Norwegian University of
Science and Technology

Characterisation of microplastic fibres and their degradation under environmental conditions

Shannen Thora Lea Sait

Environmental Toxicology and Chemistry	
Submission date:	15 May 2019
Supervisor:	Alexandros Asimakopoulos, NTNU
Co-supervisors:	Rudolf Schmid, NTNU
	Lisbet Sørensen, SINTEF Ocean
	Andy M. Booth, SINTEF Ocean

Norwegian University of Science and Technology
Department of Chemistry

Acknowledgements

I would like to thank the following people, who without this thesis would not have been possible: My external supervisors, Lisbet Sørensen and Andy Booth, for allowing me to take part in an engaging and environmentally relevant project. Huge thanks to Lisbet for your amazing availability, your constant enthusiasm and extensive and valuable feedback throughout the entire project. Your efforts have been extremely appreciated, you've taught me so much and I'm extremely grateful. Massive thanks to Andy for your great input at all stages, continual enthusiasm, great humour and treasured feedback!

My internal supervisors, Alexandros Asimakopoulos and Rudolf Schmid for all their input throughout the project. Alex, thanks for your constant passion, for guidance in the lab and for all the great stories! I look forward to doing my PhD with you! Thanks to PhD student, Kristine Vike for your help with the LC-MS/MS analysis and data processing.

The amazing laboratory staff at SINTEF Sealab: Marianne A, Oddveig, Lisbet, Marianne R, Kaja, Marianne M and Kjersti. Thanks for being so welcoming and always answering all my questions, helping me improve my Norwegian and for the much-needed afternoon coffee breaks! Thanks especially to Marianne A, Marianne R, Kjersti and Lisbet who helped me in the lab on numerous occasions.

Syverin Lierhagen for the elemental analysis, your wealth of knowledge and help with the data processing. Yingdu Ya for your invaluable expertise and training on the SEM, for the pleasant tea breaks and for all the laughs.

Thanks so much to Kjemiselskap for providing funding and to my supervisors Andy and Lisbet for the opportunity to attend the international MICRO2018 conference. A truly unforgettable experience and amazing opportunity for a master's student.

My fellow Sealab and ENVITOX students for the great conversation and the nice lunch breaks. Extra special thanks to Torbjørn, Dina, Rosalie and Giovanna!

My partner, Lars Brækken. I would not have been able to make it through these last two years if it wasn't for your unwavering support, all the home-cooked meals and for all those times you picked me up from the Uni late at night. :P Thanks for always listening to me rant about science and my thesis, and for the much-needed movie breaks! Glad i deg!

My family in Australia, for their constant support and many skype calls. Special shout out to my mum, Michele for always believing in me and sending all those comfort Tim Tams. I wouldn't be here without you!

And finally, the Norwegian Research Council for funding the Microfibre project (grant number: 268404)

List of Publications

[1] Shannen Sait, Lisbet Sørensen, Stephan Kubowicz, Alexandros Asimakopoulos, Andy M. Booth (2019)., The influence of polymer and additive chemical composition on environmental degradation of microplastic fibres. **Manuscript in preparation.**

[2] Andy M. Booth, Lisbet Sørensen, Dina Tevik Rogstad, Shannen Sait, Dag Altin, Martin Wagner, Alexandros Asimakopoulos, Iurgi Salaberria. Degradation and toxicity of microplastic fibres and their role as a source of emerging pollutants. Presentation to be held at the 29th Annual SETAC Europe meeting in Helsinki, Finland (26-30 May 2019). See Appendix J for abstract.

[3] Andy Booth, Shannen Sait, Stephan Kubowicz, Dina Tevik Rogstad, Susie Jahren, Iurgi Salaberria Lisbet Sørensen. Microfibre: How dangerous are your clothes to the ocean? Invited presentation at Ocean Week, Trondheim, Norway. (6-9 May 2019)

[4] Lisbet Sørensen, Shannen Sait, Torbjørn Nguyen, Alexandros Asimakopoulos, Rudolf Schmid, Iurgi Salaberria, Andy M. Booth. Degradation of plastic microfibres, leaching of additive chemicals and interaction with persistent organic pollutants in polar environments. Poster presented at Artic Frontiers 2019 conference in Tromsø, Norway. (20-24 Jan 2019). See Appendix J for poster.

[5] Dina Tevik Rogstad, Shannen Sait, Lisbet Sørensen, Dionis J. Lyakurwa, Dag Altin, Alexandros Asimakopoulos, Martin Wagner, Andy M. Booth, Iurgi Salaberria. Toxicity and degradation of microplastic fibres and their role as a source of emerging pollutants. Poster presented at the MICRO2018 conference in Lanzarote, Spain. (19-23 Nov 2018). See Appendix J for poster

Abstract

Despite evidence that microplastic fibres (MPFs) make up the largest proportion of microplastic pollution in aquatic environments, little is known about their degradative fate. This study investigated the UV and mechanical degradation of common MPFs: Polyester (PET), polyamide (PA) and polyacrylonitrile (PAN). Additionally, wool was included in some studies as a natural reference fibre. The characterisation of organic and inorganic additive content in the MPFs and wool, together with additive leaching was also investigated. Black and white PET, white PA, blue and orange PAN reference materials were subject to accelerated UV irradiation in seawater and freshwater media over 9 months at 65 W/m^2, representing the maximum UV exposure found globally. PET and PA MPFs showed significant fragmentation and changes in surface morphology after UV exposure. In contrast PAN did not show significant degradation under the same exposure conditions. Changes in chemical bond structures (carbonyl groups) were measured via Attenuated total reflectance-Fourier transform infrared spectroscopy (ATR-FTIR). PA showed an increase in the carbonyl index over time, while PET and PAN exhibited no observable trend in relation to carbonyl indices. The potential for mechanical degradation of pristine MPFs and wool was also assessed at 20 and 5 °C in the presence of seawater and sand. No fragmentation of any material was observed at either exposure temperature after 9 months.

Chemical additives in MPFs, and the leaching of chemical additives and polymer degradation products into freshwater and seawater was explored. A non-target approach using gas chromatography coupled to mass spectrometry (GC-MS) was first employed. The majority of the chromatographically resolved compounds could either not be identified in the NIST library or characterised based on their compound origin. Detailed investigation of the content of several bisphenols (BPs) and benzophenones (BzPs), typically employed as UV-stabilisers in MPFs and leachates, was performed via liquid chromatography coupled to tandem mass spectrometry (LC-MS/MS). BPA, BPS and BzP3 were present in all MPF samples at concentrations ranging from 4.3 - 501 ng/g, with coloured MPFs showing a higher proportion of BPs. Wool displayed the greatest total BP and BzP content at 863 and 27 ng/g, respectively. There was no detectable leaching of BPs and BzPs into water (in 14 day, and 5- and 9-month). In a final step, the targeted analysis of a broad range of known antioxidants, UV and processing stabilisers using GC-MS was conducted. All target compounds were below detectable levels in MPFs and wool. Metal content was characterised in MPFs and wool, with wool containing the highest concentration of most metals. Leaching studies conducted in seawater and freshwater media at 20 and 5 °C exhibited high levels of metal contamination, including in control samples, meaning no conclusions could be drawn about their leaching potential. The results of the current study strongly suggest that the ultimate fate and potential for detrimental effects of MPFs released to the environment are influenced significantly by multiple factors, including environmental parameters and material-specific properties. While more research is needed, the research conducted indicates that synthetic fibres may not pose a greater threat to the environment than natural fibres.

Table of Contents

List of Figures

List of Tables

Abbreviations

ANOVA	Analysis of variance
ATR-FTIR	Attenuated total reflectance Fourier transform infrared spectroscopy
BP	Bisphenol
BzP	Benzophenone
CE	Collision energy
CI	Carbonyl index
DCM	Dichloromethane
DL	Detection limit
EI	Electron ionisation
EtOAc	Ethyl acetate
FE-SEM	Field emission scanning electron microscopy
FW	Freshwater (used here specifically for TG201 medium)
GC	Gas chromatography
GC-MS	Gas chromatography mass spectrometry
HPLC	High performance liquid chromatography
ICP-MS	Inductively coupled plasma mass spectrometry
IDL	Instrument detection limit
IPA	Isopropanol
IQR	Interquartile range
IS	Internal standard
LC	Liquid chromatography
LLE	Liquid-liquid extraction
ME	Matrix effect
MeOH	Methanol
MF	Matrix factor
MP	Microplastic
MPF	Microplastic fibre
MRM	Multiple reaction monitoring

MS	Mass spectrometry
MS/MS	Tandem mass spectrometry
MSSV	Micro scale sealed vessel
NIST	National institute of standards and technology
PA	Polyamide (Nylon 6.6)
PAHs	Polycyclic aromatic hydrocarbons
PAN	Polyacrylonitrile (Polyacrylic)
PCA	Principal component analysis
PET	Polyethylene terephthalate (Polyester)
PRG	Pierre Robert Group
PVC	Polyvinyl chloride
Py-GC/MS	Pyrolysis gas chromatography mass spectrometry
Q1	Quadrupole 1
q2	Quadrupole 2
Q3	Quadrupole 3
qQq	Triple quadrupole
RIS	Recovery internal standard
RR	Relative response
RRT	Relative retention time
RSD	Relative standard deviation
RT	Retention time
SEM	Scanning electron microscope
SIS	Surrogate internal standard
SLE	Solid-liquid extraction
SRM	Single reaction monitoring
STD	Standard deviation
SW	Seawater
UV	Ultraviolet

1 Introduction

1.1 Plastic pollution

The global production of plastic has increased exponentially since the 1950s, with a staggering 348 million tonnes produced in 2017 alone (“Plastics Europe”., 2018). If production continues at this rate, global manufacture is projected to reach around 1.8 billion tonnes by 2050 (Figure 1.1). Plastics are a cheap, lightweight and durable material - desirable properties that have resulted in their high production volume. High production coupled with their disposable nature has large proportions of plastic debris entering aquatic environments. As a result, plastics are now found ubiquitously in both marine and freshwater systems including surface and subsurface waters, the water column, sediments, beaches, the deep sea and sea ice (Andrady, 2017; Browne et al., 2011).

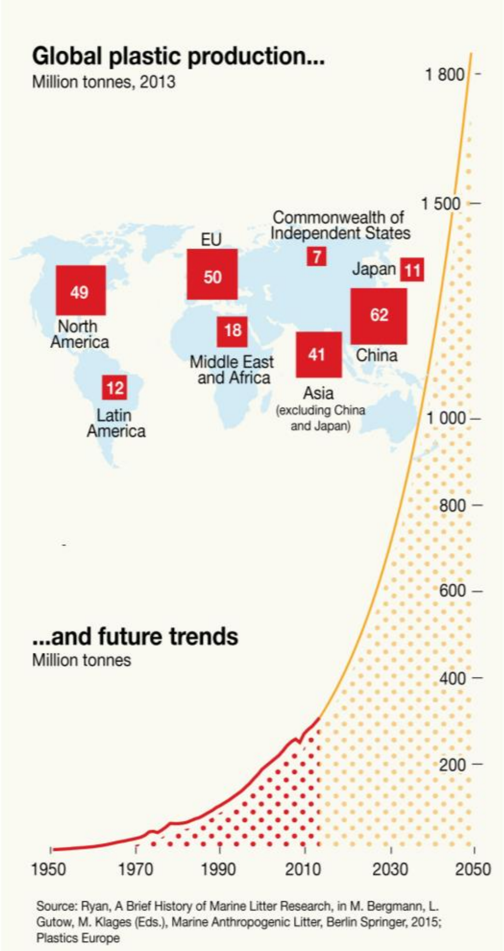

Source: Ryan, A Brief History of Marine Litter Research, in M. Bergmann, L. Gutow, M. Klages (Eds.), Marine Anthropogenic Litter, Berlin Springer, 2015; Plastics Europe

Figure 1.1. Global plastic production projection by 2050

1.1.1 Microplastics

Microplastics (MPs) are currently defined as plastic debris between 0.1 µm - 5 mm (GESAMP, 2015). The definition is however rapidly changing and new classifications are emerging such as mesoplastic (1-5 mm), microplastic (1 µm – 1 mm) and nanoplastic (< 1 µm) (Andrady, 2011; GESAMP 2017). MPs are classified as either primary or secondary. Primary MPs refer to small plastics that are specifically manufactured for direct use (e.g. cosmetic microbeads), whereas secondary MPs result from the fragmentation of larger plastic debris (E.g. microplastic fibres) (Andrady, 2017). Due their small size, MPs can be ingested by a variety of marine and freshwater biota. MPs can theoretically act as both sources and sinks of pollution, due to their potential to sorb existing metals and persistent organic pollutants (POPs) from the environment, and due to the presence of additive chemicals (Andrady, 2017; Wang et al., 2016). The extent of MP toxicity, fate and behaviour in aquatic environments is still not well understood (Andrady, 2017).

1.2 Microplastic fibres

In a recent study on the global distribution of MPs, microplastics fibres (MPFs) were determined to be the predominate microplastic debris, comprising 91% of MPs quantified in environmental samples (Barrows et al., 2018). MPF pollution is found ubiquitously in the environment with the highest density in open ocean compared to coastal regions, and the highest concentrations found in the arctic ocean according to a recent global study (Barrows et al., 2018). Other studies have shown contradictory densities with the highest concentrations found in coastal regions (Wessel et al., 2016), confounding data can be attributed to the challenges associated with working with MPFs and the lack of standard practices within the field. Similarly, MPF pollution may be overestimated due to their length and increased visibility in environmental matrices. Despite the ubiquitous occurrence of MPFs in the environment, there are few studies on their distribution, fate and behaviour in aquatic systems. Their potential effect on aquatic organisms (e.g. toxicity) is likewise poorly understood.

MPFs in the environment may originate from a number of sources including fragments of products such as fishing nets. However, the sustained increase in synthetic textile production has caused the scientific community to draw special attention to the fate and potential effects of textile fibres released through the use and washing of such products. Recent studies indicate high fibre release from both household and industrial washing of textiles.

105 million tonnes of textile fibres were produced in 2018, consisting of approximately 63% (66 million tonnes) synthetic, 25% non-synthetic (e.g. cotton, wool and silk) and the remaining a mixture of semi-synthetic blends (e.g. rayon) (Barrows et al., 2018; Lenzing, 2017). According

to a recent review, of the 6800 metric tonnes of primary plastic waste generated by the end of 2015, 700 metric tonnes was the result of polyester, polyamide and polyacrylic fibres (Geyer et al., 2017; Salvador Cesa et al., 2017). Textiles are not recycled at significant rates and are usually either incinerated or discarded with solid waste (Geyer et al., 2017). The most common synthetic textiles used within the textile industry and consequently emitted into the environment include polyester (PET), polyamide (nylon, PA), and polyacrylic (PAN).

1.2.1 Polyester (PET)

Polyester is a commonly used synthetic fibre which usually refers to either polyethylene terephthalate (PET) or poly-1,4- cyclohexylene-dimethylene terephthalate (PCDT). PET is the most popular type of polyester in textile production (Figure 1.2) (Deopura and Padaki, 2015). PET is produced via the transesterification of dimethyl terephthalate and ethylene glycol (Painter and Coleman, 1997). In 2018, 55 million tons of polyester fibre was produced globally (Lenzing, 2018). Studies have shown that PET fibre can shed between 100 000 – 500 000 fibres per a single household wash, with polyester fleece shedding significantly more than regular polyester fibre (Carney Almroth et al., 2018; Napper and Thompson, 2016).

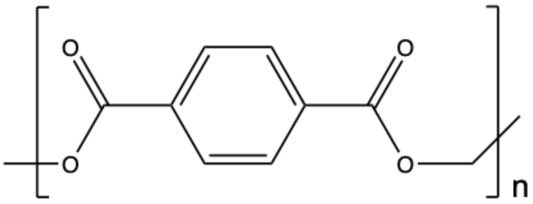

Figure 1.2. Chemical structure of polyethylene terephthalate (polyester, PET)

1.2.2 Polyamide (PA)

Polyamide fibre refers to both nylon and aramid fibres, both of which are formed from long chains of polyamides. Nylon 6 and Nylon 6.6 represent the two main fibre types used within the textile industry (Deopura and Padaki, 2015). Nylon 6 refers to polyamide which contains six carbon atoms in its monomer (Figure 1.3), and is formed from ring opening polymerisation of caprolactam before being spun into filament (Painter and Coleman, 1997). Nylon 6,6 refers to polymer made from 2 monomers containing 6 carbon atoms each (12 in total) as shown in Figure 1.3. Nylon 6.6 is produced via condensation polymerisation of hexamethylenediamine and adipic acid before being spun into filament (Painter and Coleman, 1997). In 2017, 5.7 million tons of polyamide fibre was produced globally (Lenzing, 2017). Carney Almroth et al., (2018) found that polyamide fibre can release up to 800 fibres per garment per wash, similar to polyester and polyacrylic fibres.

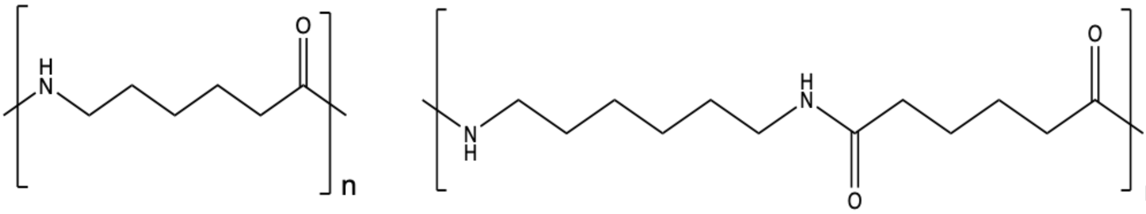

Figure 1.3. Chemical structure of common polyamide fibres. From left to right: Nylon 6, Nylon 6.6

1.2.3 Polyacrylate (PAN)

Polyacrylic fibre often refers to the polymer polyacrylonitrile (PAN). PAN fibre is produced via free-radical polymerisation of acrylonitrile (vinyl cyanide) and subsequent wet or dry spinning (Mather, 2015; Painter and Coleman, 1997). Most commercial polyacrylic fibres are copolymers, consisting of a polyacrylonitrile monomer and a comonomer such as vinyl acetate, methyl acrylate or methyl methacrylate. Comonomers are added to improve dyeability and allow for easier processing (Mather, 2015). According to the ISO and the International Synthetic Fibre Standardization Office (BISFA), for a fibre to classified as polyacrylic, it must contain at least 85% (w/w) acrylonitrile (BISFA, 2017). As of 2018, polyacrylic production is estimated to be roughly 2 million tonnes, however production rates have decreased for the seventh consecutive year (Lenzing, 2017). Acrylic fibre is often used a replacement for wool, due to its similar properties, namely it’s warmth (Mather, 2015). A study by Napper and Thompson (2016), estimated at over 700,000 acrylic fibres could be released from a single 6 kg household wash load of PAN textile.

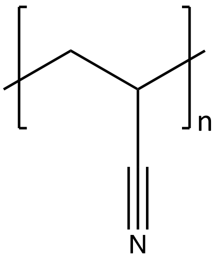

Figure 1.4. Chemical structure of polyacrylonitrile (PAN)

1.3 Natural fibres

Natural and semi-synthetic fibres make up a significant proportion of fibre pollution in aquatic environments however the impact and distribution of them are often not included when assessing microfibre contamination (Barrows et al., 2018). Cotton and wool are the most common natural fibres in textiles production.

1.3.1 Wool

Wool has a range of unique properties making it especially popular in colder climates, such as Norway (The University of Waikato, 2007). Every year, over 4000 tonnes of wool is produced in Norway alone (Norilla, 2017). Wool is a natural fibre or hair sourced from animals, generally sheep and is composed of the protein, keratin. The cellular structure of wool consists of the cuticle, cortex, cortical cells, macrofibrils, the matrix, microfibrils and twisted molecular chains (Figure 1.5). The cuticle is the outer protective layer of scales, they prevent water penetrating the fibre but allow absorption of water vapor (The University of Waikato, 2007). The cortex makes up 90% of the wool fibre. The cells of the cortex, termed cortical cells are held together by a cell membrane, this membrane contain waxy lipids and proteins and runs through the entire length of the fibres. This membrane allows for easy uptake of dye molecules (The University of Waikato, 2007). Inside the cells are long and fine filaments called macrofibrils and microfibrils which are surrounded by a matrix region. The matrix consists of a large number of thiol group (-SH) and other sulphide groups, making the interior of wool absorbent as thiol groups attract water molecules as well as organic molecules, such as dyes (Mansour et al., 2015; The University of Waikato, 2007). Wool can absorb up to 30% it's weight in water. Wool unique structure is responsible for its desirable properties including: fire resistance, natural self-cleaning and antistatic nature. (The University of Waikato, 2007).

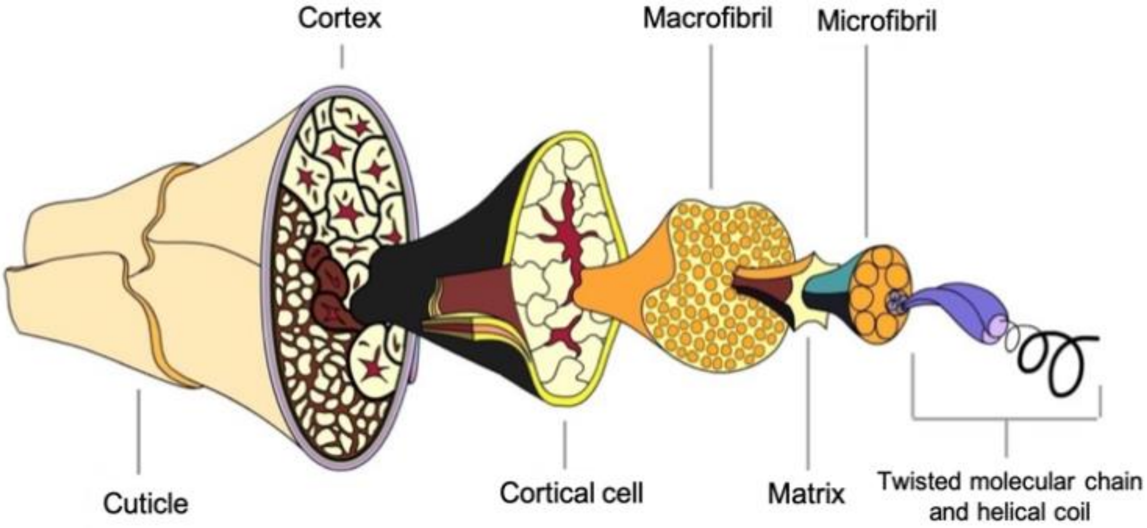

Figure 1.5. Cellular structure of wool fibre (The University of Waikato, 2007)

1.4 Sources of MPFs found in the environment

While MPFs make up the majority of MPs found in marine and freshwater environments, their sources are still relatively unknown. Studies indicate a large proportion of MPFs are released during household washing cycles (Carney Almroth et al., 2018; Napper and Thompson, 2016; Salvador Cesa et al., 2017). Modern wastewater treatment plants (WWTPs) have been shown to remove up to 99% of MP debris (including MPFs) from wastewater (Carr et al., 2016; Murphy et al., 2016; Talvitie et al., 2015) however wastewater still contributes considerably to MP pollution due to the high volumes released into the environment (Mason et al., 2016; Mintenig et al., 2017; Murphy et al., 2016; Talvitie et al., 2015). The efficiency and quality of WWTPs vary drastically across the globe with middle and low income countries often contributing higher rates of MP pollution due to poorer waste management systems (Blettler et al., 2018). Sewage sludge, a source of MPF pollution is used on agricultural land as a fertilizer allowing for potential run-off and subsequent transport of MPFs into freshwater and marine environments (Habib et al., 1998). A recent study (Li et al., 2018), showed that MPFs made up 63% of MP pollution in sludge samples collected from WWTPs across China. Furthermore, Dris et al (2016) indicates that long range transport or atmospheric fallout could be an important source of MPFs in the environment. It is estimated that between 3 – 10 tons of fibre are accumulated in the environment each year with the highest concentrations found in urban areas, these MPs can then be transported by wind or run off into marine and freshwater ecosystems (Dris et al., 2016).

1.5 Fate of microplastics in the natural environment

Once MPs or MPFs enter the environment, they can undergo several degradative processes through either biotic or abiotic pathways including: hydrolysis, photodegradation, biodegradation, mechanical and thermal degradation (Gewert et al., 2015). Degradative processes are relevant to all types of plastic debris in the natural environment; however, this thesis will focus on degradation in the context of MPFs. Due to their larger volume to surface ratio, MPFs can undergo degradation at higher rates than observed in macroplastic debris. Qualitative signs of degradation include changes in colour and so-called crazing. Crazing refers to the formation of numerous tiny cracks along the surface of MPFs, increasing the surface area and leading to embrittlement, fragmentation and subsequent disintegration (Da Costa et al., 2018; Gewert et al., 2015). Much is still unknown regarding the fate of MPs and MPFs in natural environment.

1.5.1 Hydrolysis

Hydrolysis is the breakdown of MPFs in the presence of water and an acid, base or enzyme catalyst leading to a reduction in molecular weight. In general, polymers without heteroatoms (O, N, Cl, etc) in their backbone (e.g. polyethylene and polypropylene) do not undergo hydrolysis whereas polymers with heteroatoms (e.g. polyester and polyamides) are susceptible to hydrolysis. (Gewert et al., 2015).

PET is prone to hydrolysis, though under normal environmental conditions this process is thought to occur slowly due to its aromaticity (Gewert et al., 2015). PETs aromaticity stabilises its structure thereby reducing the degree of hydrolysis. During hydrolysis, carboxylic end groups and alcohol functional groups are formed (Figure 1.6). The rate of hydrolysis will increase under basic or acidic conditions and occurs spontaneously in the presence of carboxylic acids, an end product often formed during photodegradative processes (discussed further in section 1.5.2) (Gewert et al., 2015; Muthuraj et al., 2015).

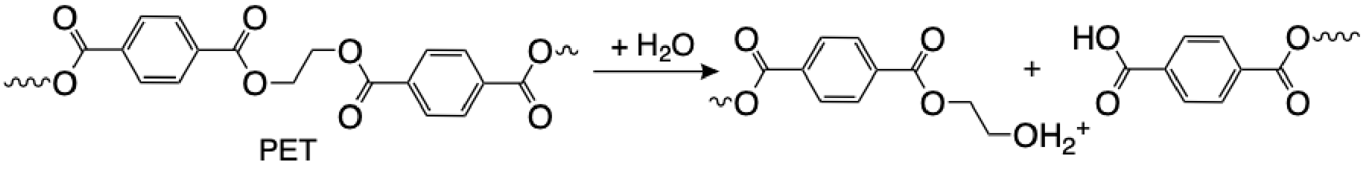

Figure 1.6. Proposed pathway of hydrolytic degradation of PET under environmental conditions (Reproduced from Gewert et al., 2015)

PA is susceptible to hydrolysis, though it is considered only an important degradative process at higher temperatures and in presence of concentrated acids or bases (Andrady, 2011). Hydrolysis of polymers is considered to not be significant form of degradation in natural marine and freshwater environments, as it usually occurs at higher temperature or in the presence of strong catalysts (Gewert et al., 2015).

1.5.2 Photodegradation

Photodegradation is expected to be the dominant degradative process in MPFs under environmental conditions (Andrady, 2011). Photodegradation occurs when MPFs are exposed to UV light (e.g. sunlight) and oxygen but can also occur in the absence of oxygen. To undergo photodegradation, the polymer must contain chromophoric groups capable of absorbing UV light. The mechanism by which photodegradation proceeds is highly dependent on polymer type and the type of chromophores present (Gewert et al., 2015). Polymers without heteroatoms usually degrade via chain scission. Chain scission refers to the breakdown of a polymer chain at random points in the backbone forming molecular fragments (Painter and Coleman, 1997). Polymers with heteroatoms (e.g. oxygen and nitrogen, like PET) are expected to degrade into low-molecular fragments (oligomers and monomers) with oxidised end groups (Gewert et al., 2018).

Environmental weathering of PET is thought to predominately occur via photodegradation and is characterised by a yellowing of the material (Gewert et al., 2015). During photodegradation, the ester bond is either cleaved resulting the formation of carboxylic acid or vinyl end groups or radicals are produced which also leads to the generation of carboxylic end groups (Figure 1.7). In short, the photodegradation of PET results in chain scission or a decrease in molecular weight and the generation of carboxylic end groups (Gewert et al., 2015).

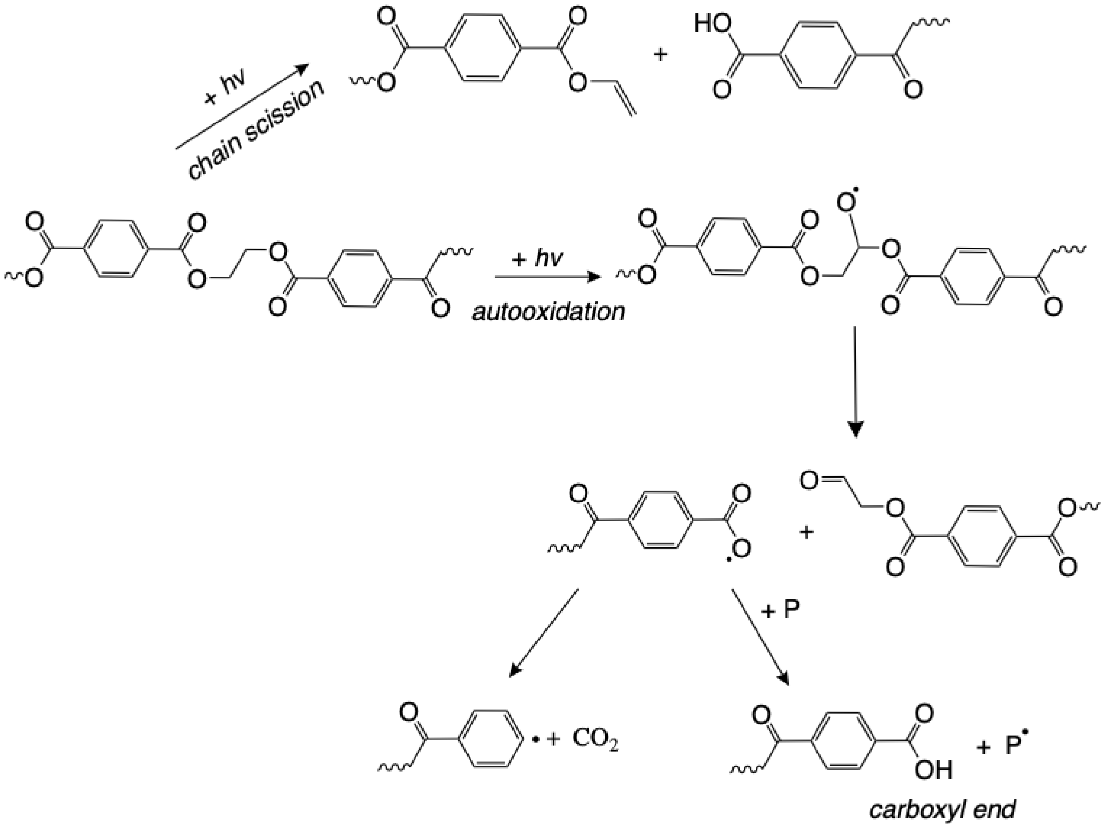

Figure 1.7. Simplified proposed pathways for the photodegradation of PET under environmental conditions. Where P represent the polymer backbone of PET and *hv* indicates energy input from UV radiation [Reproduced from Gewert et al, 2015].

Photodegradation can occur in PA via random chain scission or polymer cross-linking resulting in a decrease in molecular weight and an increase in amino end-groups (Shamey and Sinha, 2003). Few studies regarding photodegradation of PAN have been conducted, especially under environmentally relevant conditions, however it is likely that degradation would proceed via chain scission and cross linking resulting in a decrease in molecular weight, similar to what is observed in polyamide (Shamey and Sinha, 2003).

1.5.3 Mechanical degradation

Mechanical degradation of MPFs occurs due to frictional forces and interactions with any solid material. Sand and inorganic particles are relevant for the mechanical degradation of MPFs in aquatic environments. Unlike other degradative mechanisms, no specific chemical changes occur during this process (Painter and Coleman, 1997). However, photodegradation and hydrolysis reduce molecular weight, thereby increasing embrittlement making polymers more prone to fragmentation (Song et al., 2017). Preliminary chemical degradation (e.g. photodegradation) can make MPFs more brittle and susceptible to mechanical degradation resulting in an increase in surface area and a decrease in particle size. This can then result in potentially faster degradation and higher bioavailability to organisms (Song et al., 2017; Painter and Coleman, 1997).

1.5.4 Biodegradation

Once in the environment, MPFs can be quickly colonised by various microorganisms, termed biofouling which may result in possible biodegradation. Biofouling affects the fate of MPFs in aquatic systems. Colonisation of bacteria can increase MPF density which may encourage their vertical transport to sediment-benthic zones. In addition, biofouling can shield MPFs from other degradation processes. Both effects are thought to reduce the rate of environmental degradation, especially photodegradation (Kooi et al., 2017, 2017). Biodegradation of PET, PA and PAN is thought to occur very slowly under environmental conditions (Andrady, 1994; Müller et al., 2001).

1.5.5 Thermal degradation

Thermal degradation of MPFs occurs at elevated temperatures, usually close to their melting point, resulting in reductions in molecular weight via chain scission (Painter and Coleman, 1997).

In aquatic systems under environmental conditions, temperatures are not considered high enough for significant thermal degradation to occur (Gewert et al., 2015).

1.6 Factors influencing degradation rates

1.6.1 Environmental factors

The environmental conditions polymer and as such MPFs are subjected to, especially temperature, the availability of light, the level of oxygen and the presence of microorganisms will impact the extent of environmental weathering. In general, lower temperatures, lack of light, and low oxygen levels will slow down degradative processes (Booth et al., 2017; Gewert et al., 2015).

Temperature

Temperature greatly influences the rate of most types of degradation in the natural environment. With rate of degradation typically greater at higher temperatures. Temperature is also an important factor in biodegradation, which usually proceeds more rapidly at higher temperatures (Booth et al., 2017; Gewert et al., 2015.

Availability of sunlight (UV)

The availability of sunlight is a prerequisite for photodegradation, and UV intensity influences the rate of photodegradation (Gewert et al., 2015). The intensity of UV radiation is dependent mainly on geographical location, seasonality and climate conditions as well as the extent of ozone in the atmosphere. With the highest levels of UV radiation being observed at the equator and the lowest levels at the northern and southern poles. Due to this variability, polymers can experience diverse levels of photodegradation in the natural environment (Booth et al., 2017; Gewert et al., 2015).

Oxygen levels

Oxygen availability will affect the rate of degradation for all processes that require oxygen, such as photooxidation. Greater availability of oxygen will result in higher rates of degradation (Gewert et al., 2015). Oxygen availability also impacts the rate of biodegradation and the microbial composition in aquatic environments (Song et al., 2017; Gewert et al., 2015).

1.6.2 Degradation of MPFs under temperate and Arctic conditions

Rates of polymer degradation in the Norwegian environment are expected to vary significantly over the course of the year. Further north, the intensity of sunlight is lower and varies drastically between seasons, being high in summer and almost negligible in winter. Therefore, in the Norwegian environment, plastic debris (including MPFs) released to aqueous compartments is predicted to experience quite low levels of photodegradation due to low average UV intensities, commonly observed overcast conditions and the presence of sea ice in northern regions during large parts of the year (Booth et al., 2017).

1.8 Chemical additives

Plastics often contain a variety of additives chemicals in order to impart desirable properties, such as flexibility, increased durability and flame retardancy. For the purpose of this thesis chemical additives will be grouped into 3 main categories: organic additives for function (stabilisers, flame retardant, plasticisers, etc.) colorants (azo dyes, pigments, etc.) and metals (Ambrogi et al., 2017). As additive chemicals are often not covalently bonded to polymers, they have the capacity to leach into aquatic environments, especially during degradation which may impact surrounding biota (Hermabessiere et al., 2017). Analysis of chemical additives is a challenging task, not just due to the plethora of chemicals additives used within the plastics industry (> 6000 individual compounds are estimated to be in use currently), but also due to their relatively low concentrations in polymer matrices (Hahladakis et al., 2018).

The majority of plastic additives go by trade names, that are often related to their function. Examples of such trade names include: Irganox® antioxidants, Chimassorb® light stabilisers, Tinuvin® UV - absorbers and Irgafos® processing stabilisers which protect fibres and textiles from thermal and UV degradation during processing or general use (BASF, 2013; "BASF Light Stabilizers for Synthetic Fibers," 2017).

1.8.1 Functional additives

Antioxidants and photostabilisers

Antioxidants are added to plastics typically to prevent thermal degradation during the production process but also to hinder other forms of degradation during the lifetime of a product, namely photooxidation (Ambrogi et al., 2017). Antioxidants work to slow down the rate of oxidation, usually via reaction with free radicals. Antioxidants can be classified as either primary of secondary. Primary antioxidants generally consist of hindered phenolics and secondary aryl amines Secondary antioxidants typically consist of phosphites or thioesters. Primary and secondary antioxidants are often used together in the manufacture of plastics, as they work together synergistically to increase polymer stability (Ambrogi et al., 2017; Hahladakis et al., 2018). Photo- or light stabilisers are used to prevent photooxidation. As this is also mediated by free radicals, antioxidants are also classified as light stabilisers however addition classes exist outside of antioxidants such as hindered amine light stabilisers, UV absorbers and quenchers (Ambrogi et al., 2017; Choi and Jang, 2011; Hahladakis et al., 2018).

Benzophenones

Benzophenones (BzPs) are frequently used as UV light absorbers in sunscreens, cosmetics and as UV filters in plastics (including MPFs). They are classified as high production compounds and are now considered ubiquitous in natural environments. BzPs exhibit anti-estrogenic and anti-androgenic activity (Asimakopoulos et al., 2014b; Li and Kannan, 2018). Benzophenone and its various analogues are used within the textile industry to prevent photodegradation in textiles and increase their consumer lifetime (Figure 1.8) (Xue et al., 2017).

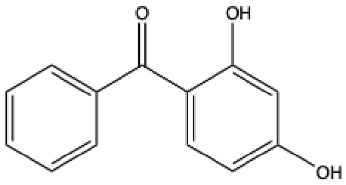

Benzophenone 1 (BzP1)

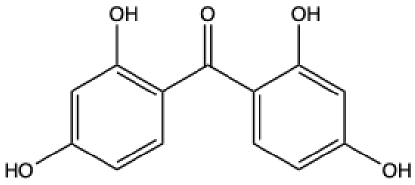

Benzophenone 2 (BzP2)

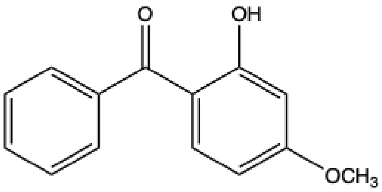

Benzophenone 3 (BzP3)

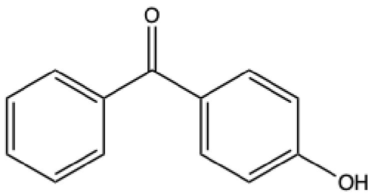

4-OH-Benzophenone (4-OH-BzP)

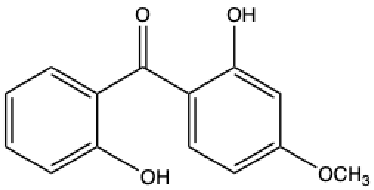

Benzophenone 8 (BzP8)

Figure 1.8. Structures of common commercial benzophenones

Bisphenols

Bisphenols (BPs) are a class of chemicals with two phenolic functional groups that include several analogues such as: Bisphenol A (BPA), Bisphenol AF (BPAF), Bisphenol B (BPB), Bisphenol F (BPF), Bisphenol S (BPS) Bisphenol M (BPM), Bisphenol P (BPP) and Bisphenol Z (BPZ) (Figure 1.9). BPs are widely used in the manufacture of various plastics and are known endocrine disruptors (Asimakopoulos et al., 2014b; Li and Kannan, 2018). While BPA has been heavily studied, concentrations of BP analogues and subsequent exposure levels of BP analogues is still an understudied area. BPA is used in a wide range of applications within the plastics industry as an intermediate chemical in the production of flame-retardants, stabilisers and antioxidants. In textile manufacturing, BPA has been reportedly used as a coating and an intermediate chemical for the manufacture of dyes and antioxidants (Xue et al., 2017). BPS and BPF are common replacements for BPA. Literature indicates that BPS is now ubiquitous in the environment, but generally with lower concentrations than BPA. Current data suggest that BPS may have adverse effects on endocrine, reproductive and nervous systems in animals and humans, and may trigger oxidative stress (Asimakopoulos et al., 2014b; Lehmler et al., 2018).

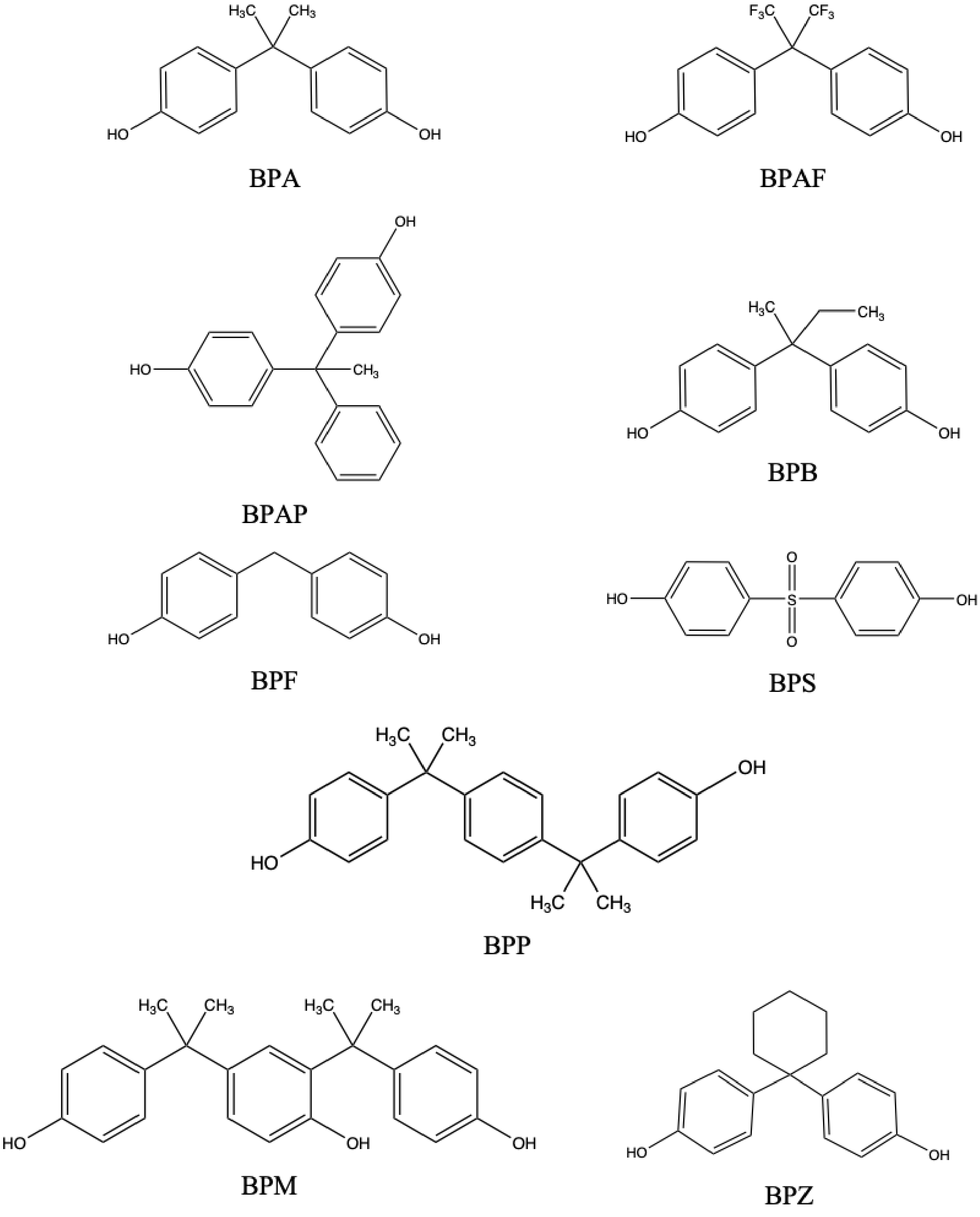
BPA

BPAF

BPAP

BPB

BPF

BPS

BPP

BPM

BPZ

Figure 1.9. Structures of common commercial bisphenols

Plasticisers

Plasticisers are added to plastic to increase their softness, flexibility and durability. The majority of plasticiser (~80%) are used in the production of a single polymer, polyvinyl chloride (PVC) (Cadogan and Howick, 2000). Phthalates make up the largest percentage of plasticisers consisting ~70%. While it's unlikely that phthalates are used directly in the production of textiles, they may be introduced through a variety of indirect pathways. Source of phthalates could arise during textile production from the use of processing chemicals e.g. dyes, incoming processing water, or chemical impurities and unknown additives in processing compounds (Le Marechal et al., 2012). Other important plasticisers include, terephthalates, epoxies and adipates (Cadogan and Howick, 2000). Phthalates represent a large source of contamination in analytical laboratories due to leaching from equipment such as plastic syringes and pipette tips and as such are difficult to quantify and avoid when conducting analytical work (Reid et al., 2007).

1.8.2 Dyes and pigments

Dyes and pigments are added to MPFs to impart colour. The choice of dye or pigment used within the textile industry is based on textile type. Azo dyes are a common colorant that provide a large range of hues and desirable properties. PET, PA and PAN MPFs are frequently coloured with dispersed azo dyes, which have an affinity for hydrophobic MPFs (Fleischmann et al., 2015; Pawar et al., 2018). It is estimated between 10-50% of colorants used during dyeing processes end up in the environment. Some dyes have shown high toxicity and mutagenicity among other undesirable environmental impacts (Drumond Chequer et al., 2013). Metal compounds are often commonly used as dyes in textiles (Rezić and Steffan, 2007).

1.8.3 Metals

Traces of various metals are used within the textile industry for a variety of applications including as: metal complex dyes; dye stripping agents; odour-preventing compounds; antifungal components and oxidising compounds. Trace heavy metals can have beneficial and negative impacts on the environment, marine biota and human health and as such it is important to determine the trace metal content in industrial textiles (Rezić and Steffan, 2007; Sungur and Gülmez, 2015a, 2015b).

1.9 Aims and objectives

This master thesis is part of the Norwegian Research Council funded project, "Microfibre", which investigates the environmental fate and behaviour of microplastic fibres (MPFs), as well as their potential for ingestion and toxicological effects on aquatic species. The degradation of MPFs, PET, PA and PAN, was investigated in marine and freshwater environments via:

- Long-term UV exposure studies under accelerated daylight conditions in marine and freshwater environments
- Long-term mechanical degradation studies in marine environments

Due to the challenges associated with additive analysis, little is known about the additive content of MPFs and their potential for leaching into aqueous environments. BPs and BzPs are high production compounds that are often employed in the manufacture of plastic products, they have known endocrine disruptors and little data exists on their occurrence in MP and wool fibres. The organic and inorganic chemical additive content in both MPFs, natural wool fibre and their respective aqueous leachates was investigated via:

- Non-target approach for the screening of additive chemicals and potential detection of emerging pollutants through gas chromatography mass spectrometry (GC-MS)
- Targeted screening of BPA and bisphenol analogues: BPAF, BPAP, BPB, BPF, BPS, BPM, BPP and BPZ in addition to 5 benzophenones: BzP1, BzP2, BzP3, 4-OH-BzP and BzP 8 in MPFs by liquid chromatography tandem mass spectrometry (LC- MS/MS)
- Target screening of common antioxidants and UV stabilisers: Cyasorb UV-5411; Irgacure 1800; Irgafos 38; Irgafos168; Irganox B220; Irganox HP 2215; Tinuvin 234; Tinuvin 327; Tinuvin 328 using GC-MS
- Examination of inorganic content with inductively coupled plasma mass spectrometry (ICP-MS)

2 Theory

2.1 Sample preparation

Prior to analytical analysis, adequate preparation of a sample is critical. It involves the extraction of analytes of interest from a sample matrix. The reliability of analytical analysis is often dependent on the selection of an appropriate preparation procedure (Skoog, 2012)

2.1.1 Solid-liquid extraction

Solid-liquid extraction (SLE) is a method used to extract organic compounds from a solid phase (e.g. plastic) into a liquid phase (e.g. organic solvent or water). Ultrasonication-assisted SLE is a simple, efficient and inexpensive extraction technique. The use of ultrasonication increases reaction kinetics and thus extraction yield (Ballesteros et al., 2014). Ultrasonication is also effective in the extraction of heat-sensitive compounds as extraction can be performed at lower temperatures than other extraction methodologies (e.g. accelerated solvent extraction). (Balcerzak and Baranowska, 2016)

2.1.2 Liquid-liquid extraction

Liquid-liquid extraction (LLE), also referred to as solvent extraction is an extraction method used to separate compounds based on their relative partitioning in two immiscible solvents, usually from an aqueous solution (e.g. water) into an organic phase (e.g. hexane). The partitioning or distribution coefficient (K_d) is given by equation (2.1):

$$K_d = \frac{[analyte]_{organic}}{[analyte]_{aqueous}} \tag{2.1}$$

Where $[\mathrm{analyte}]_{\mathrm{organic}}$ and $[\mathrm{analyte}]_{\mathrm{aqueous}}$ are the concentration of the analyte in the organic and aqueous phase, respectively. A high K_d indicates that the analyte is mostly distributed in the organic phase and conversely a low K_d indicate high concentration of analyte in the aqueous phase (Lundanes et al., 2014).

2.2 Analytical Techniques

2.2.1 Gas Chromatography-Mass Spectrometry

Chromatography separates components of mixture based on their retention time. In gas chromatography (GC), the mobile phase is a chemically inert gas, and the analytes need to be sufficiently volatile in order to be carried through the column. The applicability of GC is generally limited to volatile or semi-volatile compounds that are semi- or non-polar in nature. The analyte than interacts with the wall of the column, the stationary phase resulting in compounds eluting at different times, known as the retention time (Lundanes et al., 2014). There are several detectors that can be used with GC, depending on the application. For identification of compounds in complex mixtures, or trace amounts of compounds in samples, coupling to mass spectrometry (MS) is by far the most powerful, providing a second dimension of identification based on mass, as well as increased sensitivity. GC-MS can be used in both full scan MS or selected ion monitoring (SIM) mode in order to cover a wide range of m/z ratios or gather specific data on masses of interest, respectively (Lundanes et al., 2014; Poole, 2003).

2.2.2 Pyrolysis GC-MS

Pyrolysis gas chromatography mass spectrometry (py-GC-MS) is a valuable technique for the identification of polymers. Polymers can be identified by comparing pyrograms and MS spectra with known references (Al-Salem, 2019). In py-GC-MS, the sample is heated to decomposition into smaller fragments. Decomposition temperatures often range from 600 – 1000 °C (Basu, 2013). These small fragments or ‘pyrolysis products’ are subsequently separated and detected by direct coupling to GC-MS. Although py-GC-MS is a destructive method, it only requires a small amount of untreated sample. In addition to polymer identification, py-GC-MS allows for the detection of associated chemical additives (Al-Salem, 2019; Basu, 2013).

2.2.3 Spectral databases

Mass spectral libraries, like the National Institute of Standards and Technology’s (NIST), contain mass spectra for a plethora of compounds. When identifying compounds through such a database, the mass spectra functions like a fingerprint for that compound. When searched, the database returns a list of probable matches based on the original mass spectrum with a corresponding match percent or factor. While such databases are quite valuable, libraries have only spectra for either known compounds or those integrated into the database. Furthermore, there are many compounds which present similar or identical mass spectra (Lundanes et al., 2014; McMaster, 2005). When identifying additives and other chemical components, a 80 % match is generally considered satisfactory (Ausloos et al., 1999; Stein, 1994). Matched compounds can only be identified and quantified via analytical standards.

2.2.3 Liquid Chromatography-Mass Spectrometry

In liquid chromatography (LC), the mobile phase is a liquid, which transports the analyte of interest though the stationary phase, which may be planar or, most commonly, in the form of packed column. Components are than separated based on their polarity (Lundanes et al., 2014; McMaster, 2005). High performance liquid chromatography (HPLC) is an instrumental type of LC, where the use of a pump moves the pressurised solvent rapidly through the column. LC can be coupled to a range of detectors, where ultraviolet (UV) and MS are the most commonly applied for environmental application. LC-MS/MS (tandem MS) provides more information as it measures not only molecular weight but can also fragment the precursor ion and identify characteristic fragments of the molecule, improving accuracy and reducing experimental error (Figure 2.1). LC-MS/MS is particularly valuable for analysis that involves a large number of compounds, such as polymer matrices or environmental effluents (Barceló and Petrovic, 2007; McMaster, 2005).

The most common application mode of tandem MS is multiple reaction monitoring (MRM). In MRM, an ion of interest is first selected by the mass filter in quadrupole one (Q1), fragmented in quadrupole two (q2) and analysed in the third quadruple (Q3). Target fragment ions are counted over time, resulting in single reaction monitoring (SRM) for each transition. MRM refers to the overall process that involves multiple daughter ions from multiple precursors or parent ions. By only focusing on target ions, MRM allows for high accuracy and increased sensitivity (Lundanes et al., 2014; McMaster, 2005).

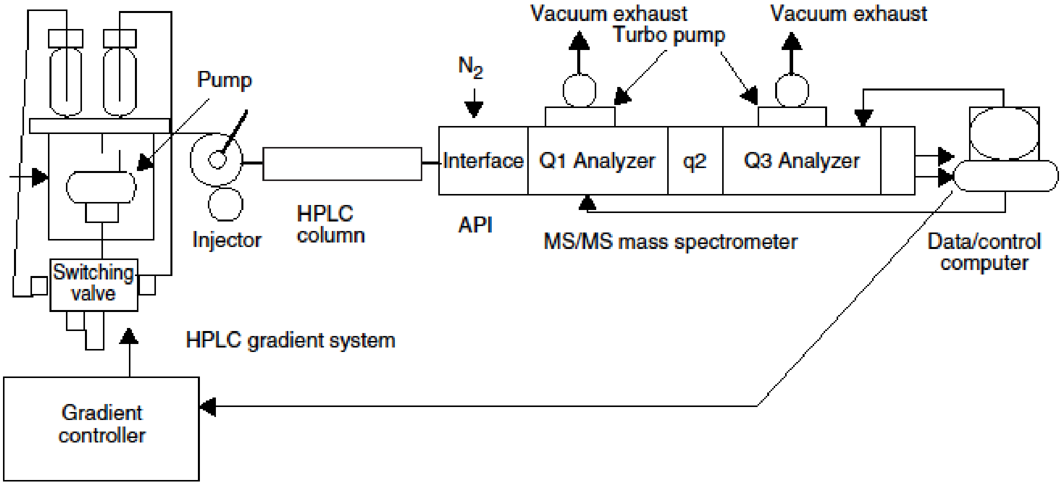

Figure 2.1. LC-MS/MS schematic (McMaster, 2005)

Retention time and relative retention time

The retention time (RT) of a compound can vary greatly between injections due to a variety of factors, including fluctuations in column and oven temperature, gas flow rate, the column length and column degradation (Wilson et al., 2014). To account for small differences in the RT, relative retention time (RRT) can be used. The RRT is determined by comparing the RT of the target analyte relative to the RT of a suitable internal standard injected under the same conditions (Equation 2.2).

$$RRT = \frac{RT_{Analyte}}{RRT_{Internal\ Standart}} \tag{2.3}$$

Relative Response

The relative response ratio (RR) is determine by comparing the signal intensity within a sample compared to the intensity in the internal standard (Equation 2.4)

$$RR = \frac{Response_{Analyte}}{Response_{Internal\ Standard}} \tag{2.4}$$

Ion ratio

The ion ratio (IR) is an addition confirmation parameter and is unique for each compound in a sample matrix (Berendsen et al., 2017). The IR is calculated by dividing the area of the confirmation ion by the area of the quantification ion (Equation 2.5).

$$IR\ \% = \frac{Area_{Confirmation\ ion}}{Area_{Quantification\ ion}} \times 100 \qquad (2.5)$$

Repeatability and reproducibility

Repeatability and reproducibility are ways to quantify precision in experimental work. Repeatability measures the variation in instrumentation taken under the same conditions for the same sample (Skoog, 2012). The mean refers the calculated ‘central’ value of a given dataset and is calculated according to equation 2.5. The mean ($\bar{x}$) can be calculated by dividing the sum of a discrete set of values by the number of values (n) (Equation 2.6).

$$\bar{x} = \frac{\sum_{i=1}^{n} x_i}{n} \qquad (2.6)$$

Where $\bar{x}$ is the mean value, n = number of samples and x_i is equal to all x values in the series (e.g. $x_1, x_2, x_3 \ldots x_n$).

Standard deviation (STD) is a measurement of the variation in a given data set. Repeatability can be determined by calculating the standard deviation (Equation 2.7) or the relative standard deviation (Equation 2.7).

$$STD = \sqrt{\frac{\sum_{i=1}^{n}(x_1 - \bar{x})^2}{n-1}} \qquad (2.7)$$

Relative standard deviation (RSD) is the preferred measure of repeatability or precision as it allows for the comparison of uncertainty between measurements of different magnitude (Skoog, 2012). RSD can be determined by dividing the standard deviation of a given set of measurements by its respective mean (Equation 2.8).

$$RSD\% = \frac{STD}{\bar{x}} \times 100 \qquad (2.8)$$

Absolute and relative recovery

Recovery is a measurement of the efficiency of a sample extraction procedure. The absolute recovery is determined by comparing the area of an analyte in a pre-extraction matrix spiked sample with the response of the analyte in the post-extraction spiked sample (Equation 2.9)

$$Absolute\ recovery\ \% = \frac{A_{pre-ext.\ spike}}{A_{post-ext.\ spike}} \times\ 100 \qquad (2.9)$$

Where $A_{pre-ext.\ spike}$ is the area of the pre-extraction spiked analyte and $A_{post-ext.\ spike}$ is the area of the post-extraction spiked analyte.

The relative recovery is determined by comparing the ratio of samples that were spiked with target analytes prior to extraction with those that were spiked after extraction to the internal standard (Equation 2.9)

$$Relative\ recovery\ \% = \frac{RR_{pre-ext.\ spike}}{RR_{post-ext.\ spike}} \times\ 100 \qquad (2.10)$$

Where $RR_{pre-ext.\ spike}$ is the relative response of the pre-extraction spiked sample and $RR_{post-ext.\ spike}$ is the relative response of the post-extraction spiked sample

Matrix factor (MF) and matrix effects (ME)

Evaluating matrix effects is extremely important for LC-MS (and LC-MS/MS) analysis as coeluting compounds present in a matrix can impact ionisation efficiency and reproducibility, resulting in ion suppression or enhancement (Asimakopoulos et al., 2014a; Ito and Tsukada, 2002).

$$MF = \frac{Area_{post-ext.\ spike}}{Area_{Solvent\_10ppb}} \qquad (2.11)$$

The percentage matrix effect can then be expressed according to equation 2.12.

$$ME\ \% = (MF - 1) \times\ 100 \qquad (2.12)$$

Limit of detection and lower level of quantification

The limit of detection (LOD) and lower level of quantification (LLOQ) can vary within a sample due to matrix effects and needs to fit the purpose of the research and analytical method (Asimakopoulos et al., 2014a). In this thesis, the LLOQ of each compound was set the lowest concentration detected in the calibration curve and the LOD determined from Equation 2.13.

$$LOD = \frac{LLOQ}{3} \tag{2.13}$$

Internal standard method

Internal standards are compounds that are similar to a target compound, but not identical and as such are easily distinguishable from the target analyte. Deuterated or isotopically labelled forms of the target analyte are often used for this purpose (Wang et al., 2007). The internal standard method consists of using a calibration curve, constructed for every target analyte, from the ratio of the analyte response and the internal standard response in a set of standard solutions, plotted against the analyte concentration (Skoog, 2012). Validation criteria (i.e. accuracy and reproducibility) can be calculated in accordance to this ratio (Asimakopoulos et al., 2014).

2.2.5 Inductively Couple Plasma-Mass Spectrometry

Inductively coupled plasma mass spectrometry (ICP-MS) is a form of mass spectrometry that can detect metal and several non-metals at very low concentrations (e.g. parts per billion). ICP-MS allows for multi-elemental analysis, good precision and low detection limits, making it a powerful too in trace element analysis (Skoog, 2012).

2.2.6 Scanning Electron Microscopy

Scanning electron microscopy (SEM) is a technique useful for examining fine changes in surface morphology. SEM creates an image by scanning a focused beam of electrons over a samples surface. The electrons interact with the sample to produce various signals that provide information about surface topography. SEM can produce further focused and magnified images than tradition light microscopy as electrons have shorter wavelengths, allowing greater resolution (typically between 1 – 20 nm) (Egerton, 2016). Non-conductive samples (e.g. polymers) will build up electrostatic charge that interferes with the signals used to create an SEM image. To avoid charge build up in non-conductive materials are generally coated in a thin conductive layer of (often gold (Au) or platinum (Pt)) prior to imaging (Käppler et al., 2015).

2.2.7 ATR-FTIR

Fourier transform infrared (FT-IR) spectroscopy is an important technique for the identification of functional groups in a molecule. FTIR measures the range of wavelengths in the IR region that are absorbed by a sample, certain functional groups have characteristic absorbances. FT-IR spectroscopy can be used for compound identification in addition to examining phenomena such as degradation over time (Skoog, 2012). Attenuated total reflectance (ATR) FT-IR spectroscopy is a technique commonly used to examine the surface properties of materials rather than their bulk properties (Bokria and Schlick, 2002). The photooxidation of polymers results in an increase in carbonyl (C=O) and hydroxyl (-OH) groups in a majority of polymers, as such carbonyl and hydroxyl indices can be determined. Carbonyl index (CI) is the most commonly employed indicator in ATR-FTIR to measure the extent of chemical oxidation in polymers. It has mostly been employed in degradative studies on polyethylene and polypropylene and can be calculated according to equation 2.2 (Allen and Edge, 1992; Rouillon et al., 2016).

$$Carbony\ Index = \frac{Area_{C=O\ stretch}}{Area_{reference\ peak}} \tag{2.2}$$

Where the C=O stretch generally occurs between 1600 -1700 cm^{-1} and the reference peak is peak not impacted by degradation and varies in location based on the material of interest.

2.2.8 Dynamic light scattering

A Zetasizer system determines size distribution by measuring the Brownian motion of particles via dynamic light scattering (DLS). Brownian motion can be related to the size of the particles. (Malvern Instruments Ltd, 2009). The Zetasizer determines particle size by illuminating particles with a laser and analysing fluctuations in intensity. The Zetasizer contains a digital correlator, which measures similarities between two signals over a period of time to produce a correlation function. The rate of decay in the recorded correlation functions can be related to particle size. The rate of decay is faster for smaller particles and slower for larger particles. By using the determined correlation functions, a size distribution can be constructed based on decay rates (Malvern Instruments Ltd, 2009).

2.4 Statistics

2.4.1 Descriptive statistics

When performing any statistical analysis, the distribution of a dataset should be verified. This is an important first step, as the majority of statistical tests assume normal distribution. Log transformation can be performed to attain normality, although this is not always achievable. In the case of the latter non-parametric measures can be applied. Normal distribution can be confirmed through either visual inspection of histograms or the Shapiro-Wilk test (Shapiro and Wilk, 1965), where a given dataset is considered normal when the p-value is greater than 0.05 (De Veaux et al., 2018). Comparisons between more than one group can be performed using a one-way ANOVA for normal distributed data, or the Kruskal-Wallis H-test for non-normal data. To understand where the significance lies, pairwise comparisons can be performed using a Tukey HSD post-hoc test. If a dataset shows non-homogenous variance, the Games-Howell post hoc test is generally applied. For non-normal data, pairwise comparisons can be performed with the Dunn's tests (Weaver et al., 2017).

2.4.2 Correlation

Correlation is a measure of the degree of association between two variables. The strength of a correlation is related to its respective correlation coefficient (r). Generally, an R-value between 0.9 to 1 is considered a very high correlation, 0.70 to 0.89 a high correlation, 0.5 to 0.69 a moderate correlation and <0.5 a low correlation (Asuero et al., 2006). The p-value in the context of correlations, indicates the likelihood of a 'true' correlation, the higher the p -value ($p > 0.05$) the higher probability of it being a 'false' correlation (De Veaux et al., 2018).

2.4.3 Multivariate statistics

Principal component analysis (PCA) can be used to reveal trends within large datasets. This is achieved by reducing the data into two dimensions or principal components (PC), making it possible to visualise a dataset with multiple variables within the same plot. In two dimensional PCA plots, the first two PCs should describe as much variation as possible within a dataset (preferably over 70%) (Jolliffe and Cadima, 2016; Tabachnick and Fidell, 2013). By combining scores and loading plots it is possible to evaluate which variables or groups influence specific samples by examining the direction of the loading vectors (Tabachnick and Fidell, 2013).

3 Materials and Methods

3.1 Chemicals and materials

3.1.1 Chemicals

Analytical grade methanol (MeOH) was purchased from Merck (Darmstadt, Germany) and Sigma Aldrich (Steinheim, Germany). *N*-hexane and isopropanol (IPA) were supplied by Fluka Analytical (Steinheim, Germany). Analytical grade ethyl acetate and ammonium acetate was obtained from Sigma-Aldrich (Steinheim, Germany). Analytical grade dichloromethane (DCM) was supplied by Rathburn Chemicals (Walkerburn, UK). Concentrated nitric acid (UltraPure grade) was obtained by distillation with Milestone SubPur (Sorisole BG, Italy). Colourless Richard-Allan Scientific^{TM} Neg-50^{TM} frozen section medium (glycol solution) was purchased from Thermo Fischer Scientific. Corning$^{®}$ sterile nylon cell strainer (40 um) were purchased from Sigma-Aldrich (Steinheim, Germany). 37% Hydrochloric acid (HCl) and Sodium sulphate (Na_2SO_4) were purchased from Merck (Darmstadt, Germany). Aquarium sand (Rådassand, 0 - 0.5 mm) was obtained from a Tam Lade pet shop (Trondheim, Norway).

Seawater and freshwater media were used as exposure mediums in this study. Natural seawater was obtained from 80 m depth in the Trondheim fjord and sterile filtered (0.22 µm, Sterivex filtered). Freshwater media (TG 201) was prepared according to OECD Guideline 2011 (OECD, 2011), which can be found in Appendix C.

Antioxidants, UV and thermal stabilising additive standards (Chimassorb 81; Chimassorb119; Chimassorb 2020; Cyasorb UV-5411; Irgacure 369; Irgacure 1800; Irgacure 2959; Irgafos 38; Irgafos168; Irgafos P-EPQ; Irganox 1010FF; Irganox 1076; Irganox1081; Irganox B220; Irganox 1330; Irganox 1425; Irganox HP 2215; Tinuvin 234; Tinuvin 327; Tinuvin 328 and Tinuvin 622) were provided by SINTEF Industry, Oslo (no further details provided). Surrogate and recovery internal standards were made in house from naphtalene-*d*8, phenanthrene-*d*10, perylene-d12, chrysene-*d*12, acenaphtene-*d*10 and fluorene-*d*10 standards purchased from Sigma-Aldrich (Steinheim, Germany) and made up respective standards according to the composition detailed in Table 3.1. Water was purified with a Milli-Q grade water purification system (Q-option, Elga Labwater, Veolia Water Systems LTD, U.K.).

Table 3.1. Surrogate (SIS) and recovery (RIS) internal standards chemical content (µg/mL)

Standard ID	Chemical	Concentration (µg/mL)	Standard ID	Chemical	Concentration (µg/mL)
SIS A703	naphtalene-*d*8	25.1	RIS A705	acenaphtene-*d*10	10.6
	phenanthrene-*d*10	5.00		fluorene-*d*10	9.84
	perylene-*d*12	5.08			
	chrysene-*d*12	4.86			

Analytical standards of Bisphenol A (BPA), Bisphenol AF (BPAF), Bisphenol AP (BPAP), Bisphenol B (BPB), Bisphenol F (BPF), Bisphenol M (BPM), Bisphenol P (BPP), Bisphenol S (BPS), Bisphenol Z (BPZ), Benzophenone-1 (BzP-1), Benzophenone-2 (BzP-2), Benzophenone-3 (BzP-3), Benzophenone8 (BzP-8) and 4-Hydroxybenzophenone (4-OH BzP) were purchased from Sigma-Aldrich (Steinheim, Germany). Internal Standards: Bisphenol A $^{13}C_{12}$ (BPA $^{13}C_{12}$), Bisphenol S $^{13}C_{12}$ (BPS $^{13}C_{12}$), Bisphenol B $^{13}C_{12}$ (BPB $^{13}C_{12}$), Bisphenol AF $^{13}C_{12}$ (BPAF $^{13}C_{12}$), Bisphenol F $^{13}C_{12}$ (BPF $^{13}C_{12}$), were supplied by Cambridge Isotope Laboratories, Inc. (Massachusetts, United States).

3.1.2 Materials

Synthetic and natural fibres were supplied by the garment manufacturers: Helly Hansen; Pierre Robert Group (PRG) and Varner. Detailed specifications of the materials used in this project are provided in Table 3.2.

Table 3.2. Synthetic and natural fibre specifications

Fibre type	Supplier	Colour(s)	Density (g/mL)*
Polyester	Helly Hansen	black	1.387 ± 0.001
		white	1.339 ± 0.009
Polyamide	PRG	white	1.146 ± 0.006
Polyacrylonitrile, worsted	Varner	blue	1.178 ± 0.004
		pink	N/A
Polyacrylonitrile, carded	Varner	orange	1.170 ± 0.007
Wool	Helly Hansen	white	1.312 ± 0.004

*Determined by displacement of ethanol at 18.5 °C. n=2

3.2 Preparation of microplastic fibres

3.2.1 Scalpel method

Fibres were aligned by wrapping them around a custom manufactured spool as described by Cole (2016) and shown in Figure 3.1. The number of rounds varied between material. Wrapped fibres were coated with water-soluble glycol solution and frozen for 5-10 min at -80 °C. After freezing, fibres were manually cut with a scalpel to yield particles between 1 - 2.5 mm in length. The fibres were then added to Milli-Q grade water and placed in an oven at 60 °C for approximately 10 min to dissolve the glycol. The solution was filtered using a Duran® glass filtration apparatus through cellulose (0.45 µm) filters, rinsed with MilliQ, collected and dried at 40 °C for ~76 hours. The scalpel method was used to prepare 1-2.5 mm fibres for UV and mechanical degradation studies.

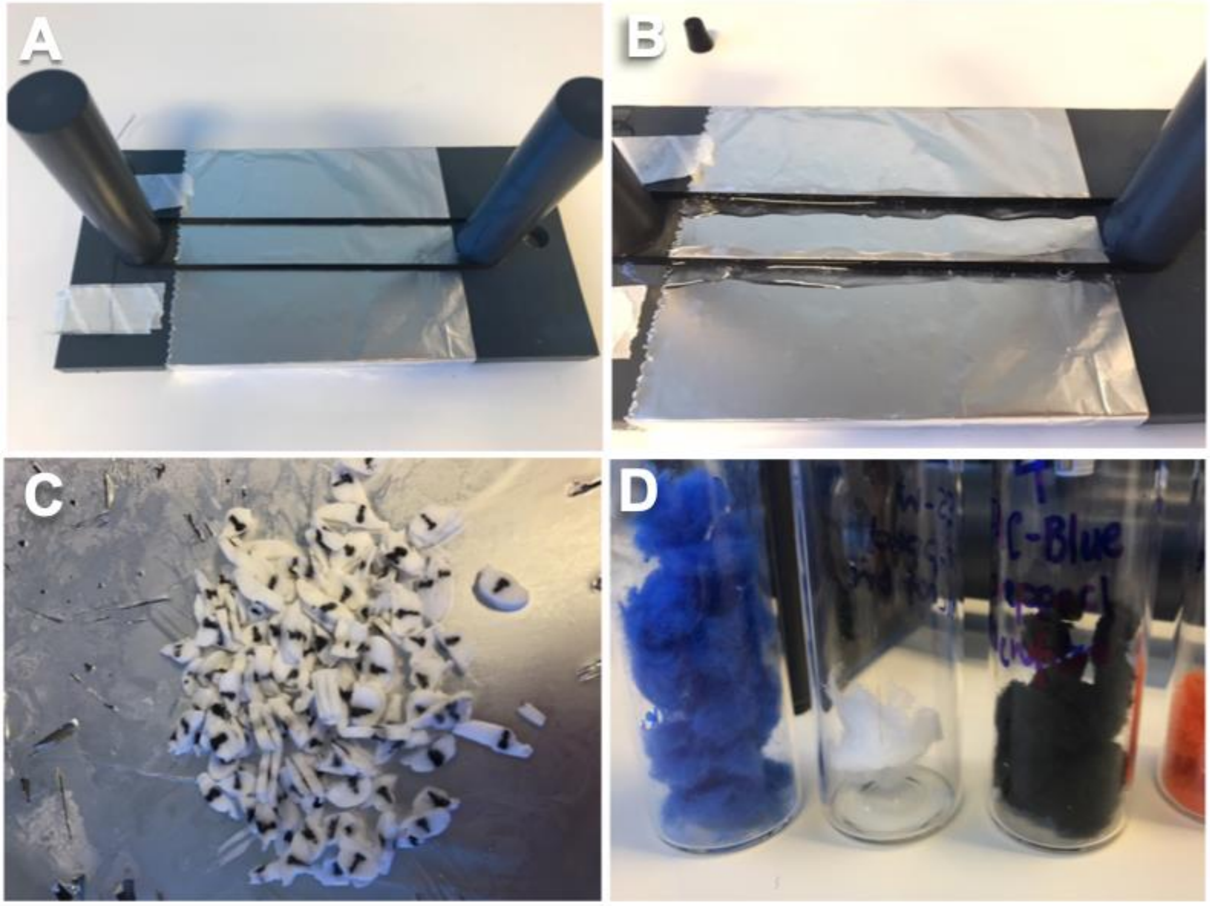

Figure 3.1. Preparation of 1 - 2.5 mm MPFs via the scalpel method. A: PET (Black) wrapped around custom made spool, B: PET coated in glycol solution prior to freezing, C: cut PET fibres in frozen glycol solution, and D: filtered and dried fibres stored in glass vials.

3.2.2 Scissor method

Using surgical scissors, fibres were prepared by manually cutting to approximately 5 mm and collecting them in a glass beaker with Milli-Q grade water. The fibres were filtered using a Duran® glass filtration apparatus with cellulose (0.45 µm) filters, collected and dried at 40 °C for ~76 hours. The scissor method was used to prepare 5 mm fibres for short leachate studies (as described in section 3.5).

3.3 UV exposure studies

3.3.1 Experimental set-up

MPF UV studies were conducted in seawater and freshwater median. UV exposure was performed using an Atlas Suntest CPS+ instrument fitted with a xenon lamp (1500 W) and daylight filter regulated at 300-400 nm. Single samples of 5 different MPFs (1 - 2.5mm), PET black, PET white, PA, PAN blue and PAN orange were prepared in 40 mL quartz tubes at a concentration of 1 mg MPF/mL. All MPF samples were irradiated in both freshwater media and seawater at 65 W/m^2. A detailed list of samples used in the experiment can be found in Appendix B (Table B.1.). The exposure temperature was 24 ± 3 °C inside the Atlas instrument. Samples were gently shaken by hand twice a week throughout the 9-month exposure period to ensure a relatively even level of UV exposure. Control samples were kept in the dark at room temperature (~ 20 °C) and shaken gently at the same frequency as the exposed samples. Sampling was conducted after ~5 months (153 days) and 9 months (292 days). Evaporation was dealt with by regularly replacing lost water.

After 5-month exposure, samples (~10 mg) were filtered through nylon filters (Corning® 40 µm). The filtrate was retained, and triplicate 2 mL samples were collected for analysis of additive chemical leaching. After sampling from the 40 mL quartz tubes, the entire volume was replaced with fresh aqueous media. The MPFs were rinsed with Milli-Q water and dried at 40 °C for ~76 hours. At 9-month exposure, a different sampling procedure was employed to maximise recovery of the smallest degradation products and avoid contamination of the filtrate (used for leachate analysis). Samples were filtered using a Duran® glass filtration apparatus through cellulose (0.45 µm) filters, rinsed with Milli-Q water and dried at 40 °C for ~76 hours. Leachate samples (2 mL) were collected in triplicate for subsequent sample processing and analysis via GC-MS (n=3) and LC-MS/MS (n=3).

Figure 3.2. UV exposed MPFs in Atlas Suntest CPS+ chamber. (From left to right: PET (white) in SW, PET (white) in FW, PET (black) in SW, PET (black) in FW, PAN (orange) in SW, PAN (orange) in FW, PA in SW, PA in FW, PAN (blue) in SW and PAN (blue) FW.

The total irradiance that MPFs were exposed to over 9-months was determined according to equation 3.1

$$\text{Total irradiance exposed} = \text{Intensity } [\mathrm{W/m^2}] \times \text{ hours of exposure } [\mathrm{h}] \qquad (3.1)$$

To determine the actual number of days relative to the total irradiance and the European mean irradiance equation 3.2 was used.

$$\text{Simulated days} = \frac{\text{Total irradiance exposed}}{\text{Mean European UV irradiance}} \times 365 \qquad (3.2)$$

Where European mean irradiance $\approx 1200\ \mathrm{kWh/(m^2 \cdot year)}$, 5% of which is considered UV light giving a mean UV irradiance of $60\ \mathrm{kWh/(m^2 \cdot year)}$ ((Gewert et al., 2018))

$$\text{Simulated days} = \frac{\text{Total irradiance exposed}}{\text{Mean European UV irradiance}} \times 365$$

$$\text{Total irradience exposed} = 65\mathrm{W/m^2} \times 24\ \mathrm{h} \times 291 \text{ days } (\sim 9 \text{ months}) = 453.96\ \mathrm{kWh/m^2}$$

$$\text{Simulated days} = \frac{453.96\ \text{kWh/m}^2}{60\ \text{kWh/m}^2} \times\ 365 = 2761\ \text{days}\ (\sim 7.5\ \text{years})$$

The 9 months UV exposure in this experiment therefore corresponds to 2761 days or ~7.5 years of sunlight exposure according to European mean solar irradiance.

3.3.2 Light microscopy

All light microscopy was performed using a Nikon Eclipse E200 microscope and post-processed in ImageJ® (Schneider et al., 2012). The scale was set according to the objective lens used and calibration using a stage micrometre slide. MPF lengths were measured manually using the measure function in ImageJ, with the use of either straight or segmented lines. At least 30 MPFs were measured in each sample and where images contained many MPFs, up to 250 individual fibres were measured. For statistical analysis, 30 measurements from each data set were randomly selected using a random number generator ("Random Integer Generator," 1998) to avoid sampling bias.

3.3.3 Data treatment

Statistical analysis of fragmentation data was conducted in GraphPad Prism version 8.02 for Mac. An ordinary one-way ANOVA was performed within textile groups (PET, PA, PAN) where data was normally distributed. In the case of non-normal data, the Kruskal-Wallis test was performed. For pairwise comparisons, Tukey HSD and Dunn's tests were employed for parametric and non-parametric tests, respectively.

3.3.4 Scanning electron microscopy

To examine changes in surface morphology of MPFs after UV exposure, a Zeiss Ultra 55LE field emission SEM (FEG-SEM, Carl Zeiss AG) was used. All samples were thinly coated with gold (Au) via low vacuum sputtering (Edwards S150b Gold sputter coater, Edwards, UK) prior to analysis to minimize charge build up. SEM images were captured under the following conditions: 2-10 kV accelerating voltage and 10 mm working distance. Images were captured at five different magnifications (100, 200, 500, 1000 and 2000) to allow for both an overview of the sample and a detailed view of the surface morphology. For samples that showed significant changes in surface morphology, additional images were taken at 5000x magnification. Scale bars were added in ImageJ®.

3.3.5 ATR-FTIR

To investigate changes in polymer composition of MPFs during degradation, ATR-FTIR analysis was carried out using a Bruker ALPHA ATR-FTIR spectrometer equipped with a diamond crystal. Three spectra were recorded at 4 cm^{-1} resolution with 47 scans for both pristine UV exposed MPF samples. Background subtraction, baseline correction and normalisation to a pre-determined reference peak were performed using OPUS software. The crystal and clamp were cleaned with isopropanol and air dried between each analysis. Carbonyl indices were calculated according to equation 3.1.

$$Carbony\ Index = \frac{Area_{C=O\ stretch}}{Area_{reference\ peak}} \tag{3.1}$$

3.3.6 Investigation of formation of nanosized plastic particles

To investigate the presence of nanosized particles, the size distribution of filtered UV leachates (5- and 9-months) were measured using a Zetasizer ZS (Malvern Instruments, UK). Three measurements consisting of 5 runs with 10 sec duration were performed with an initial 30 sec equilibration time. Data was analysed using Dispersion Technology Software v 5.00 (Malvern Instruments, UK).

3.4 Mechanical degradation

3.4.1 Experimental set-up

Mechanical degradation studies of black and white PET, white PA, blue and orange PAN, as well as white wool fibres (all 1 - 2.5mm) were performed in seawater with sand at two temperatures. Fibre samples were dispersed into seawater at a concentration of 1.5 mg MPF/mL (n=1) in 250 mL glass bottles with Teflon lined caps and placed in shaking incubators at either 5 or 20 °C with 5 g sand (total 12 individual samples, 6 at each exposure temperature) to simulate mechanical abrasion of fibres in a natural environment, a process also referred to as mechanical degradation. In addition, control samples (n=1), with only MPFs (including wool) and seawater were also shaken for the duration of the study at the same exposure temperatures (5 and 20 °C), including control samples without MPFs (seawater alone, and seawater and sand). The samples were shaken at a speed of 175 rpm (horizontal, circular motion). A detailed list of samples can be found in Appendix D (Table D.1). After 5 months, 10 - 40 mg of MPF was ‘fished out’ of the samples using tweezers, washed in Milli-Q water, dried at 40 °C for ~76 hours and photographed using traditional photography to investigate any changes. Length characterisation was attempted on 5-month samples, but not enough free fibres were present to allow for statistical analysis (i.e. $n < 30$). The main sampling and analysis were conducted after 9 months.

3.4.2 Sample collection after 9-month exposure via density separation

In a density separation, materials of dissimilar densities are placed in a liquid of intermediate density, where the less dense material (i.e. MPFs) will float and separate from the denser material (i.e. sand) (Quinn et al., 2017). Prior to working with the 9-month samples from the mechanical degradation studies, a density separation method using zinc chloride ($ZnCl_2$) as a density modifier for water was established and validated. First, $ZnCl_2$ was added in small increments to 100 mL of filtered seawater to determine the saturation point (~1.8 g/mL). Recovery tests were then performed with samples containing 150 mg of each MPF and wool in 100 mL seawater. $ZnCl_2$ was dissolved gradually in each MPF-SW sample (100 mL) over an ice bath and shaken vigorously for 60 seconds. Once the $ZnCl_2$ was fully dissolved, each sample was transferred to a separating funnel and left to settle for ~12 hours. After settling, the sand and roughly a quarter of the solution was removed through the bottom of the funnel (Figure 3.3). The remaining water sample with fibres were vacuum-filtered using a Duran® glass filtration apparatus through 20 μm metal filters, and the collected fibres washed with Milli-Q grade water, dried at 40 °C for 76 hrs and imaged. Free MPFs were imaged and measured under light microscopy according to section 3.3.2. MPF length before and after mechanical degradation were statistically analysed according to section 3.3.3.

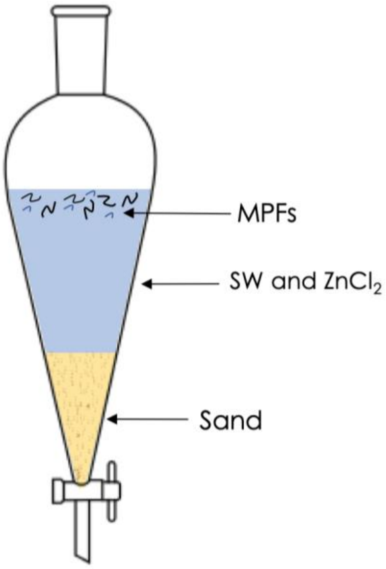

Figure 3.3. Schematic of density separation

3.5 Short-term leachate studies

In a preliminary study to determine an appropriate MPF concentration, leachates of the black and white PET, PA, blue and orange PAN MPFs, and wool were obtained by shaking 100 mg of MPF (including wool) (all 5 mm) in 200 mL seawater (0.5 mg MPF/mL) at 20 °C. Sampling was conducted after 14 days. Samples (2 mL) of each leachate was filtered through a 40 μm nylon filter and collected for further analysis. Samples were shaken on a Gerhardt shaking Table (horizontal, back and forth motion), at a speed of 8 (8 of 10, ~2-3 Hz). Preliminary results indicated that the leachate concentration was too low, and that the MPF concentration needed to be increased to allow investigation of the leachates.

The main short-term leachate studies were conducted at a concentration of 10 mg MPF/mL in filtered SW (5 and 20 °C) and TG201 as freshwater medium (20 °C), with control samples consisting of each media without fibres added. A detailed list of samples can be found in Appendix G (Table G.1). Exposure conditions were otherwise as described for the preliminary study. After 14 days, samples were filtered through 40 μm nylon filters and the particulate-free leachates retained for further analysis.

Leachate samples (2 or 15 mL) were prepared for GC-MS analysis using the LLE method described in section 3.8.2. Separate samples (3 mL) were prepared for LC-MS/MS analysis using LLE (as described in section 3.6.1). Samples for ICP-MS (1 mL) were prepared as described in section 3.10.2.

3.6 Bisphenol and benzophenone analysis

3.6.1 Sample preparation by liquid/liquid extraction (LLE)

A volume of 2 mL of the aqueous UV (5- and 9-months) and short-term (14 day) leachates were transferred to 15 mL polypropylene tubes. All samples were spiked with 10 μL of known IS (1ppm mix of BPA $^{13}C_{12}$, BPS $^{13}C_{12}$, BPB $^{13}C_{12}$, BPAF $^{13}C_{12}$, BPF $^{13}C_{12}$) before extraction, and 300 μL of 1M ammonium acetate and 3 mL of EtOAc added. Samples were vortex-mixed and ultrasonicated for 45 mins prior to centrifugation at 4000 rpm for 5 mins and the organic phase collected. This process was repeated twice more to yield ~9 mL of EtOAc extract. 1 mL Milli-Q grade water was added to each EtOAc extract to remove any excess salt, centrifuged at 4000 rpm for 5 min and the organic phase collected. Samples were evaporated under a gentle stream of N_2

to near dryness, reconstituted to 500 µL with MeOH, and transferred into a vial for LC-MS/MS analysis.

3.6.2 Sample preparation by solid/liquid extraction

Solid liquid extraction (SLE) was used to extract pristine MPFs (PET black, PET white, PA, PAN blue, PAN orange) and wool (N=3). For each material, 200 mg was inserted into 15 mL polypropylene tubes. All samples were spiked with 10 µL of known IS (1ppm mix of BPA $^{13}C_{12}$, BPS $^{13}C_{12}$, BPB $^{13}C_{12}$, BPAF $^{13}C_{12}$, BPF $^{13}C_{12}$) and 1 mL of 1M ammonium acetate and 3 mL of EtOAc added before extraction. Samples were vortex-mixed and ultrasonicated for 45 mins. After ultrasonication, samples were centrifuged at 4000 rpm for 5 mins and the organic phase collected. This process was repeated twice more to yield ~9 mL of EtOAc extract. 1 mL Milli-Q water was added to each EtOAc extract, centrifuged at 4000 rpm for 5 min and the organic phase collected. Samples were evaporated under a gentle stream of nitrogen to approximately 250 µL, and reconstituted to 500 µL with MeOH, and transferred to a vial for LC-MS/MS analysis (section 3.6.3).

3.6.3 LC-qQq-MS/MS analysis

BP and BzP analysis of pristine MPFs (including wool), and aqueous leachates (UV and short 14 day leachate studies) was performed using an Acquity UHPLC system (Waters, USA) equipped with column, flow through needle (FTN) and binary pump. Target analytes were separated on a Kinetex C18 column (30 x 2.1 mm, 1.3 µm) serially connected to a C18 Phenomenex guard column (4.0 mm x 2.1 mm, 1.3 µm) maintained at 30 °C. LC-grade water with 0.1% v/v ammonium hydroxide (A) and MeOH (B) were used for the elution of analytes. The total run time was 4 min. For the analysis of BPs and BzPs, separation was performed by gradient elution at a flow rate of 300 µL/min starting at 75% A, held for 3.4 min, decreased to 25% A, held for 2 min, then further decreased to 1% A, held for 30 seconds (3.5 min), and reverted to 75% A (3 min and 54 sec/3.9 min) and held for 6 sec, for a total run time of 4 min. Sample volume injected was 4 µL and the final in-vial composition of all samples and standard solutions were in MeOH. The mass spectrometer Xevo TQ-S triple quadrupole mass analyser (QqQ), with a ZSpray ESI function (Waters, USA) was operated in multiple reaction monitoring (MRM) mode. Electron spray ionisation was conducted in negative ion mode (ESI-) with capillary voltage −1.5 V, where ionisation and desolvation temperatures were 150 °C and 350 °C, respectively. Nitrogen was used as desolvation and cone gas, with flow rates of 150 L/hr and 650 L/hr respectively.

Analyte specific MS/MS parameter can be found in Appendix E (Table E.2). Prior to analysis, the cone was cleaned, a series of acetone blanks ran, followed by multiple injections of target analyte standard (mix of 10 ppb BPA, BPAF, BPAP, BPB, BPF, BPM, BPP, BPS, BPZ, BzP-1, BzP-2, BzP-3, 4-OH BzP and BzP-8) to saturate the cone.

3.6.4 Data treatment

LC-MS/MS data was acquired with IntelliStart and processed with MassLynx and TargetLynx software packages (v 4, Waters, USA). Residual data processing was performed in Excel.

3.7 Screening of antioxidant, UV and processing stabilising chemical additives

Additive stock solutions were prepared by adding ~2.5 mg of each additive standard (Chimassorb 81; Chimassorb119; Chimassorb 2020; Cyasorb UV-5411; Irgacure 369; Irgacure 1800; Irgacure 2959; Irgafos 38; Irgafos168; Irgafos P-EPQ; Irganox 1010FF; Irganox 1076; Irganox1081; Irganox B220; Irganox 1330; Irganox 1425; Irganox HP 2215; Tinuvin 234; Tinuvin 327; Tinuvin 328; Tinuvin 622) to 25 mL DCM. Irganox 1010FF and Irganox 1425 were made up in 50 mL due to difficulties dissolving at higher concentrations. All stock solutions were than diluted to 5 µg/mL and analysed via GC-MS according to section 3.8.3.

3.8 Non-target analysis of chemical additives

3.8.1 Sample preparation by solid-liquid extraction (SLE)

Initial polymer extractions were performed using ~100 mg of each yarn (black and white PET, PA, blue and orange PAN) and wool. Samples were added to 12 mL Kimax® glass tubes and extracted with 4 mL of either hexane, DCM, IPA, EtOAc and MeOH, respectively. Samples were ultrasonicated for 30 min at temperatures below each solvents' boiling point (Table 3.3). After ultrasonication, extracts were filtered through a glass pipette packed with Bilsom cotton and a small amount of anhydrous Na_2SO_4 into a glass tube. IPA, EtOAc and MeOH samples were evaporated under a gentle stream of N_2 to dryness and the solvent replaced with DCM. Hexane and DCM samples were evaporated under the same conditions to ~200 µL, as they can be analysed directly in the GC-MS. Kimax® glass tubes were washed three times with DCM, transferred to a GC vial and evaporated down to a final volume of 400 µL. RIS-A705 (100 µL) was added before GC-MS analysis. After investigation of the resulting chromatograms, polymer extractions were repeated in triplicate using both DCM and EtOAc. SIS A703 (100 µL) was added to each sample prior to the addition of solvent to allow for semi-quantification.

Table 3.3. Solvent boiling points and ultrasonication conditions

Solvent	Boiling Point (°C)	Temperature of ultrasonication (°C)
DCM	39.6	Room temperature
MeOH	64.7	45
Hexane	68.0	50
EtOAc	77.1	60
IPA	82.5	70

3.8.2 Sample preparation by liquid-liquid extraction (LLE)

Samples (2 or 15 mL) of aqueous leachate from UV exposure studies (after 5- and 9-months) was transferred to a glass tube and pH adjusted to approximately 2 using 15% HCl. All samples were spiked with SIS-A703 (100 µL) before extraction, and a volume (1 mL for 2 mL samples, 5 mL for 15 mL samples) of DCM:*n*-hexane (1:1 v/v) added. Samples were vortexed for 1 minute followed by centrifugation for 2 min at 2000 rpm, and the organic phase collected. Addition of solvent, vortex and centrifugation was repeated twice. A small amount of anhydrous Na_2SO_4 was added to each solution to remove any water. Samples were vortexed and centrifuged for 2 min at 2000 rpm, the organic phase collected and the remaining Na_2SO_4 was washed 3 times with 500 µL DCM. Samples were evaporated under a gentle stream of N_2 to ~500 µL, glass tubes were washed three times with DCM, transferred to a GC vial and evaporated down to a final volume of 400 µL. RIS A705 (100 µL) was added before GC-MS analysis.

3.8.3 GC-MS analysis

All non-target samples (polymer extractions of MPFs and wool, UV leachates and short-term 14-day leachates) were analysed by an Agilent 7890A GC equipped with an Agilent 5975C Mass Selective Detector (MSD). The inlet was set to 250 °C, the transfer line to 300 °C, the ion source to 230 °C and the quadrupole to 150 °C. The carrier gas was helium, at a constant flow of 1.1 mL/min. 1 µL of sample was injected via spitless injection. An Agilent DB5MS ultra-inert column (30 m, 0.25 µm film thickness, 0.25 mm internal diameter) was used and the GC oven was held at 40 °C (2 minute), ramped by 6 °C/min to 320 °C (20 min hold). Mass spectra were recorded from 50-500 m/z after a 12 min hold time.

3.8.4 Data treatment

GC chromatograms and mass spectra were recorded in Chemstation software, further investigated using MassHunter Unknowns Analysis ("Unknowns") and exported to csv format for further processing using R (R Core Team, 2017). After initial inspection of chromatograms in MassHunter Qualitative Analysis B.07.00, peaks were deconvoluted in Unknowns software and best hits from the NIST 14 library were extracted (IST Standard Reference Database 1A v14). In R, compounds were filtered based on their observed presence in at least 2 of 3 replicates and >80 % match to NIST 2017 library mass spectra. Further filtering was performed in Microsoft Excel to remove duplicates.

3.9 Pyrolysis-GC-MS

3.9.1 Analysis of pristine MPFs

Samples of pristine MPFs (black and white PET, PA, blue and orange PAN) were analysed directly without any pre-treatment except rinsing of the pristine MPFs in Milli-Q grade water and drying. The samples (a few mm of each, corresponding to 0.5 - 1.0 mg) were placed in a 45 µL glass micro scale sealed vessel (MSSV) and subsequently sealed. An Agilent 7890A GC coupled to an Agilent 5975C MS, fitted with a ZB5MSplus column (60 m x 0.25 mm x 0.25 µm) and an EI source operated at 230 °C and 70 eV was applied for the analysis. The carrier gas was helium (grade 6.0) at a constant flow rate of 1.0 mL/min. The instrument was fitted with a pyrolysis oven, which had a maximum operating temperature of 625 °C. The sample was introduced into the pyrolysis chamber at 230 °C, and the chamber temperature increased to the final temperature (600 °C) and held for 2 minutes, before the vial was manually broken, and the analytes released into the cold trap. The GC temperature was held at 40 °C (2 min), ramped to 90 °C at 5 °C/min (12 min hold), then ramped up to 300 °C and held (49 mins). The MS was operated in full scan mode (m/z 50-500), spectra recorded using MassHunter GC-MS software and peaks tentatively identified based on match to NIST libraries.

3.10 Elemental analysis

3.10.1 Sample preparation of MPFs

Samples of MPFs (black and white PET, PA, blue and orange PAN) and wool were prepared for elemental analysis by weighing 150 - 250 mg of each MPF (N=3) into 18 mL PTFE-Teflon vials and adding 6 mL 50 vol% HNO_3 (UltraPure grade). Sample digestion was carried out in a high-pressure microwave system (Milestone UltraClave, EMLS, Leutkirch, Germany) according to a temperature profile which increases gradually from room temperature to 250 °C over 1 hr at a constant pressure of 160 bar, as shown in Appendix F (Table F.1). Digested samples were diluted to 60 ± 3 mL with ultrapure water to achieve a final HNO_3 concentration of approximately 0.6 M, and subsequently transferred to polypropylene vials for ICP-MS analysis.

3.10.2 Sample preparation of water leachates

Leachate samples (1 mL) from the 14-day leachate study was diluted to 15 ± 3 mL and acidified with 6 drops of 50% v/v nitric acid (HNO_3) before analysis via ICP-MS.

3.10.3 ICP-MS analysis

Elemental analysis was performed using a Thermo Finnigan model Element 2 ICP-HR-MS (Bremen, Germany) equipped with a SC2 DX auto-sampler and UPLA filter, applying a SC-FAST flow injection analysis system (Elemental Scientific, Omaha, USA). The instrument was calibrated using 0.6 M HNO_3 solutions of multi-element standards (Elemental Scientific). The calibration curve consists of five different concentrations made from multi-element standards. Detection limits (DL) were based either on three times the standard deviation of the blanks, or on the instrument detection limits (IDL). Detection limits are given Table F.2. (Appendix F). The IDL was determined from concentration equal to 25 % RSD at three scans and based on the sample amount analysed. Results of leachates were corrected for reagent blank values. Where the concentrations of metals were below the DL in >50% of samples, the metal removed from the dataset. When analysing the 14-day leachates only 42 elements were included based on the preliminary screening. Results were corrected for dilution and the blank values subtracted where relevant.

4 Results and Discussion

4.1 Initial characterisation of synthetic fibres and wool

In the following, an initial characterisation of the study materials is briefly presented.

4.1.2 Structural confirmation of textiles types

Polymer composition of the MPFs was confirmed via ATR-FTIR analysis and FTIR spectra of PET, PA and PAN MPFs are presented in Figures 4.1, 4.2 and 4.3, respectively. The FTIR spectrum for pristine black PET is shown in Figure 4.1. The spectrum of PET has characteristic peaks at 2915, 1712, 1406, 1238, 1088, 870 and 721 cm^{-1}. The peak at 2915 corresponds to C-H stretching. The strong band at 1712 cm^{-1} corresponds to carbonyl (C=O) stretching. Strong bands at 1238 and 1088 are attributed to C-O stretching. The weak C=C stretching, C-C out of plane bending and intense C-H bending vibrations of the benzene rings appear at 1406, 870 and 721 cm^{-1}, respectively (Ioakeimidis et al., 2016; Parvinzadeh and Ebrahimi, 2011). The spectrum was compared to reference spectra to verify its identify as PET (Vahur et al., 2016). White PET MPF showed the same characteristic peaks, with small variations in absorbance (Appendix A, Figure A.1).

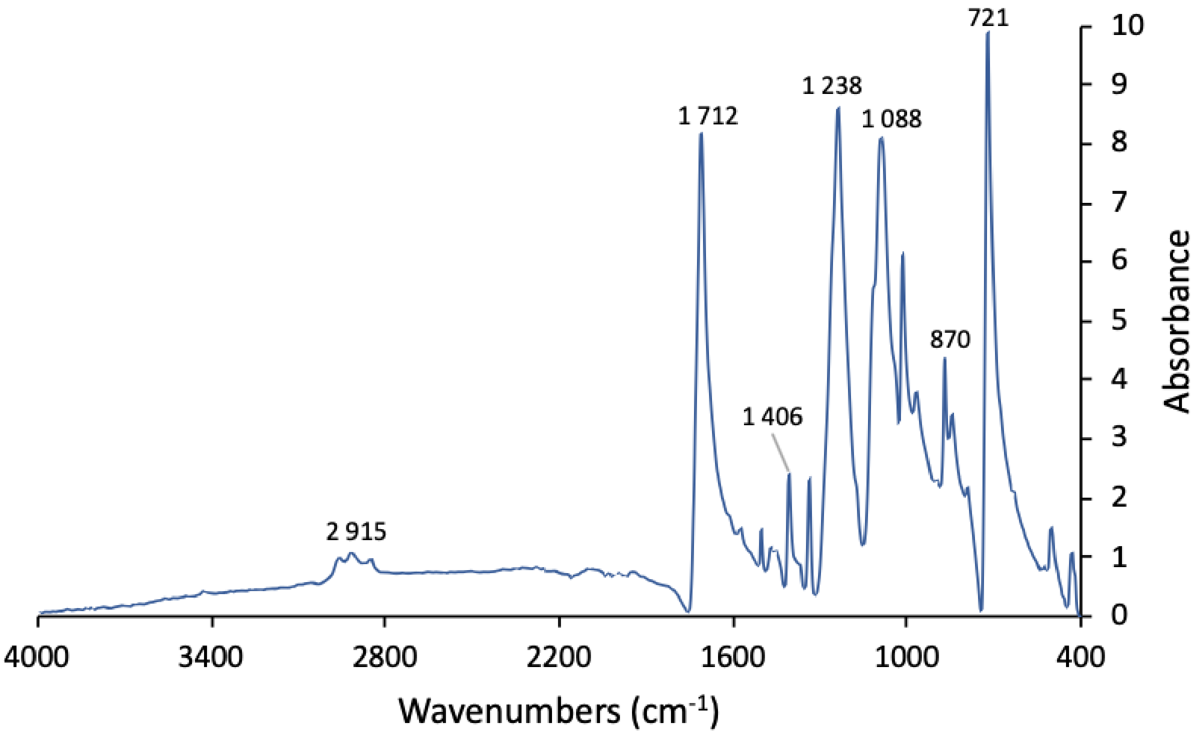

Figure 4.1. FTIR spectrum of pristine black PET

The FTIR spectrum for pristine PA fibre is presented in Figure 4.2. The spectrum of PA has characteristic peaks at 3285, 3075, 2934, 2860, 1632, 1526 and 930 cm^{-1}. The bands at 3285 and 3075 cm^{-1} are attributed to NH stretching and NH angular deformation, respectively. Peaks at 2934 and 2860 cm^{-1} are assigned to CH_2 asymmetric and symmetric stretching, respectively. The band at 1631 cm^{-1} corresponds to carbonyl (C=O) stretching. In plane N-H deformation is attributed to the band at 1529 cm^{-1}. Lastly, the band at 930 cm^{-1} corresponds to C-O stretching in the crystalline phase of the polymer. (Porubská et al., 2012) Characteristic peaks confirm the identify of PA (Vahur et al., 2016).

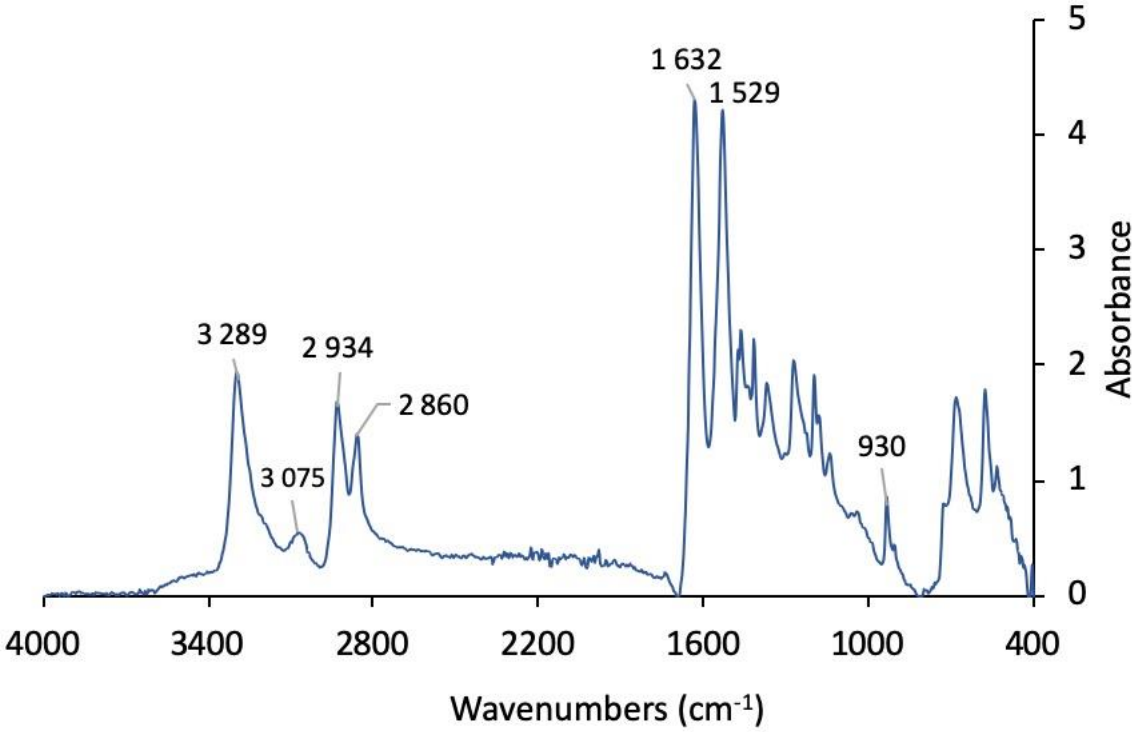

Figure 4.2. FTIR spectrum of pristine PA

The FTIR spectrum for pristine orange PAN MPF is presented in Figure 4.3. The spectrum of PAN has characteristic peaks at 2921, 2851, 2240, 1733, 1624, 1449, 1367, 1230 and 1039 cm^{-1}. The bands at 2921 and 2851 are attributed to C-H stretching. The band at 2240 cm^{-1} is assigned to the nitrile (C≡N) stretching. As previously stated, PAN is often polymerised with the addition of a vinyl comonomer to improve fibre processability. The moderate C=O stretching and C=C stretching vibration of the vinyl co-monomer appear at 1733 and 1624 cm^{-1}, respectively. Characteristics from aliphatic CH groups along the PAN backbone appear at 1449 (in plane deformation of CH (δ_{C-H} in CH_2) and 1367 cm^{-1} (δ_{C-H} in CH), respectively. The moderate peak at 1039 cm^{-1} may be attributed to 1,2,3-propantriol, a plasticiser used during fibre spinning of

PAN (Ribeiro et al., 2015). Characteristic peaks confirms the identify of PAN fibre (Vahur et al., 2016). Blue PAN MPF shows the same characteristic peaks, with some variations in absorbance. (Appendix A, Figure A.2)

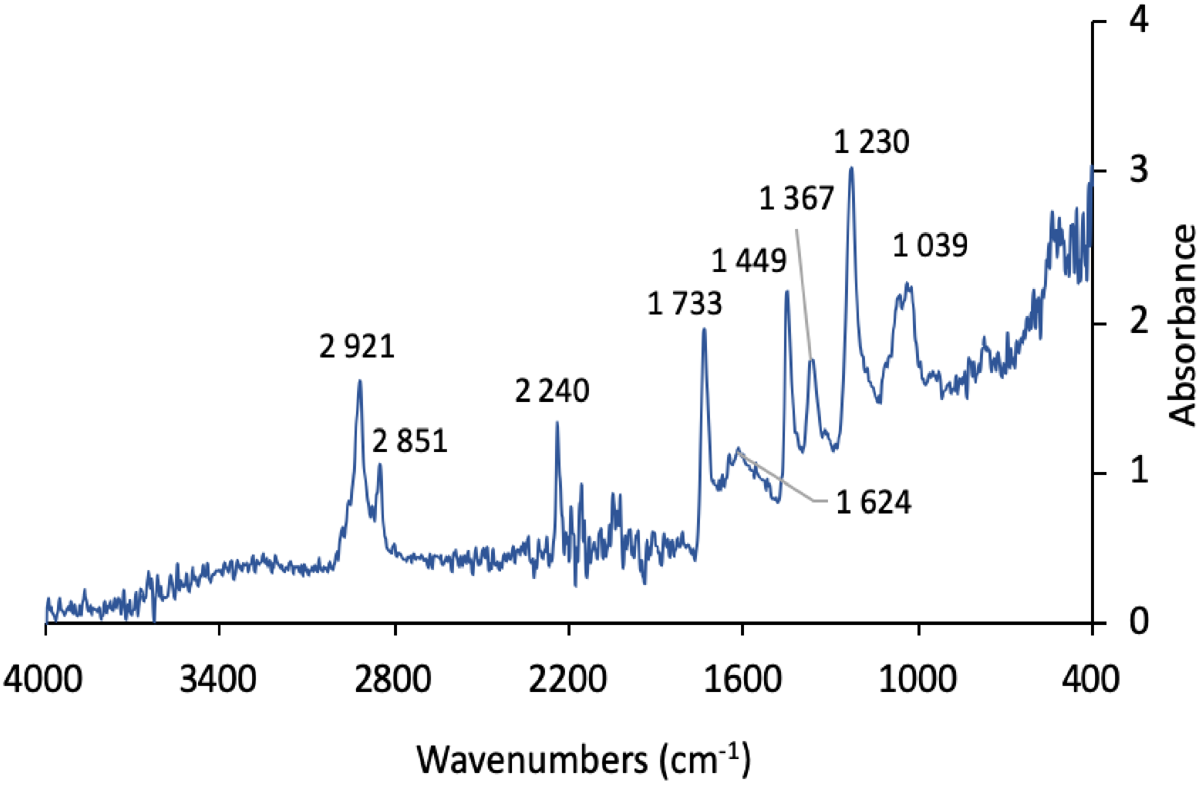

Figure 4.3. FTIR spectrum of pristine PAN orange

4.1.3 Characterisation of synthetic fibres by pyrolysis GC-MS

Each MPF sample (black and white PET, PA, blue and orange PAN) were pyrolysed at 600 °C for initial characterisation of MPF structure and any potential additives. MPF identity was further validated by comparing pyrograms to those published in the Pyrolysis-GC-MS data book of synthetic polymers (Tsuge et al., 2011). Published pyrograms are based on literature collected from pyrolysis studies at pyrolysis temperatures ranging from 600 - 1000 °C. Not all peaks classified in Tsuge et al., (2011) for the following MPFs were able to be identified in this chromatogram, which is possibly attributed to the lower pyrolysis temperature (600) used in the current study, this due to limitations of the available instrumentation. The pyrogram of black PET MPF is presented in Figure 4.4. The pyrogram displays seven characteristic peaks at 3.02, 5.06, 10.91, 22.47, 25.23, 27.73 and 28.83 min, respectively. Peak assignments are displayed in Table 4.1 Characteristic peaks are consistent with data on the pyrolysis of PET at 600 °C

(Sugimura and Tsuge, 1979). White PET shows the same characteristic peaks, with some variations in intensity (Appendix A, Figure A.3).

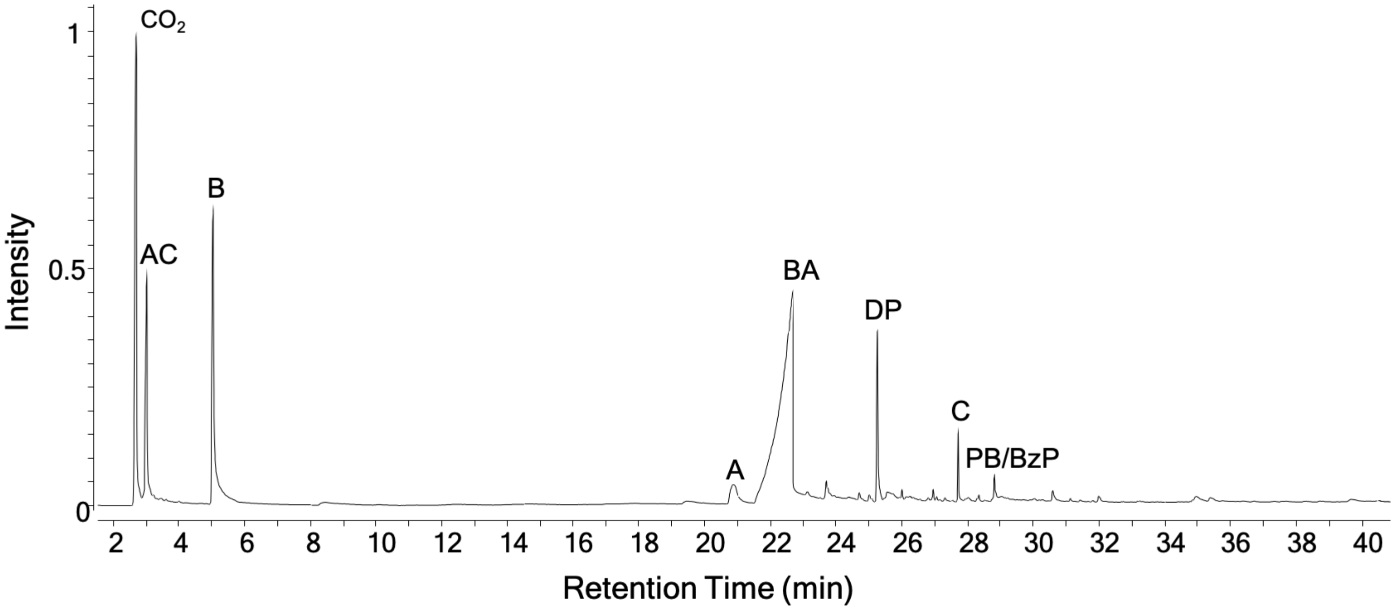

Figure 4.4. Pyrogram of black PET, pyrolysed at 600 °C

Table 4.1. Assignment of main peak in pyrogram for PET MPF

Abbreviation	Peak Assignment	Molecular Weight	Retention time (min)
CO_2	Carbon dioxide	244	2.66
AC	Acetaldehyde	44	3.02
B	Benzene	78	5.06
A	Vinyl benzoate	148	20.91
BA	Benzoic acid	122	22.47
DP	Diphenyl	154	25.23
C	Divinyl terephthalate* CH_2=CHOCOCC$_6$H$_4$COOCH=CH2	218	27.73
PB/BzP	Phenyl benzoate* C_6H_5-C_6H_4COOH	198	28.83

* Where C_6H_5 represents phenyl group; C_6H_4 represents p-phenylene group (Tsuge et al., 2011)

The pyrogram of PA is presented in Figure 4.5. The chromatogram displays two identified peaks at 8.95, and 32.06 min, respectively (Table 4.2). Peak assignments are displayed in Table 4.2. Many high intensity peaks could not be identified but may be attributed to the presence additive chemicals or degradation products that are not available in the NIST library. PA was challenging to analyse via py-GC-MS with replicate samples showing variations between pyrograms. It is unclear as to why this occurred. The presence of CP and NA6 in the pyrogram, in combination with FTIR data were considered enough to confirm the material as nylon 6,6.

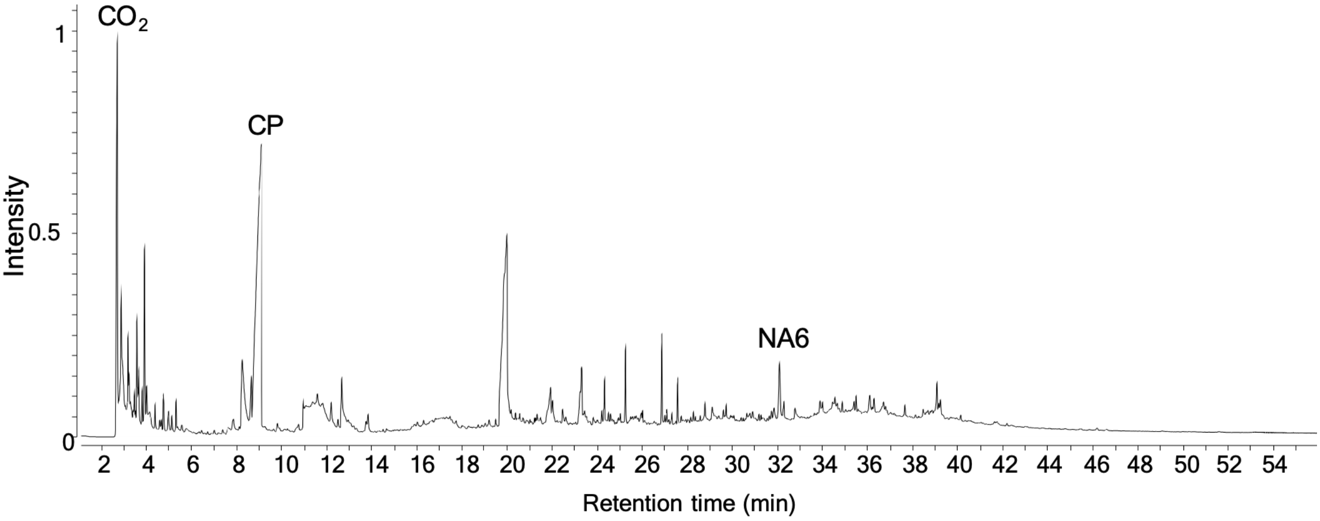

Figure 4.5. Pyrogram of PA MPF, pyrolysed at 600 °C

Table 4.2. Assignment of main peak in pyrogram for PA MPF

Abbreviation	Peak Assignment	Molecular Weight	Retention time (min)
CO_2	Carbon dioxide	44	2.45
CP	Cyclopentanone	84	8.95
NA_6	$CH_2=CH(CH_2)_4NHCO(CH_2)_4CN$	208	32.06

The pyrogram of Blue PAN MPF is presented in Figure 4.6. The chromatogram displays 5 characteristic peaks at 3.63, 4.29, 19.07, 27.89 and 29.59 min, respectively. Peak assignments are displayed in Table 4.3. Characteristic peaks are consistent with data on the pyrolysis of PAN at 600 °C (Yamamoto et al., 1972), confirming the identity of PAN. Orange PAN shows the same characteristic peaks in its pyrogram, with some variations in intensity (Appendix A, Figure A.4).

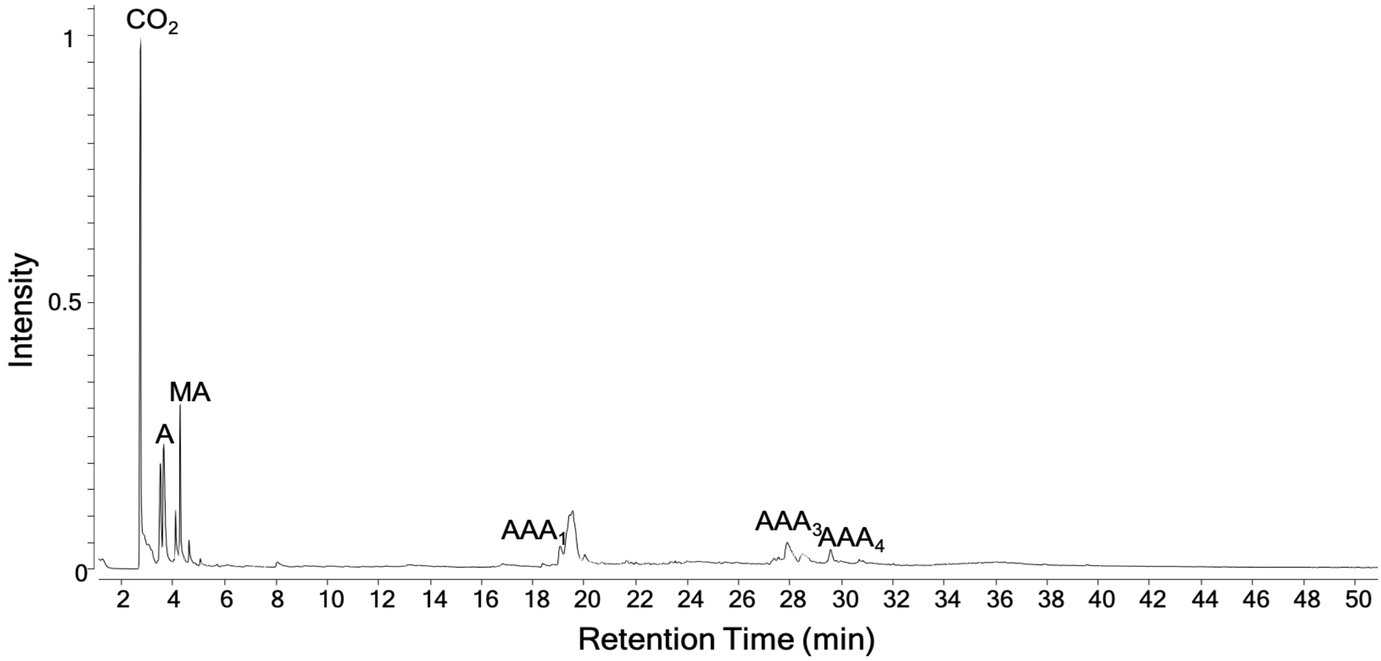

Figure 4.6. Pyrogram of blue PAN MPF, pyrolysed at 600 °C

Table 4.3. Assignment of main peak in pyrogram for PAN MPF

Abbreviation	Peak Assignment	Molecular Weight	Retention time (min)
CO_2	Carbon dioxide	244	2.78
A	Acrylonitrile (monomer)	53	3.63
MA	Methyl acrylonitrile	67	4.29
AAA_1	C=C(CN)-C-C(CN)-C-C-CN (trimer)	159	19.07
AAA_3	C(CN)-C-C(CN)-C-C-CN (trimer)	147	27.89
AAA_4	C-C(CN)-C-C(CN)-C=C-CN (trimer)	159	29.59

4.1.4 Characterisation of inorganic content of synthetic fibres and wool

Figure 4.7 displays the concentrations of a selection of elements detected in MPFs (including wool). A full Table of detected elements in MPFs and wool can be found in Appendix F (Tables F.3 and F.4) Elemental concentrations in MPFs were lower than reported by other studies (Table 4.4). In general, higher metal content was found in wool samples, relative to MPFs. Animal and human hair are accumulative bioindicators for metal pollution, which may explain the higher concentrations observed in wool fibres (Aydin, 2008; McLean et al., 2009). Wet processing, a finishing technique in textile manufacturing involves bleaching, printing and dying and can be a source of metals in textiles, where Cobalt (Co), Chromium (Cr), Copper (Cu) and Nickel (Ni) are often components of textile dyes (Menezes et al., 2010). In MPFs (including wool), Ni was present in the highest concentration in coloured PAN fibres, likely attributed to its use in dyes. Titanium in the form of TiO_2 is used in the manufacture of synthetic textiles as a delustering agent, for matting and gloss reduction, which explains its higher concentration in MPFs and lower concentration in wool. TiO_2 is a known radical producer and may impact a materials susceptibility to photodegradation (Barker, 1975). Antimony (Sb) was found at high levels in PET and PA, respectively. Sb in the form of antimony oxide (Sb_2O_3) is used as a catalyst in the production of PET, which accounts for the higher levels present in the PET samples (Haldimann et al., 2013). Sb is used synergistically along with various flame-retardants, which may explain the high levels identified in PA (Horrocks, 2008). PA showed high levels of Manganese (Mn) relative to other MPFs, but the source of Mn in the production of PA remains unclear. Heavy metals Cd, Cr, Hg and Pb were present in low concentrations across all MPFs (including wool). The Oeko-Tex Standard 100 is an international certification system for textiles, limiting the use of certain inorganic and organic chemicals and is considered an important standard within Europe (Sungur and Gülmez, 2015a). All heavy metals in Figure 4.9 were below the limit values for textiles suggested by Oeko-Tex Standard 100 (Table 4.5) .

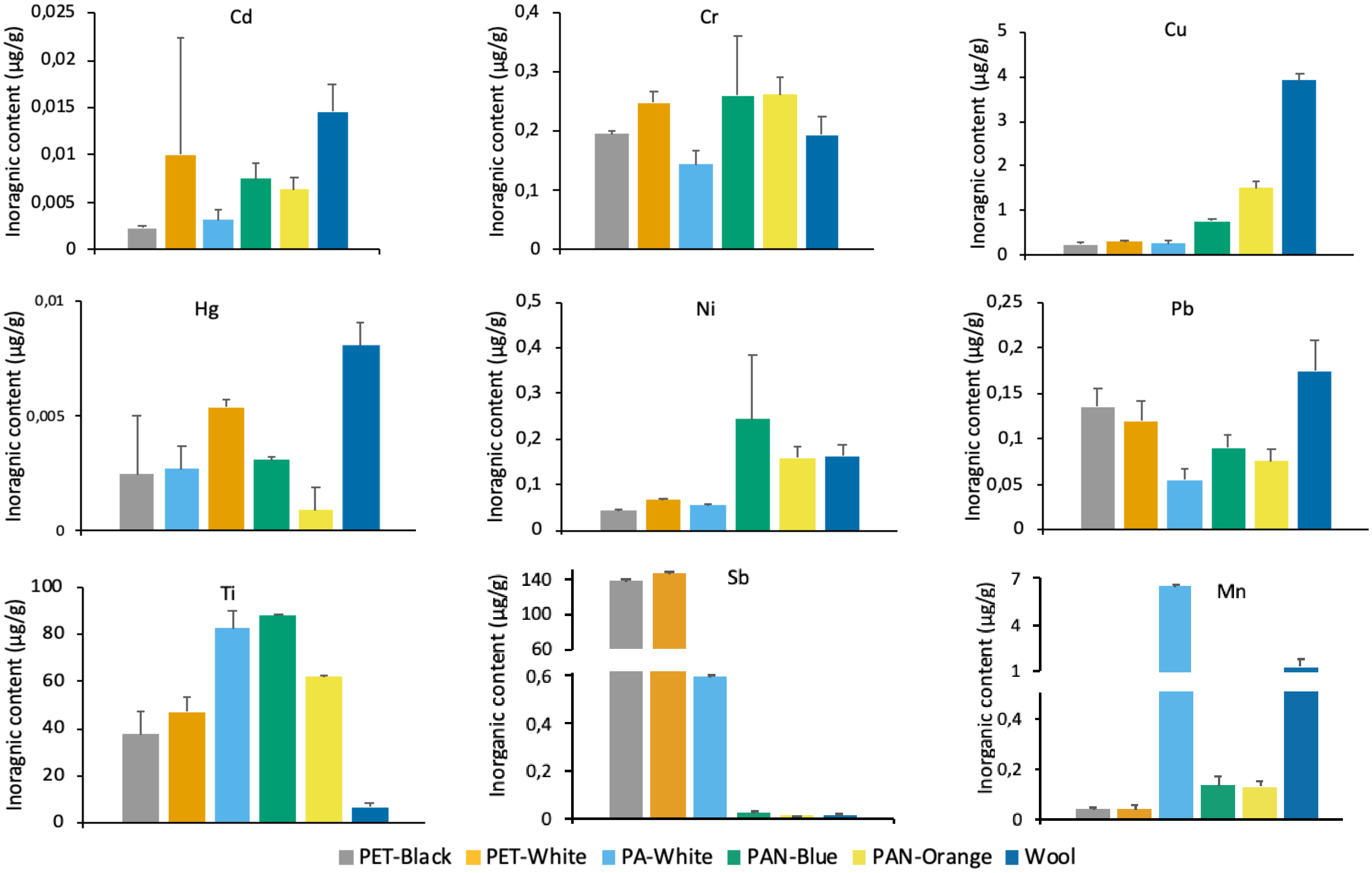

Figure 4.7. Mean concentration of select metals in MPFs and wool (N=3). Error bars show standard deviation.

Table 4.4. Literature values of trace metals (μg/g) in textile samples*

Literature	Metals	PET	PA	PAN	Wool
Saracoglu et al., (2003)	Cu	n.d. – 0.36	n.d.– 0.48	—	—
	Fe	0.23 – 28.90	3.42 – 29.90	—	—
	Ni	0.29 – 3.63	0.76 – 3.63	—	—
	Pb	n.d.– 0.76	0.31 – 3.76	—	—
	Zn	0.90 – 4.70	n.d.– 0.90	—	—
Doğan et al., (2002)	Cu	0.04 – 0.34	0.04 – 0.32	—	—
	Ni	0.20 – 0.24	0.24 – 0.26	—	—
	Pb	0.05 – 1.08	1.08 – 2.50	—	—
	Cr	n.d.– 0.42	n.d.	—	—
	Zn	0.92 – 4.04	0.14–0.92	—	—
	Co	0.08 – 0.16	0.12 – 0.16	—	—
Rezić and Steffan, (2007)	Cu	0.05	—	—	—
	Mn	1.17 – 2.1	—	—	—
	Ni	0.08	—	—	—
Sungur and Gülmez, (2015)	Cd	7.94 – 8.98	5.45 – 6.45	5.81 – 6.61	—
	Cr	0.72 – 0.80	0.67 – 0.75	0.66 – 0.74	—
	Cu	4.70 – 5.30	3.11 – 3.5.1	3.63 – 4.07	—
	Fe	63.36 – 71.56	51.17 – 57.79	74.92 – 74.58	—
	Mn	0.96 – 1.10	1.06 – 1.20	1.48 – 1.62	—
	Ni	1.90 – 2.16	1.77 – 2.01	1.48 – 1.68	—
	Pb	18..69 – 20.11	19.06 – 21.61	17.69 – 19.99	—
Rezić et al., (2011)	Cr	—	—	—	3.1
	Cu	—	—	—	—
	Fe	—	—	—	19.3
	Ni	—	—	—	2.3
	Pb	—	—	—	0.7
	Zn	—	—	—	n.d.
Current study	Cr	0.002 – 0.022	0.002 – 0.004	0.005 – 0.01	0.012 – 0.018
	Cu	0.23 – 0.35	0.20 – 0.32	0.71 – 1.66	3.75 – 4.07
	Fe	2.60 – 2.44	2.45 – 2.53	8.57 – 10.13	17.06 – 22.31
	Mn	0.03 – 0.05	6.47 – 6.60	0.10 – 0.18	0.83 – 1.78
	Ni	0.04 – 0.07	0.05 – 0.06	0.10 – 0.39	0.14 – 0.19
	Pb	0.04 – 0.07	0.053 – 0.063	0.10 – 0.385	0.137 – 0.986
	Zn	0.624 – 1.03	0.46 – 1.20	8.02 – 24.60	100.81 – 102.78

*Where "n.d." indicates not detected and "—" indicates not included in study

Table 4.5. Limits for heavy metals suggested by Oeko-Tex Standard 100 for textiles

Element	Amount (µg/g)
Sb	30
Cd	0.1
Cr	1.0 – 2.0
Co	1.0 – 4.0
Cu	25 – 50
Pb	0.2 – 1.0
Ni	1.0 – 4.0
Hg	0.02

4.2 Preparation of MPFs

4.1.1 Visual characterisation of MPFs

PET, PA and PAN MPFs were visually characterised via light microscopy after scalpel preparation into 1 - 2.5 mm MPFs (Figure 4.8). MPFs (including wool) were prepared to a similar size range to those collected from a washing machine after washing a fleece textile for environmental relevance (Figure 4.9). In addition, 5 mm fibres were prepared for short leachate studies but could not be imaged with light microscopy to show their entire length.

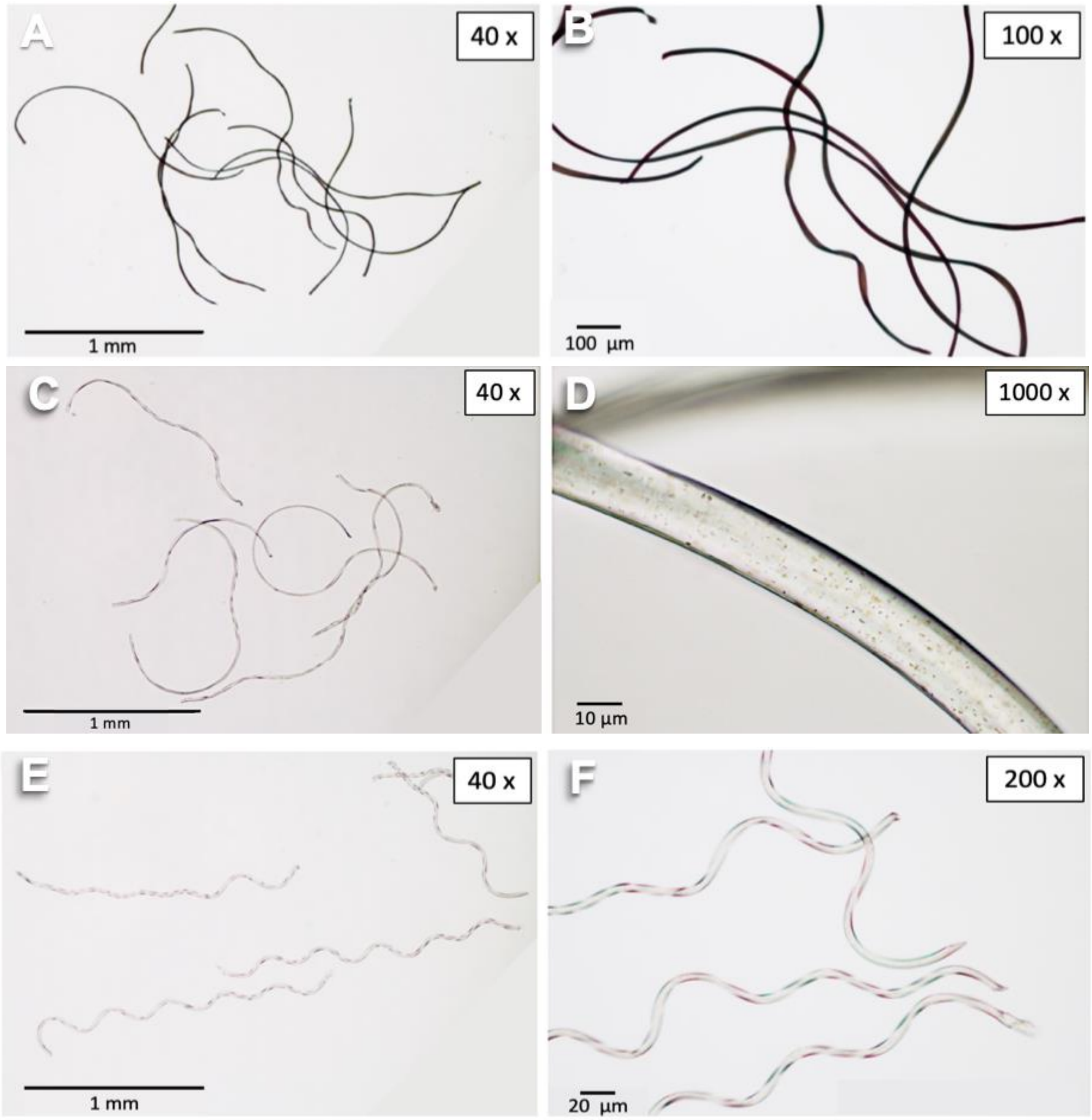

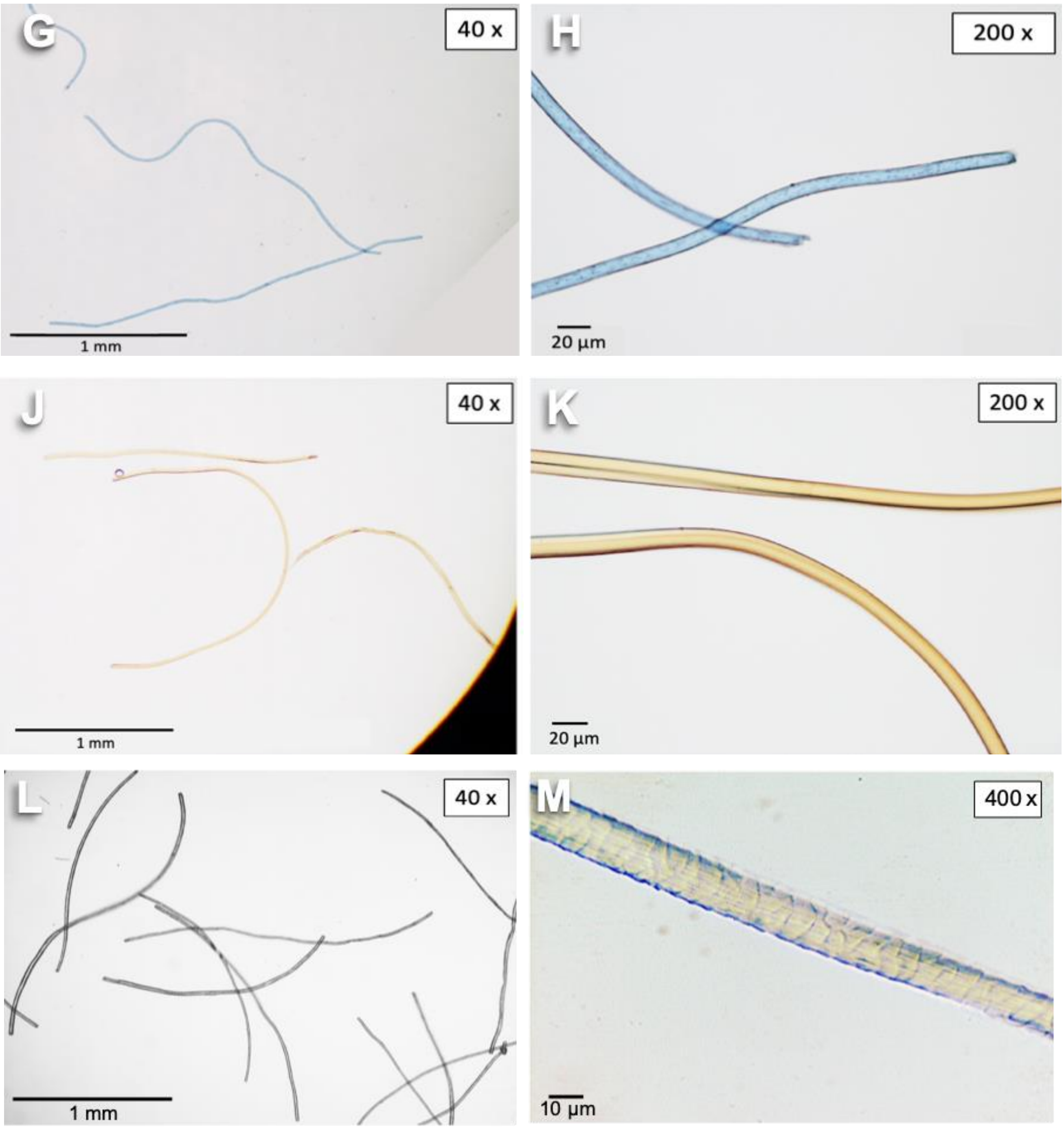

Figure 4.8. Light microscopy images of MPFs. Where: A and B show black PET at 40x and 100x magnification, respectively; C and D show white PET MPF at 40x and 1000x magnification, respectively; E and F show white PA MPF at 40x and 200x magnification, respectively; G and H show blue PAN MPF at 40x and 200x magnification, respectively; J and K shown orange PAN MPF at 40x and 200x magnification, respectively and L and M showing wool fibre at 40x and 400x magnification, respectively.

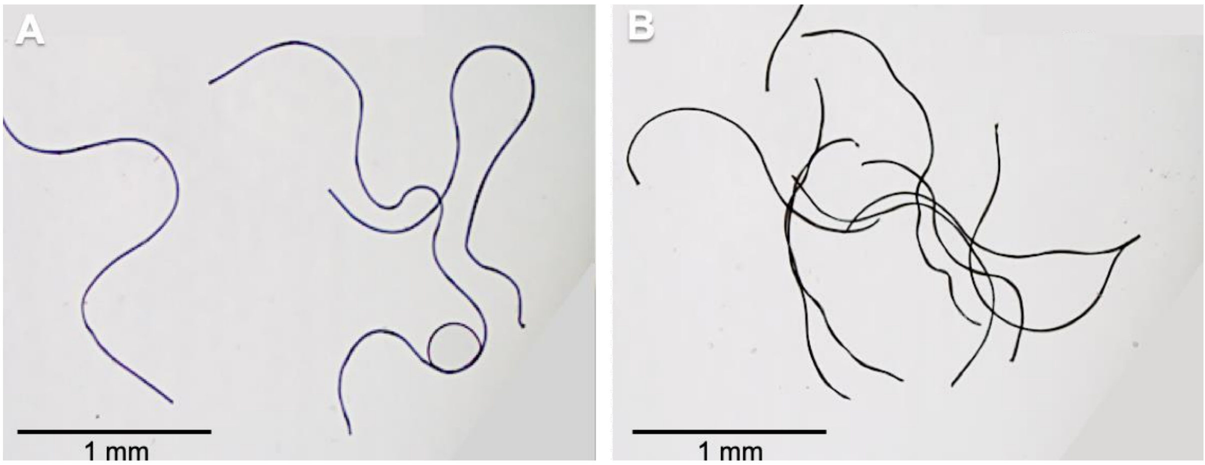

Figure 4.9. Light microscope images showing a comparison of PET MPFs collected from washing machine after washing a commercially available fleece textile (A) and scalpel prepared PET (B)

4.2.1 Validation of scalpel preparation procedure

The size distribution of MPF fibres (including wool) prepared for UV and mechanical degradation studies using the scalpel method are presented in Figure 4.10. While a significant difference ($p<0.05$) is observed between PAN fibres (blue and orange) and the other MPFs (including wool), all median and mean values fell within the intended 1 - 2.5 mm size range. PAN showed greater size variation, which maybe be due to either PAN yarns containing significantly more fibre filaments per single length of yarn than other test materials, or to human error during preparation. While the scalpel method was effective for preparing fibres of environmentally relevant size, it is quite time intensive. Furthermore, the method requires the use glycol, a potential contaminant. To minimize the potential impact of glycol residue on the studies, the prepared fibres were washed thoroughly with water before use in experiments.

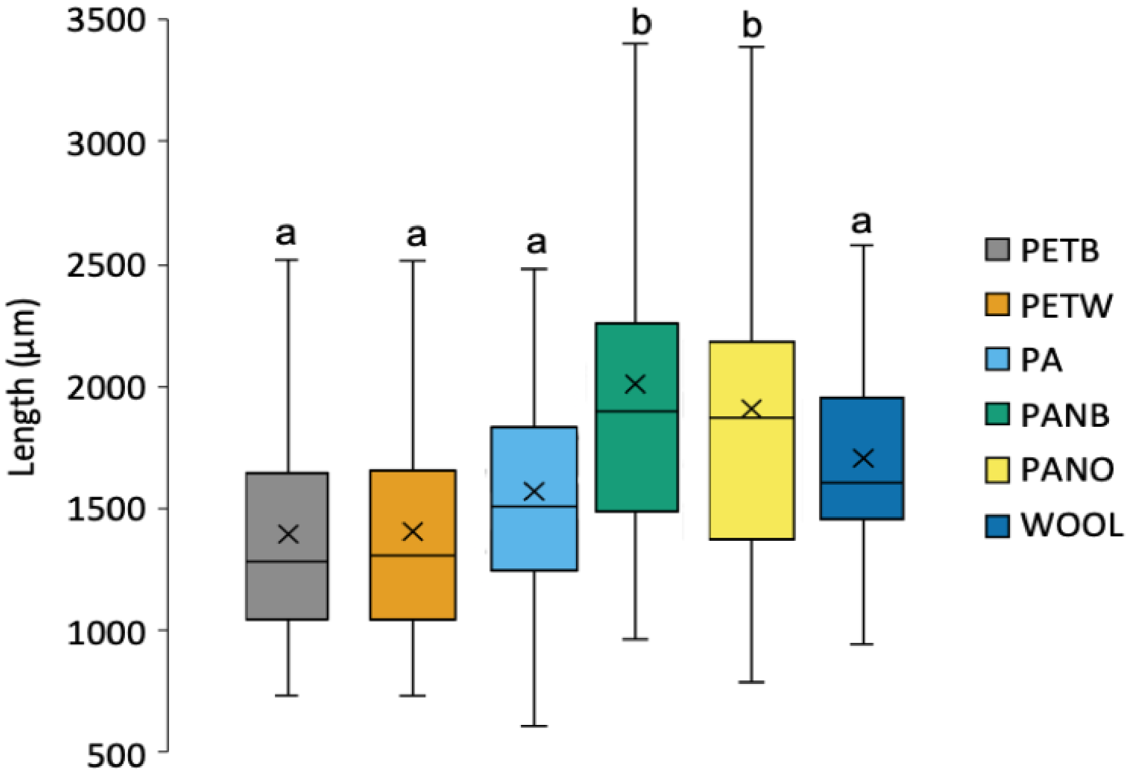

Figure 4.10. Size distribution of black and white PET (PETB, PETW), PA, blue and orange PAN (PANB, PANO) MPFs and wool. Boxplots show median length and interquartile range (IQR), where N = 60 for all samples. Significant differences ($P<0.05$) between groups are shown by letter codes (where the same letter indicates no significant difference ($p > 0.05$))

4.2.2 Validation of scissor preparation procedure

MPFs (and wool) were prepared via the scissor method for short 14-day leachate studies. The scissor method proved to be a quick, cheap and effective technique for the production of 5 mm fibres. It does not require specialised equipment and avoids the introduction of additional chemicals during preparation (e.g. glycol solution). However, size distribution of prepared MPFs (including wool) could not be measured successfully and therefore accuracy of the scissor method was not quantifiable. This was due to 5 mm MPFs being too long for the whole fibre to be in the field of view under the lowest magnification in light microscopy, but also too small to distinguish and measure individual fibres in images obtained by "regular" photography. Since a large amount of material was required for leaching, and accurate fibre length was not a relevant factor for the outcome of these studies, the scissor method was deemed suitable or this application. While the scissor method is a quick and effective technique it is not deemed suitable for the production of smaller fibres (e.g. below ~3 mm) due to practical constraints. It is neither suitable for applications where accurate and quantifiable fibre lengths are necessary.

4.3 UV Degradation Studies

4.3.1 Visual observations

Colour fading and changes that occurred after 9-month UV exposure in black and white PET, PA, blue and orange PAN are shown in Figure 4.11. Black PET did not change in colour and no obvious colour fading was evident, it did however appear to change in texture moving from a softer material to a rougher material with UV exposure. White PET changed from white in colour to yellow/brown within 3 months and continued to darken in colour with ongoing UV exposure. PA was white in colour and showed no signs of yellowing throughout the 9-month UV exposure period. Both PAN MPFs showed evidence of colour fading. PAN orange went from a bright orange to white within 3 months and PAN blue went from a bright blue to a very pale blue gradually over the 9-month exposure period.

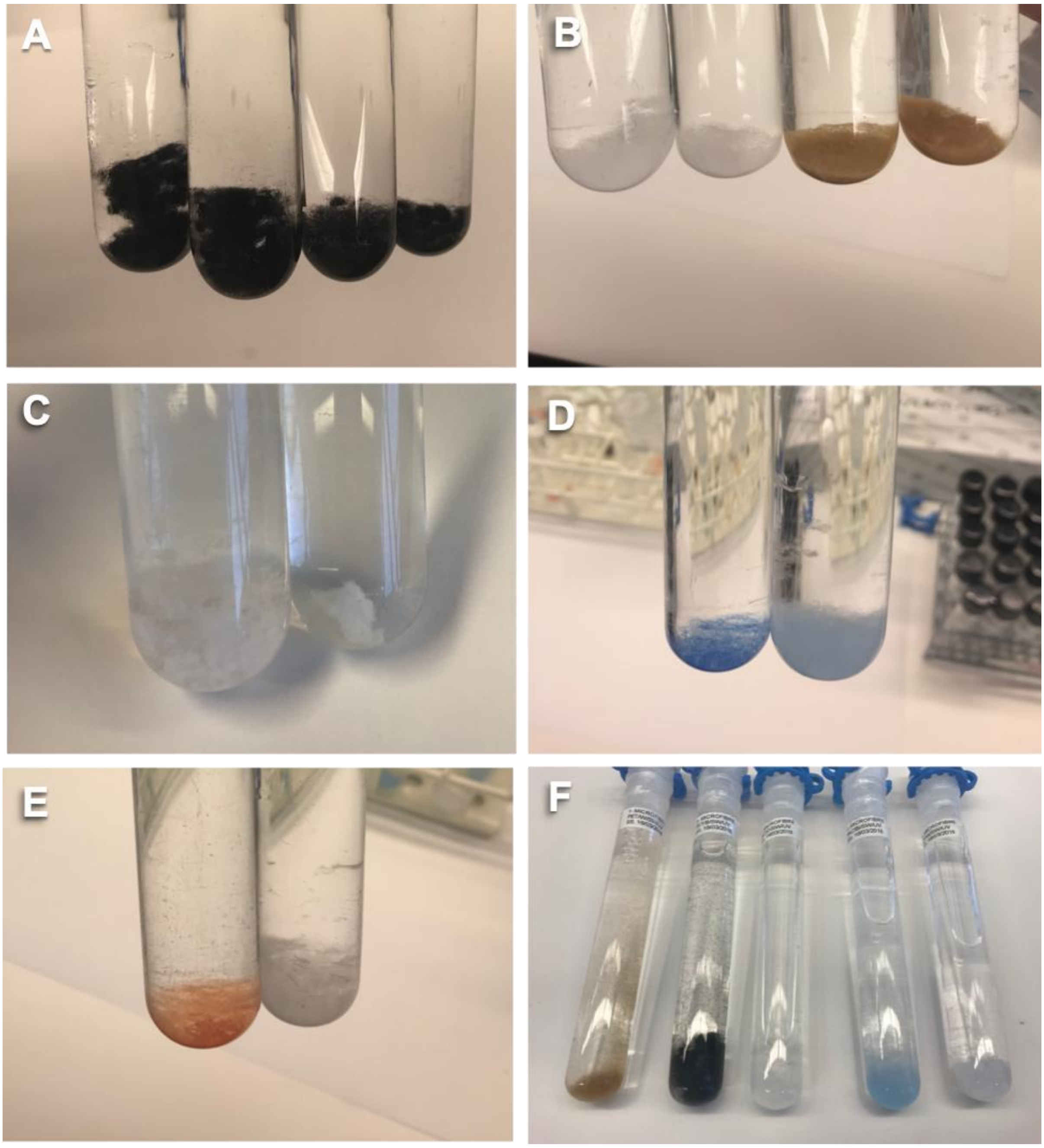

Figure 4.11. Qualitative changes in 9-month UV exposed MPFs. Panel A shows black PET. From left to right: Control in SW, Control in FW, UV exposed in SW and UV exposed in FW; B displays PET white, from left to right: Control in SW, Control in FW, UV exposed in SW and UV exposed in FW; C shows PA control (left) and exposed samples and after (right) UV exposure in SW; D shows blue PAN before (left) and after (right) UV exposure in SW; E shows orange PAN before (left) and after (after) UV exposure in SW and F shows UV exposed MPFs in SW, from left to right: PA, black PET, white PET, blue PAN and orange PAN.

4.3.2 MPF fragmentation

The change in length of black and white PET after 5- and 9-month UV exposure in seawater and freshwater media is shown in Figure 4.12. PET black significantly decreased in length ($p < 0.001$) after 5- and 9-month UV exposure. There was decrease in mean MPF length between 5 (217 µm) and 9 months (140 µm) in seawater, though this was not significant ($p > 0.05$), suggesting that the majority of photodegradation may have occurred in the first 5 months of exposure. White polyester also exhibited a significant decrease in length ($p < 0.001$) after UV exposure. The higher extent of fragmentation observed in PET white after the 5-month exposure in freshwater media, likely resulted from overhandling of the sample resulting in the production of smaller fragments due to its increased brittleness. Although white PET showed a larger change in length, this was not significant (>0.05) relative to black PET, suggesting the use of dyes in this case does not impact the rate of photodegradation. There were no significant changes ($p > 0.05$) in length after UV exposure between SW and freshwater mediums in PET, suggesting that the increased salinity in seawater does not significantly contribute to the degree of photodegradation.

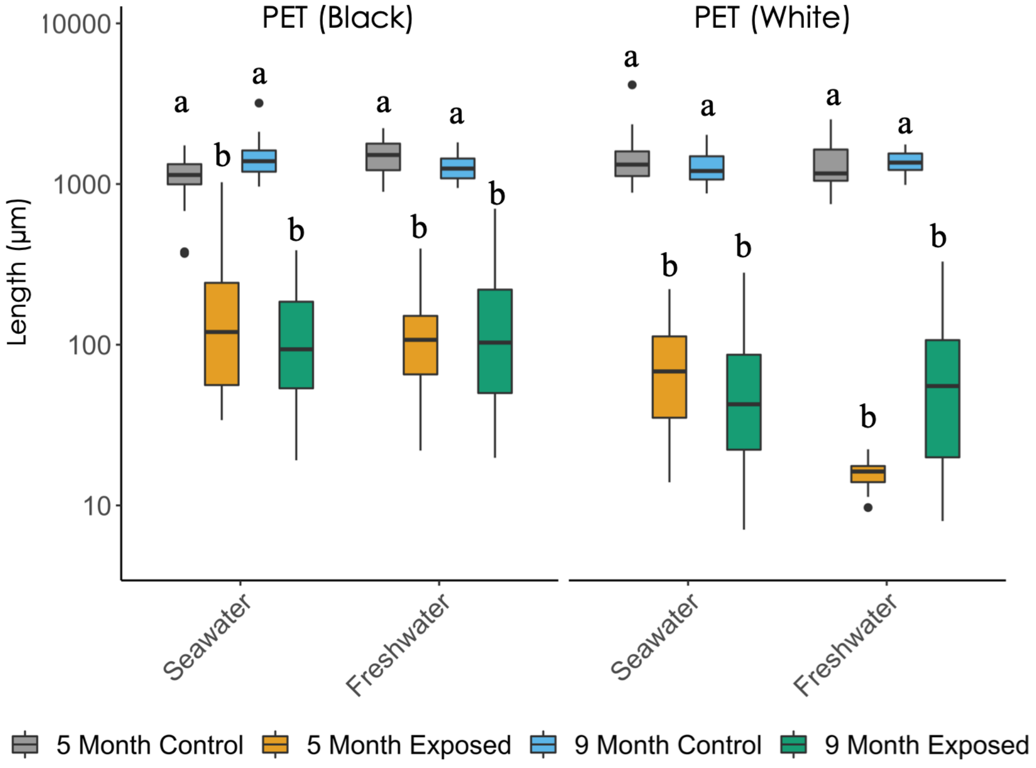

Figure 4.12. Change in length (in µm) of black and white PET after 5- and 9-month UV exposure. Boxplots show median length and interquartile range (IQR), where N = 30 for all samples. Significant differences ($p < 0.001$) between groups are shown by letter codes (where the same letter indicates no significant difference ($p > 0.05$))

The change in length of PA MPFs after 5- and 9-month UV exposure in seawater and freshwater media is shown in Figure 4.13. PA showed significant fragmentation ($p < 0.0001$) after 5- and 9-month UV exposure, with a decrease in mean MPF length in seawater from 1622 µm before exposure to 550 µm after 5 months and further to 373 µm after 9 months. However, the change between 5 and 9 months was not statistically significant ($p = 0.33$). This indicates that majority of photodegradation may have occurred in the first 5 months as observed in PET samples. There were no significant changes ($p > 0.05$) in length after UV exposure between SW and freshwater mediums in PA suggesting that the increased salinity in seawater does not significantly contribute to the degree of photodegradation.

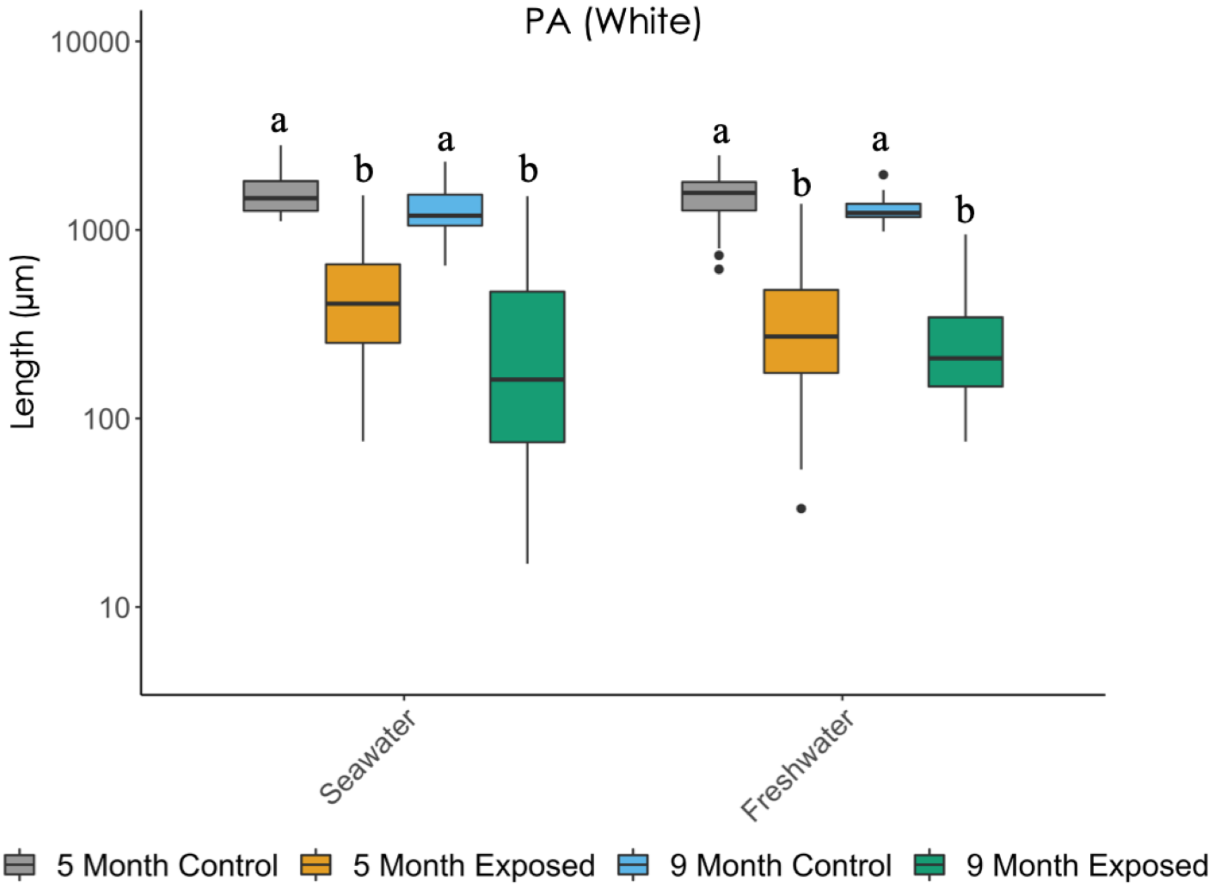

Figure 4.13. Change in length (in µm) in PA after 5- and 9-month UV exposure. Boxplots showing median length and interquartile range (IQR). N = 30 for all samples. Significant difference ($p < 0.001$) between groups are shown by letter codes (where the same letter indicates no significant difference ($p > 0.05$)).

As shown in Figure 4.14, there was no change in length in either the blue or the orange PAN MPFs after 5- and 9-month UV exposure in seawater and freshwater media ($p > 0.05$).

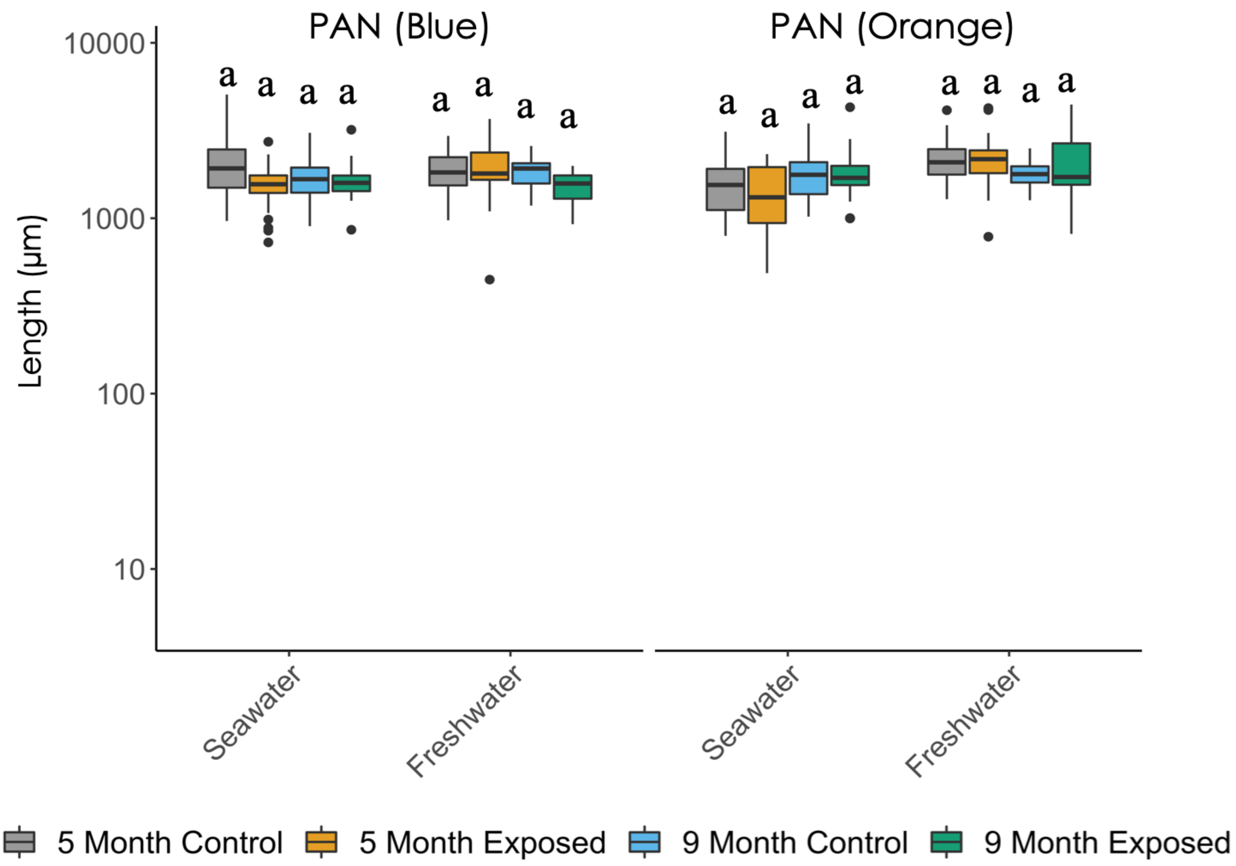

Figure 4.14. Change in length (µm) in blue and orange PAN MPFs after 5- and 9-month UV exposure. Boxplots show median length and interquartile range (IQR), where N = 30 for all samples. Significant difference between groups are shown by letter codes (where the same letter indicates no significant difference ($p > 0.05$))

Fragmentation results suggest that PET and PA will degrade more readily in surface waters of marine and freshwater environments, while PAN may be more persistent in such environments. Photodegradation of PET is known to result in increased brittleness and yellowing consistent with findings in this study (Andrady, 2003). PA is likewise known to increase in brittleness and undergo yellowing under UV irradiation. Interestingly, no yellowing of PA occurred during UV exposure, though the use of anti-yellowing agents are often employed in the manufacture of various polyamides, which likely explain this observation (Andrady, 2003; Weedon and Decaprio, 1971). According to literature, PAN *can* undergo photodegradation, however no available literature have reported studies of this under environmentally relevant conditions (Aggour and Aziz, 2000; Jellinek and Bastien, n.d.; Jellinek and Schlueter, 1960).

Photodegradation rates depend on many intrinsic and extrinsic factors, and while PET and PA showed a higher degree of degradation in this study, these materials are not necessarily representative of all types of PET, PA and PAN MPFs used in textiles or found in the environment. Material physicochemical properties, for example the presence of UV stabilisers, will significantly hinder the rate of environmental degradation and prolong environmental lifetimes. In contrast, the presence of other chemical additives may again lead to an increase in degradation susceptibility (Deterre et al., 2014).

4.3.3 Changes in surface morphology

Changes in surface morphology were characterised by SEM microscopy. SEM images of black and white PET, PA, blue and orange PAN are presented in Figures 4.15, 4.16, 4.17, 4.18 and 4.19, respectively. SEM images of black PET reveal visible crazing or cracking along the surface after UV exposure in seawater (Figure 4.15). There appears to be an increase in cracking at the surface after 9 months of UV exposure. While there was no significant change in length of black PET between the 5- and 9-month exposures, it is apparent that the sample has undergone additional photodegradation based on the increased frequency of surface cracking observed after 9 months. A study investigating mechanical properties of recycled PET fibres in an alkaline concrete environment exhibited comparable crazing following their degradation (Pelisser et al., 2012). The same observations were seen in black PET exposed in freshwater media (Appendix B Figure B.1). In the current study, MPFs appear to have degraded non-homogenously, which may be attributed to a variety of factors including shading effects as a result of static exposure conditions, nanoscale defects or inconsistencies in the polymer matrix such as, uneven distribution of additive chemicals.

SEM images of white PET display the formation of small holes or dimples along the surface after 5-month UV exposure (Figure 4.16). The surface morphology of white PET after 9-month UV exposure appeared similar to the surface morphology observed at 5 months, however, there did appear to be an increase in surface cracking. The appearance of surface cracking implies an increase in sample brittleness, suggesting that PA has undergone further photodegradation. Analogous observations were observed in white PET irradiated in freshwater media (Appendix B Figure B.2). While, both PET MPFs showed significant fragmentation after UV exposure, their surfaces appeared visibly different. Crazing is often reported in the photodegradation of PET, however the formation of holes on the surface as observed in white PET have not been reported prior to the current study. Similar holes have been reported to be observed on the surface of polycyclic carbonate films after hydrolytic degradation studies, indicating that hydrolysis may be occurring in combination with photodegradation (Chandure et al., 2014).The rate of hydrolysis in PET is known to increase in the presence of acid or base. Furthermore, photodegradation is known to produce carboxylic acid end groups (Gewert et al., 2015). Differences observed in surface morphology between PET fibres after UV exposure is may be related to differences in chemical additive content.

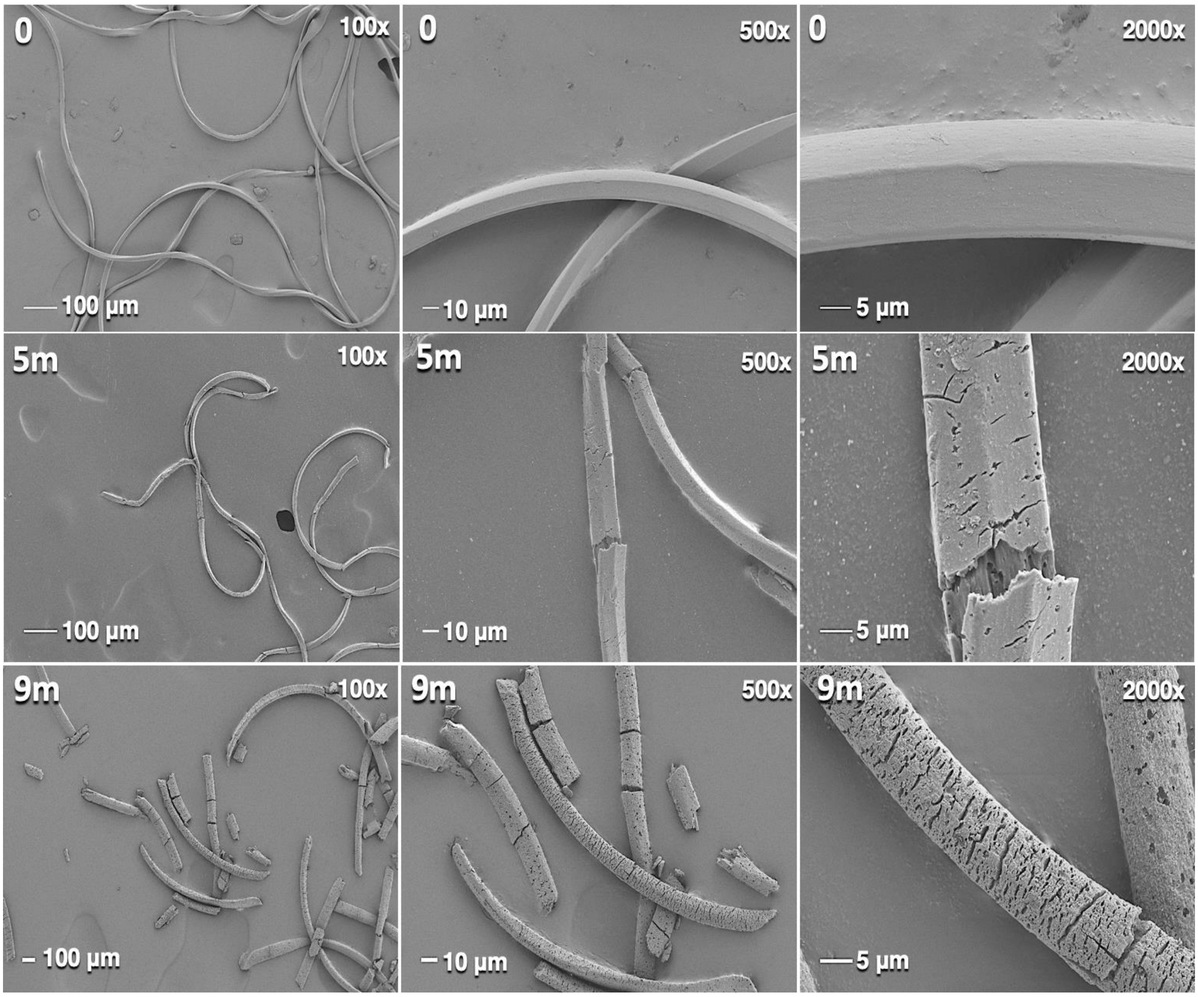

Figure 4.15. SEM images showing changes in surface morphology in black PET MPFs before (0) and after 5-month (5m) and 9-month (9m) UV exposure in seawater. Images are shown at 100, 500 and 2000x magnification.

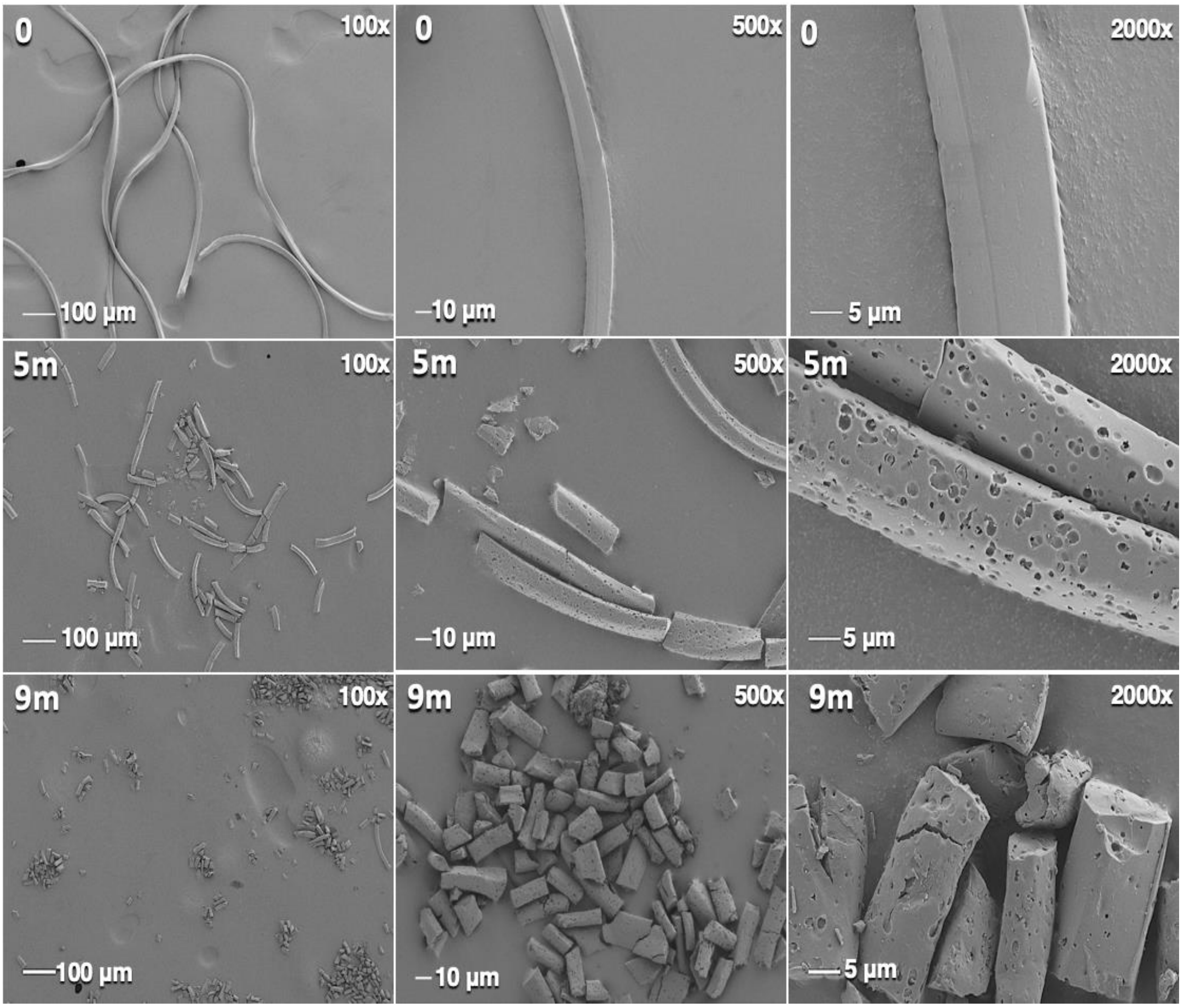

Figure 4.16. SEM images showing changes in surface morphology of white PET MPFs before (0) and after 5-month (5m) and 9-month (9m) UV exposure in seawater. Images are shown at 100, 500 and 2000x magnification.

The formation of relatively deep holes and crevices along the surface of PA after 5-month UV exposure in seawater are seen in Figure 4.17. Crevices and holes on the surface of PA were considerably more pronounced after the 9-month exposure compared to the 5-month exposure in SW. In freshwater exposed samples, surface morphology was not as severely degraded after the 9-month UV exposure (Appendix B Figure B.3.). This difference could be attributed to either nanoscale defects or inconsistencies in the polymer matrix such as, uneven distribution of additive chemicals. Despite a thorough literature search, this extent of UV initiated surface morphology changes appear to have not been characterised in PA before. Surface crazing has been previously imaged with SEM in photodegraded PA films (Ksouri and Haddar, 2018), but the formation of deep crevices has not been described in literature. This drastic change in polyamide surface morphology during photodegradation suggests probable formation of small micro- and nano-sized particles, especially when combined with external mechanical forces. This is an important finding as nano-sized fragments are considered more bioavailable and may translocate into biotic tissues. (Dawson et al., 2018; Revel et al., 2018).

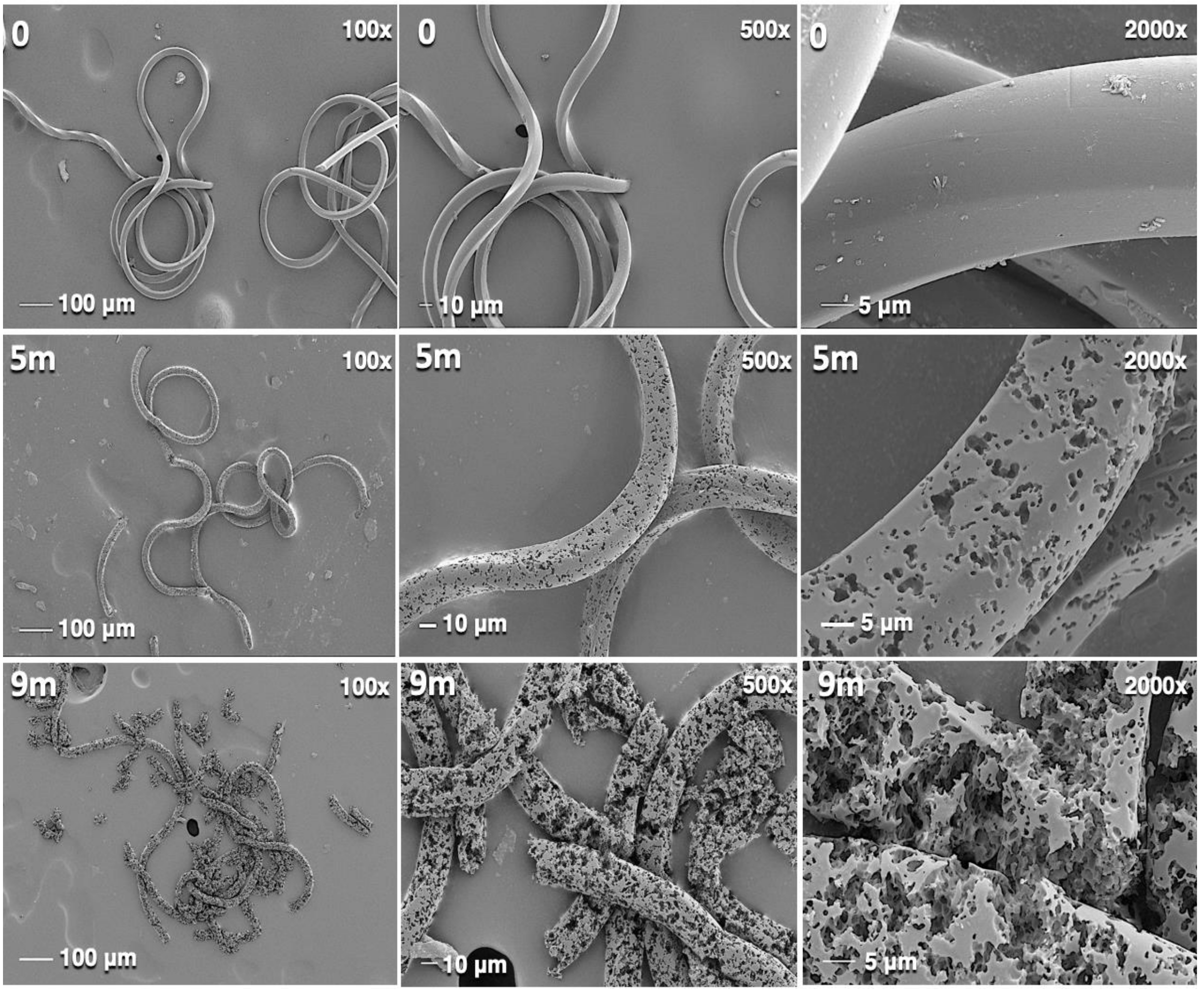

Figure 4.17. SEM images showing changes in surface morphology of PA MPFs before (0) and after 5-month (5m) and 9-month (9m) UV exposure in seawater. Images are shown at 100, 500 and 2000x magnification.

SEM images of blue PAN MPFs show the formation of small holes in the surface after 5-month UV exposure in SW (Figure 4.18). These small holes increased in both frequency and size after 9 months of UV exposure in seawater relative to 5-month exposed samples. The same observations were seen in the blue PAN exposed in freshwater media (Appendix B Figure B.4). SEM images of orange PAN MPFs show little change to surface morphology after 5-months UV exposure. After 9-months UV exposure in SW, the formation of tiny holes is evident at the surface (Figure 4.19) compared to pristine and 5-month UV exposed PAN. Non-homogenous polymer degradation is likely attributed to shading effects as a result of static exposure conditions. The same observations were seen in the orange PAN exposed in freshwater media (Appendix B Figure B.5). Blue PAN showed a greater frequency of small holes on the surface than evident in orange PAC. It is unclear why blue PAN presented larger changes to surface morphology, but it is hypothesized that this may be related to differences in chemical additive content.

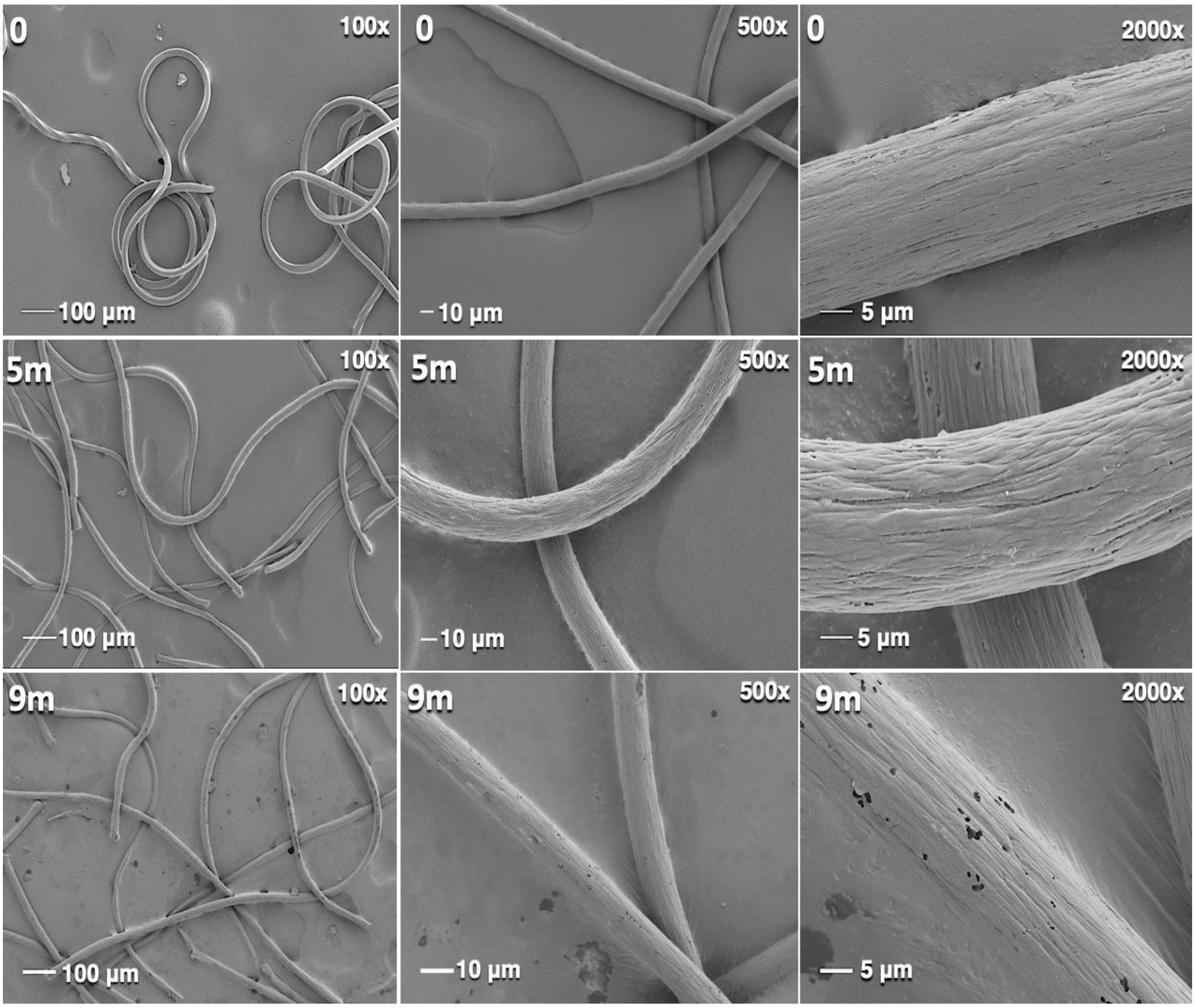

Figure 4.18. SEM images showing changes in surface morphology of blue PAN MPFs before (0) and after 5-month (5m) and 9-month (9m) UV exposure in seawater. Images are shown at 100, 500 and 2000x magnification.

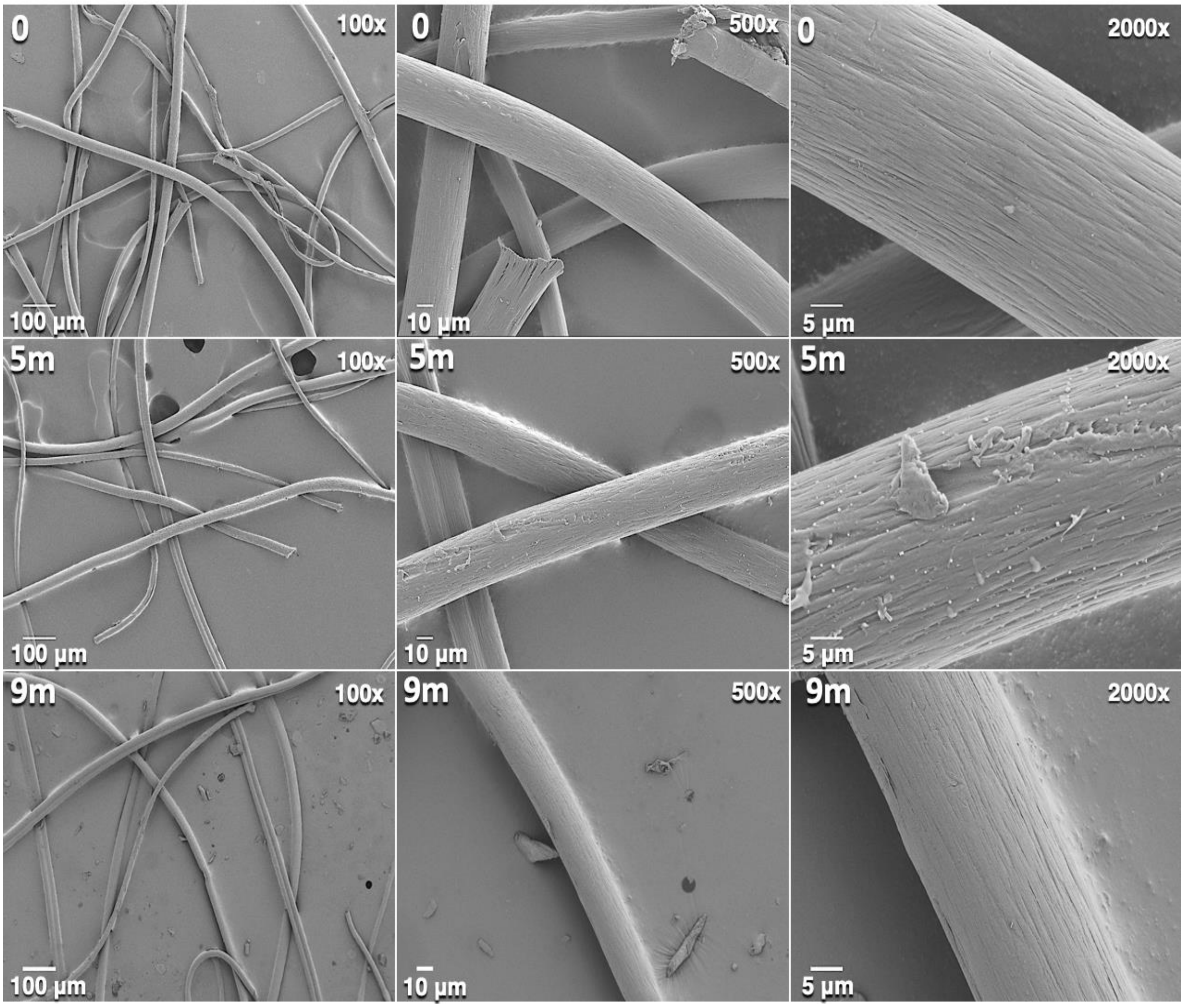

Figure 4.19. SEM images showing changes in surface morphology of orange PAN MPFs before (0) and after 5-month (5m) and 9-month (9m) UV exposure in seawater. Images are shown at 100, 500 and 2000x magnification.

In the UV degradation studies, significant fragmentation and changes to surface morphology were observed with PET and PA, whereas little degradation was seen in PAN during the exposure period. A greater extent of fragmentation occurred in PET relative to PA, likely due to an increase in brittleness of PET. Gentle shaking and sample handling may also have resulted in greater fragmentation of PET MPFs relative to PA MPFs as a result of the increased brittleness. Based on changes in length and surface morphology it is hypothesised that the generation of nano-sized particles is likely, and that this would also occur in natural environments. Variations in photodegradation between MPFs is likely attributed to variations in both chemical structure and chemical additive content.

4.3.4 Generation of nanosized particles

The significant fragmentation of PET and PA MPFs raised the question about whether nanosized particles were being formed. To investigate this, the presence and size distribution nanosized particles in all UV exposed leachates and respective control samples were analysed by dynamic light scattering (Zetasizer). The obtained data are shown in Appendix B, Figures B.6 - B.10. There was evidence of nanosized particles present in both UV-exposed and control samples, which made reliable identification of nano-sized plastic degradation products challenging. The presence of nano-sized particulates in the control samples may be explained by the use of natural seawater in experiments. The seawater was only filtered to 0.22 µm, meaning naturally occurring nanoparticles will be present. Furthermore, the Zetasizer is optimised to measure spherical particles (sized between 0.3 nm – 10 µm), and can have difficulties measuring irregular shaped nanofragments – which is likely to be formed from MPF degradation. The Zetasizer determined that the sample polydispersity was very high, indicating that the particle size range was too large to measure effectively and as such a detailed analysis of the nano-fraction was not possible to perform in the current study.

4.3.5 Changes in polymer chemistry

Changes in polymer chemistry were investigated using ATR-FTIR. FTIR spectra of black and white PET, PA and blue and orange PAN MPFs are presented in Figures 4.20, 4,21, 4.22, 4.23 and 4.24, respectively. PET spectra were normalised to the C-H peak at 1407 cm^{-1} as this is expected to remain unaltered during photodegradation (Nguyen-Tri and Prud'homme, 2019). Characteristic peaks for PET are discussed in detail in section 4.1.2, and a summary of main peaks for both black and white PET can be found in Table 4.6, below. For black PET UV-exposed in seawater, a decrease in absorbance is observed at peaks 1711 (C=O), 1238 (C-O) and 1090 cm^{-1} (C-O) in UV exposed fibres (Figure 4.20) relative to control. The decrease in absorption in UV exposed PET is in line with observations from another study examining the extent of environmental degradation on PET bottles in marine environments (Ioakeimidis et al., 2016). Formation of new functional groups at 1435 and 620 cm^{-1} indicating formation of an alkyne bond (C≡H) and a new C-H bond are expected in significantly weathered PET (Ioakeimidis et al., 2016).

No new peaks were observed after UV exposure in this study, suggesting that the degree of weathering was not sufficient to promote the formation of degradation products responsible for respective peaks. A slight decrease in absorbance occurred in dark controls, which could be the result of either hydrolysis or variation between FTIR measurements due to variations in sample thickness. PET is susceptible to hydrolysis, though under normal environmental conditions this process is expected to occur very slowly due to its aromaticity (Gewert et al., 2015). The same observations were seen in the FTIR spectra of black PET exposed in freshwater media (Appendix, B Figure B.6), indicating no significant impact on photodegradation in the presence of dissolved salts in seawater relative to freshwater. The carbonyl indices (CI) for black PET after UV exposure were determined (Figure 4.22) relative to the C=C stretching peak at 1407 cm^{-1}. Even though changes in length and morphology were observed in PET, it is likely that oxidation has not occurred to a sufficient extent to observe an increase in the CI with exposure time. Similar findings were observed in the CI of white PET (Appendix B, Figure B.11)

The appearance of an OH stretching band in PET white after 5-month UV exposure may indicate oxidation has occurred (Figure 4.21) but is more likely associated with inadequate rinsing of white PET prior to analysis. Residual salts from seawater can result in moderate to strong peaks in the 3000 – 3500 cm^{-1} range, this was evident when unwashed MPFs were first analysed with FTIR. All samples exposed in seawater presented a high intensity peak in the OH region, after washing with Milli-Q this peak completely disappeared in the majority of samples. In addition, the reduced intensity of the OH peak observed in 9m exposure supports this, as if oxidation had occurred, the peak would be expected to appear at a similar intensity or higher. The lack of OH peak seen in freshwater exposed samples and in black PET samples further supports this statement. (Appendix A, Figure A.6. Similarly to black PET, a decrease in absorbance is observed at peaks 1711 (C=O), 1238 (C-O) and 1090 cm-1 (C-O) in UV exposed white PET (Figure 4.21) relative to control The same observations were seen in the FTIR spectra of white PET exposed in freshwater medium (Appendix B, Figure B.7, indicating no significant impact on photodegradation in the presence of dissolved salts in seawater relative to freshwater.

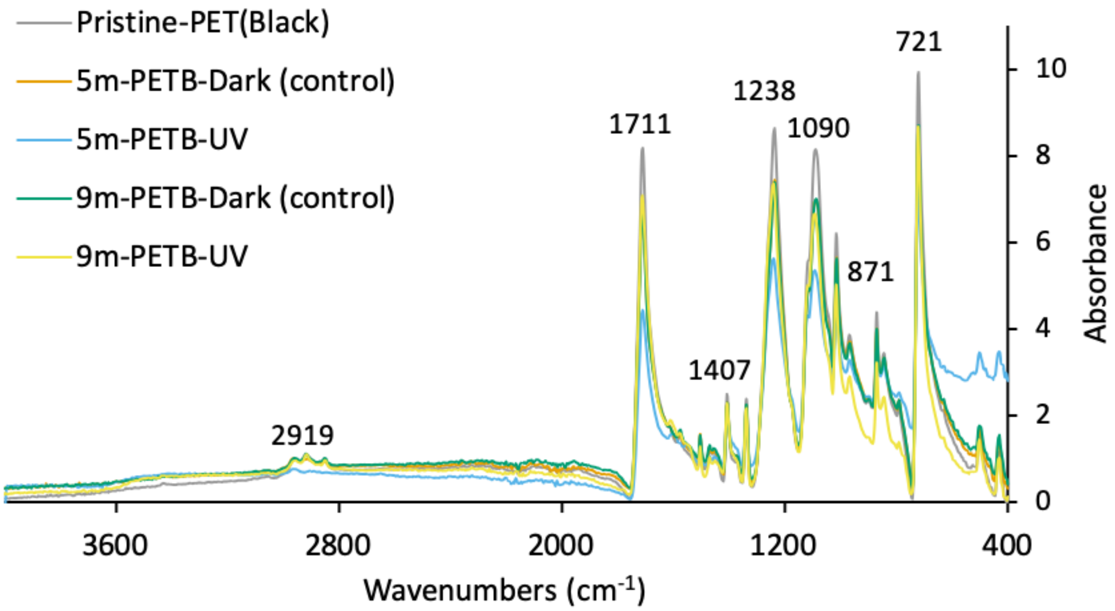

Figure 4.20. ATR-FTIR spectrums of UV exposed black polyester (PETB) in SW, normalised to CH reference peak at 1407 cm^{-1}.

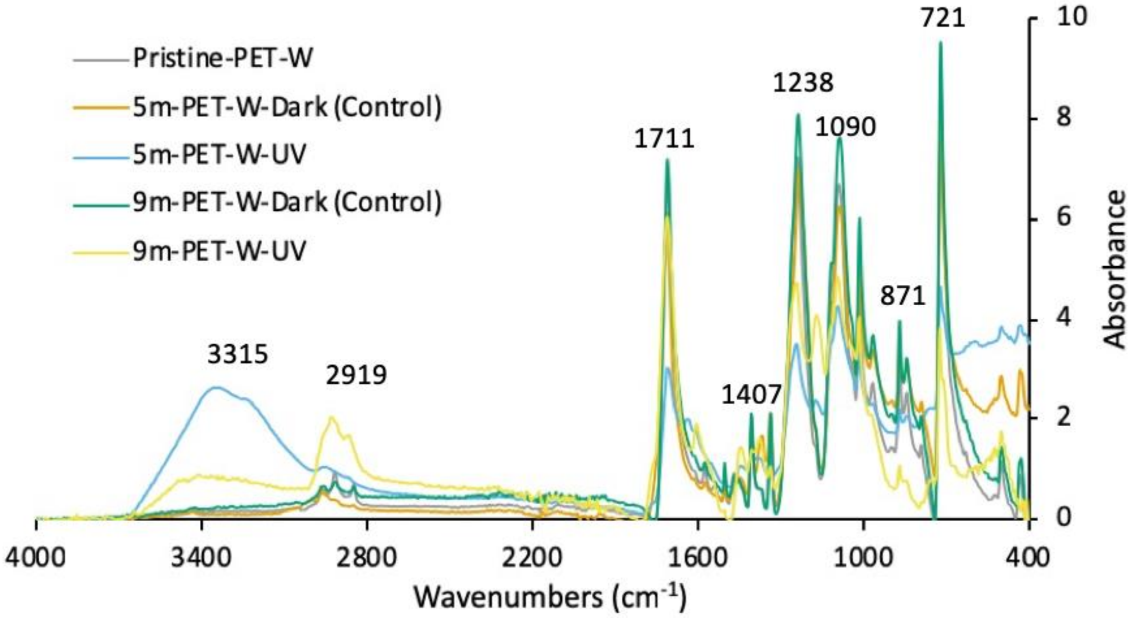

Figure 4.21. ATR-FTIR spectrums of UV exposed white PET (PET-W) in SW, normalised to CH reference peak at 1407 cm^{-1}

Table 4.6. FTIR band assignment for black and white PET

Band (cm^{-1})	Assignment	Intensity	References
3315	O-H stretching	weak-moderate	Ioakeimidis et al., (2016)
2960	C-H stretching	weak-moderate	Ioakeimidis et al., (2016)
2919	C-H stretching	weak-moderate	Ioakeimidis et al., (2016)
2852	C-H stretching	weak-moderate	Ioakeimidis et al., (2016)
1711	C=O stretching	strong	Ioakeimidis et al., (2016)
1407	C=C stretching	weak	Ioakeimidis et al., (2016)
1238	C-O stretching	strong	Ioakeimidis et al., (2016)
1090	C-O stretching	strong	Ioakeimidis et al., (2016)
871	C-C out of plane bending	moderate	Ioakeimidis et al., (2016)
721	C-H bending	very strong	Ioakeimidis et al., (2016)

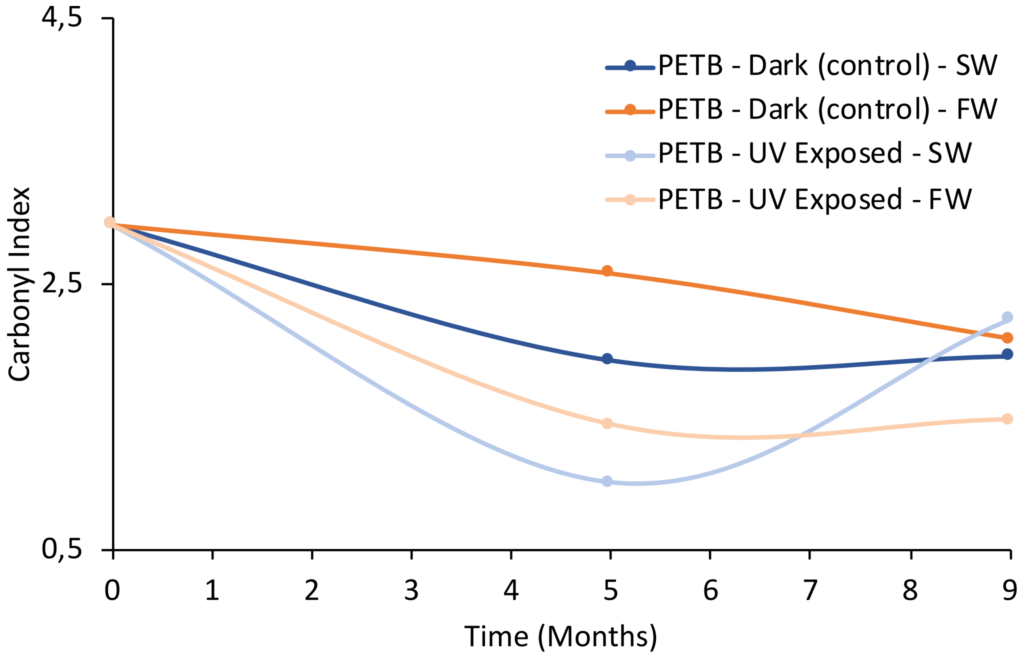

Figure 4.22. Change in carbonyl indices of black PET after 9-month UV exposure

PA spectra were normalised to the C-H peak at ~930 cm^{-1} as this is thought to remain stable under photodegradation. Characteristic peaks for PA were discussed in detail in section 4.1.2, and a summary of main peaks can be found in Table 4.7, below. An increase in absorption was observed in UV exposed PA relative to control samples at peaks 3295 (N-H), 2921 (C-H), 1631 (C=O) and 1530 (δ_SN-H) cm^{-1}(Figure 4.23). The increase in absorption in UV exposed PA is consistent with a study examining the accelerated photodegradation of nylon 6,6 and is likely attributed to imide formation due to photooxidation (Thanki and Singh, 1998). The same observations were seen the FTIR spectra of PA exposed in freshwater media as (Appendix B Figure B.8). The carbonyl indices for PA after UV exposure were determined (Figure 4.24) relative to the C-H peak at ~930 cm^{-1}. PA fibres exposed to UV radiation in SW showed a logarithmic increase (R^2 = 0.99) in carbonyl index with respect to UV exposure time. PA exposed to UV radiation in freshwater medium showed an exponential increase (R^2 = 0.96) in their carbonyl indices with respect to exposure time. Increases in carbonyl indices in UV exposed samples is likely due to the formation of imide groups during photodegradation, increasing the intensity of the carbonyl stretch at 1631 cm^{-1}. It is unclear what was responsible for the variation in CI change between SW and freshwater samples, but likely related to non-homogenous degradation. Dark controls showed a logarithmic (R^2 =1) and exponential increase (R^2 = 1) in regard to UV exposure in freshwater and SW medium, respectively. The observed increase in CI in dark controls may be explained by slow degradation via hydrolysis.

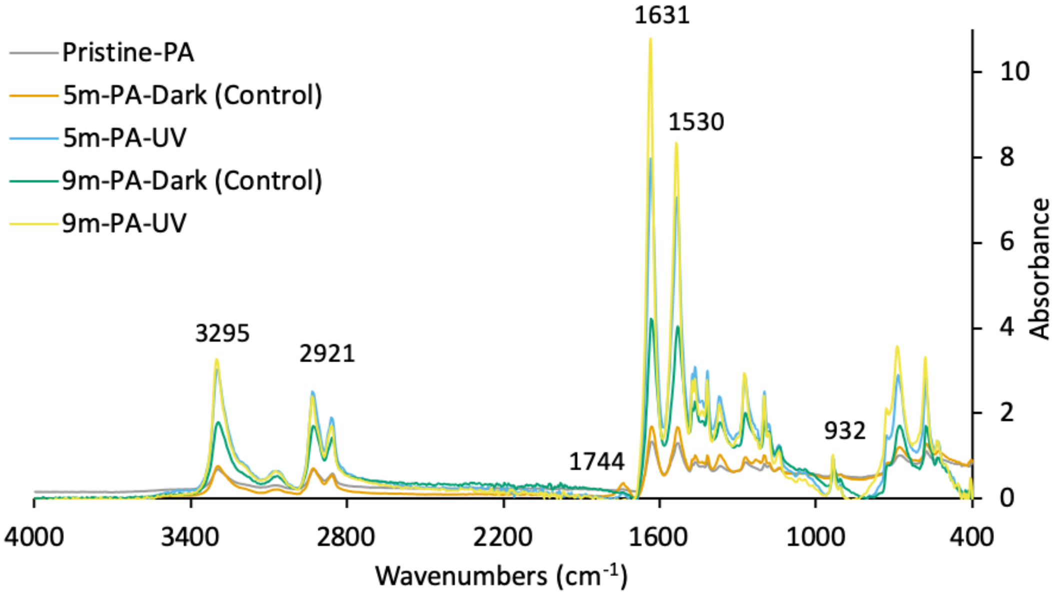

Figure 4.23. ATR-FTIR spectra of UV exposed PA in SW, normalised to CH reference peak at 932 cm^{-1}.

Table 4.7. FTIR band assignment PA

Band (cm^{-1})	Assignment	Intensity	Reference
3295	NH stretching	moderate	Porubská et al., (2012)
3070	NH angular deformation	weak	Porubská et al., (2012)
2921	CH_2 asymmetric stretching	weak-moderate	Porubská et al., (2012)
2851	CH_2 symmetric stretching	weak-moderate	Porubská et al., (2012)
1631	C=O band	very strong	Porubská et al., (2012)
1530	In plane N-H deformation	strong	Porubská et al., (2012)
932	C-CO stretching	weak	Porubská et al., (2012)

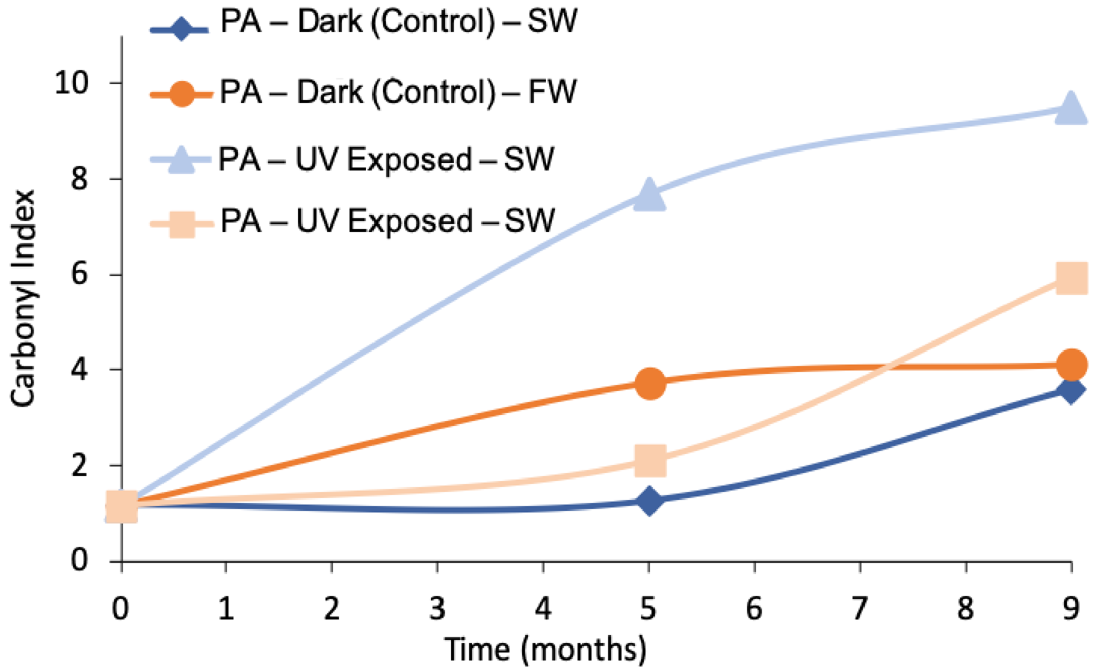

Figure 4.24. Change in carbonyl indices of PA after 9-month UV exposure

ATR-FTIR spectra of PAN MPFs in pristine, control UV exposed samples (Figure 4.25 and 4.26) were challenging to interpret due to low signal to noise ratio (i.e. high background noise). It appears characteristic of PAN to create a low signal in FTIR (Coleman and Sivy, 1981; Jellinek and Schlueter, 1960). Characteristic peaks for PAN were discussed in detail in section 4.1.2, and a summary of main peaks for both blue and orange PAN can be found in Table 4.8, below. The appearance of two peaks at ~1600 cm^{-1} and increased intensity at 2915 and 2446 cm^{-1} can be attributed to bacterial growth, this was not observed in UV exposed samples as UV is a known growth inhibitor (Aggour and Aziz, 2000; Hijnen et al., 2006).

No obvious trends in changes in absorbance are observed in the FTIR spectra of UV exposed blue PAN (Figure4.25). However, there appears to be a subtle increase in absorbance at peaks 2240 (C≡N), 1733 (C=O), 1450 (C−H) in orange PAN (Figure 4.26). It is unclear why there is an observed difference between blue and orange PAN spectra. Given the low degree of surface changes in PAN fibres after UV exposure, chemicals changes were not expected in the respective FITR spectra. Analogous observations were seen in the FTIR spectra of blue and orange PAN in freshwater medium (Appendix B, Figure B.9 and B.10, respectively), indicating no significant impact on results due to the presence of dissolved salts in seawater relative to freshwater. Carbonyl indices were measured in PAN spectra (Figure 4.27). Due to lack of studies on PAN photodegradation, carbonyl indices have not been used to quantify degradation in PAN before this study. No obvious trends were observed in calculated carbonyl indices, likely a result of the low degree of photodegradation in PAN MPFs.

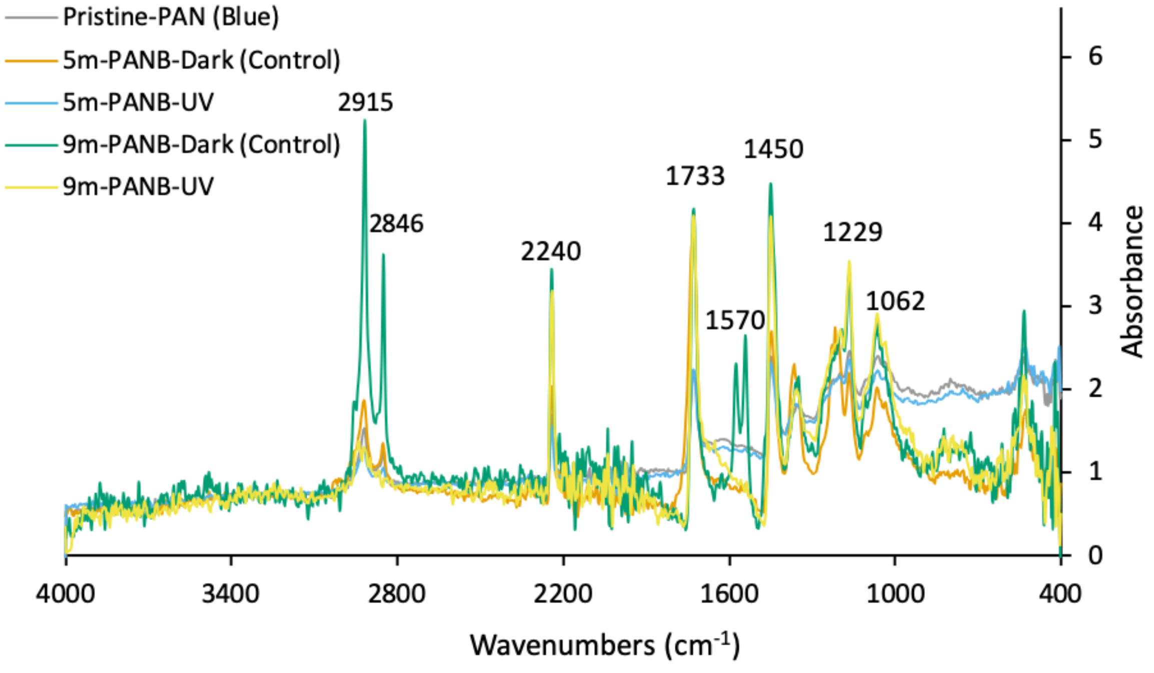

Figure 4.25. ATR-FTIR spectrums of UV exposed blue PAN (PANB) in SW, normalised to peak at 1360 cm^{-1}

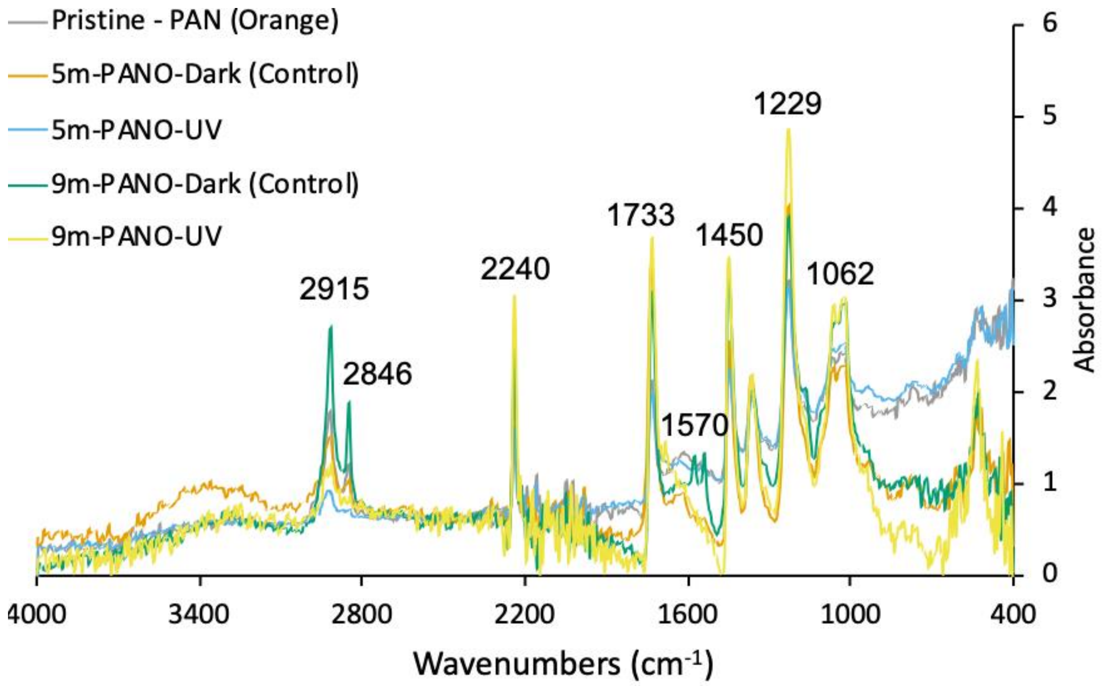

Figure 4.26. ATR-FTIR spectrums of UV exposed orange PAN (PANO) in SW, normalised to the peak at 1360 cm^{-1}

Table 4.8. FTIR band assignment PAN (blue and orange).

Band (cm^{-1})	Assignment	Intensity	Reference
2915	C-H stretching	moderate	Farsani et al., (2009)
2846	C-H stretching	weak/moderate	Farsani et al., (2009)
2240	C≡N	moderate	Farsani et al., (2009)
1733	C=O from comonomer	moderate	Farsani et al., (2009)
1537	Bacteria	weak	(Ojeda and Dittrich, 2012)
1450	C−H in CH2	moderate	Farsani et al., (2009)
1366	CH bend	weak/moderate	Farsani et al., (2009)

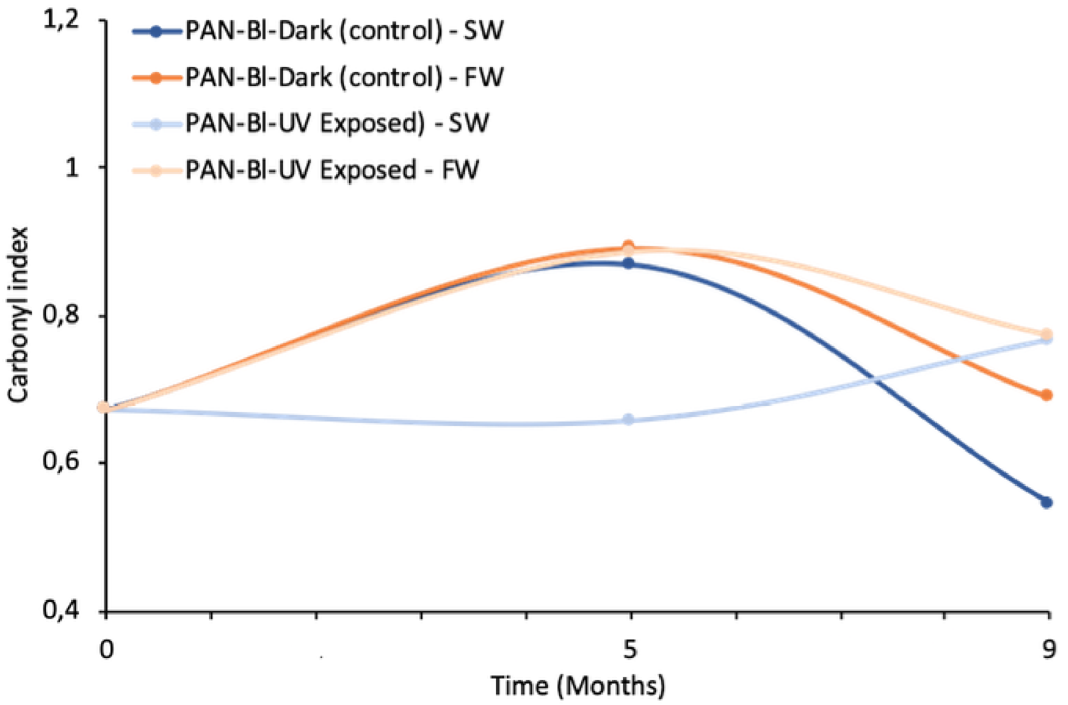

Figure 4.27. Change in carbonyl indices with time in blue PAN after 9-month UV exposure

PET showed decreases in absorption in FTIR spectra with weathering time, consistent with literature and surface morphology changes. However, no temporal trends in the determined carbonyl indices were observed for PET. PA displayed increased absorption and carbonyl indices relative to exposure time indicating photodegradation. This is consistent with the extent of fragmentation and changes to surface morphology seen in this study. No obvious trends were identified in the FTIR spectra or the determined carbonyl indices for PAN after UV exposure, as a result of a lower degree of photodegradation. No visual difference between seawater and freshwater imply photodegradation would occur at similar rates in these environments. It is plausible that degradation may occur at comparatively quicker rates in freshwater environments due to the higher proportion of shallow regions (i.e. higher potential for UV exposure) relative to marine environments. Carbonyl indices appear to be a suitable measure for the extent of photodegradation in MPFs, but only when sufficient degree of weathering has occurred.

4.3.6 Method considerations

UV exposure studies were completed with only one replicate of each material in SW and freshwater media due to instrument size constraints. Very few studies have been conducted on the fate of both semi-synthetic (e.g. rayon) and natural fibres in the environment (Barrows et al., 2018).

No natural fibre reference was included in this study due to size constraints, but its inclusion in future studies is recommended to improve understanding of the fate of natural fibres in the environment relative to MPFs. Vials were capped and sealed with parafilm to reduce evaporative losses of the medium during UV exposure. Although some loss of media was observed, this confirmed that O_2 exchange into the system occurred throughout the study, ensuring that this did not becoming limiting for degradative processes, however the flow of O_2 was not regulated. In surface waters, MPFs will typically have a steady supply of available oxygen for any potential photodegradative reactions, which is known to increase rates of photodegradation (Gewert et al., 2015). A daylight filter was used to simulate realistic levels of UV radiation that would occur in the natural environment, however laboratory-based exposures can fail to replicate the complexity of outdoor weathering as photodegradation will occur simultaneously with other degradative processes. The advantages of laboratory-based tests compared to outdoor weathering are increased reproducibility and repeatability.

4.4 Mechanical degradation studies

4.4.1 Visual observations

Within 3 weeks of exposure, all MPFs and wool had formed large, dense clusters of entangled fibres in the majority of samples. These ranged in size from 0.13 to 1.76 cm, as shown in Figure 4.28 and Appendix D (Figures D.2 and D.3). MPF clusters appeared more compact and denser in samples containing sand. No change in colour was evident in any of the MPF samples over the 9-month exposure period. As expected, MPF and wool samples containing sand appeared visibly dirtier and clusters also contained sand particles (Figure 4.29).

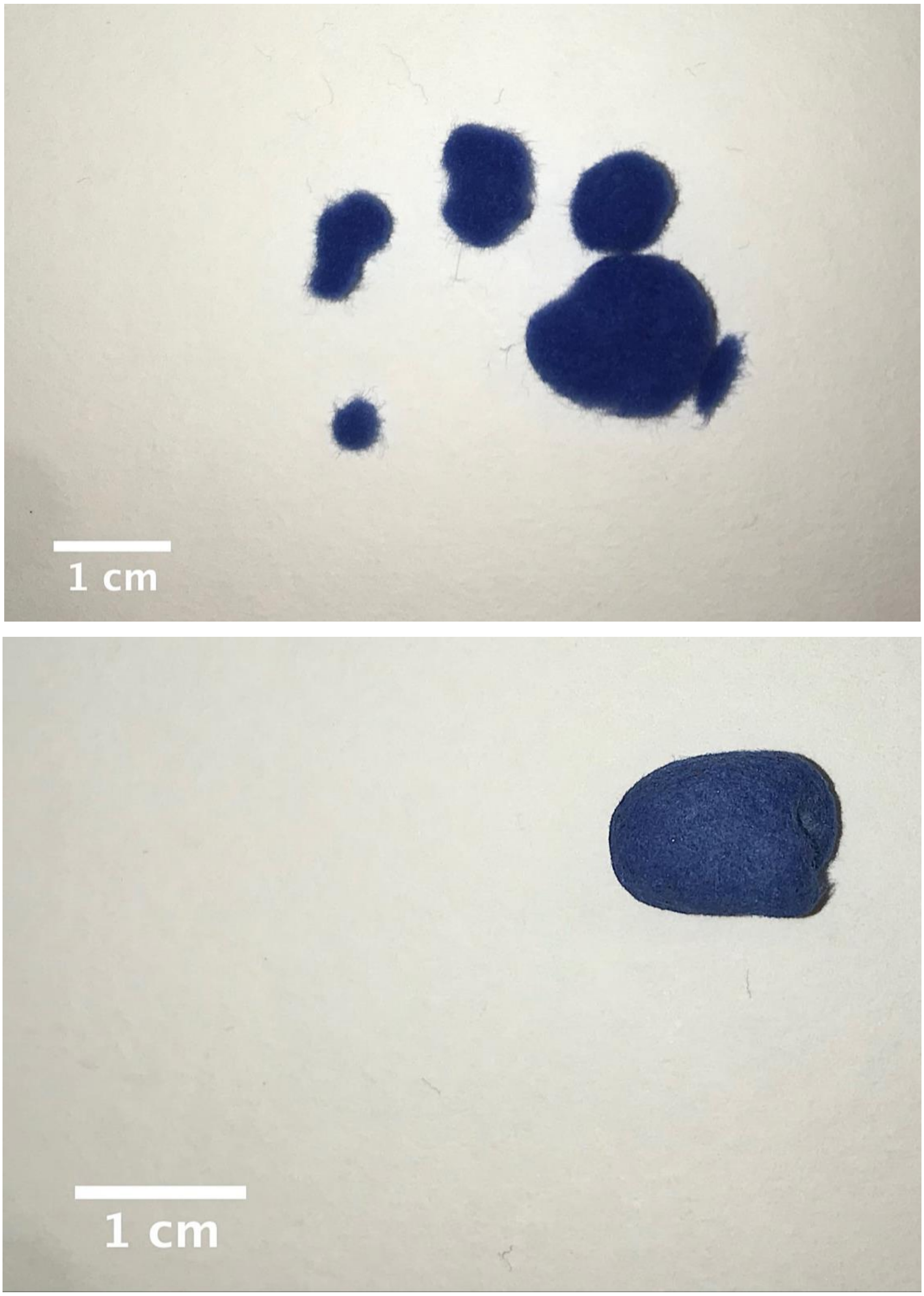

Figure 4.28. Blue PAN MPF after 9-month mechanical degradation experiments. Top: blue PAN without sand. Bottom: PAN blue with sand.

Figure 4.29. Separated orange PAN fibre cluster showing integration of sand particles

The formation of such dense fibre clusters does not appear to have been reported in environmental MPF distribution studies. This could be attributed to that fact that clusters observed in the current study are typically larger than the common microplastic size range (< 5 mm) and may therefore be categorised as mesoplatsic. The current study indicates that their formation in the natural environment *may* occur under the right tidal conditions and with high concentrations of MPFs. However, the mechanical studies were conducted in a cyclical shaking incubator and this cyclical motion appears likely to be the reason for the development of the MPF clusters. This cyclical motion may not be representative of the complex tidal and wave forces present in natural environments. When conducting mechanical degradation studies, a back and forth shaking table may be more representative of waves crashing against beaches and shorelines and should be considered for future studies. Fibre clusters were extremely robust and difficult to separate into individual fibres, suggesting that if they do occur in natural environments, they may very stable which could impact their fate. Fibre cluster if ingested by aquatic organisms, may lead to longer retention times in the gut and an associated impact on organism health (Welden and Cowie, 2016).

After 9-month exposure, the MPFs and wool in the mechanical degradation studies were separated from sand (as much as possible in the case of fibre clusters) and seawater via density separation with $ZnCl_2$. The recovery rates for black and white PET, PA, blue and orange PAN MPFs and wool using $ZnCl_2$ after 9 months exposure are presented in Table 4.9.

Table 4.9. Percent (%) recovery of MPFs for mechanical degradation experiments after 9 months

Samples Description	Recovery rate (%) at 20 °C	Recovery rate (%) at 5 °C
PET (black) w/ sand	158.7	155.1
PET (black)	96.8	95.5
PET (white) w/ sand	197.6	154.7
PET (white)	95.0	95.6
PA w/ sand	102.4	120.7
PA	98.2	95.6
PAN (blue) w/ sand	136.1	160.7
PAN (blue)	91.0	94.0
PAN (orange) w/sand	168.3	175.0
PAN (orange)	98.4	95.6
Wool w/ sand	95.1	96.0
Wool	90.9	92.7

Density separation with $ZnCl_2$ yielded high recoveries for the collection of MPFs and wool fibres from free sand. Recovery rates for mechanical degradation studies ranged between 91 – 175%, with higher recovery rates (>100) observed for those containing sand. In samples without sand, recovery rates were high and reasonable (91-98 %), validating the adequacy of the density separation procedure. Average recovery rates well above 100 in samples with sand present are likely due to the integration of sand particles into MPF clusters formed during exposure (Figure 4.29). Although not observed in the current study, embedding of sand directly into the surface of MP particles has previously been observed (Hepsø, 2018), and could contribute to the higher recovery rates observed. Wool was the only fibre to not experience a significant uptake of sand into the fibre cluster, and also appeared slightly 'cleaner' than other MPFs exposed to sand, although this is highly subjective. It is suggested that wools natural cleaning ability, may explain the reduced uptake of sand and the visibly cleaner appearance after mechanical degradation studies (The University of Waikato, 2007).

4.4.2 Extent of fragmentation

The length of MPFs before and after mechanical degradation studies of black and white PET, PA, blue and orange PAN and wool fibres in seawater at 5 and 20 °C is shown in Figure 4.30. Samples were only collected and analysed after 9 months, as there were not enough available free fibres from 5-month samples to yield a large enough sample size for statistical comparison. After 9 months, there was no significant fragmentation ($p > 0.05$) or change in mean length ($p > 0.05$) in any sample at any temperature. It was not possible to measure the length of fibres within developed fibre clusters, as disentanglement by force could have caused fibre damage and potential fragmentation. However, it is assumed that any smaller fibre fragments would be less likely to associate with fibre clusters, and as such would have been observed floating freely in the exposure medium. Mechanical degradation is considered an important degradative mechanism for MPFs that have already undergone other forms of degradation leading to their embrittlement (Gewert et al., 2015). Prior to conducting this study, it was hypothesised that negligible UV degradation would occur in MPFs over the 9-month exposure period, as such only pristine MPFs were prepared for mechanical degradation studies. The effect of photodegradation coupled with mechanical degradation should be investigated by either performing sand abrasion studies with UV exposed MPFs or under simultaneous degradation mechanisms (i.e. UV exposure in the presence of mechanical shaking).

Further analytical investigations (e.g. SEM, FTIR, analysis of leachates) were not performed on mechanically degraded MPFs for a variety of reasons. Primarily, mechanical degradation is known to not result in the chemical degradation of polymers only fragmentation. Based on 9-month fragmentation results and visual inspection of MPFs using light microscopy, no significant changes to either length or surface morphology were observed to warrant further investigation.

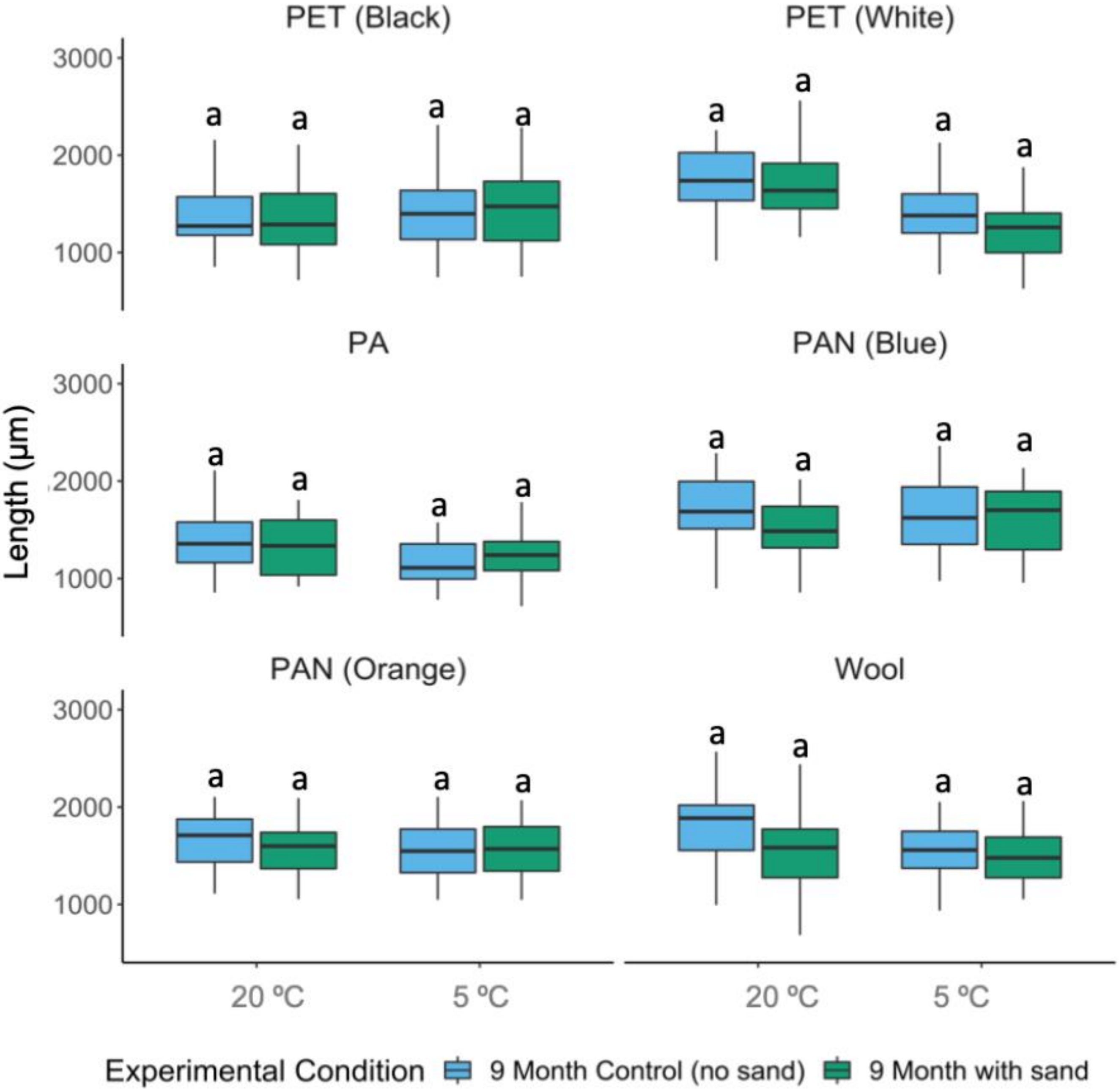

Figure 4.30. Fibre length (in µm) before and after 9-months of simulated mechanical degradation in seawater of black and white PET, PA, blue and orange PAN MPFs and wool. Statistical analysis was performed within groups: PET, PA, PAN and Wool respectively. Boxplots showing median length and interquartile range (IQR). N = 30 for all samples. Significant difference ($p < 0.05$) between groups are shown by letter codes, where the same letter indicates no significant difference ($p > 0.05$).

4.5 Identification of 'unknown' chemical additives

A wide variety of chemical compounds were tentatively identified in MPFs: black (B) and white (W) PET, white PA; blue (Bl) and orange (O) PAN and wool. Textile extractions were performed in various solvents: DCM, EtOAc, IPA, MeOH and hexane (Hex). Furthermore, tentatively identified compounds in aqueous leachates from UV and short 14-day leachate studies were also included. Compounds were only included in presented tables if they appeared in 2 or 3 replicates and had >80% match in the NIST database, unless otherwise stated. (Table 4.10, 4.11, 4.12 and 4.13, respectively). All tables are sorted by potential compound origin and ascending retention time. As described, these are tentatively identified compounds and should be discussed with a certain degree of caution, to confirm the identity of such compounds, appropriate standards should to be purchased. Dichloromethane and ethyl acetate extracted the highest percentage of compounds relative to other solvents and should be employed in the analysis of chemical additives in MPFs in future work. Oligomers (e.g. hydrocarbon) are excluded from the following discussion for simplicity but it should be noted that a high proportion of tentatively identified components in MPFs and wool were classified as oligomers and can be found in Appendix H, Table H.1. H.2, H.3 and H.4 for PET, PA, PAN and wool, respectively. In PET, approximately 50% of tentatively identified compounds were present in both PET types, with approximately 60 and 80% identified in white and black PET, respectively (Table 4.10). Degradation products were classified in PET, based on their occurrence in only UV leachates and the presence of carboxylic acid end groups. The majority of degradation products were found in both black and white PET fibres, suggesting a similar mechanism of photodegradation in both PET types, regardless of colour. PA contained few tentatively identified compounds that were not also present in procedural blanks (Table 4.11). The lack of identified plastic additives in PA may explain the high degree photodegradation observed after UV exposure. In PAN, approximately 85% of tentatively identified compounds were present in both PAN types, with approximately 80 and 92% identified in orange and blue PAN, respectively (Table 4.12). Variance in additive chemical composition may be the reason for the variations observed in photodegradation of these MPFs. Wool also contained a high proportion of unidentifiable compounds, perhaps due to them being of biogenic origin (Table 4.13). Distribution of tentatively identified compounds according to compound origin are presented in Figure 4.35. Principal component analysis (PCA) was attempted for non-target results, but the explained variance was very low, and statistical data treatment was therefore not investigated further in the current study. Investigation of non-target additive chemicals should be a focus of future work. It is evident from this non-target approach that a considerable proportion of chemical compounds are either not available in spectral databases or very little literature exist about their use and potential environmental impact. This emphasises the importance of continued work in non-target analysis to identify potential emerging contaminants.

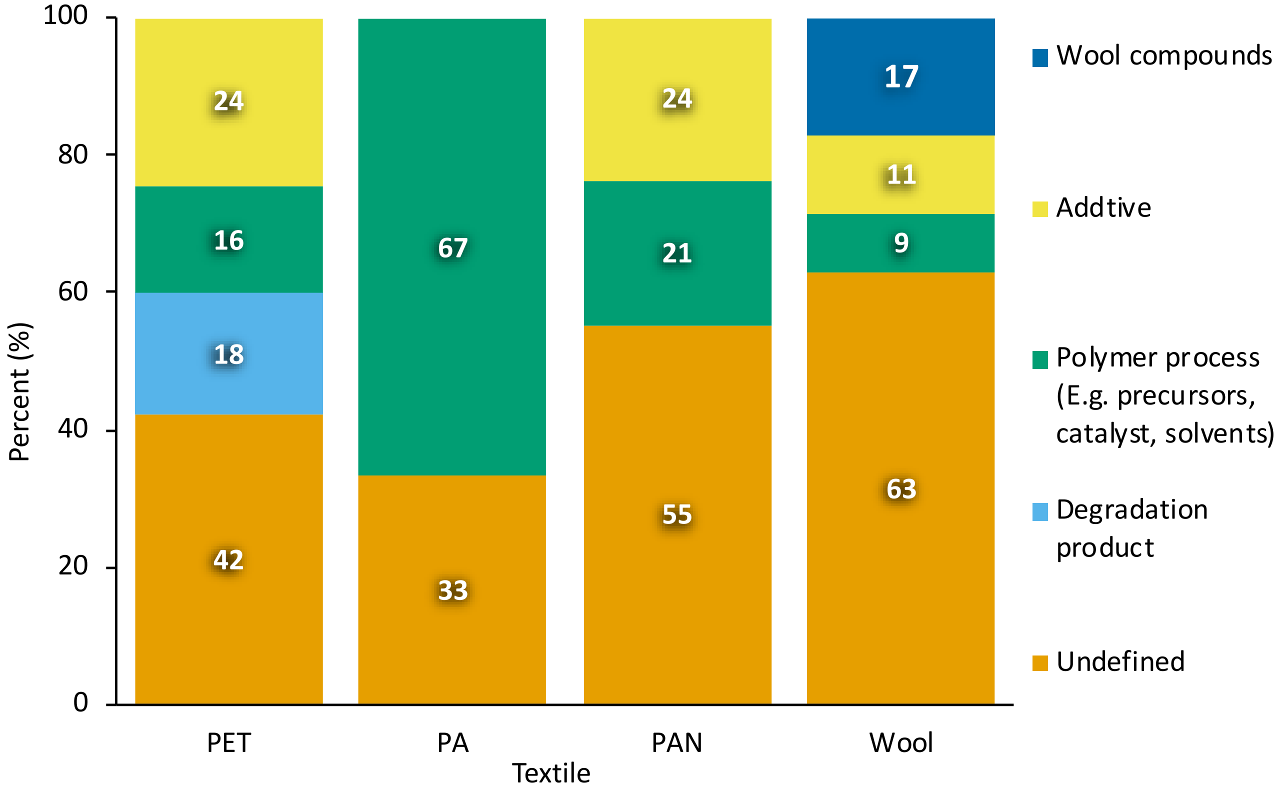

Figure 4.31. Distribution of type of compounds present in PET, PA, PAN and wool natural fibres according to the origin of the compound (Compounds identified as hydrocarbons and contamination and were not included in this graph)

Table 4.10. Tentative identified compounds in black (B) and white (W) PET MPFs

Compound Name	Formula	CAS ID	RT	Match	Polymer Extracts					Aqueous Leachates			Colour		Compound origin
					DCM	EtOAc	IPA	MeOH	Hex	14 days	UV (5 m)	UV (9 m)	B	W	
Benzoic acid, hydrazide	$C_7H_8N_2O$	613-94-5	12.99	94							×	×	×	×	Degradation product
Benzoic acid, methyl ester	$C_8H_8O_2$	93-58-3	13.01	98							× (SW)			×	Degradation product
2-Chloroethyl benzoate	$C_9H_9ClO_2$	939-55-9	14.6	84									×	×	Degradation product
Benzoic acid	$C_7H_6O_2$	65-85-0	14.6	96							×	×	×	×	Degradation product
Benzoic acid, 4-methyl-	$C_8H_8O_2$	99-94-5	17.23	94							×	×		×	Degradation product
Ethyl 4-methylbenzoate	$C_{10}H_{12}O_2$	94-08-6	17.79	91							× (SW)			×	Degradation product
Ethanone, 1-(2,4-dimethylphenyl)-	$C_{10}H_{12}O$	89-74-7	19.53	83							× (SW)	×* (SW)		×	Degradation product
2-Propanamine**	C_3H_9N	75-31-0	12.88	99	×	×								×	Dye related product
1(3H)-Isobenzofuranone	$C_8H_6O_2$	87-41-2	19.18	89								× (SW)	×	×	Dye related product
Nonanoic acid	$C_9H_{18}O_2$	112-050	17.16	84		×					× (FW)		×	×	Plastic additive
Octocrylene	$C_{24}H_{27}NO_2$	6197-30-4	40.7	92	×	×	×						×	×	Plastic additive – Photostabiliser
Isopropyl phenyl ketone	$C_{10}H_{12}O$	611-70-1	23.38	91							×			×	Plastic additive – UV coating
Benzophenone	$C_{13}H_{10}O$	119-61-9	24.97	88	×	×							×	×	Plastic additive – UV filter

Compound Name	Formula	CAS ID	RT	Match	Polymer Extracts					Aqueous Leachates			Colour		Compound origin
					DCM	EtOAc	IPA	MeOH	Hex	14 days	UV (5 m)	UV (9 m)	B	W	
2-Ethylhexyl salicylate	$C_{10}H_{18}O$	118-60-5	28.15	95	×	×	×	×	×				×	×	Plastic additive – UV filter
Dodecanoic acid	$C_{12}H_{24}O_2$	143-07-7	23.46	90	×	×							×		Plastic additive *but also high production compound
1,2-Ethanediol, monobenzoate	$C_9H_{10}O_3$	94-33-7	20.64	80	×	×						× (FW)	×	×	Polymer process
Terephthalic acid	$C_{12}H_{14}O_6$	959-26-2	34.27	85	×	×							×	×	Polymer process
2-Butenedioic acid (E)-, bis(2-ethylhexyl) ester	$C_{20}H_{36}O_4$	141-02-6	34.69	90	×	×							×*	×*	Polymer process
1,4-Benzenedicarboxylic acid, bis(2-ethylhexyl) ester	$C_{24}H_{38}O_4$	6422-86-2	41.48	93	×	×	×		×				×	×	Polymer process
4-Ethylbenzoic acid	$C_9H_{10}O_2$	619-64-7	19.33	89							× (SW)	× (SW)		×	Polymer process - Similar to starting product
Acetophenone	C_8H_8O	98-86-2	12.26	93	×	×					×	×	×	×	Polymer process - Solvent
3,4-Hexanedione, 2,2,5trimethyl-**	$C_9H_{16}O_2$	20633-03-8	13.06	88	×	×	×	×		×		×* (SW)	×	×	Undefined
nonanal	$C_9H_{18}O$	124-19-6	13.22	95	×	×	×	×	×				×	×	Undefined
Ethyl mandelate	$C_{10}H_{12}O_3$	774-40-3	14.44	89							× (SW)			×	Undefined

Compound Name	Formula	CAS ID	RT	Match	Polymer Extracts					Aqueous Leachates			Colour		Compound origin
					DCM	EtOAc	IPA	MeOH	Hex	14 days	UV (5 m)	UV (9 m)	B	W	
(+)-Dibenzoyl-L-tartaric acid anhydride	$C_{18}H_{12}O_7$	64339-95-3	14.63	89	×						× (SW)		×		Undefined
3-Phenyl-1-propanol, acetate	$C_{11}H_{14}O_2$	122-72-5	14.67	82								× (SW)		×	Undefined
Decanal	$C_{10}H_{30}O_5Si_5$	112-31-2	15.76	91	×	×		×*	×*					×	Undefined
2-Decenal, (E)-	$C_{10}H_{18}O$	3913-81-3	17.08	90	×	×									Undefined
1,2-Ethanediol, 1,2-diphenyl-, [R-(R,R)]-	$C_{14}H_{14}O_2$	52340-78-0	18.66	85							× (SW)			×	Undefined
Benzenemethanol, .alpha.-methyl-.alpha.-(1-methyl-2-propenyl)-	$C_{12}H_{16}O$	61967-11-1	18.94	87							× (SW)			×	Undefined
Diphenyl ether	$C_{12}H_{10}O$	101-84-8	20.33	83	×								×		Undefined
3-Methylbenzoic acid, 3-pentyl ester	$C1_3H_{18}O_2$	100032571-1	22.85	89	×	×					×* (SW)		×	×	Undefined
1-(2-(3-Cyclohexenyl)ethyl)silatrane	$C_{14}H_{25}NO_3Si$	1000427-34-2	23.99	81							×		×*	×*	Undefined
4-Ethylbenzoic acid, 2-methylbutyl ester	$C_{14}H_{20}O_2$	1000331-30-8	25.03	85							× (SW)			×	Undefined
Phenylglyoxylic acid, 2-butyl ester	$C_{12}H_{14}O_3$	1000453-46-5	25.17	85							× (SW)			×	Undefined

Compound Name	Formula	CAS ID	RT	Match	Polymer Extracts					Aqueous Leachates			Colour		Compound origin
					DCM	EtOAc	IPA	MeOH	Hex	14 days	UV (5 m)	UV (9 m)	B	W	
Sulfurous acid, 2-ethylhexyl hexyl ester	$C_{14}H_{30}O_3S$	1000309-20-2	26.93	80	×	×	×	×	×				×	×	Undefined
Oxalic acid, allyl nonyl ester	$C_{14}H_{24}O_4$	1000309-23-7	27.23	85									×	×	Undefined
1-Iodoundecane	$C_{11}H_{23}I$	4282-44-4	34.28	85	×*	×			×				×*		Undefined
Oxalic acid, allyl pentyl ester	$C_{10}H_{16}O_4$	1000309-23-2	35	84										×	Undefined

** indicates compound was identified by NIST at more than one RT across samples; * indicates compound was present in only 1 sample

Table 4.11. Tentatively identified compounds in Polyamide MPF

Compound Name	Formula	CAS ID	RT	Match	Polymer					Leachates			Compound origin
					DCM	EtOAc	IPA*	MeOH*	Hex*	14 days	UV (5 m)	UV (9 m)	
Caprolactam	$C_6H_{11}NO$	10560-2	16.8	85	×	×	×	×		× (SW)	× (SW)		Precursor product
Cyclopentanone, 2 cyclopentylidene-	$C_{10}H_{14}O$	825252	20.00	92	×					× (SW)			Polymer process
2-Butenal, 2-methyl-	C_5H_8O	111511-3	12.93	90								× (SW)	Undefined

** indicates compound was identified by NIST at more than one RT across samples; * indicates compound was present in only 1 sample

Table 4.12. Tentatively identified compounds in blue (Bl) and orange (O) PAN MPFs

Compound Name	Formula	CAS ID	RT	Match	Polymer Extracts					Aqueous Leachates			Colour		Compound origin
					DCM	EtOAc	IPA*	MeOH*	Hex*	14 days	UV (5 m)	UV (9 m)	Bl	O	
1-Hepten-3-one	$C_7H_{12}O$	2918-13-0	15.38	80							× (inc. D)		×	×	Plastic additive
Pentanoic acid, 2,2,4-trimethyl-3-carboxyisopropyl, isobutyl ester	$C_{16}H_{30}O_4$	1000140-77-5	24.26	87						× (FW)			×*	×	Plastic additive
1-Hexadecanol	$C_{16}H_{34}O$	36653-82-4	29.27	94	×	×	×	×					×	×	Plastic additive
Phthalic acid, 6-ethyl-3-octyl butyl ester	$C_{22}H_{34}O_4$	100031517-4	30.69	86								× (FW)		×	Plastic additive
Octadecanamide	$C_{18}H_{37}NO$	124-26-5	36.89	84	×*	×	×	×	×				×	×*	Plastic additive
Nonanoic acid	$C_9H_{18}O_2$	112-050	17.15	85							× (SW inc. D)		×*	×	Plastic additive - Lubricant for textiles
Cyclohexanol, 2-methyl-, propionate, trans-	$C_{10}H_{18}O_2$	15287-79-3	28.2	85		×							×		Plastic additive - Dye
1-Dodecanamine, N,N-dimethyl-	$C_{14}H_{31}N$	112-18-5	22.32	92	×	×	×	×					×	×	Polymer
Caprolactam	$C_6H_{11}NO$	10560-2	16.8	84	×*						× (inc. D)		×	×	Polymer process
Propanoic acid, 2-methyl-, propyl ester	$C_7H_{14}O_2$	644-49-5	19.66	85								× (FW)	×	×*	Polymer process

Compound Name	Formula	CAS ID	RT	Match	Polymer Extracts					Aqueous Leachates			Colour		Compound origin
					DCM	EtOAc	IPA*	MeOH*	Hex*	14 days	UV (5 m)	UV (9 m)	Bl	O	
Nonanamide	$C_9H_{19}NO$	1120-07-6	32.73	84	×	×	×						×*	×	Polymer process
2-Butenedioic acid €-, bis(2-ethylhexyl) ester	$C_{20}H_{36}O_4$	141-02-6	34.69	84						×			×	×	Polymer process
Ethanol, 2-ethoxy-	$C_4H_{10}O_2$	110-80-5	32.74	86	×			×		×* (FW)	× (FW)		×	×	Polymer process - Solvent
Acetophenone	C_8H_8O	98-86-2	12.24	82						× (FW)			×	×	Polymer process - Solvent for resins
3,4-Hexanedione, 2,2,5trimethyl-**	$C_9H_{16}O_2$	20633-03-8	13.06	92	×		×	×		× (FW)		×	×	×	Undefined
Nonanal	$C_9H_{18}O$	124-19-6	13.19	85	×	×	×	×					×	×	Undefined
Heptanediamide, N,N'-di-benzoyloxy-	$C_{21}H_{22}N_2O_6$	1000253-26-4	14.64	85	×								×		Undefined
2,4,4-Trimethyl-1-pentanol, trifluoroacetate	$C_{10}H_{17}F_3O_2$	100036519-5	15.38	82	×	×							×	×	Undefined
2-Butanone, 1,1,1-trifluoro-	$C_4H_5F_3O$	381-88-4	15.74	80	×	×							×	×	Undefined
DL-2,3-Butanediol**	$C_4H_{10}O_2$	6982-258	15.75	80	×	×*							×	×*	Undefined
Decane, 1-iodo-	$C_{10}H_{21}I$	2050-77-3	17.93	84	×*	×	×	×		×		×* (SW)	×	×	Undefined

Compound Name	Formula	CAS ID	RT	Match	Polymer Extracts					Aqueous Leachates			Colour		Compound origin
					DCM	EtOAc	IPA*	MeOH*	Hex*	14 days	UV (5 m)	UV (9 m)	Bl	O	
Propane, 1-(chloromethoxy)-2-methyl-	$C_5H_{11}ClO$	34180-11-5	19.44	87	×								×		Undefined
1,2,4,5Tetrazin-3-amine	$C_2H_3N_5$	79329-74-1	19.97	83	×							×* (FW)	×	×*	Undefined
Acetic acid, trifluoro-, 2,2-dimethylpropyl ester**	$C_7H_{11}F_3O_2$	7556-79-8	19.99	80	×									×	Undefined
Diazene, dimethyl-	$C_2H_6N_2$	503-28-6	22.38	91	×								×*	×	Undefined
Benzoic acid, 4-ethoxy-, ethyl ester	$C_{11}H_{14}O_3$	23676-09-7	22.86	91						×* (FW)		×	×	×	Undefined
Methyl[(1-methyl-2,3-dihydropyrrol-3-yl)methyl]amine	$C_7H_{14}N_2$	1000436-31-5	26.4	81									×		Undefined
Oxalic acid, allyl hexadecyl ester	$C_{21}H_{38}O_4$	1000309-24-4	29.27	90	×				×				×		Undefined
2,2'-Bi-1,3-dioxolane	$C_6H_{10}O_4$	670589-1	34.50	82		×		×						×	Undefined
4-Amino-1,6-dihydro-1-methyl-6-oxopyrimidine **	$C_5H_7N_3O$	1122-46-9	40.6	84	×	×							×		Undefined
Sulfurous acid, 2-ethylhexyl hexyl ester**	$C_{14}H_{30}O_3S$	1000309-20-2	41.57	86	×	×							×*	×	Undefined

** indicates compound was identified by NIST at more than one RT across samples; * indicates compound was present in only 1 sample; where ‘inc. D’ indicates that tentatively identified compound was also present in dark controls of UV leachates.

Table 4.13. Tentatively identified compounds in natural wool fibre

Compound Name	Formula	CAS ID	RT	Match	Polymer					14-day leachates	Compound origin
					DCM	EtOAc	IPA*	MeOH*	Hex*		
Nonanoic acid, 9-oxo-, methyl ester	$C_{10}H_{18}O_3$	1931-63-1	20.92	95	×	×	×	×	×		Additive
Pentanoic acid, 2,2,4-trimethyl-3-carboxyisopropyl, isobutyl ester	$C_{16}H_{30}O_4$	1000140-77-5	24.26	82						×* (FW)	Additive
Bis(2-ethylhexyl) maleate	$C_{20}H_{36}O_4$	142-16-5	33.58	83						× (FW)	Additive - Fibre production process
Oxalic acid, allyl tridecyl ester	$C_{18}H_{32}O_4$	1000309-24-1	44.65	82	×						Additive - Fibre production process
1,14-Tetradecanediol	$C_{14}H_{30}O_2$	19812-64-7	20.37	87	×	×	×				Polymer
2-Butenedioic acid (E)-, bis(2-ethylhexyl) ester	$C_{20}H_{36}O_4$	141-02-6	34.7	86			×	×		×	Polymer
1,4-Benzenedicarboxylic acid, bis(2-ethylhexyl) ester	$C_{24}H_{38}O_4$	6422-86-2	41.44	85	×	×	×	×	×		Polymer
Ethanol, 2-ethoxy-	$C_4H_{10}O_2$	110-80-5	33.99	82		×	×			×* (SW/FW)	Polymer - solvent in dye bath
Octanoic acid, methyl ester	$C_9H_{18}O_2$	111-11-5	13.71	82	×	×					Wool compound
Pentadecanal-	$C_{15}H_{30}O$	9112765	24.49	95		×					Wool compound
Eicosanoic acid, methyl ester	$C_{21}H_{42}O_2$	1120-28-1	36.06	87	×	×	×				Wool compound

Compound Name	Formula	CAS ID	RT	Match	Polymer					14-day leachates	Compound origin
					DCM	EtOAc	IPA*	MeOH*	Hex*		
Desmosterol	$C_{27}H_{44}O$	313-04-2	46.24	90	×*	×	×	×	×		Wool compound
Cholesta-3,5-dien-7-one	$C_{27}H_{42}O$	567-72-6	46.78	85		×	×				Wool compound
9-Octadecenoic acid, methyl ester, (E)-	$C_{19}H_{36}O_2$	1937-62-8	32.8	99	×	×	×	×	×		Wool compound - Oil
Nonanal	$C_9H_{18}O$	124-19-6	13.19	98	×	×	×	×	×		Undefined
Cyclobutane-1,1-dicarboxamide, N,N'-di-benzoyloxy-	$C_{20}H_{18}N_2O_6$	1000253-25-3	14.71	95						× (SW)	Undefined
Nonanoic acid	$C_9H_{18}O_2$	112-05-0	17.17	87	×	×	×	×			Undefined
3,4-Hexanedione, 2,2,5-trimethyl-	$C_9H_{16}O_2$	20633-03-8	17.96	85	×			×	×		Undefined
Benzoic acid, 4-ethoxy-, ethyl ester	$C_{11}H_{14}O_3$	23676-09-7	22.86	96						× (20)	Undefined
Cyclohexanepropanol-	$C_9H_{18}O$	1124-63-6	24.49	82	×			×			Undefined
2-Bromotetradecane	$C_{14}H_{29}Br$	74036-95-6	31.2	89	×	×	×				Undefined
Sulfurous acid, 2-ethylhexyl isohexyl ester**	$C_{14}H_{30}O_3S$	1000309-19-0	31.22	88	×	×		×		×	Undefined
Docosane, 1-iodo-	$C_{22}H_{45}I$	1000406-31-9	37.85	89	×	×	×	×	×		Undefined
Oxalic acid, allyl nonyl ester**	$C_{14}H_{24}O_4$	1000309-23-7	39.27	91	×					×* (SW)	Undefined
Tetracosane, 1-iodo-	$C_{24}H_{49}I$	1000406-32-0	40.38	93	×	×	×	×	×		Undefined

Compound Name	Formula	CAS ID	RT	Match	Polymer					14-day leachates	Compound origin
					DCM	EtOAc	IPA*	MeOH*	Hex*		
Decane, 1-iodo-	$C_{10}H_{21}I$	2050-77-3	42.01	89						×(FW)	Undefined
Pyrrolidine, 1-methyl-	$C_5H_{11}N$	120-94-5	43.71	87		×					Undefined
Cycloheptane, bromo-	$C_7H_{13}Br$	2404-35-5	44.65	84	×						Undefined
Sulfurous acid, cyclohexylmethyl heptadecyl ester	$C_{24}H_{48}O_3S$	1000309-22-5	44.73	82	×						Undefined
Octacosane, 1-iodo-	$C_{28}H_{57}I$	1000406-32-2	44.91	87	×	×	×				Undefined
2-Propyn-1-amine, N,N-dimethyl-	C_5H_9N	7223-38-3	45.44	81	×	×	×				Undefined
Sulfurous acid, butyl decyl ester	$C_{14}H_{30}O_3S$	1000309-17-7	46.35	83	×					× (FW)	Undefined
Sulfurous acid, 2-ethylhexyl hexyl ester	$C_{14}H_{30}O_3S$	1000309-20-2	46.97	87		×		×			Undefined
Sulfurous acid, hexyl pentadecyl ester	$C_{21}H_{44}O_3S$	1000309-13-7	53.04	89	×	×					Undefined
Oxalic acid, allyl hexadecyl ester	$C_{21}H_{38}O_4$	1000309-24-4	54.71	87	×	×					Undefined
2-Propyl-1-pentanol	$C_8H_{18}O$	58175-57-8	55.3	83	×						Undefined

** indicates compound was identified by NIST at more than one RT across samples; * indicates compound was present in only 1 sample

4.6 Bisphenol and benzophenone investigation

4.6.1 Method performance

Absolute recoveries of bisphenols and benzophenones in black PET, white PET, PA, blue PAN, orange PAN MPFs and wool ranged from 57 to 77 %, with >70 % for the majority of target analytes (Appendix E, Table E.3.). The recoveries of target analytes are similar to a previous study investigating BzP and BPs in textiles (Xue et al., 2017). All ion ratios (IR%) met the criteria of tolerance stated in the European Commission Decision 2002/657/EC (European Commission, 2002) and can be found in Appendix E (Table E.4). The LODs of the target analytes in textiles ranged from 0.03 to 0.17 ng/mL (Table E.5). Concentrations detected below the LOD have been removed from the dataset. Relative standard deviation (RSDs) for all target analytes were below 6% (Table E.6). Contamination was evaluated by the analysis of procedural blanks. For each batch of ten samples analysed, one procedural blank was analysed. BPA, BPS, BzP1, BzP2, BzP3 and 4-OH-BzP were detected in all blanks. In all cases, the concentration in procedural blanks were subtracted from measured concentrations in MPFs and wool. It is acknowledged that evaporation is likely responsible for observed contamination. The matrix effects (MEs) were found for all target analytes and measured at a fortification level of 20 ng/ml. MEs ranged from +19.4 to –34.6% (Table E.7). Slight ionisation enhancement was demonstrated for BzP8 (7.3), BPF (16.6), 4-OH-BzP (18.5) and BPAF (19.4), whereas ionisation suppression in the range of –2.1 to –34.6 % was found for remining target analytes.

4.6.2 BPs and BzPs content in fibres

The concentration of BPs and BzPs in MP and wool fibres are presented in Figure 4.32 and 4.33, respectively. Mean concentration and detection rates can be found in Appendix E, Table E.1. BPA is the major bisphenol component across all samples, with median concentrations ranging from 25.36 to 500.60 ng/g. BPA has been reportedly used in polyester as a finisher, however this is the first study investigating its occurrence in PA, PAN and wool (Xue et al., 2017). BPA is often used as an intermediate in the manufacture of dyes, which may explain the higher median BPA levels observed in coloured MPFs (black PET, blue PAN and orange PA) compared to undyed MPFs (white PA and PET). Wool showed the highest median concentration of BPA at 500.60 ng/g, it is unclear as to why this may be the case and what the source of BPA as there is no existing literature on the use of BPA in the processing of wool fibres. It was thought wools high levels of BPA may be attributed to its capacity to sorb chemicals, however in-house adsorption studies undertaken alongside this project indicate PA adsorbs polycyclic aromatic hydrocarbons (PAHs) at a higher rate relative to other MPFs (including wool) (Mansour et al., 2015; Nguyen, T,. 2019). BPA would be expected to behave differently PAHs due to variation in relative hydrophilicity. The next most abundant BP in MPFs (including wool) was BPS with median concentrations between 0.43 and 1.95 ng/g. BPS is a common replacement for BPA in industry, and according to the European Chemical Agency (EHCA) 10 000 – 100 000 tonnes is either manufactured or imported in the European Economic Area each year (European Chemicals Agency, 2019). Despite a detailed literature search, little information was available on the use and sources of BPS, BPF, BPAF and BPAP. The presence of BPAF in PAN blue and not PAN orange is unclear but may indicate its use as an intermediate chemical in certain dyes.

BzPs are employed as UV coatings in textiles (Mavrić and Simončič, 2018). BzP3 is the major benzophenone component across all samples (Figure 4.33). Lower median concentration of BzP3 were found in blue and orange PAN at 4.33 and 7.77 ng/g, respectively. Higher, but similar median BzP3 concentrations were seen in black PET, white PET, PA MPFs and wool at 17.91, 16.98, 13.61 and 20.74 ng/g, respectively. BzP3 has been shown to transfer to humans through dermal exposure through clothing (Morrison et al., 2017). Little literature exists about specific uses of BzP1 and 4-OH-BzP outside of the standard BzP applications (E.g. UV filter in plastics and use in personal care products like sunscreens and cosmetics). Similar to BPs, wool showed the highest total BzP content at 26.93 ng/g.

BPA, BPS and BzP3 were found to be the most prominent BP and BzP analytes in MPFs and wool, consistent with a recent study examining these analytes in children’s textiles (Carr et al., 2016). Higher median concentrations of BPA and BPS were observed in coloured textiles than in white or undyed textiles, similarly to Xue et al, findings (2017). In contrast to Xue findings, which found synthetic clothing to have higher levels of BPs and BzPs, compared to natural cotton textiles. However, most textiles employed in Xue’s study were not homogenous (e.g. 100% polyester). Textile blends (e.g. spandex and PET) may account for higher observed concentrations in synthetic fibres relative to natural fibres. Many BP and BzP are employed in a wide range of personal care products (e.g. cosmetics, hair products, sunscreens). Although steps were taken to minimise contamination and blanks subtracted, introduced contamination is always a challenge when working with trace pollutants.

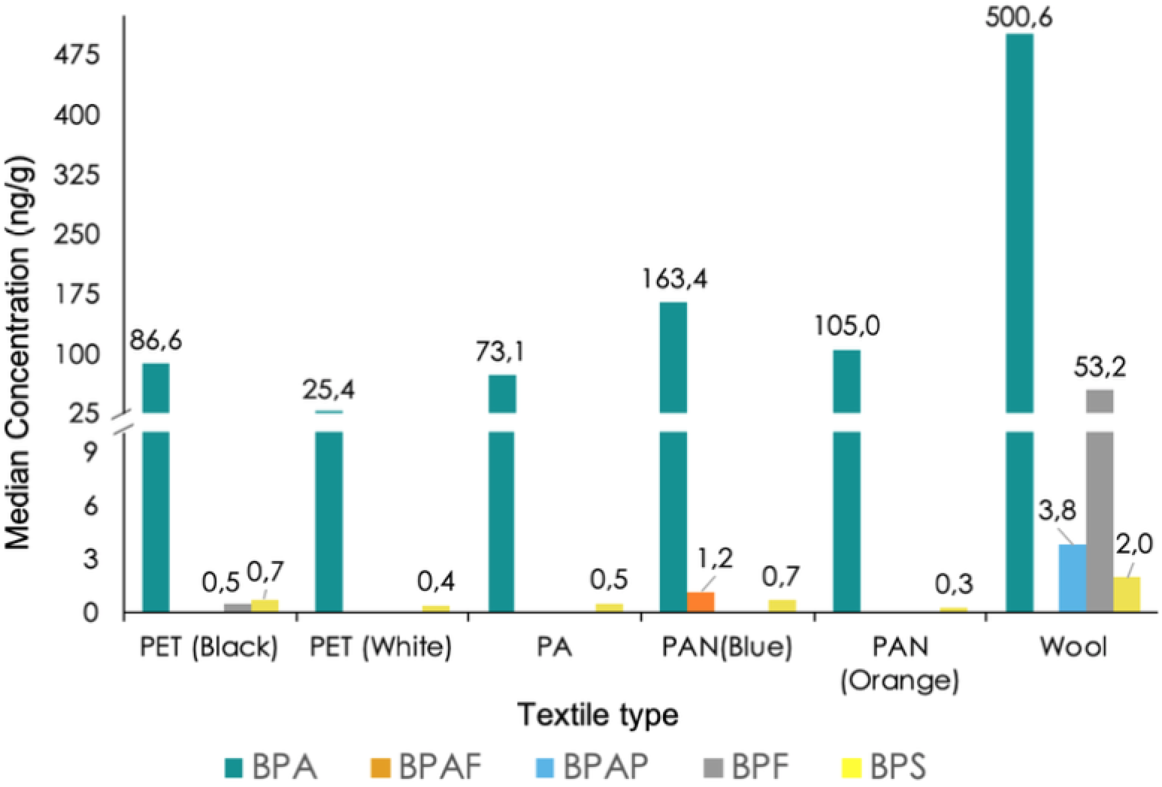

Figure 4.32. Median concentration of bisphenol compounds in black PET, white PET, PA, blue PAN, orange PAN MPFs and natural wool fibre

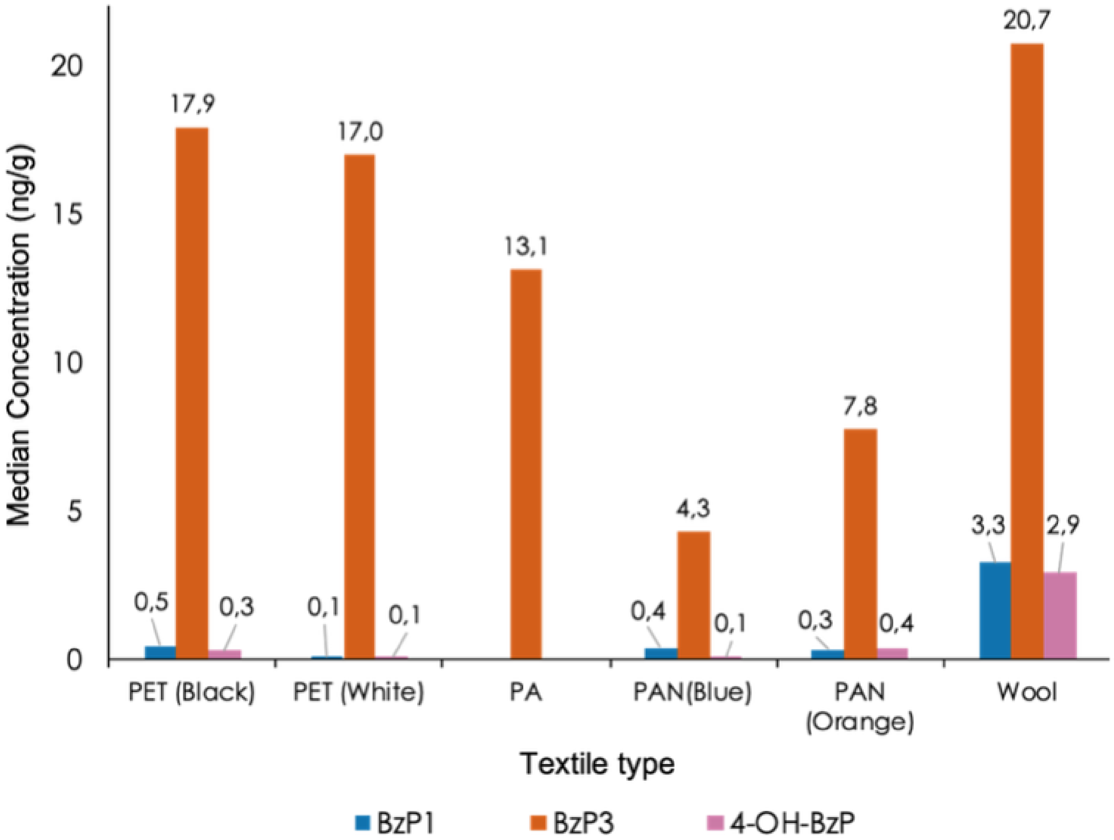

Figure 4.33. Median concentration of benzophenones in black PET, white PET, PA, blue PAN, orange PAN MPFs and natural wool fibre

4.6.3 BP and BzP content in leachates

All BP and BzP compounds were found below the limit of detection in short 14-day leachates, as well as in the 5- and 9-month UV leachates. With the exception of BPA, the BP and BzP content in pristine fibres was at quite low concentrations across all samples, which is likely why no leaching was detected. While BPA and BzP compounds have been found to leach from plastic materials, these studies are often conducted at higher temperatures with lower environmental relevance (Sajiki and Yonekubo, 2003; Tan and Mustafa, 2003). BPA has been shown to undergo photodegradation under simulated environmental conditions which could suggest that any leached BPA in UV leachates may have photodegraded (Sajiki and Yonekubo, 2003). Though, no detectable leaching of BPA in UV leachates is likely accredited to low MPF concentrations (1 mg MPF/mL). According to literature, benzophenones exhibit various levels of photostability when exposed to UV radiation, BzP3 is considered to be quite photostable where as BzP2 is highly susceptible to photodegradation (Liu et al., 2011). In short leachate studies, exposure concentration was high and performed in the dark, so no photodegradation would occur. Similarly, leaching of BP or BzP compounds was not detected. In short leachate studies. Despite a comprehensive literature search, comparable leaching studies do not appear to have been performed with textiles before this study.

4.7 Correlation between organics and inorganics (BPs, BzPs and Metals)

To study the relationships between inorganic variables (Appendix F, Tables F.3 and F.4) and organic bisphenol (BP) and benzophenone (BzP) content (Table 4.14), in MPF and wool fibres a PCA was performed (Figure 4.34) and a correlation heat map constructed (Figure 4.35). The variance explained by the first two principal components was 61.4%. Ideally, the variance of the first two components should be over 70%, but >60% allows for the discussion of any general trends. PET and PA MPFs showed a tendency to group together and were influenced by Ni, Cr, Mn, Sb and Mo and to a lesser extent by Hf, Zr, and Co. As previously stated, Antimony (Sb) is used a catalyst in the manufacture of PET fibres, and also is employed as a co-synergist in combination with flame retardants. PAN fibres were grouped together in the bottom right quadrant. BPAF was highly correlated with blue PAN as it was detectable only in blue PAN, which may indicate that it was an intermediate used in the production of the blue dye. PAN fibres appear to be influenced by Sn, K, U, Ta, Na, Se and Ba. And through a lesser extent by Mg, Li, Ca, P and Al. PAN appears to be the lowest potential for toxicity of all textile types according to its associated metals. BPA, BPAF+BPF, BPS, Sum BPs were strongly correlated to wool, as all BPs were found at the highest concentrations in wool. Wool samples appear to be are influenced by Hg, Au, Fe, S, Cu, Sc, Zn and Bi and to a lesser extent by Pb, La, Ce, Cs, Zn, Sc, Y, Th and Nd. Wool shows high variance across triplicates, which may be attributed to it complex heterogenous structure (The University of Waikato, 2007). Ti was present at similar concentrations across MPFs and low concentrations in wool, due to its use as a delustering agent in fibre processing. The biplot indicates strong correlation between BPA and BP analogues (namely BPS and BPF), as they are often employed as replacement chemicals in the phase out of BPA. According to the correlation heatmap (Figure 4.35), no strong correlations are observed between metals and BzPs. Hg showed strong positive correlation with BPAF and BPF ($r = 0.79$). Cs showed strong correlations to BPA ($r = 0.78$), BPS ($r = 0.75$) and total BPs ($r = 0.75$). Organic-metal correlations are most likely related to the higher observed concentrations of both metals and organic analytes (Bps and BzPs) in wool rather than an analogous source of inorganic and organic contamination. Regarding metal-metal correlations, Cu and Zn were strongly positively correlated ($r = 0.96$), as were Hg and S ($r = 0.81$). Hg and S are likely correlated due to higher presence of both these elements in wool, wool and other mammalian hair have high S content due to the presence of thiol (SH) groups on their surface, allowing for the adsorption of inorganic molecules (McLean et al., 2009).

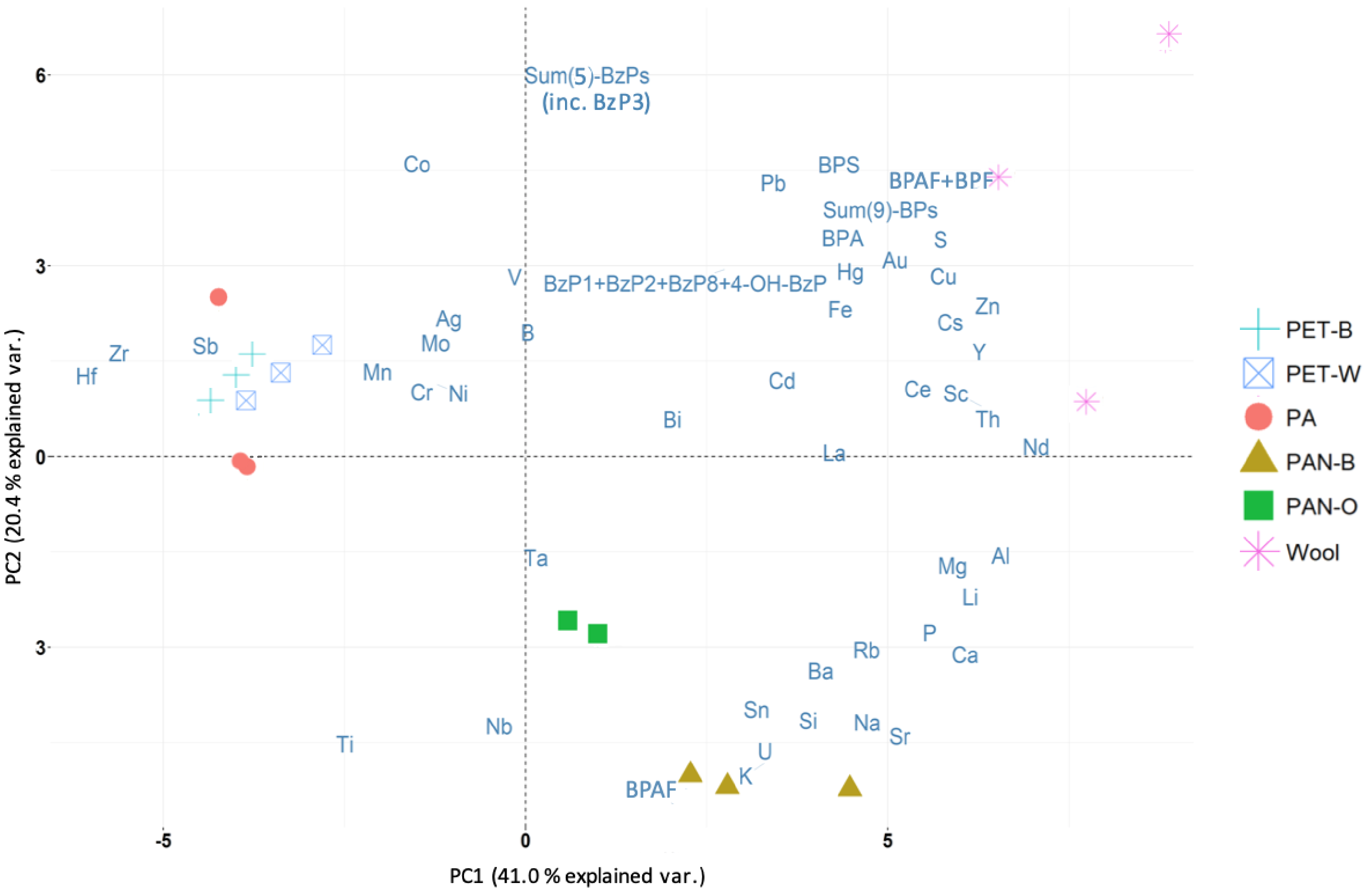

Figure 4.34. PCA bi plot (combined scores and loading plot) of metals, BPs and BzPs.

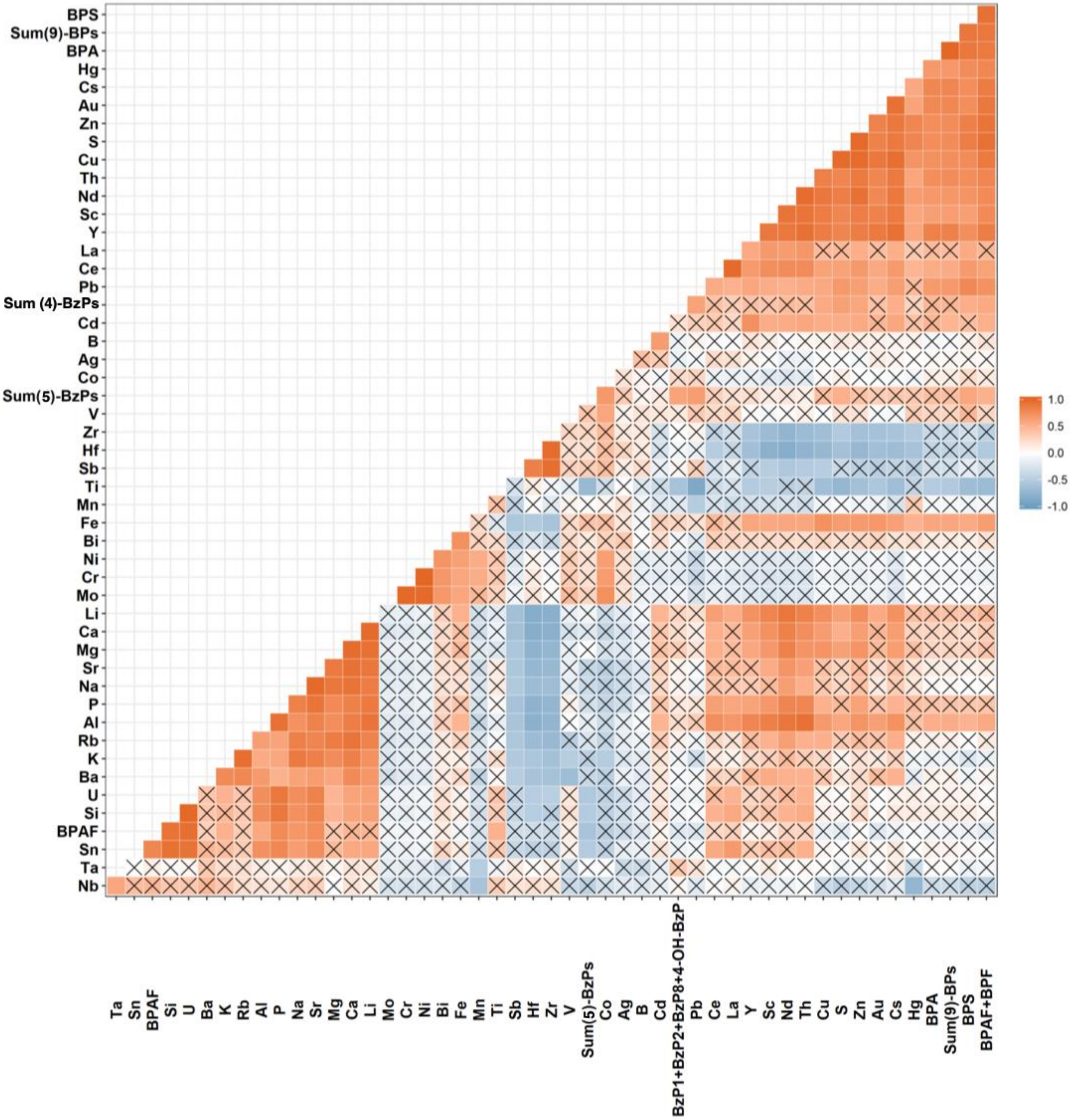

Figure 4.35. Correlation heat map matrix of BPs, BzP and metals, where dark orange indicates strong positive correlations, blue indicates strong negative correlations and ‘✕’ indicates statistically insignificant correlations ($p > 0.05$)

4.8 Screening of antioxidants, UV and thermal stabilising additives

All MPFs and wool were screened for the presence of several antioxidant, UV and thermal stabilising chemical additives (Chimassorb 81; Chimassorb119; Chimassorb 2020; Cyasorb UV-541; 1Irgacure 369; Irgacure 1800; Irgacure 2959; Irgafos P-EPQ; Irgafos168; Irgafos 38; Irganox 1010FF; Irganox 1076; Irganox1081; Irganox 1330; Irganox 1425; Irganox B220; Irganox HP 2215 and Tinuvin 622; Tinuvin 234; Tinuvin 327; Tinuvin 328). Analyte specific conditions can be found in Appendix I, Table I.1. Several chemical additives (Chimassorb 81; Chimassorb119; Chimassorb 2020; Irgacure 369; Irgacure 2959; Irgafos P-EPQ; Irganox 1010FF; Irganox 1076; Irganox1081; Irganox 1330; Irganox 1425 and Tinuvin 622) could not be successfully analysed via GC-MS due to their respective size and/or polarity. Cyasorb UV-5411; Irgacure 1800; Irgafos 38; Irgafos168; Irganox B220; Irganox HP 2215; Tinuvin 234; Tinuvin 327; Tinuvin 328 were able to be analysed with GC-MS but were not detected in MPFs or wool. Tinuvin 324 and 328 are used in the manufacture of industrial synthetic fibres (e.g. carpets and insulation), but little data exist on their use in conventional textiles ("BASF Light Stabilizers for Synthetic Fibers," 2017). Cyasorb UV 5411, Irgafos 168 and Tinuvin 327 are known skin irritants, and as such may be specifically avoided in textiles that are designed to be in close and prolonged contact with skin (BASF, 2016; Cytec, 2012) Despite a thorough literature search, little information could be found on either the specific application or safety of Irgacure 1800; Irgafos 38 Irganox B220 and Irganox HP 2215. Irganox® and Irgafos® are additives that are often added to account for high temperatures during fibre processing. The lack of detection of target plastic additives in MPFs is likely not representative of the overall additive content in test materials.

4.9 Inorganic content from short leachate studies

The percent leaching of select metals from Black PET, PA, Orange PAN MPFs and wool to aqueous leachates (freshwater media (20 °C) and seawater at 5 and 20 °C, respectively) is displayed in Figure 4.36. Full inorganic content from short leachate studies can be found in Appendix F (Tables F.3 and F.4) Even after subtracting average blank concentrations, a majority of analysed elements were found at higher concentrations in aqueous media than determined in the MPFs and wool. This indicates that there is a source of metal contamination from either the exposure system or the sample processing step. Metal contamination could have been introduced at multiple stages in the current study but is likely due to the use of glass sample vessels that were not pre-washed with acid. Glass was chosen for this study to avoid any potential leaching of additives from plastic containers. Contamination was likely also introduced during filtration of the MPFs. A higher degree of metal leaching is observed at higher temperatures for most metals, which is consistent with previous studies (Fu et al., 2018; Muzenda et al., 2011). However, due to high levels of contamination, no conclusions should be drawn from this data. Leachate studies should be repeated in acid-washed plastic vials to minimise contamination, but this would need to be conducted as a dedicated study separate to that of organics. MPFs contained low concentrations of nearly all analysed metals indicating that leaching may not be of environmental concern, although this is worth further investigation due to the sheer volume of MPFs that end up in marine and freshwater environments.

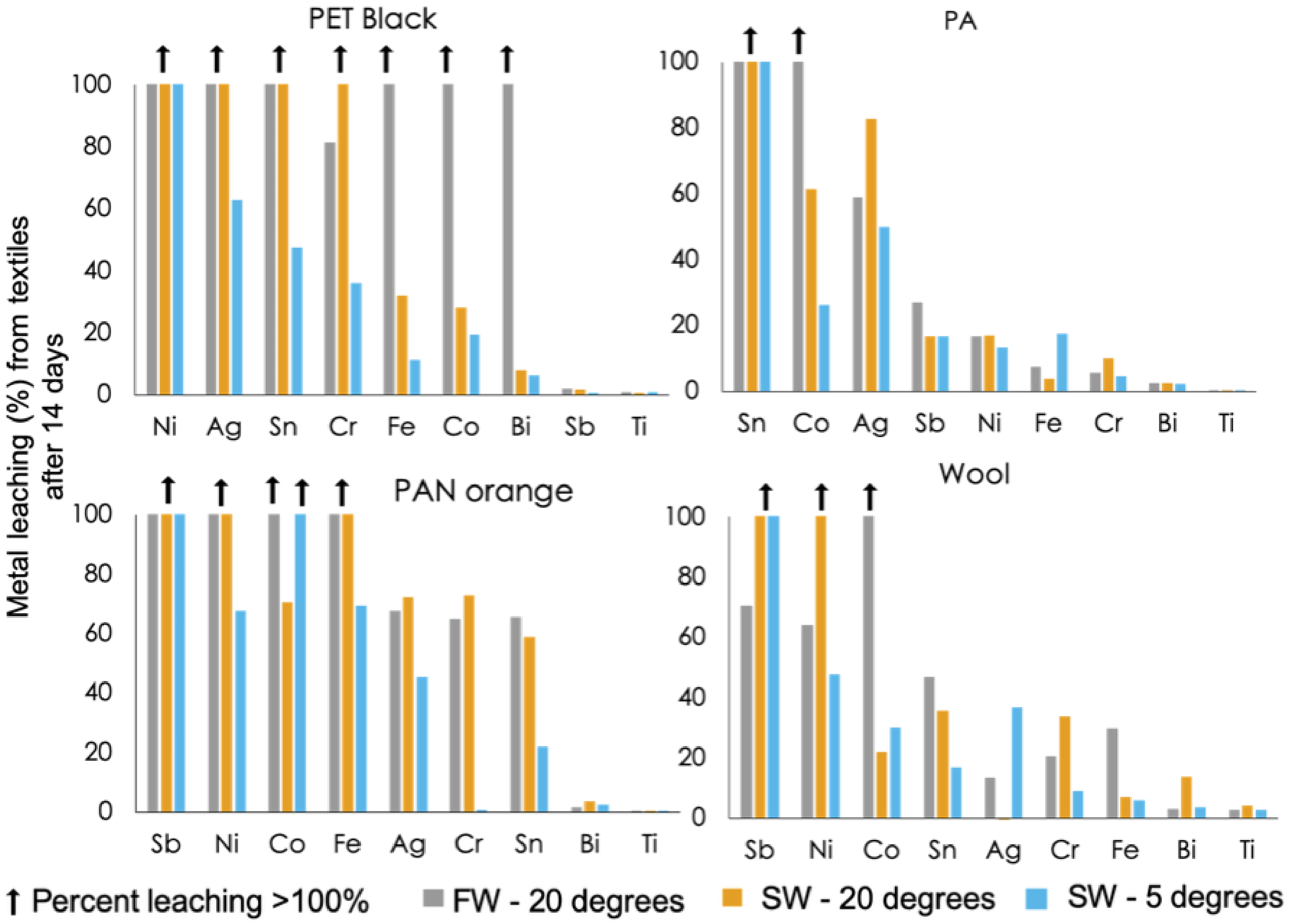

Figure 4.36. Percent leaching of select metals are shown for black PET, PA, orange PAN MPFs and wool fibres.

4.10 Implications of findings

The broader implications of these findings for identifying and selecting MPF materials for synthetic textiles are not immediately clear. It may be desirable for MPFs to degrade at quicker rates, instead of remaining persistent in aquatic environments. Conversely, greater rates of degradation and subsequent fragmentation could result in the formation of nano-sized particles and increases in particle surface area. When considering the degradative fate of a single MPF, slow rates of fragmentation will increase the potential of exposure to many types of aquatic organisms. Its subsequent fragmentation will cause the formation of smaller particles each of which has the potential to be exposed to an aquatic organism. Increased fragmentation will likely lead to a greater number of exposures or interactions. It is proposed that faster degradation rates are more desirable as all MPFs will eventually undergo complete degradation and remineralisation into CO_2. It is suggested that faster degradation will result in fewer interactions or potential exposures with aquatic biota before complete degradation.

Findings suggest that without prior UV-mediated embrittlement, mechanical degradation, even under high energy abrasive scenarios has little impact on MPF fragmentation. Suggesting that, only sediment interaction in shallow water would result in significant fragmentation of MPFs. MPFs in deep sea would likely remain relatively intact if not sufficiently embrittled by other degradative means. No obvious differences were observed between seawater and freshwater exposure indicating that photodegradation is not significantly impacted by relative differences in salinity. However, freshwater ecosystems can be quite sensitive to small changes relative to marine environments as a result it is likely that any potential impacts of fragmentation and subsequent exposure may be greater in freshwater environments.

It is also important to consider the exposure conditions used within this study in terms of potential exposure scenarios that are likely natural environments. Based on mean European UV irradiance, this 9-month UV exposure study is equivalent to approximately 7.5 years. However, when plastics or MPFs enter aquatic environments they will not be exposed to UV at an even rate and likely will not stay in surface shallow waters, where they can undergo photodegradation. The majority of plastics and MP are thought to sink to sediments as a result of materials naturally having a higher density than natural waters, or when density increases due to processes including biofouling and heteroaggregation. In all cases, transport of plastic and MP to sediments will significantly retard UV-derived degradation. It is therefore important to note that the rate of photodegradation observed in this investigation is expected to be considerably faster than what would be observed in natural environments. High rates of degradation are expected along beaches or shorelines, due to the availability of sunlight, in combination with waves and high energy forces. In deep sea regions, you would expect minimal degradation due to the absence of UV in conjunction with low energy.

PET MPFs underwent surface changes and significant fragmentation after UV exposure Differences observed in the surface are likely attributed to chemical additive content. The use of additives can result in either increased or decreased UV degradation depending on their intrinsic properties. Additives can be designed to prevent UV degradation (e.g. light stabilisers) or incorporated for other reason (e.g. as a dye) which may increase a materials susceptibility to degradation. Given the wide range of functions and properties of chemical additives, it is difficult to interpret their potential impact on materials in relation to degradation. PET black had considerably higher median concentrations of BPA relative to white PET at 86.64 and 25.36 ng/g, respectively. This difference is likely attribute to BPAs use as a dye intermediate. Little is known about how BPA might influence the degree of photodegradation, but any chemical impurities which contain chromophoric groups (i.e. groups capable of absorbing UV) are thought to increase a materials susceptibility to photodegradation (Rabek, 1996). PA underwent the greatest degree of degradation based on surface chemical changes. Interestingly, the lowest number of tentatively identified compounds (including UV additives) were found in PA, which could explain its higher rate of photodegradation in relation to other MPFs. Photodegradation was observed in a higher degree in blue PAN relative to orange PAN. PAN blue did contain a higher number of components (including chemical additives) identified through non-target analysis, which may increase its susceptibility to photodegradation. In addition, a higher BzP content was observed in orange PAN, which may explain the smaller degree of surface photodegradation comparative to blue PAN. The impact of inorganic content on photo susceptibility should be further investigated. TiO_2 as discussed previously is a known photo-initiator (Barker, 1975; Glass et al., 2018). It's high presence in PA, may be responsible for the degree of photodegradation observed. Similarly, Ti was present in high amounts in PAN blue, which conversely exhibited low levels of photodegradation. While no leaching of BP and BzPs was detectable, degradation studies should be repeated at higher MPF concentration, to determine if leaching can occur under environmental conditions. The characterisation of chemical additive content is difficult but crucial for understanding the fate and potential effects of MPFs in natural environments.

Conclusions

The aim of this research was to investigate the degradative fate of polyester (PET), polyamide (PA) and polyacrylic (PAN) MPFs in marine and freshwater environments by conducting long-term UV exposure and mechanical abrasion studies under environmentally relevant conditions. The study also investigated the organic and inorganic additive content in both MP and wool fibres, and their respective potential for leaching into seawater and freshwater media.

Accelerated UV exposure studies were conducted over a 9-month period in seawater and freshwater media. PET and PA showed significant photodegradation after UV exposure, characterised by changes in colour, fibre length (fragmentation) and surface morphology. Despite exhibiting strong colour fading, PAN MPFs did not undergo significant photodegradation during the 9-month exposure period. The results clearly show that PET and PA degrade and fragment much faster under environmentally relevant conditions than PAN MPFs. Although nano-sized fragments could not be identified, it seems likely that they are formed during the photodegradation of MPFs. In contrast to UV degradation, mechanical abrasion studies conducted with sand at 5°C and 20°C showed no signification changes in fibre length after the 9-month exposure ($p > 0.05$). It is proposed that mechanical abrasion could be a more significant degradative pathway when it occurs in combination with other degradation mechanisms (e.g. photodegradation) that increase particle brittleness, but this was not explored in this investigation.

A non-target approach for analysis of chemical additives in MPFs and their leachates was performed. The majority of chromatographically resolved compounds could either not be identified in the NIST database or characterised based on their potential origin or source. This emphasises the importance of continued work in non-target analysis to identify potential emerging contaminants. The content of bisphenols (BPs) and benzophenones (BzPs) was investigated in MPFs and wool. BPA and BPS were present in all samples, with BPA at the highest concentrations ranging from ~25 - 500 ng/g. BzPs were found in all MP and wool fibres, with BzP3 at the highest concentrations ranging from ~4 - 20 ng/g. Wool exhibited the highest total concentration of BPs and BzPs, which may be attributed to the nature of its structure, allowing high absorption of organic molecules. Given the known endocrine disrupting effects associated with bisphenols and benzophenones, their use in textiles in not trivial. BPs or BzPs could not be detected in aqueous leachates from either the short (14-day) leaching studies or the 9-month UV exposures. This may be due to the low concentration of analytes in the fibres themselves and, in the case of the UV exposed leachates, to the photosensitivity of some target analytes (e.g. BPA). Screening of the MPFs and wool for the presence of several common UV and thermal stabilising additives indicated these were not present at detectable levels. Many of these additives are known to cause skin irritation, so it is probable that they are not present in the test materials as they derive from textile yarns manufactured for producing clothing.

For the majority of inorganic elements measured in textile fibres, wool showed higher concentrations relative to MPFs. Mammalian hair is known to adsorb metals and is often used as an accumulative bioindicator for metal pollution. MPFs displayed low levels of metals with Sb, Cd, Cr, Co, Cu, Pb, Ni and Hg, all below the allowed limit values set by international textile standard, Oeko-Tex 100. Due to high levels of metal contamination in leachate studies, no conclusions were drawn about the potential for inorganic leaching from MP and wool fibres.

Through principal component analysis (PCA), it was possible to visualise possible associations between MPFs and determined BP, BzP and metal content. Wool was grouped closely with the majority of target BPs and BzPs, as well as toxic metals, Hg, Pb and Cd. These findings suggest that wool may represent a greater exposure risk to both organic and inorganic chemicals than MPFs.

Based on the current study, it is evident that the eventual fate and possible effects of MPFs released to the environment are likely influenced significantly by numerous factors, including environmental parameters and intrinsic material-specific properties. While more research is necessary, synthetic fibres may not pose a greater environmental risk than natural fibres.

Recommendations for further work

The UV exposure equipment used in the current study had limited capacity to include many different test materials. Furthermore, the timescale required to conduct UV degradation studies prevented more than one experiment from being conducted. The degradative fate of other textile types needs to be investigated including natural and semi-synthetic textiles. Given, the results of this study and the potential impact of wool, UV exposure studies should be repeated both with replicates and a natural fibre control (e.g. wool or cotton). It would be valuable to conduct UV exposure studies with a constant supply of O_2 in order to have more control over the rate of photodegradation. In the natural environment, degradative processes are complex and generally occur simultaneously as such, the cumulative effect of photodegradation coupled with mechanical degradation should also be investigated by, either performing sand abrasion studies with UV exposed MPFs or under simultaneous degradation mechanisms (i.e. UV exposure in the presence of mechanical shaking).

Based on preliminary non-target findings, future work should investigate the tentatively identified compounds present in the MPFs, in addition to determining any toxicity of these chemicals towards aquatic organisms. Some elucidation of MS spectra would also be advantageous to identify potential compounds that are not present in spectral databases. Given that a majority of chemical additives are either large or very polar, non-target screening of additive content via LC-MS would give a better impression of total additive chemical content in MPFs. While a workflow method was developed to analyse non-target compounds, it is time intensive and needs to be automated to a greater extent to allow for faster and more efficient processing. Given the high level of metal contamination in leachate studies, these should be repeated separately from any organic leachate studies and conducted in acid washed plastic vials. Metal analysis of UV leachates should also be performed, to gain an understanding on the impact of degradation of inorganic leaching in MPFs.

Bibliography

Aggour, Y.A., Aziz, M.S., 2000. Degradation of polyacrylonitrile by low energy ion beam and UV radiation. Polym. Test. 19, 261–267. https://doi.org/10.1016/S0142-9418(98)00087-7

Allen, N.S., Edge, M., 1992. Fundamentals of polymer degradation and stabilisation. Elsevier Applied Science, London ; New York.

Al-Salem, S.M. (Ed.), 2019. Plastics to energy: fuel, chemicals, and sustainability implications, Plastics design library. William Andrew Applied Science Publishers, Oxford Cambridge, MA.

Ambrogi, V., Carfagna, C., Cerruti, P., Marturano, V., 2017. Additives in Polymers, in: Modification of Polymer Properties. Elsevier, pp. 87–108. https://doi.org/10.1016/B978-0-323-44353-1.00004-X

Andrady, A.L., 2017. The plastic in microplastics: A review. Mar. Pollut. Bull. 119, 12–22. https://doi.org/10.1016/j.marpolbul.2017.01.082

Andrady, A.L., 2011. Microplastics in the marine environment. Mar. Pollut. Bull. 62, 1596–1605. https://doi.org/10.1016/j.marpolbul.2011.05.030

Andrady, A.L. (Ed.), 2003. Plastics and the environment. Wiley-Interscience, Hoboken, N.J.

Andrady, A.L., 1994. Assessment of Environmental Biodegradation of Synthetic Polymers. J. Macromol. Sci. Part C 34, 25–76. https://doi.org/10.1080/15321799408009632

Asimakopoulos, A.G., Thomaidis, N.S., Kannan, K., 2014a. Widespread occurrence of bisphenol A diglycidyl ethers, p-hydroxybenzoic acid esters (parabens), benzophenone type-UV filters, triclosan, and triclocarban in human urine from Athens, Greece. Sci. Total Environ. 470–471, 1243–1249. https://doi.org/10.1016/j.scitotenv.2013.10.089

Asimakopoulos, A.G., Wang, L., Thomaidis, N.S., Kannan, K., 2014b. A multi-class bioanalytical methodology for the determination of bisphenol A diglycidyl ethers, p-hydroxybenzoic acid esters, benzophenone-type ultraviolet filters, triclosan, and triclocarban in human urine by liquid chromatography–tandem mass spectrometry. J. Chromatogr. A 1324, 141–148. https://doi.org/10.1016/j.chroma.2013.11.031

Asuero, A.G., Sayago, A., González, A.G., 2006. The Correlation Coefficient: An Overview. Crit. Rev. Anal. Chem. 36, 41–59. https://doi.org/10.1080/10408340500526766

Ausloos, P., Clifton, C.L., Lias, S.G., Mikaya, A.I., Stein, S.E., Tchekhovskoi, D.V., Sparkman, O.D., Zaikin, V., Zhu, D., 1999. The critical evaluation of a comprehensive mass spectral library. J. Am. Soc. Mass Spectrom. 10, 287–299. https://doi.org/10.1016/S1044-0305(98)00159-7

Aydin, I., 2008. Comparison of dry, wet and microwave digestion procedures for the determination of chemical elements in wool samples in Turkey using ICP-OES technique. Microchem. J. 90, 82–87. https://doi.org/10.1016/j.microc.2008.03.011

Balcerzak, M., Baranowska, I., 2016. Handbook of trace analysis: fundamentals and applications. Springer, Cham [etc.

Ballesteros, L.F., Teixeira, J.A., Mussatto, S.I., 2014. Selection of the Solvent and Extraction Conditions for Maximum Recovery of Antioxidant Phenolic Compounds from Coffee Silverskin. Food Bioprocess Technol. 7, 1322–1332. https://doi.org/10.1007/s11947-013-1115-7

Barceló, D., Petrovic, M., 2007. Challenges and achievements of LC-MS in environmental analysis: 25 years on. TrAC Trends Anal. Chem. 26, 2–11.

Barker, R.H., 1975. Additives in fibers and fabrics. Environ. Health Perspect. 11, 41–45.

Barrows, A.P.W., Cathey, S.E., Petersen, C.W., 2018. Marine environment microfiber contamination: Global patterns and the diversity of microparticle origins. Environ. Pollut. 237, 275–284. https://doi.org/10.1016/j.envpol.2018.02.062

BASF, 2016. Technical Data Sheet - Irgafos 168.

BASF, 2013. Plastic Additives for Fibers & Textile : BASF [WWW Document]. URL http://www.plasticadditives.basf.com/ev/internet/plastic-additives/en_GB/content/plastic-additives/Industries/Textiles_Fibers/index (accessed 5.14.19).

BASF Light Stabilizers for Synthetic Fibers [WWW Document], 2017. . Alpha-Plast. URL http://www.alpha-plast.com.ua/basf-light-stabilizers-for-synthetic-fibers/ (accessed 5.11.19).

Basu, P., 2013. Biomass gasification, pyrolysis, and torrefaction: practical design and theory, Second edition. ed. Academic Press is and imprint of Elsevier, Amsterdam ; Boston.

Berendsen, B.J.A., Meijer, T., Mol, H.G.J., van Ginkel, L., Nielen, M.W.F., 2017. A global inter-laboratory study to assess acquisition modes for multi-compound confirmatory analysis of veterinary drugs using liquid chromatography coupled to triple quadrupole, time of flight and orbitrap mass spectrometry. Anal. Chim. Acta 962, 60–72. https://doi.org/10.1016/j.aca.2017.01.046

Blettler, M.C.M., Abrial, E., Khan, F.R., Sivri, N., Espinola, L.A., 2018. Freshwater plastic pollution: Recognizing research biases and identifying knowledge gaps. Water Res. 143, 416–424. https://doi.org/10.1016/j.watres.2018.06.015

Bokria, J.G., Schlick, S., 2002. Spatial effects in the photodegradation of poly(acrylonitrile–butadiene–styrene): a study by ATR-FTIR. Polymer 43, 3239–3246. https://doi.org/10.1016/S0032-3861(02)00152-0

Booth, A.M., Kubowicz, S., Beegle-Krause, C., Skancke, J., Nordam, T., Landsem, E., Jahren, S., 2017. Microplastic in global and Norwegian marine environments: Distributions, degradation mechanisms and transport (No. M-918|2017). Sintef.

Browne, M.A., Crump, P., Niven, S.J., Teuten, E., Tonkin, A., Galloway, T., Thompson, R., 2011. Accumulation of Microplastic on Shorelines Woldwide: Sources and Sinks. Environ. Sci. Technol. 45, 9175–9179. https://doi.org/10.1021/es201811s

Cadogan, D.F., Howick, C.J., 2000. Plasticizers, in: John Wiley & Sons, Inc. (Ed.), Kirk-Othmer Encyclopedia of Chemical Technology. John Wiley & Sons, Inc., Hoboken, NJ, USA, p. 1612011903010415.a01. https://doi.org/10.1002/0471238961.1612011903010415.a01

Carney Almroth, B.M., Åström, L., Roslund, S., Petersson, H., Johansson, M., Persson, N.-K., 2018. Quantifying shedding of synthetic fibers from textiles; a source of microplastics released into the environment. Environ. Sci. Pollut. Res. 25, 1191–1199. https://doi.org/10.1007/s11356-017-0528-7

Carr, S.A., Liu, J., Tesoro, A.G., 2016. Transport and fate of microplastic particles in wastewater treatment plants. Water Res. 91, 174–182. https://doi.org/10.1016/j.watres.2016.01.002

Chandure, A.S., Bhusari, G.S., Umare, S.S., 2014. Synthesis, Characterization, and Biodegradation Studies of Poly(1,4-cyclohexanedimethylene-adipate-carbonate)s. J. Polym. 2014, 1–11. https://doi.org/10.1155/2014/547325

Choi, S.-S., Jang, J.-H., 2011. Analysis of UV absorbers and stabilizers in polypropylene by liquid chromatography/atmospheric pressure chemical ionization-mass spectrometry. Polym. Test. 30, 673–677. https://doi.org/10.1016/j.polymertesting.2011.05.011

Cole, M., 2016. A novel method for preparing microplastic fibers. Sci. Rep. 6. https://doi.org/10.1038/srep34519

Coleman, M.M., Sivy, G.T., 1981. Fourier transform ir studies of the degradation of polyacrylonitrile copolymers—I: Introduction and comparative rates of the degradation of three copolymers below 200°c and under reduced pressure. Carbon 19, 123–126. https://doi.org/10.1016/0008-6223(81)90118-4

Cytec, 2012. Product safety summary - CYASORB® UV-5411.

Da Costa, J.P., Nunes, A.R., Santos, P.S.M., Girão, A.V., Duarte, A.C., Rocha-Santos, T., 2018. Degradation of polyethylene microplastics in seawater: Insights into the environmental degradation of polymers. J. Environ. Sci. Health Part A Tox. Hazard. Subst. Environ. Eng. 53, 866–875. https://doi.org/10.1080/10934529.2018.1455381

Dawson, A.L., Kawaguchi, S., King, C.K., Townsend, K.A., King, R., Huston, W.M., Nash, S.M.B., 2018. Turning microplastics into nanoplastics through digestive fragmentation by Antarctic krill. Nat. Commun. 9, 1001. https://doi.org/10.1038/s41467-018-03465-9

De Veaux, R.D., Velleman, P.F., Bock, D.E., 2018. Intro stats, Fifth edition. ed. Pearson, Boston.

Deopura, B.L., Padaki, N.V., 2015. Chapter 5 - Synthetic Textile Fibres: Polyamide, Polyester and Aramid Fibres, in: Sinclair, R. (Ed.), Textiles and Fashion, Woodhead Publishing Series in Textiles. Woodhead Publishing, pp. 97–114. https://doi.org/10.1016/B978-1-84569-931-4.00005-2

Deterre, R., Feller, J.-F., Hamaide, T., 2014. Environmental impact of polymers. ISTE, Ltd. ; Wiley, London; Hoboken.

Doğan, M., Soylak, M., Elçi, L., von Bohlen, A., 2002. Application of Total Reflection X-Ray Fluorescence Spectrometry in the Textile Industry. Microchim. Acta 138, 77–82. https://doi.org/10.1007/s006040200012

Dris, R., Gasperi, J., Saad, M., Mirande, C., Tassin, B., 2016. Synthetic fibers in atmospheric fallout: A source of microplastics in the environment? Mar. Pollut. Bull. 104, 290–293. https://doi.org/10.1016/j.marpolbul.2016.01.006

Drumond Chequer, F.M., de Oliveira, G.A.R., Anastacio Ferraz, E.R., Carvalho, J., Boldrin Zanoni, M.V., de Oliveir, D.P., 2013. Textile Dyes: Dyeing Process and Environmental Impact, in: Gunay, M. (Ed.), Eco-Friendly Textile Dyeing and Finishing. InTech. https://doi.org/10.5772/53659

Egerton, 2016. Physical principles of electron microscopy. Springer Berlin Heidelberg, New York, NY.

European Chemicals Agency, 2019. 4,4’-sulphonyldiphenol - Substance Information - ECHA [WWW Document]. URL https://echa.europa.eu/substance-information/-/substanceinfo/100.001.137 (accessed 5.10.19).

Farsani, R.E., Raissi, S., Shokuhfar, A., Sedghi, A., 2009. FT-IR Study of Stabilized PAN Fibers for Fabrication of Carbon Fibers. World Acad. Sci. Eng. Technol. 50.

Fleischmann, C., Lievenbrück, M., Ritter, H., 2015. Polymers and Dyes: Developments and Applications. Polymers 7, 717–746. https://doi.org/10.3390/polym7040717

Fu, S., Lu, J.M., Yuan, F.Q., 2018. Multivariate analysis of Co, Fe and Ni leaching from tailings following simulated temperature change. IOP Conf. Ser. Earth Environ. Sci. 191, 012125. https://doi.org/10.1088/1755-1315/191/1/012125

Gewert, B., Plassmann, M., Sandblom, O., MacLeod, M., 2018. Identification of Chain Scission Products Released to Water by Plastic Exposed to Ultraviolet Light. Environ. Sci. Technol. Lett. 5, 272–276. https://doi.org/10.1021/acs.estlett.8b00119

Gewert, B., Plassmann, M.M., MacLeod, M., 2015. Pathways for degradation of plastic polymers floating in the marine environment. Environ. Sci. Process. Impacts 17, 1513–1521. https://doi.org/10.1039/C5EM00207A

Geyer, R., Jambeck, J.R., Law, K.L., 2017. Production, use, and fate of all plastics ever made. Sci. Adv. 3, e1700782. https://doi.org/10.1126/sciadv.1700782

Glass, S., Trinklein, B., Abel, B., Schulze, A., 2018. TiO2 as Photosensitizer and Photoinitiator for Synthesis of Photoactive TiO2-PEGDA Hydrogel Without Organic Photoinitiator. Front. Chem. 6, 340. https://doi.org/10.3389/fchem.2018.00340

Habib, D., Locke, D.C., Cannone, L.J., 1998. Synthetic Fibers as Indicators of Municipal Sewage Sludge, Sludge Products, and Sewage Treatment Plant Effluents. Water. Air. Soil Pollut. 103, 1–8. https://doi.org/10.1023/A:1004908110793

Hahladakis, J.N., Velis, C.A., Weber, R., Iacovidou, E., Purnell, P., 2018. An overview of chemical additives present in plastics: Migration, release, fate and environmental impact during their use, disposal and recycling. J. Hazard. Mater. 344, 179–199. https://doi.org/10.1016/j.jhazmat.2017.10.014

Haldimann, M., Alt, A., Blanc, A., Brunner, K., Sager, F., Dudler, V., 2013. Migration of antimony from PET trays into food simulant and food: determination of Arrhenius parameters and comparison of predicted and measured migration data. Food Addit. Contam. Part Chem. Anal. Control Expo. Risk Assess. 30, 587–598. https://doi.org/10.1080/19440049.2012.751631

Hepsø, M.O., 2018. Experimental weathering of microplastic under simulated environmental conditions.

Hermabessiere, L., Dehaut, A., Paul-Pont, I., Lacroix, C., Jezequel, R., Soudant, P., Duflos, G., 2017. Occurrence and effects of plastic additives on marine environments and organisms: A review. Chemosphere 182, 781–793. https://doi.org/10.1016/j.chemosphere.2017.05.096

Hijnen, W.A.M., Beerendonk, E.F., Medema, G.J., 2006. Inactivation credit of UV radiation for viruses, bacteria and protozoan (oo)cysts in water: A review. Water Res. 40, 3–22. https://doi.org/10.1016/j.watres.2005.10.030

Horrocks, A.R. (Ed.), 2008. Advances in fire retardant materials, Woodhead publishing in materials. Woodhead Publ. [u.a.], Cambridge.

Ioakeimidis, C., Fotopoulou, K.N., Karapanagioti, H.K., Geraga, M., Zeri, C., Papathanassiou, E., Galgani, F., Papatheodorou, G., 2016. The degradation potential of PET bottles in the marine environment: An ATR-FTIR based approach. Sci. Rep. 6. https://doi.org/10.1038/srep23501

Ito, S., Tsukada, K., 2002. Matrix effect and correction by standard addition in quantitative liquid chromatographic-mass spectrometric analysis of diarrhetic shellfish poisoning toxins. J. Chromatogr. A 943, 39–46.

Jellinek, H.H.G., Bastien, I.J., n.d. PHOTOLYSIS OF POLYACRYLONITRILE 13.

Jellinek, H.H.G., Schlueter, W.A., 1960. Photodegradation of polyacrylonitrile in solution. J. Appl. Polym. Sci. 3, 206–212. https://doi.org/10.1002/app.1960.070030810

Jolliffe, I.T., Cadima, J., 2016. Principal component analysis: a review and recent developments. Philos. Transact. A Math. Phys. Eng. Sci. 374. https://doi.org/10.1098/rsta.2015.0202

Käppler, A., Windrich, F., Löder, M.G.J., Malanin, M., Fischer, D., Labrenz, M., Eichhorn, K.-J., Voit, B., 2015. Identification of microplastics by FTIR and Raman microscopy: a novel silicon filter substrate opens the important spectral range below 1300 cm−1 for FTIR transmission measurements. Anal. Bioanal. Chem. 407, 6791–6801. https://doi.org/10.1007/s00216-015-8850-8

Kooi, M., Nes, E.H. van, Scheffer, M., Koelmans, A.A., 2017. Ups and Downs in the Ocean: Effects of Biofouling on Vertical Transport of Microplastics. Environ. Sci. Technol. 51, 7963–7971. https://doi.org/10.1021/acs.est.6b04702

Ksouri, I., Haddar, N., 2018. Long term ageing of polyamide 6 and polyamide 6 reinforced with 30% of glass fibers: temperature effect. J. Polym. Res. 25, 153. https://doi.org/10.1007/s10965-018-1551-1

Le Marechal, A.M., Krianec, B., Vajnhandl, S., Volmajer, J., 2012. Textile Finishing Industry as an Important Source of Organic Pollutants, in: Puzyn, T. (Ed.), Organic Pollutants Ten Years After the Stockholm Convention - Environmental and Analytical Update. InTech. https://doi.org/10.5772/32272

Lehmler, H.-J., Liu, B., Gadogbe, M., Bao, W., 2018. Exposure to Bisphenol A, Bisphenol F, and Bisphenol S in U.S. Adults and Children: The National Health and Nutrition

Examination Survey 2013–2014. ACS Omega 3, 6523–6532. https://doi.org/10.1021/acsomega.8b00824

Lenzing, A.G., 2017. Annual Report 2017.

Li, A.J., Kannan, K., 2018. Elevated Concentrations of Bisphenols, Benzophenones, and Antimicrobials in Pantyhose Collected from Six Countries. Environ. Sci. Technol. 52, 10812–10819. https://doi.org/10.1021/acs.est.8b03129

Li, X., Chen, L., Mei, Q., Dong, B., Dai, X., Ding, G., Zeng, E.Y., 2018. Microplastics in sewage sludge from the wastewater treatment plants in China. Water Res. 142, 75–85. https://doi.org/10.1016/j.watres.2018.05.034

Liu, Y.-S., Ying, G.-G., Shareef, A., Kookana, R.S., 2011. Photostability of the UV filter benzophenone-3 and its effect on the photodegradation of benzotriazole in water. Environ. Chem. 8, 581–588. https://doi.org/10.1071/EN11068

Lundanes, E., Reubsaet, L., Greibrokk, T., 2014. Chromatography basic principles, sample preparations and related methods.

Malvern Instruments Ltd, 2009. Zetasizer Nano User Manual. Malvern Instruments Ltd., England.

Mansour, E., Ormondroyd, G.A., Curling, S.F., 2015. Absorption of formaldehyde by different wool types, in: ResearchGate. Presented at the International Panel Products Symposium, Llandudno.

Mason, S.A., Garneau, D., Sutton, R., Chu, Y., Ehmann, K., Barnes, J., Fink, P., Papazissimos, D., Rogers, D.L., 2016. Microplastic pollution is widely detected in US municipal wastewater treatment plant effluent. Environ. Pollut. 218, 1045–1054. https://doi.org/10.1016/j.envpol.2016.08.056

Mather, R.R., 2015. Chapter 6 - Synthetic Textile Fibres: Polyolefin, Elastomeric and Acrylic Fibres, in: Sinclair, R. (Ed.), Textiles and Fashion, Woodhead Publishing Series in Textiles. Woodhead Publishing, pp. 115–138. https://doi.org/10.1016/B978-1-84569-931-4.00006-4

Mavrić, Z., Simončič, B., 2018. Recent advances in the ultraviolet protection finishing of textiles. TEKSTILEC 61, 201–220. https://doi.org/10.14502/Tekstilec2018.61.201-220

McLean, C.M., Koller, C.E., Rodger, J.C., MacFarlane, G.R., 2009. Mammalian hair as an accumulative bioindicator of metal bioavailability in Australian terrestrial environments. Sci. Total Environ. 407, 3588–3596. https://doi.org/10.1016/j.scitotenv.2009.01.038

McMaster, M.C., 2005. LC/MS: a practical user’s guide. John Wiley, Hoboken, N.J.

Menezes, E.A., Carapelli, R., Bianchi, S.R., Souza, S.N.P., Matos, W.O., Pereira-Filho, E.R., Nogueira, A.R.A., 2010. Evaluation of the mineral profile of textile materials using inductively coupled plasma optical emission spectrometry and chemometrics. J. Hazard. Mater. 182, 325–330. https://doi.org/10.1016/j.jhazmat.2010.06.033

Mintenig, S.M., Int-Veen, I., Löder, M.G.J., Primpke, S., Gerdts, G., 2017. Identification of microplastic in effluents of waste water treatment plants using focal plane array-based micro-Fourier-transform infrared imaging. Water Res. 108, 365–372. https://doi.org/10.1016/j.watres.2016.11.015

Morrison, G.C., Bekö, G., Weschler, C.J., Schripp, T., Salthammer, T., Hill, J., Andersson, A.-M., Toftum, J., Clausen, G., Frederiksen, H., 2017. Dermal Uptake of Benzophenone-3 from Clothing. Environ. Sci. Technol. 51, 11371–11379. https://doi.org/10.1021/acs.est.7b02623

Müller, R.-J., Kleeberg, I., Deckwer, W.-D., 2001. Biodegradation of polyesters containing aromatic constituents. J. Biotechnol., Tailored Biopolymers 86, 87–95. https://doi.org/10.1016/S0168-1656(00)00407-7

Murphy, F., Ewins, C., Carbonnier, F., Quinn, B., 2016. Wastewater Treatment Works (WwTW) as a Source of Microplastics in the Aquatic Environment. Environ. Sci. Technol. 50, 5800–5808. https://doi.org/10.1021/acs.est.5b05416

Muthuraj, R., Misra, M., Mohanty, A.K., 2015. Hydrolytic degradation of biodegradable polyesters under simulated environmental conditions. J. Appl. Polym. Sci. 132, n/a-n/a. https://doi.org/10.1002/app.42189

Muzenda, E., Ramatsa, I., Ntuli, F., Belaid, M., Tshwabi, P., 2011. An Investigation into the Effect of Temperature on the Leaching of Copper-Matte. Eng. Technol. 52.

Napper, I.E., Thompson, R.C., 2016. Release of synthetic microplastic plastic fibres from domestic washing machines: Effects of fabric type and washing conditions. Mar. Pollut. Bull. 112, 39–45. https://doi.org/10.1016/j.marpolbul.2016.09.025

Nguyen-Tri, P., Prud'homme, R.E., 2019. Nanoscale analysis of the photodegradation of polyester fibers by AFM-IR. J. Photochem. Photobiol. Chem. 371, 196–204. https://doi.org/10.1016/j.jphotochem.2018.11.017

Norilla, 2017. Norilia [WWW Document]. Norilla. URL https://www.norilia.com/ (accessed 4.25.19).

OECD, 2011. Test No. 201: Freshwater Alga and Cyanobacteria, Growth Inhibition Test. https://doi.org/10.1787/9789264069923-en

Ojeda, J.J., Dittrich, M., 2012. Fourier Transform Infrared Spectroscopy for Molecular Analysis of Microbial Cells. Microb. Syst. Biol. 881, 187–211. https://doi.org/10.1007/978-1-61779-827-6_8

Painter, P.G., Coleman, M.M., 1997. Fundamentals of Polymer Science. CRC Press LLC.

Parvinzadeh, M., Ebrahimi, I., 2011. Influence of atmospheric-air plasma on the coating of a nonionic lubricating agent on polyester fiber. Radiat. Eff. Defects Solids 166, 408–416. https://doi.org/10.1080/10420150.2011.553230

Pawar, A.B., More, S.P., Adivarekar, R.V., 2018. Dyeing of Polyester and Nylon with Semi-synthetic Azo Dye by Chemical Modification of Natural Source Areca Nut. Nat. Prod. Bioprospecting 8, 23–29. https://doi.org/10.1007/s13659-017-0144-8

Pelisser, F., Montedo, O.R.K., Gleize, P.J.P., Roman, H.R., 2012. Mechanical properties of recycled PET fibers in concrete. Mater. Res. 15, 679–686. https://doi.org/10.1590/S1516-14392012005000088

Plastics Europe [WWW Document], 2018. URL https://www.plasticseurope.org/en/resources/publications/619-plastics-facts-2018 (accessed 3.18.19).

Poole, C.F., 2003. The Essence of Chromatography. Elsevier Science Limited.

Porubská, M., Szöllős, O., Kóňová, A., Janigová, I., Jašková, M., Jomová, K., Chodák, I., 2012. FTIR spectroscopy study of polyamide-6 irradiated by electron and proton beams. Polym. Degrad. Stab. 97, 523–531. https://doi.org/10.1016/j.polymdegradstab.2012.01.017

Quinn, B., Murphy, F., Ewins, C., 2017. Validation of density separation for the rapid recovery of microplastics from sediment. Anal. Methods 9, 1491–1498. https://doi.org/10.1039/C6AY02542K

Rabek, J.F., 1996. Photodegradation of polymers: physical characteristics and applications. Springer, Berlin ; New York.

Random Integer Generator [WWW Document], 1998. URL https://www.random.org/integers/ (accessed 5.13.19).

Reid, A.M., Brougham, C.A., Fogarty, A.M., Roche, J.J., 2007. An investigation into possible sources of phthalate contamination in the environmental analytical laboratory. Int. J. Environ. Anal. Chem. 87, 125–133. https://doi.org/10.1080/03067310601071183

Revel, M., Châtel, A., Mouneyrac, C., 2018. Micro(nano)plastics: A threat to human health? Curr. Opin. Environ. Sci. Health 1, 17–23. https://doi.org/10.1016/j.coesh.2017.10.003

Rezić, I., Steffan, I., 2007. ICP-OES determination of metals present in textile materials. Microchem. J., Papers Presented at the XIIth Hungarian - Italian Symposium on Spectrochemistry 85, 46–51. https://doi.org/10.1016/j.microc.2006.06.010

Rezić, I., Zeiner, M., Steffan, I., 2011. Determination of 28 selected elements in textiles by axially viewed inductively coupled plasma optical emission spectrometry. Talanta 83, 865–871. https://doi.org/10.1016/j.talanta.2010.10.031

Ribeiro, R.F., Pardini, L.C., Alves, N.P., Brito Júnior, C.A.R., Ribeiro, R.F., Pardini, L.C., Alves, N.P., Brito Júnior, C.A.R., 2015. Thermal Stabilization study of polyacrylonitrile fiber obtained by extrusion. Polímeros 25, 523–530. https://doi.org/10.1590/0104-1428.1938

Rouillon, C., Bussiere, P.-O., Desnoux, E., Collin, S., Vial, C., Therias, S., Gardette, J.-L., 2016. Is carbonyl index a quantitative probe to monitor polypropylene photodegradation? Polym. Degrad. Stab. 128, 200–208. https://doi.org/10.1016/j.polymdegradstab.2015.12.011

Sajiki, J., Yonekubo, J., 2003. Leaching of bisphenol A (BPA) to seawater from polycarbonate plastic and its degradation by reactive oxygen species. Chemosphere 51, 55–62. https://doi.org/10.1016/S0045-6535(02)00789-0

Salvador Cesa, F., Turra, A., Baruque-Ramos, J., 2017. Synthetic fibers as microplastics in the marine environment: A review from textile perspective with a focus on domestic washings. Sci. Total Environ. 598, 1116–1129. https://doi.org/10.1016/j.scitotenv.2017.04.172

Saracoglu, S., Divrikli, U., Soylak, M., Elci, L., Dogan, M., 2003. Determination of Trace Elements of Some Textiles by Atomic Absorption Spectrometry. J. Trace Microprobe Tech. 21, 389–396. https://doi.org/10.1081/TMA-120020273

Schneider, C.A., Rasband, W.S., Eliceiri, K.W., 2012. NIH Image to ImageJ: 25 years of image analysis. Nat. Methods 9, 671–675. https://doi.org/10.1038/nmeth.2089

Shamey, R., Sinha, K., 2003. A review of degradation of nylon 6. 6 as a result of exposure to environmental conditions. Rev. Prog. Color. Relat. Top. 33, 93–107. https://doi.org/10.1111/j.1478-4408.2003.tb00147.x

Skoog, D.A., 2012. Fundamentals of analytical chemistry, 9th Ed. ed. Cengage - Brooks/Cole, Belmont, CA.

Song, Y.K., Hong, S.H., Jang, M., Han, G.M., Jung, S.W., Shim, W.J., 2017. Combined Effects of UV Exposure Duration and Mechanical Abrasion on Microplastic Fragmentation by Polymer Type. Environ. Sci. Technol. 51, 4368–4376. https://doi.org/10.1021/acs.est.6b06155

Stein, S.E., 1994. Estimating probabilities of correct identification from results of mass spectral library searches. J. Am. Soc. Mass Spectrom. 5, 316–323. https://doi.org/10.1016/1044-0305(94)85022-4

Sugimura, Y., Tsuge, S., 1979. Studies on thermal degradation of aromatic polyesters by pyrolysis-gas chromatography. J. Chromatogr. Sci. 17, 269–272.

Sungur, Ş., Gülmez, F., 2015a. Determination of Metal Contents of Various Fibers Used in Textile Industry by MP-AES. J. Spectrosc. 2015, 1–5. https://doi.org/10.1155/2015/640271

Sungur, Ş., Gülmez, F., 2015b. Determination of Metal Contents of Various Fibers Used in Textile Industry by MP-AES [WWW Document]. J. Spectrosc. https://doi.org/10.1155/2015/640271

Sungur, Ş., Gülmez, F., 2015c. Determination of Metal Contents of Various Fibers Used in Textile Industry by MP-AES. J. Spectrosc. 2015, 1–5. https://doi.org/10.1155/2015/640271

Tabachnick, B.G., Fidell, L.S., 2013. Using multivariate statistics, 6th ed. ed. Pearson Education, Boston.

Talvitie, J., Heinonen, M., Pääkkönen, J.-P., Vahtera, E., Mikola, A., Setälä, O., Vahala, R., 2015. Do wastewater treatment plants act as a potential point source of microplastics? Preliminary study in the coastal Gulf of Finland, Baltic Sea. Water Sci. Technol. 72, 1495–1504. https://doi.org/10.2166/wst.2015.360

Tan, B.L.L., Mustafa, A.M., 2003. Leaching of Bisphenol A from New and Old Babies' Bottles, and New Babies' Feeding Teats. Asia Pac. J. Public Health 15, 118–123. https://doi.org/10.1177/101053950301500208

Thanki, P.N., Singh, R.P., 1998. Photo-oxidative degradation of nylon 66 under accelerated weathering. Polymer 39, 6363–6367. https://doi.org/10.1016/S0032-3861(97)10390-1

The University of Waikato, 2007. Wool fibre structure and properties [WWW Document]. Sci. Learn. Hub. URL https://www.sciencelearn.org.nz/image_maps/61-wool-fibre-structure-and-properties (accessed 4.25.19).

Tsuge, S., Ohtani, H., Watanabe, C., 2011. Pyrolysis-GC/MS data book of synthetic polymers: pyrograms, thermograms and MS of pyrolyzates, 1st ed. ed. Elsevier, Amsterdam ; Boston.

Vahur, S., Teearu, A., Peets, P., Joosu, L., Leito, I., 2016. ATR-FT-IR spectral collection of conservation materials in the extended region of 4000-80 cm–1. Anal. Bioanal. Chem. 408, 3373–3379. https://doi.org/10.1007/s00216-016-9411-5

Wang, J., Tan, Z., Peng, J., Qiu, Q., Li, M., 2016. The behaviors of microplastics in the marine environment. Mar. Environ. Res. 113, 7–17. https://doi.org/10.1016/j.marenvres.2015.10.014

Wang, S., Cyronak, M., Yang, E., 2007. Does a stable isotopically labeled internal standard always correct analyte response? J. Pharm. Biomed. Anal. 43, 701–707. https://doi.org/10.1016/j.jpba.2006.08.010

Weaver, K.F., Morales, V., Dunn, S.L., Godde, K., Weaver, P.F., 2017. An Introduction to Statistical Analysis in Research: With Applications in the Biological and Life Sciences. John Wiley & Sons, Inc., Hoboken, NJ, USA. https://doi.org/10.1002/9781119454205

Weedon, G.C., Decaprio, J.D., 1971. Prevention of yellowing in polyamides.

Welden, N.A., Cowie, P.R., 2016. Long-term microplastic retention causes reduced body condition in the langoustine, Nephrops norvegicus. Environ. Pollut. 218, 895–900.

Wessel, C.C., Lockridge, G.R., Battiste, D., Cebrian, J., 2016. Abundance and characteristics of microplastics in beach sediments: Insights into microplastic accumulation in northern Gulf of Mexico estuaries. Mar. Pollut. Bull. 109, 178–183. https://doi.org/10.1016/j.marpolbul.2016.06.002

Wilson, M.B., Barnes, B.B., Boswell, P.G., 2014. What Experimental Factors Influence the Accuracy of Retention Projections in Gas Chromatography-Mass Spectrometry? J. Chromatogr. A 1373, 179–189. https://doi.org/10.1016/j.chroma.2014.11.030

Xue, J., Liu, W., Kannan, K., 2017. Bisphenols, Benzophenones, and Bisphenol A Diglycidyl Ethers in Textiles and Infant Clothing. Environ. Sci. Technol. 51, 5279–5286. https://doi.org/10.1021/acs.est.7b00701

Yamamoto, Y., Tsuge, S., Takeuchi, T., 1972. Study on the Distribution of Dyads in Acrylonitrile-Methyl Acrylate Copolymers by Pyrolysis Gas Chromatography. Macromolecules 5, 325–327.

Appendices

Appendix A. Characterisation of synthetic fibres

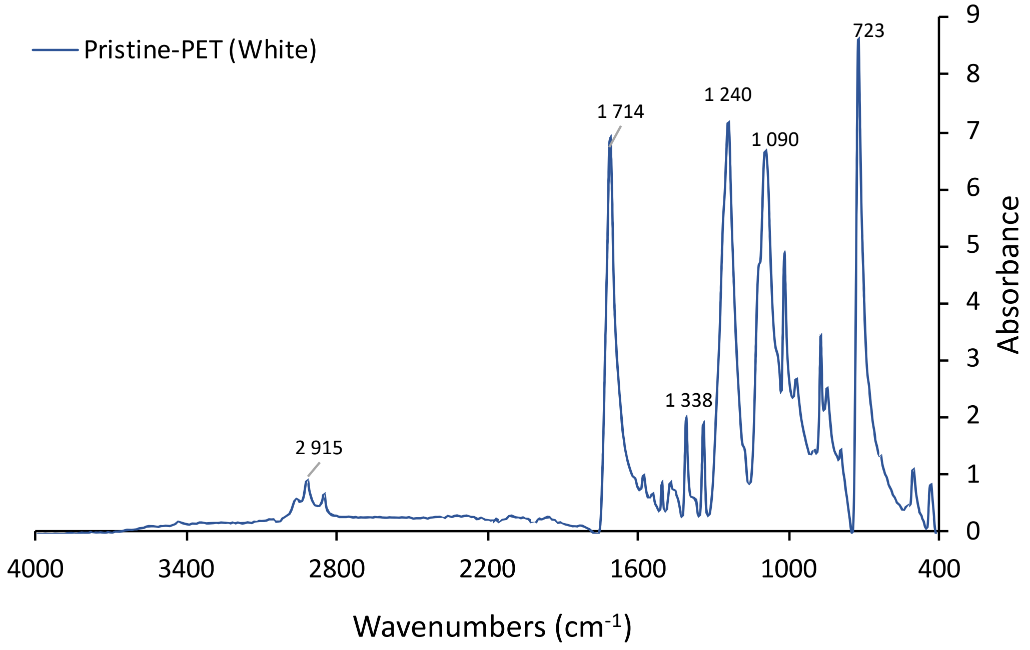

Figure A.1. ATR-FTIR spectra of white PET

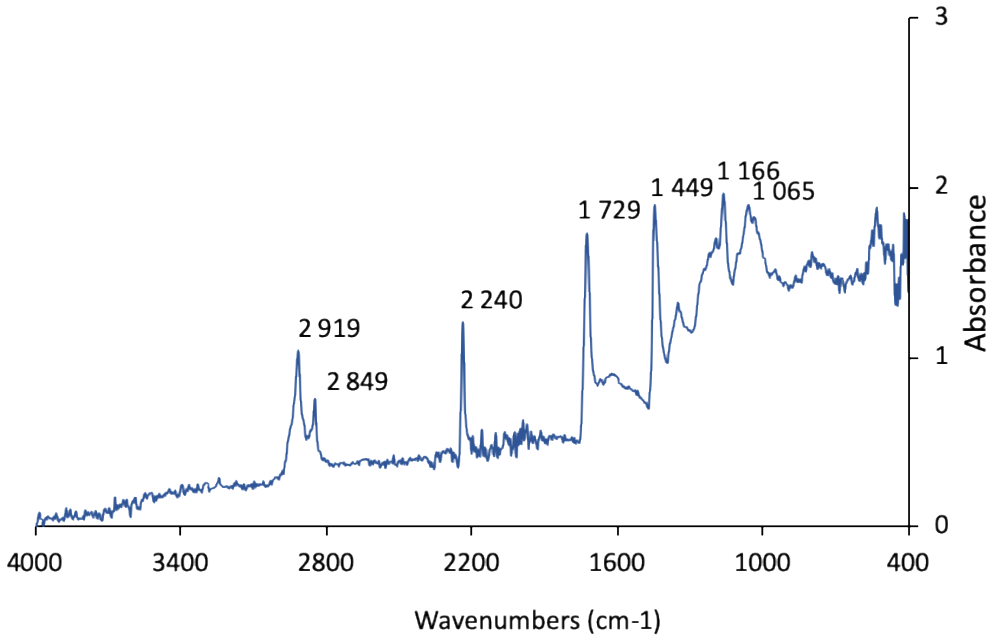

Figure A.2. ATR-FTIR spectra of blue PAN

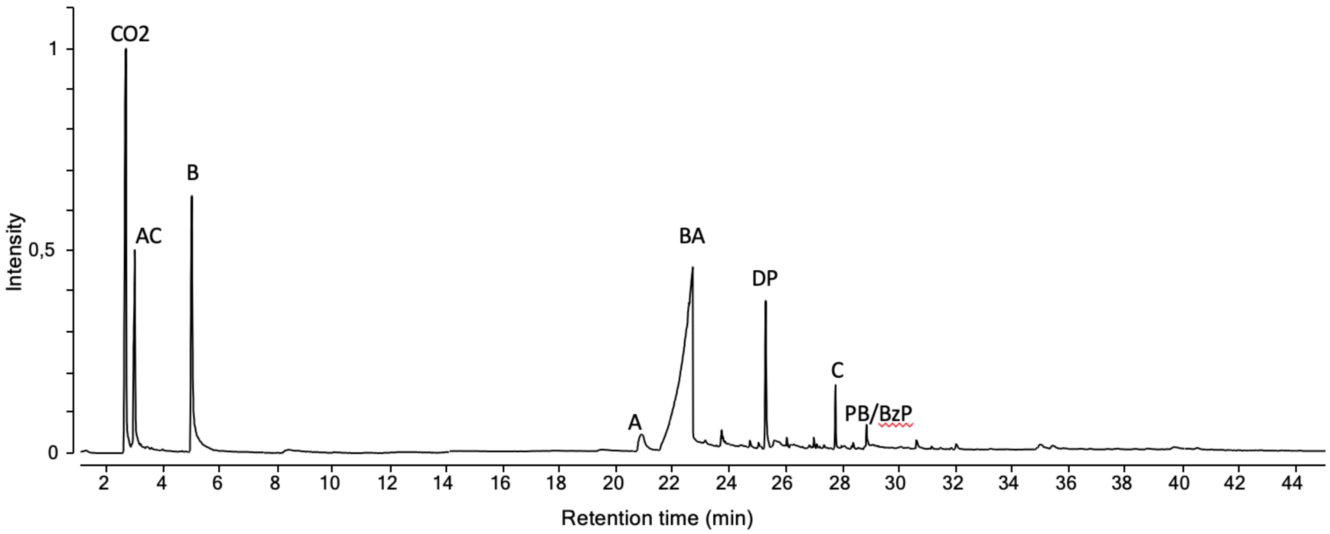

Figure A.3. Pyrogram of white PET, pyrolysed at 600 °C

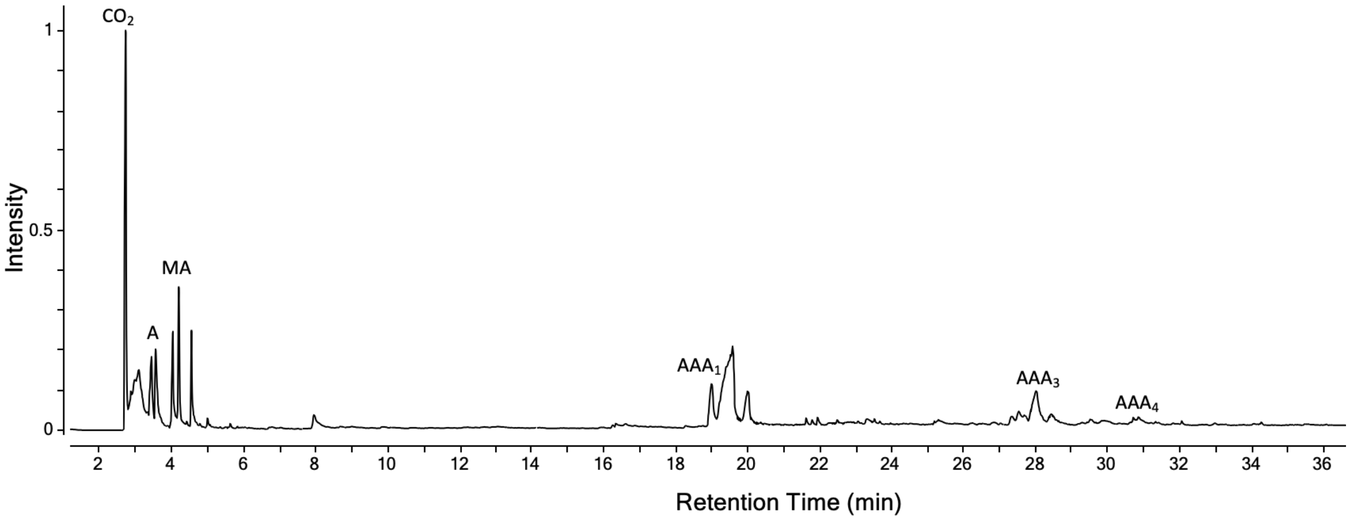

Figure A.4. Pyrogram of orange PAN, pyrolysed at 600 °C

Appendix B. UV exposure study

Table B.1 Detailed sample description of 9 month long UV exposure studies with subsampling at 5 months

Samples name	Fibre type (colour)	MPF amount (mg)	MPF size (mm)	Medium	Medium amount (mL)	Exposure time	Avg. temp (°C)	UV exposed
PET-B SW UV	Polyester (Black)	28.23	1 - 2.5	SW	30	9 months	25	×
PET-W SW UV	Polyester (White)	29.15	1 - 2.5	SW	30	9 months	25	×
PA-W SW UV	Polyamide fibre (White)	29.59	1 - 2.5	SW	30	9 months	25	×
PAN-B SW UV	Polyacrylonitrile (Blue)	30.38	1 - 2.5	SW	30	9 months	25	×
PAN-O SW UV	Polyacrylonitrile (Orange)	30.00	1 - 2.5	SW	30	9 months	25	×
PET-B FW UV	Polyester (Black)	29.15	1 - 2.5	FW (TG201)	30	9 months	25	×
PET-W FW UV	Polyester (White)	31.54	1 - 2.5	FW (TG201)	30	9 months	25	×
PA-W FW UV	Polyamide fibre (White)	29.93	1 - 2.5	FW (TG201)	30	9 months	25	×
PAN-B FW UV	Polyacrylonitrile (Blue)	30.11	1 - 2.5	FW (TG201)	30	9 months	25	×
PAN-O FW UV	Polyacrylonitrile (Orange)	31.38	1 - 2.5	FW (TG201)	30	9 months	25	×

PET-B SW Dark	Polyester (Black)	31.18	1 - 2.5	SW	30	9 months	20
PET-W SW Dark	Polyester (White)	29.80	1 - 2.5	SW	30	9 months	20
PA-W SW Dark	Polyamide fibre (White)	30.53	1 - 2.5	SW	30	9 months	20
PAN-B SW Dark	Polyacrylonitrile (Blue)	29.26	1 - 2.5	SW	30	9 months	20
PAN-O SW Dark	Polyacrylonitrile (Orange)	30.53	1 - 2.5	SW	30	9 months	20
PET-B FW Dark	Polyester (Black)	31.54	1 - 2.5	FW (TG201)	30	9 months	20
PET-W FW Dark	Polyester (White)	30.13	1 - 2.5	FW (TG201)	30	9 months	20
PA-W FW Dark	Polyamide (White)	31.01	1 - 2.5	FW (TG201)	30	9 months	20
PAN-B FW Dark	Polyacrylonitrile (Blue)	29.97	1 - 2.5	FW (TG201)	30	9 months	20
PAN-O FW Dark	Polyacrylonitrile (Orange)	31.01	1 - 2.5	FW (TG201)	30	9 months	20
SW	N/A	N/A	N/A	SW	30	9 months	20
FW	N/A	N/A	N/A	FW (TG201)	30	9 months	20

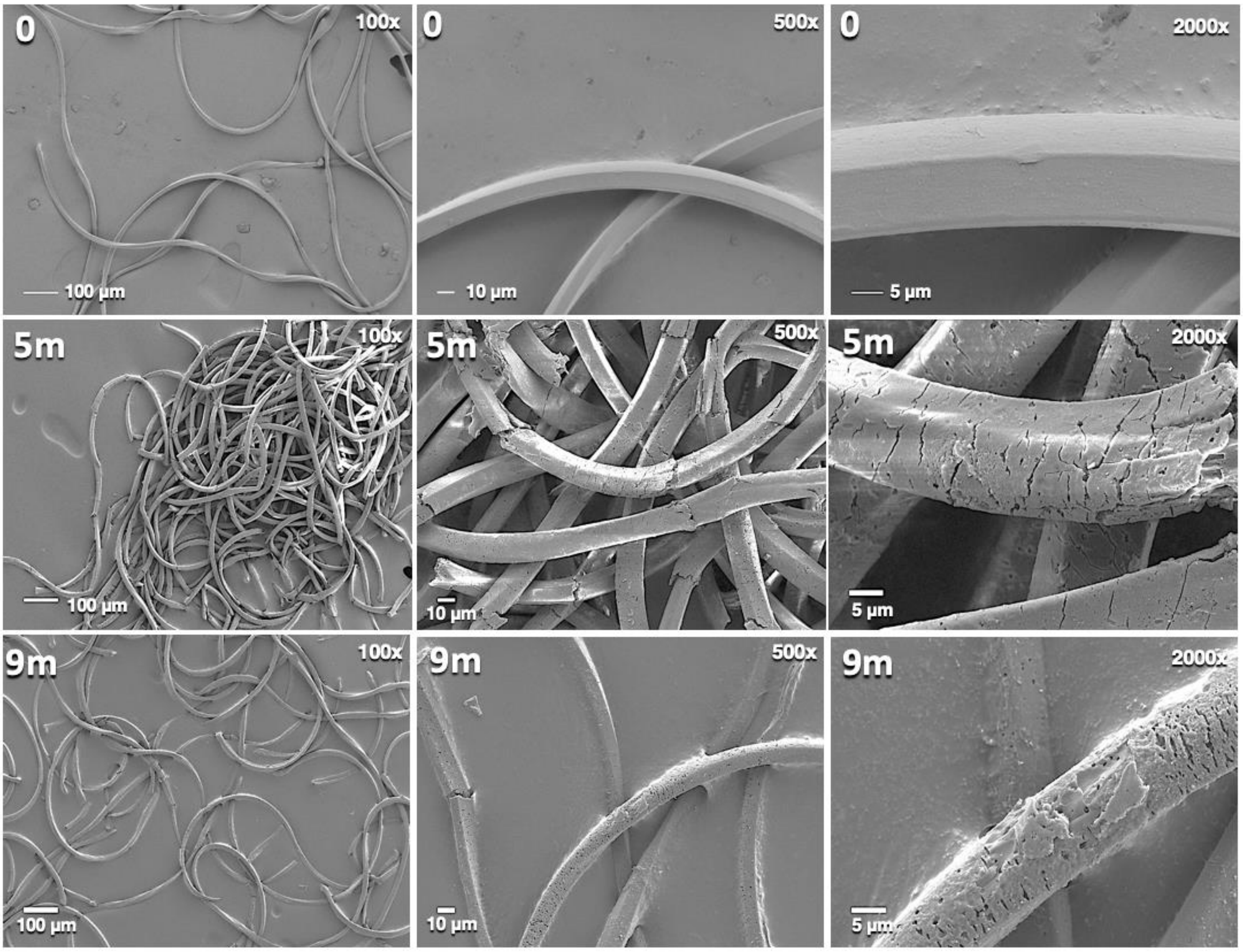

Figure B.1. SEM images showing changes in surface morphology of PET (black) between pristine fibre (0), 5 month UV exposure in FW (5 m) and 9 month UV exposure in SW (9m) at 100, 500 and 2000x magnification.

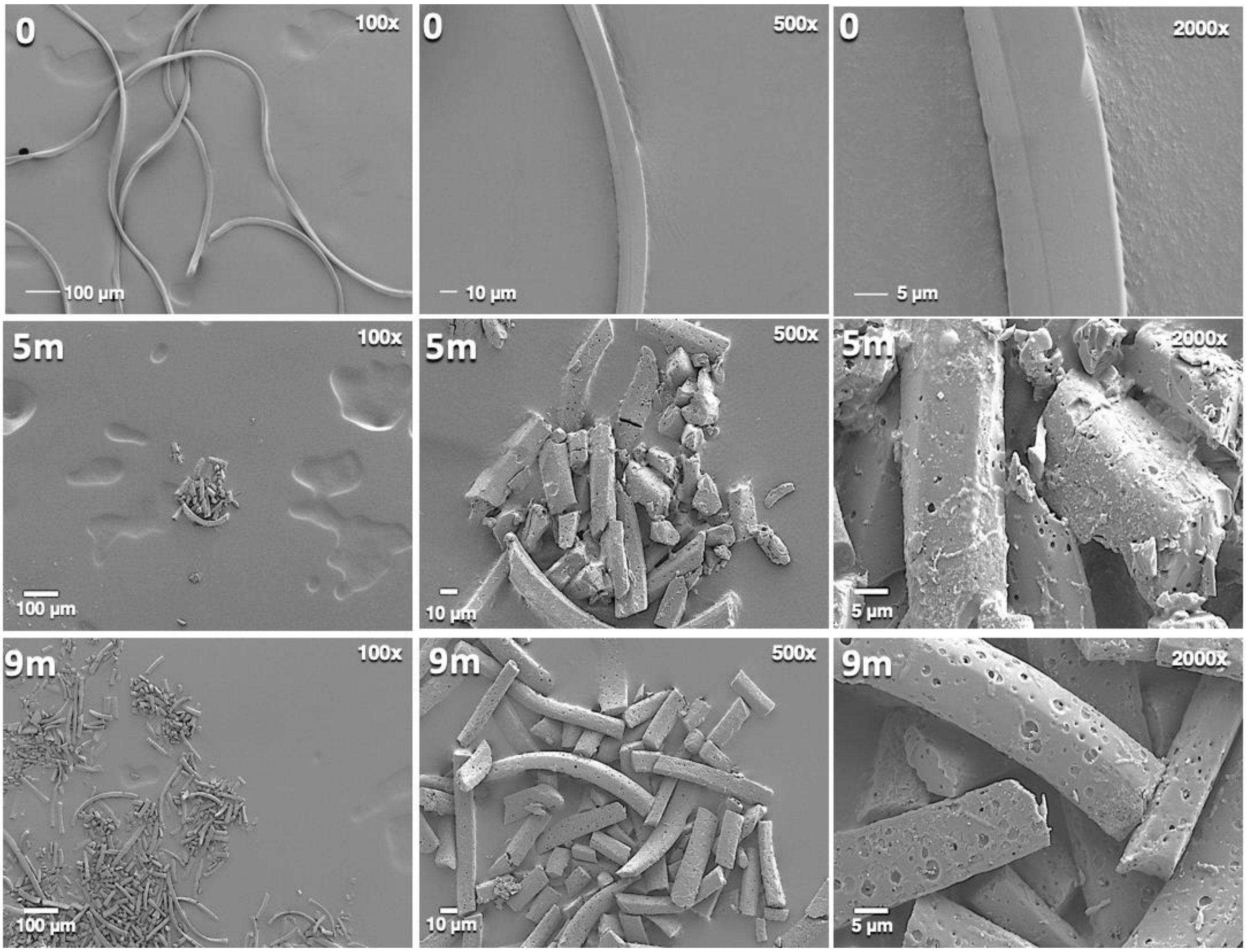

Figure B.2. SEM images showing changes in surface morphology of PET (white) between pristine fibre (0), 5 month UV exposure in FW (5 m) and 9 month UV exposure in SW (9m) at 100, 500 and 2000x magnification.

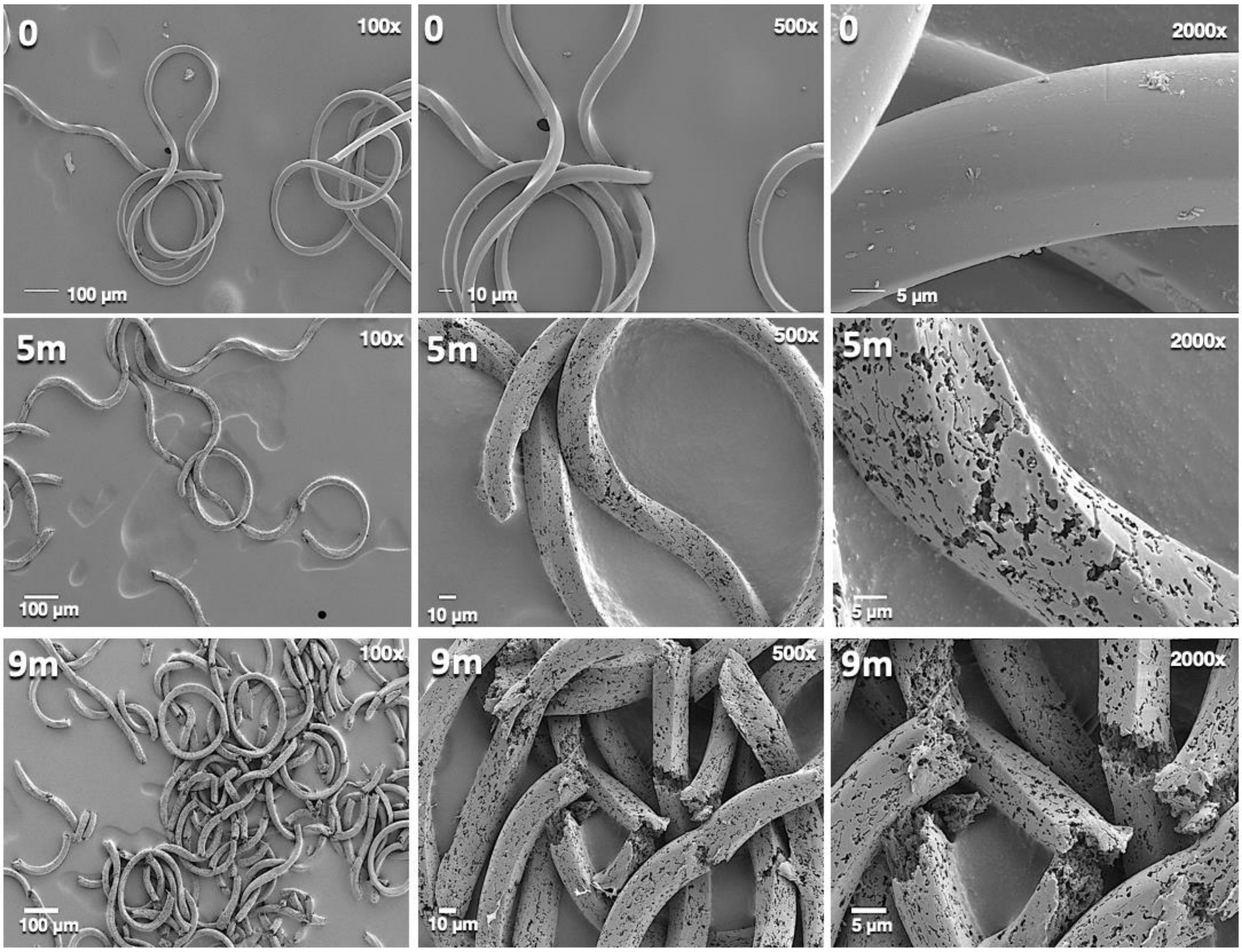

Figure B.3. SEM images showing changes in surface morphology of PA (white) between pristine fibre (0), 5 month UV exposure in FW (5 m) and 9 month UV exposure in SW (9m) at 100, 500 and 2000x magnification.

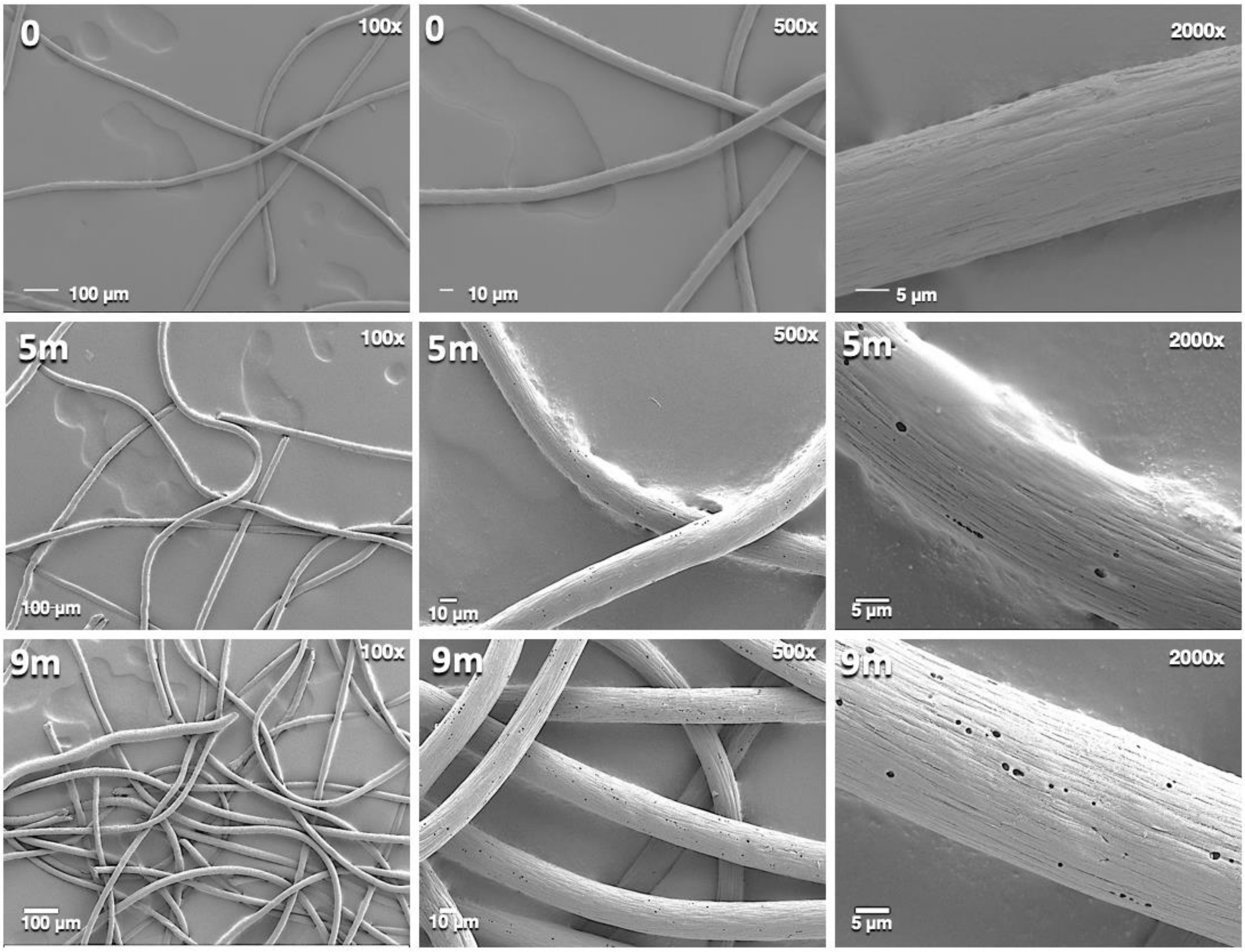

Figure B.4. SEM images showing changes in surface morphology of PAN (blue) between pristine fibre (0), 5 month UV exposure in FW (5 m) and 9 month UV exposure in SW (9m) at 100, 500 and 2000x magnification.

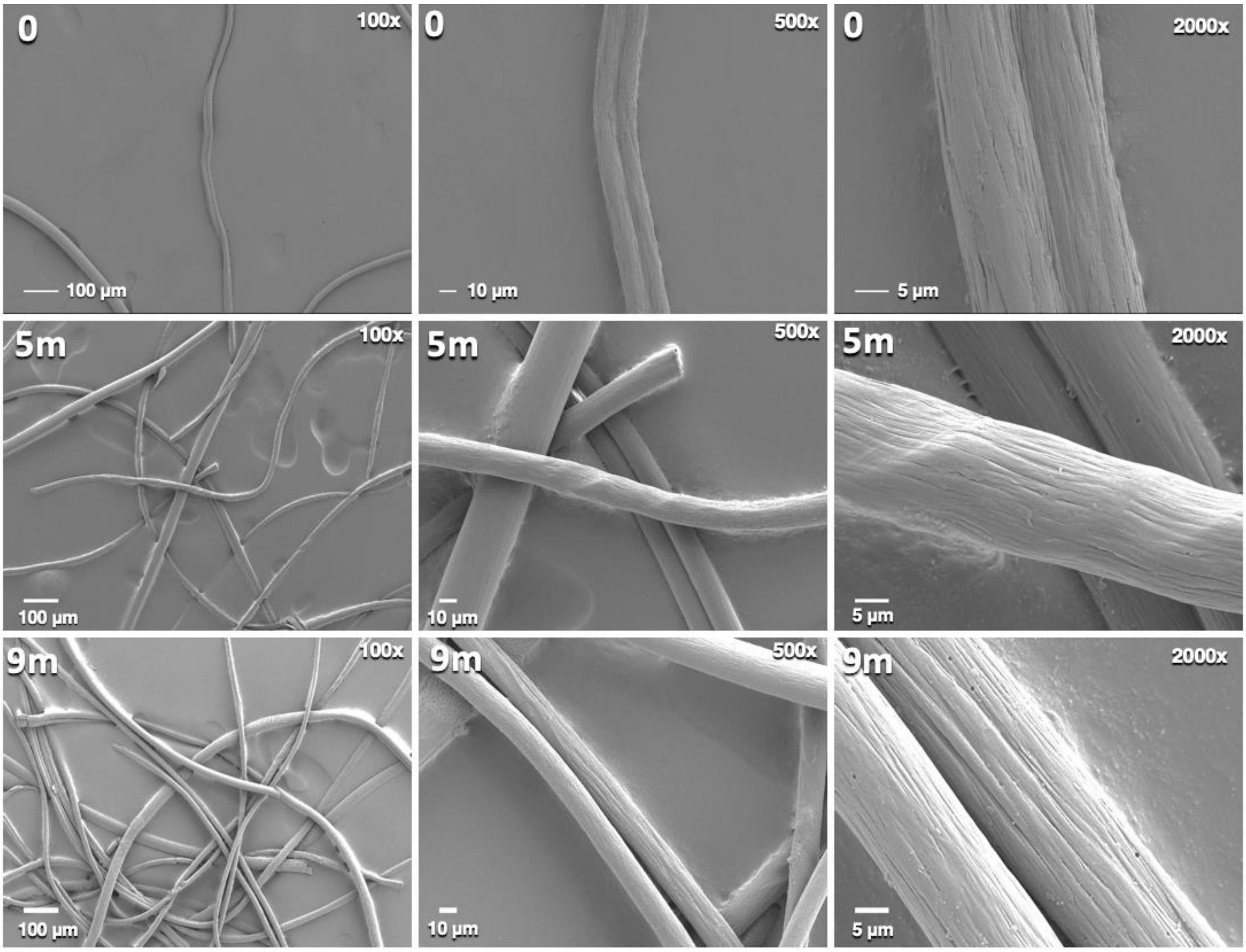

Figure B.5. SEM images showing changes in surface morphology of PAN (orange) between pristine fibre (0), 5 month UV exposure in FW (5 m) and 9 month UV exposure in SW (9m) at 100, 500 and 2000x magnification.

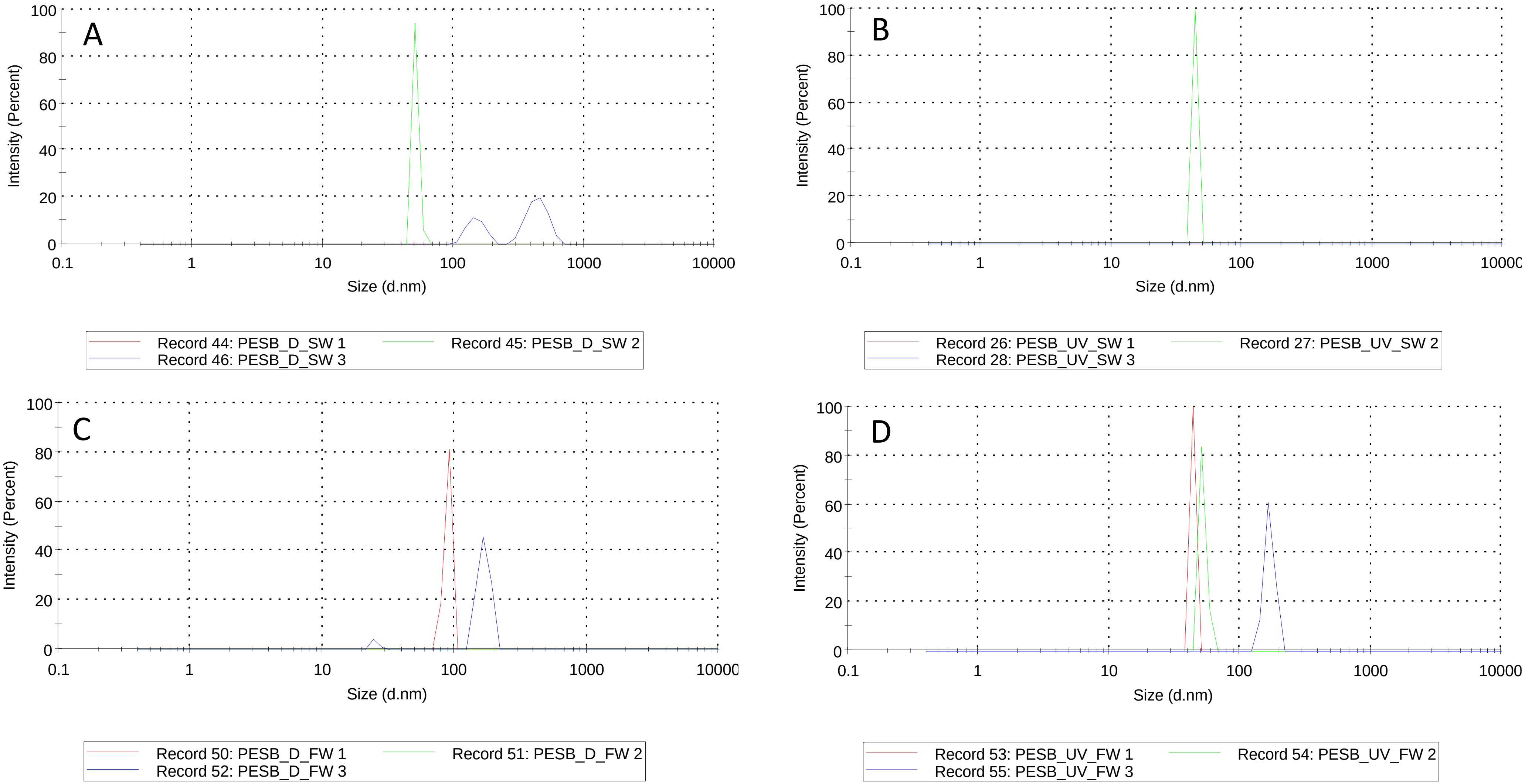

Figure B.6. Size distribution of leachates from UV expsodure studies. A:Black PET control in SW, B: Black PET UV exposed in SW ,C: Black PET control in FW and D: black PET UV exposed in FW

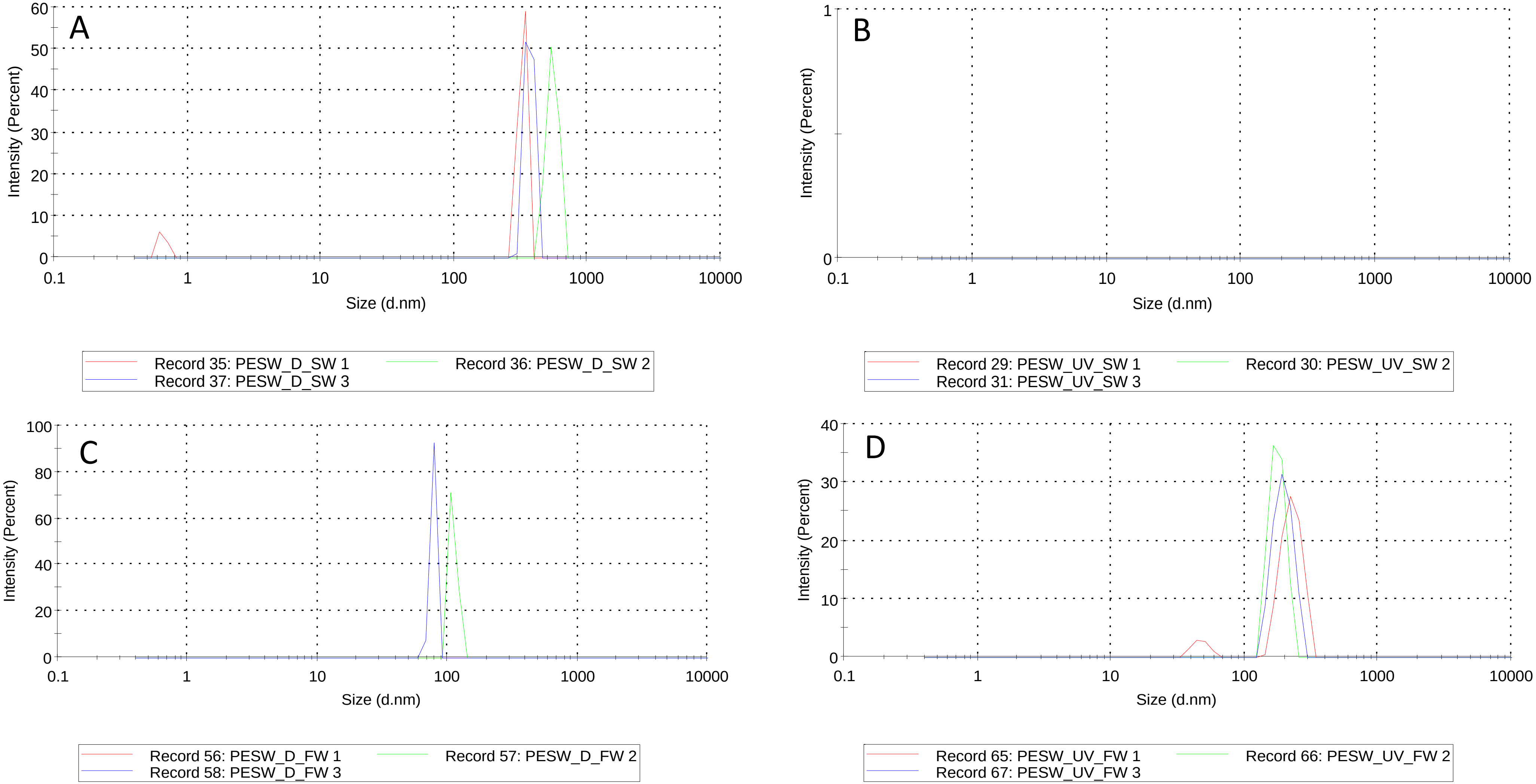

Figure B.7. Size distribution of leachates from UV expsodure studies. A: white PET control in SW, B:white PET UV exposed in SW ,C: white PET control in FW and D: white PET UV exposed in FW

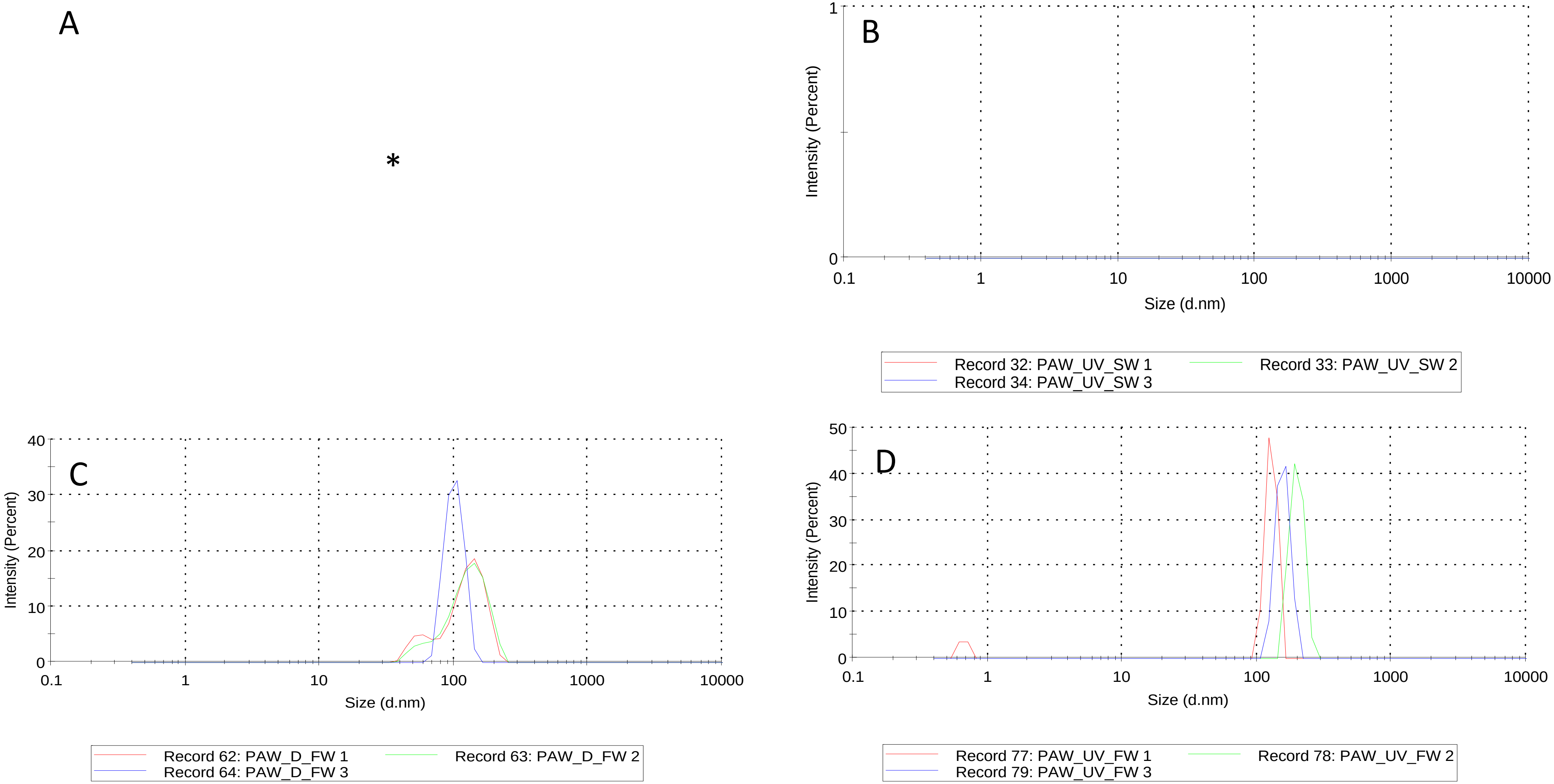

Figure B.8. Size distribution of leachates from UV expsodure studies. A*: PA SW control was not analysed due to inadquate remaining leachate after organic analysis, B:PA UV exposed in SW ,C: PA control in FW and D: PA UV exposed in FW

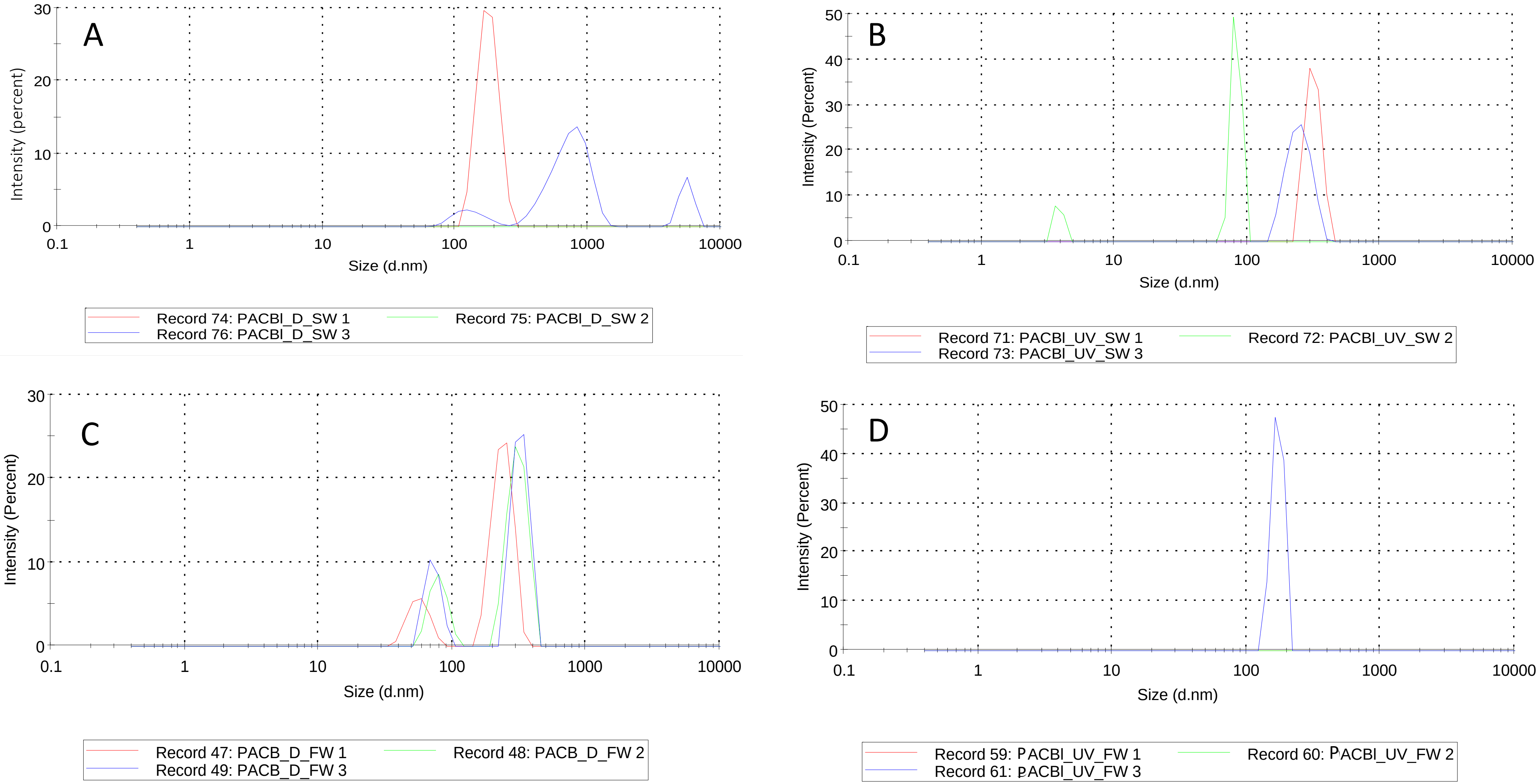

Figure B.9. Size distribution of leachates from UV expsodure studies. A: Blue PAN control in SW, B:Blue PAN UV exposed in SW ,C: Blue PAN control in FW and D: Blue PAN UV exposed in FW

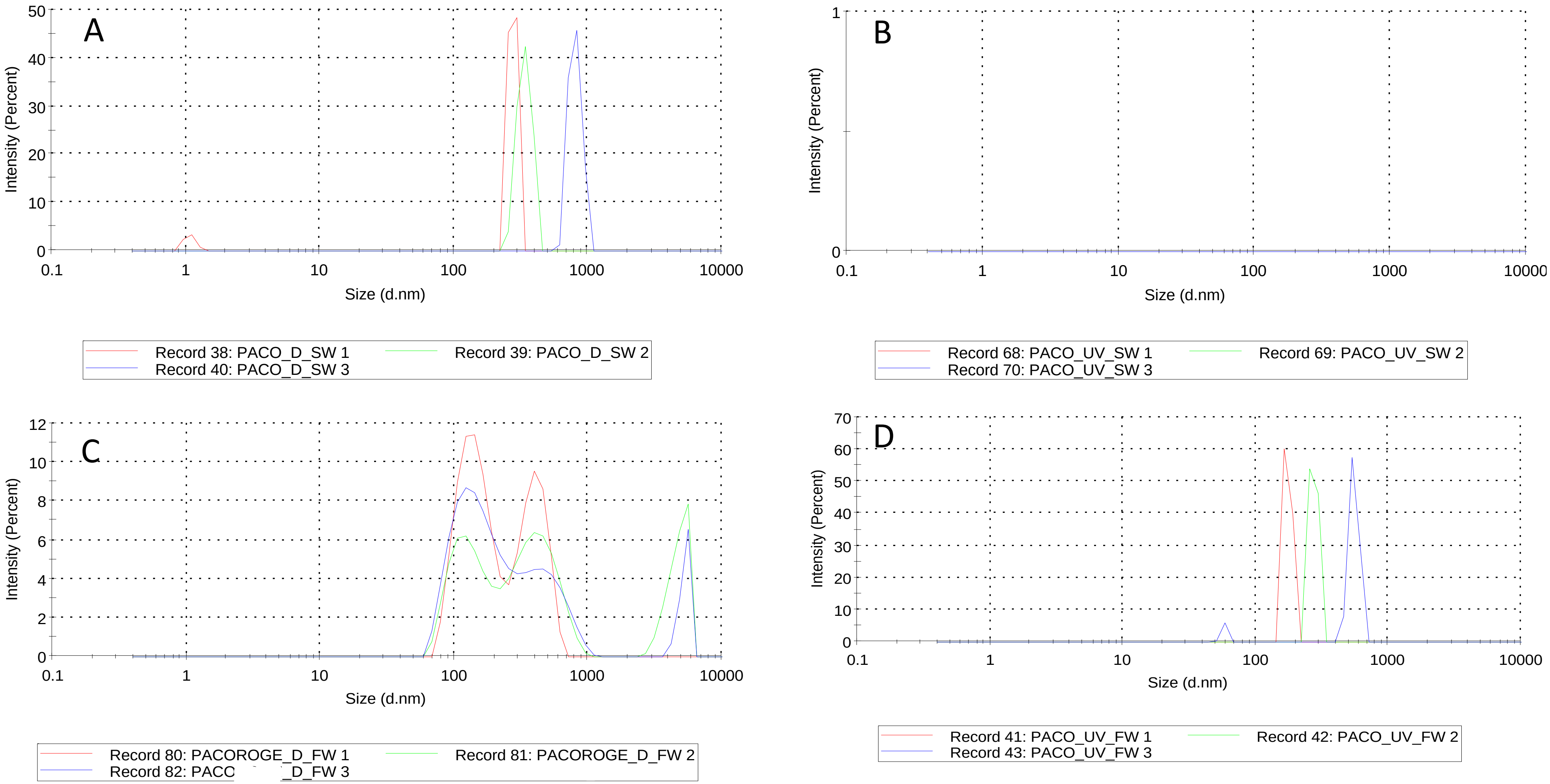

Figure B.10. Size distribution of leachates from UV expsodure studies. A: Orange PAN control in SW, B: Orange PAN UV exposed in SW ,C: Orange PAN control in FW and D: Orange PAN UV exposed in FW

FTIR Spectra – UV exposure studies in freshwater

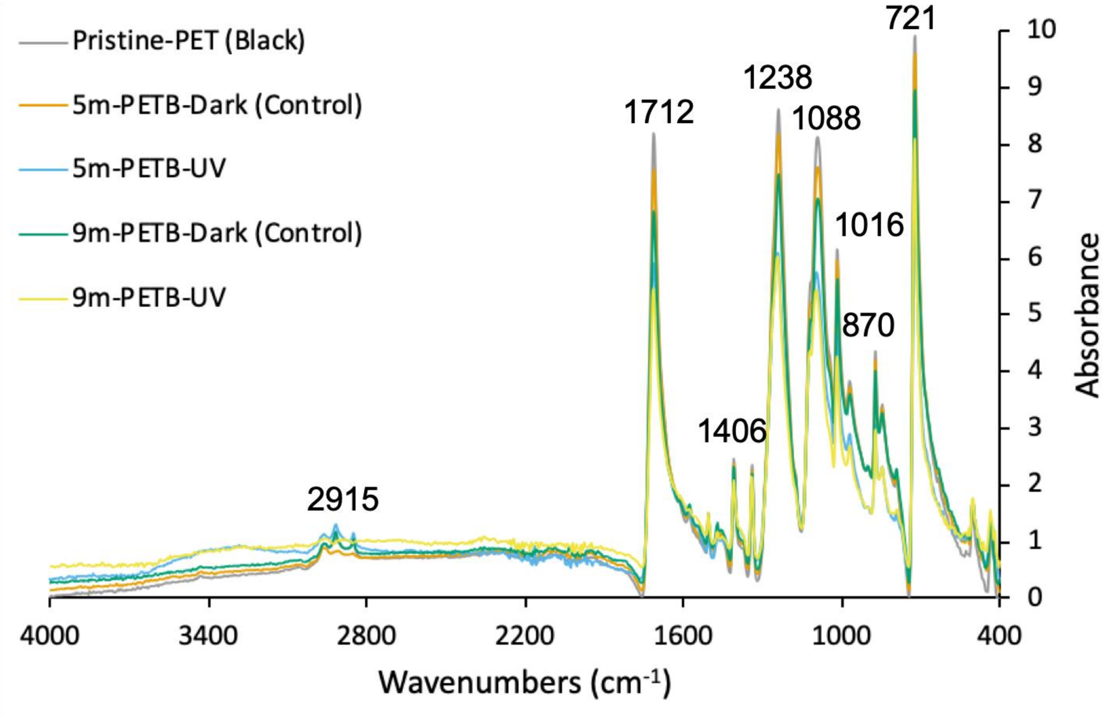

Figure B.6. ATR-FTIR spectrums of UV exposed black polyester (PETB) in FW, normalised to CH reference peak at 1407 cm^{-1}

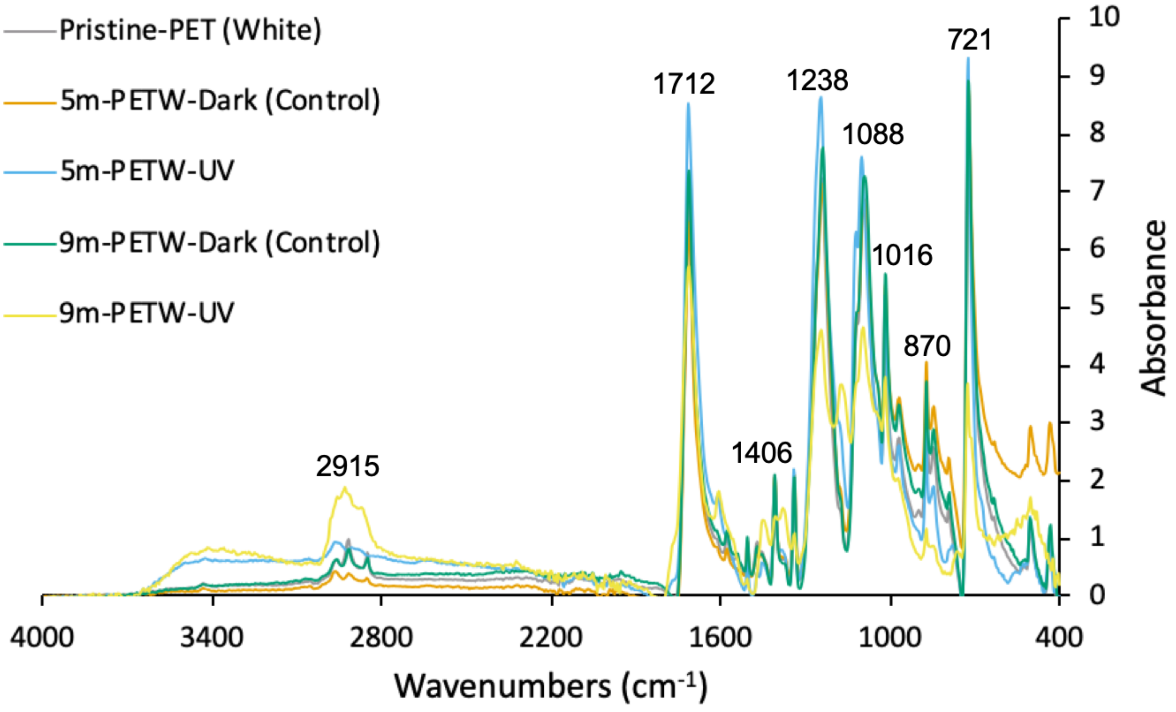

Figure B.7. ATR-FTIR spectrums of UV exposed white polyester (PET-W) in FW, normalised to CH reference peak at 1407 cm^{-1}

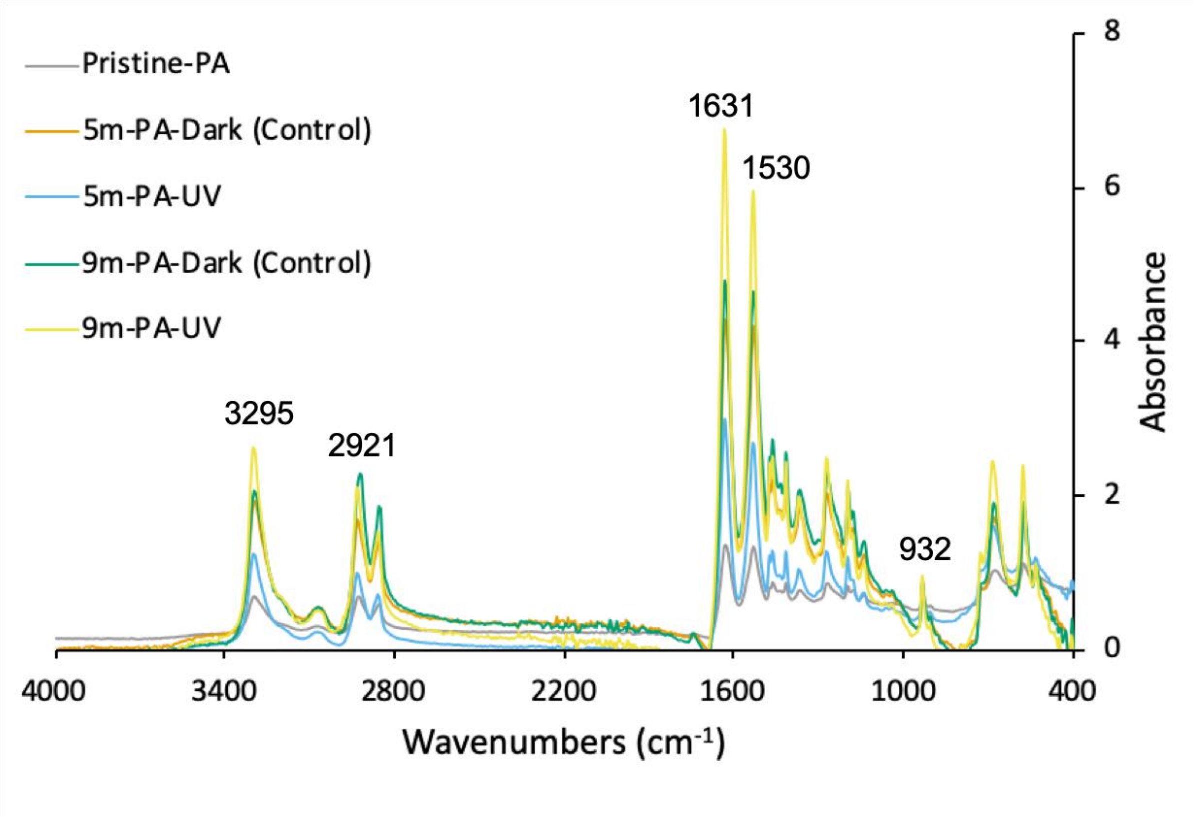

Figure B.8. ATR-FTIR spectra of UV exposed PA in FW, normalised to CH reference peak at 932 cm^{-1}

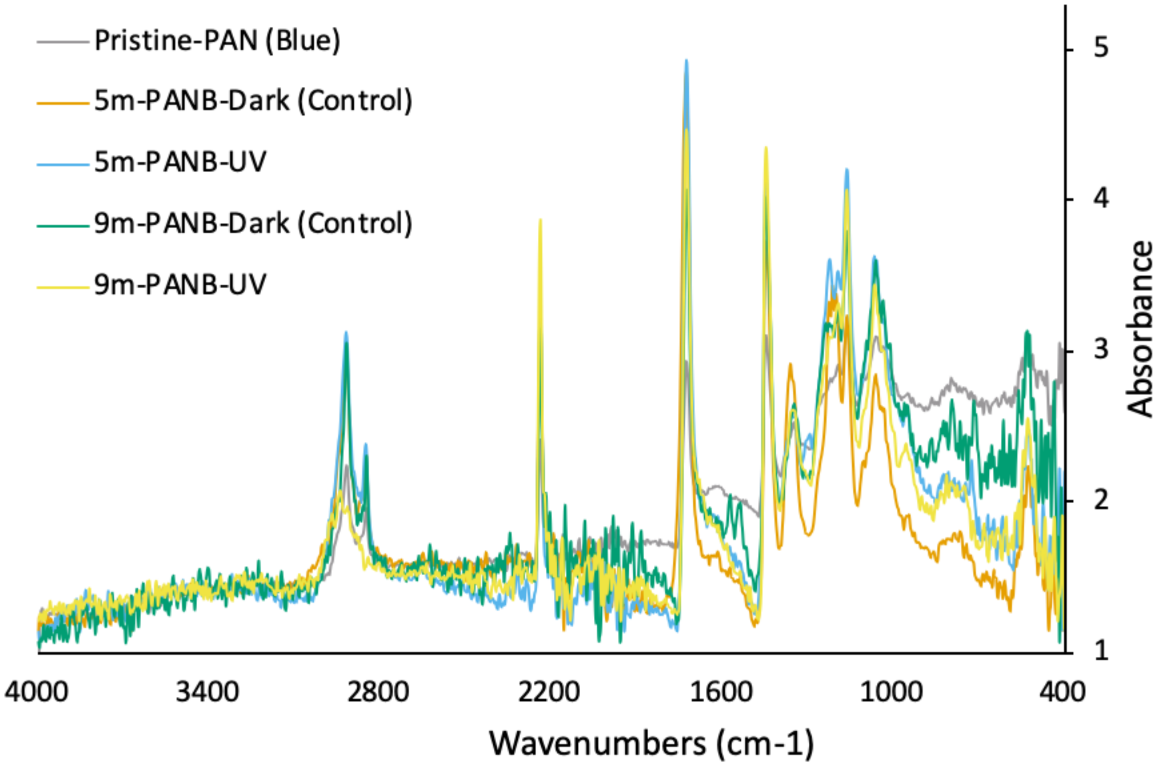

Figure B.9. ATR-FTIR spectrums of UV exposed blue polyacrylic (PANB) in FW, normalised to peak at 1360 cm^{-1}

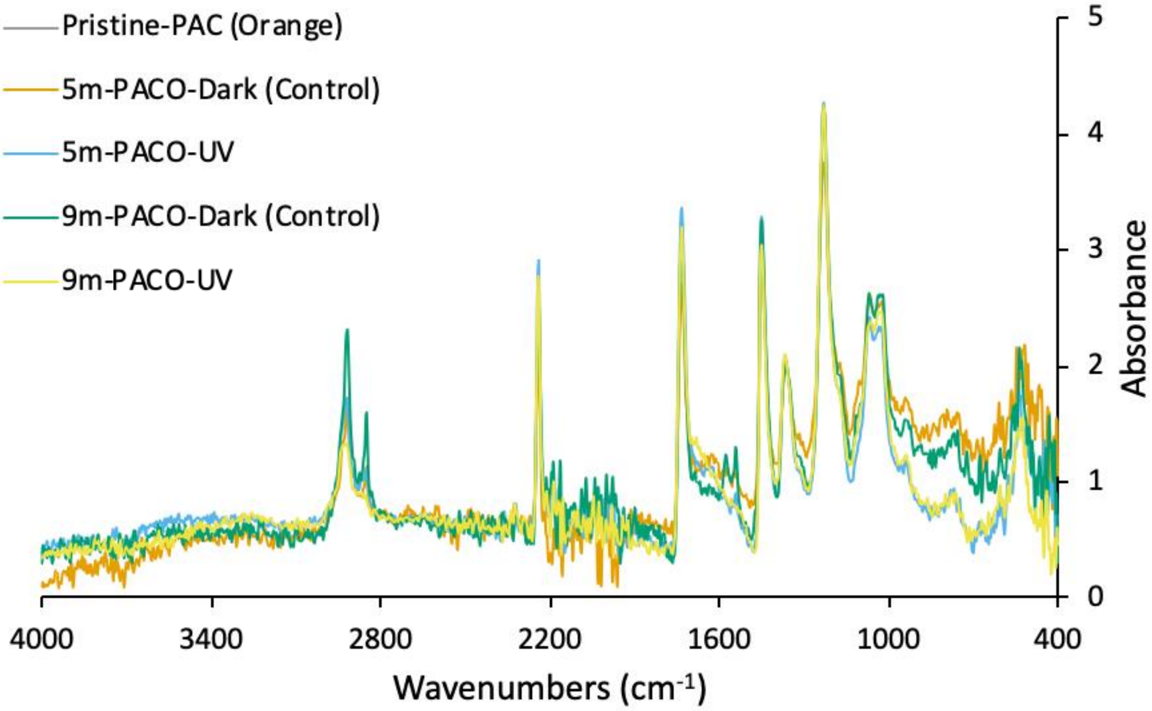

Figure B.10. ATR-FTIR spectrums of UV exposed orange polyacrylic (PANO) in FW, normalised to peak at 1360 cm^{-1}

UV exposure studies - Carbonyl indices

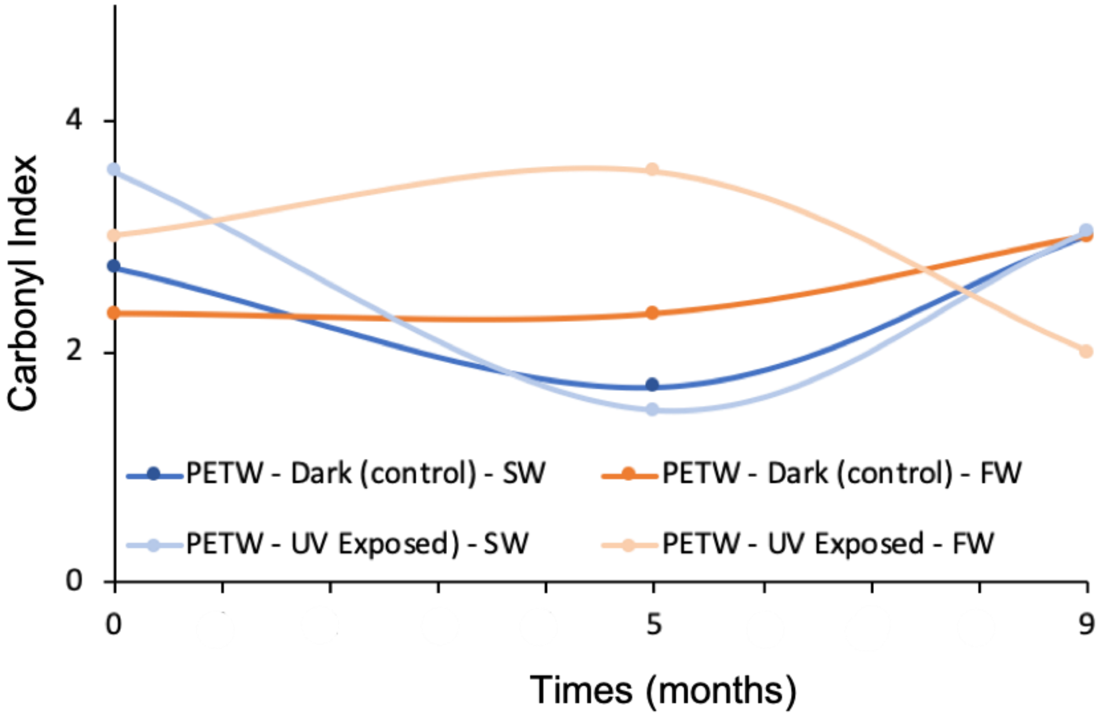

Figure B.11. Change in carbonyl indices with time in white PET after 9-month UV exposure

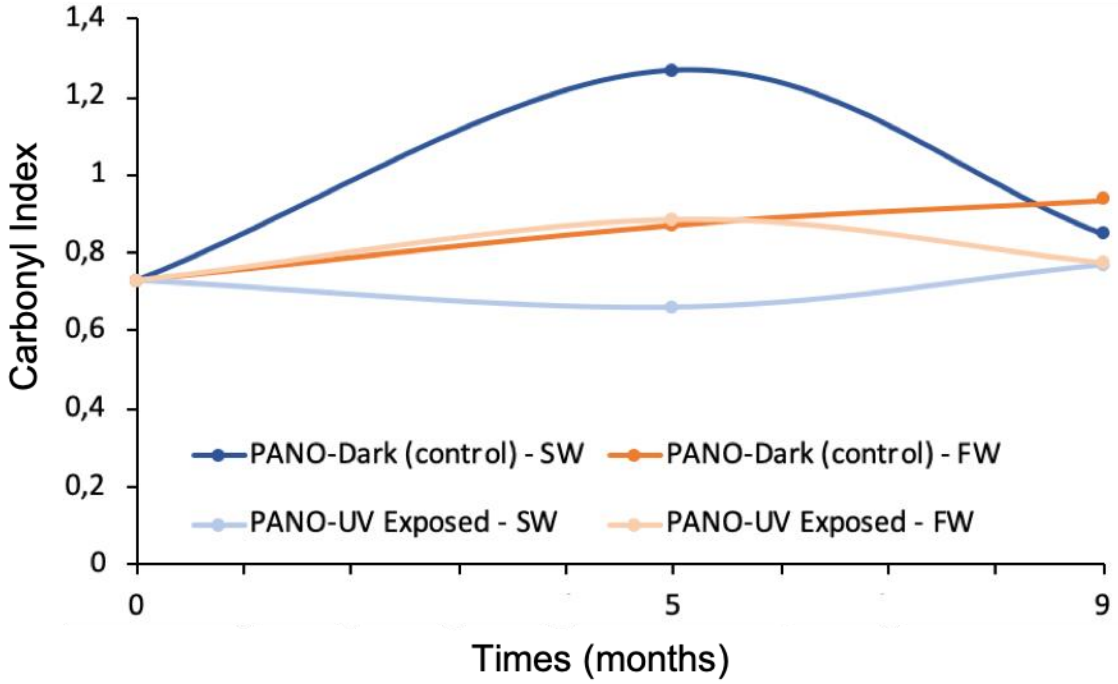

Figure B.12. Change in carbonyl indices with time in orange PAN after 9-month UV exposure

Appendix C. TG201 Media preparation

Preparation of OECD medium

Nutrient	**Concentration in stock solution**
Stock solution 1: macro nutrients	
NH_4Cl	1.5 g/L
$MgCl_2 \cdot 6H_2O$	1.2 g/L
$CaCl_2 \cdot 2H_2O$	1.8 g/L
$MgSO_4 \cdot 7H_2O$	1.5 g/L
KH_2PO_4	0.16 g/L
Stock solution 2: iron	
$FeCl_3 \cdot 6H_2O$	64 mg/L
$Na_2EDTA \cdot 2H_2O$	100 mg/L
Stock solution 3: trace elements	
H_3BO_3	185 mg/L
$MnCl_2 \cdot 4H_2O$	415 mg/L
$ZnCl_2$	3 mg/L
$CoCl_2 \cdot 6H_2O$	1.5 mg/L
$CuCl_2 \cdot 2H_2O$	0.01 mg/L
$Na_2MoO_4 \cdot 2H_2O$	7 mg/L
Stock solution 4: bicarbonate	
$NaHCO_3$	50 g/L
$Na_2SiO_3 \cdot 9H_20$	

Sterilize the stock solutions by membrane filtration (mean pore diameter 0.2 µm) or by autoclaving (120 °C, 15 min). Store the solutions in the dark at 4 °C.
Do not autoclave stock solutions 2 and 4, but sterilise them by membrane filtration.

Prepare a growth medium by adding an appropriate volume of the stock solutions 1-4 to water:

Add to 500 ml of sterilised water:
- 10 ml of stock solution 1
- 1 ml of stock solution 2
- 1 ml of stock solution 3
- 1 ml of stock solution 4

Make up to 1 000 mL with sterilised water.

Allow sufficient time for equilibrating the medium with the atmospheric CO_2, if necessary by bubbling with sterile, filtered air for some hours.

Appendix D. Mechanical degradation studies

Table D.1 Detailed sample description of 9 month long mechanical abrasion studies with subsampling at 5 months

Samples name	Fibre types (colour)	MPF amount (mg)	MPF size (mm)	Medium	Medium amount (mL)	Exposure time	Exposure temp (°C)	Amount of sand (g)
PES-B_Sand_20	Polyester (Black)	149.33	1 - 2.5	SW	100	9 months	25	5
PES-W_Sand_20	Polyester (White)	150.99	1 - 2.5	SW	100	9 months	25	5
PA-W_Sand_20	Polyamide (White)	148.76	1 - 2.5	SW	100	9 months	25	5
PAC-B_Sand_20	Polyacrylonitrile (Blue)	147.69	1 - 2.5	SW	100	9 months	25	5
PAC-O_Sand_20	Polyacrylonitrile (Orange)	147.20	1 - 2.5	SW	100	9 months	25	5
Wool_Sand_20	Wool (white/beige)	148.86	1 - 2.5	SW	100	9 months	25	5
SW_Sand_20	N/A	N/A	N/A	SW	100	9 months	25	5
PES-B_20	Polyester (Black)	150.00	1 - 2.5	SW	100	9 months	25	0
PES-W_20	Polyester (White)	152.67	1 - 2.5	SW	100	9 months	25	0
PA-W_20	Polyamide (White)	148.27	1 - 2.5	SW	100	9 months	25	0
PAC-B_20	Polyacrylonitrile (Blue)	150.69	1 - 2.5	SW	100	9 months	25	0

PAC-O_20	Polyacrylonitrile (Orange)	150.50	1 - 2.5	SW	100	9 months	25	0
Wool_20	Wool (white/beige)	148.89	1 - 2.5	SW	100	9 months	25	0
SW_20	N/A	N/A	N/A	SW	100	9 months	25	0
PES-B_Sand_5	Polyester (Black)	150.32	1 - 2.5	SW	100	9 months	5	5
PES-W_Sand_5	Polyester (White)	150.78	1 - 2.5	SW	100	9 months	5	5
PA-W_Sand_5	Polyamide (White)	149.91	1 - 2.5	SW	100	9 months	5	5
PAC-B_Sand_5	Polyacrylonitrile (Blue)	148.62	1 - 2.5	SW	100	9 months	5	5
PAC-O_Sand_5	Polyacrylonitrile (Orange)	149.01	1 - 2.5	SW	100	9 months	5	5
Wool_Sand_5	Wool (white/beige)	151.21	1 - 2.5	SW	100	9 months	5	5
SW_Sand_5	N/A	N/A	N/A	SW	100	9 months	5	5
PES-B_5	Polyester (Black)	149.56	1 - 2.5	SW	100	9 months	5	0
PES-W_5	Polyester (White)	145.67	1 - 2.5	SW	100	9 months	5	0
PA-W_5	Polyamide (White)	151.42	1 - 2.5	SW	100	9 months	5	0
PAC-B_5	Polyacrylonitrile (Blue)	148.22	1 - 2.5	SW	100	9 months	5	0
PAC-O_5	Polyacrylonitrile (Orange)	148.78	1 - 2.5	SW	100	9 months	5	0
Wool_5	Wool (white/beige)	148.39	1 - 2.5	SW	100	9 months	5	0
SW_5	N/A	N/A	N/A	SW	100	9 months	5	0

MPFs and wool after 9 month mechanical degradation

PET (Black) – SW medium (No sand)

PET (Black) – SW medium with sand

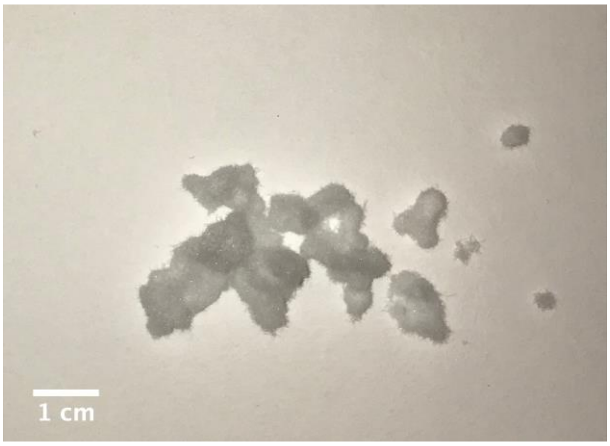

PET (White) – SW medium (No sand)

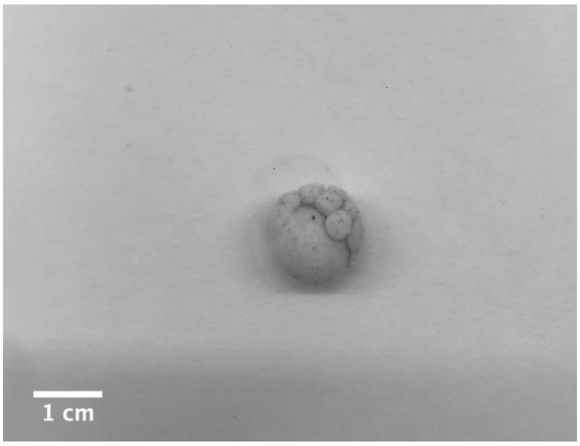

PET (White) – SW medium with sand

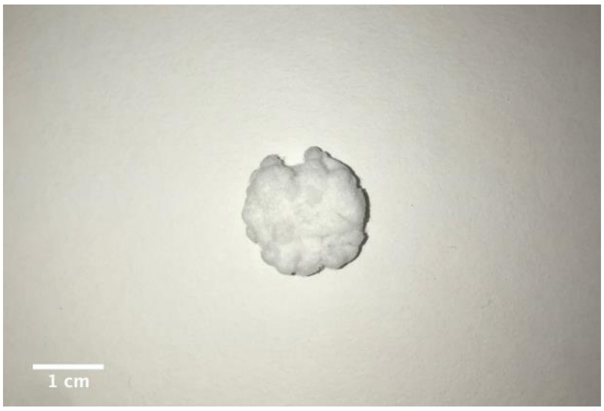

PA (White) – SW medium (No Sand)

PA (White) – SW medium with sand

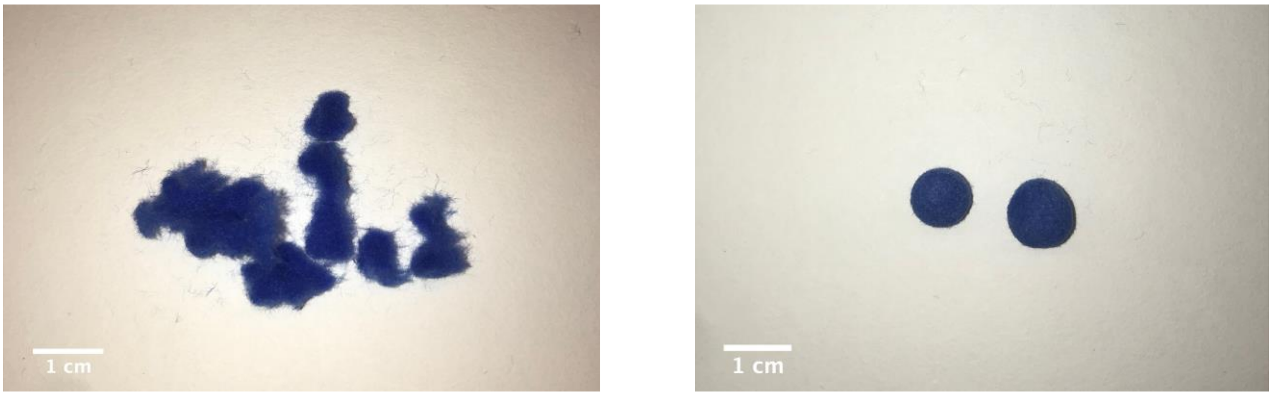

PAN (Blue) – SW medium (No Sand) PAN (Blue) – SW medium with sand

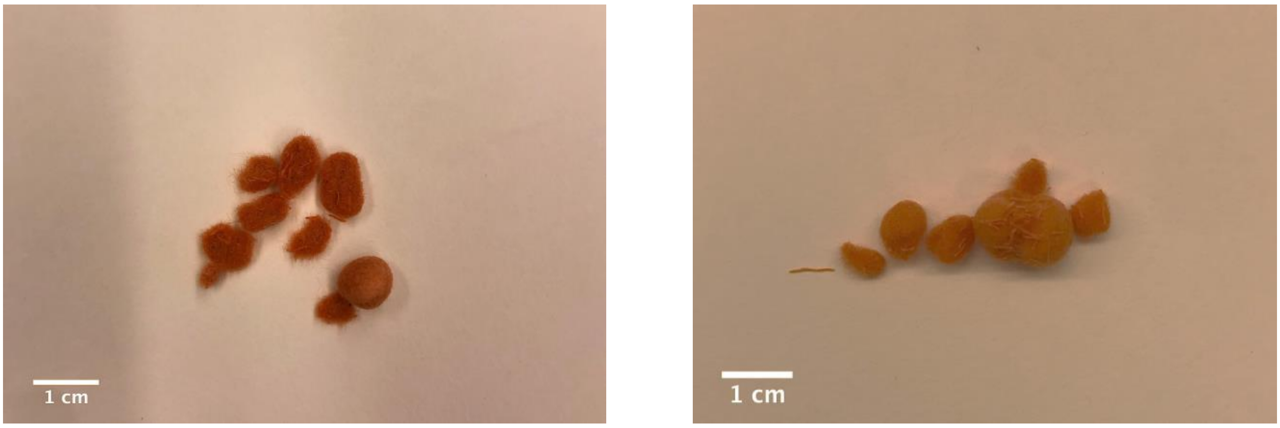

PAN (Orange) – SW medium (No Sand) PAN (Orange) – SW medium with sand

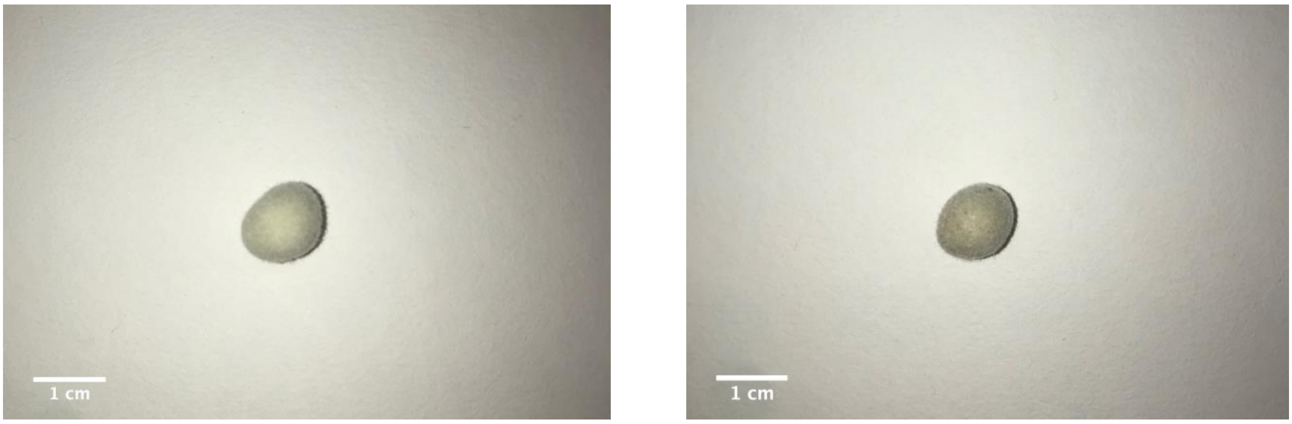

Wool – SW medium (No Sand) Wool – SW medium with Sand

Figure D.1. MPFs and wool after mechanical abrasion studies at 20 degrees

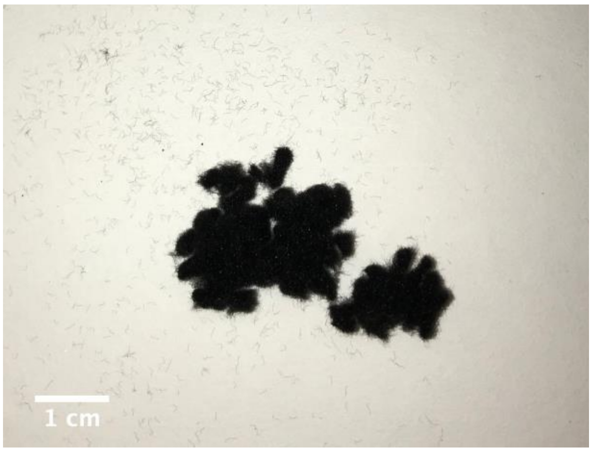

PET (Black) – SW medium (No sand)

PET (Black) – SW medium with sand

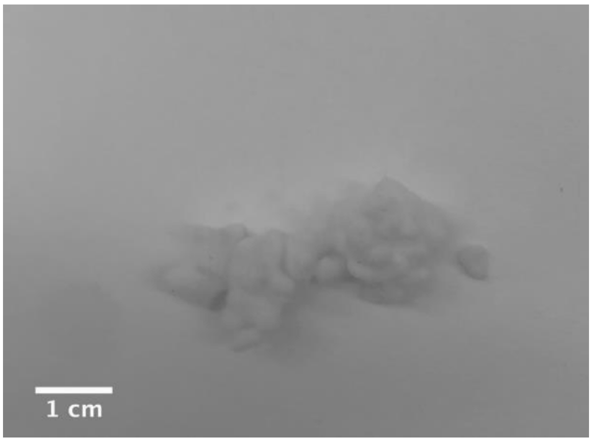

PET (White) – SW medium (No sand)

PET (White) – SW medium with sand

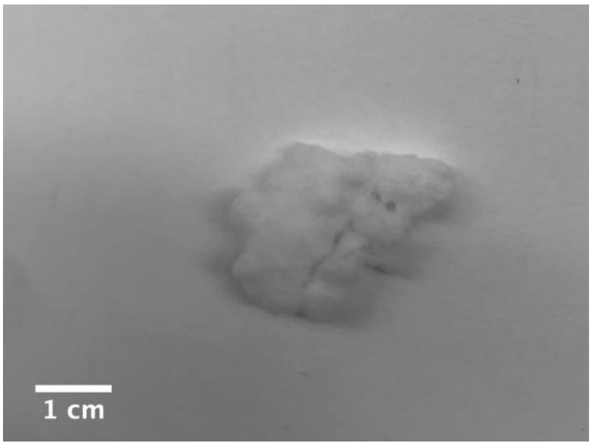

PA (White) – SW medium (No Sand)

PA (White) – SW medium with sand

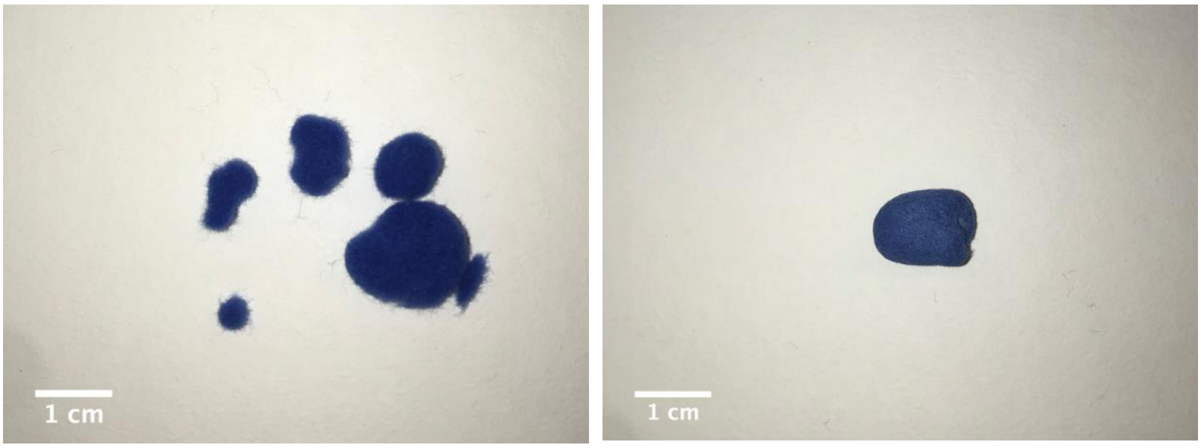

PAN (Blue) – SW medium (No Sand)

PAN (Blue) – SW medium with sand

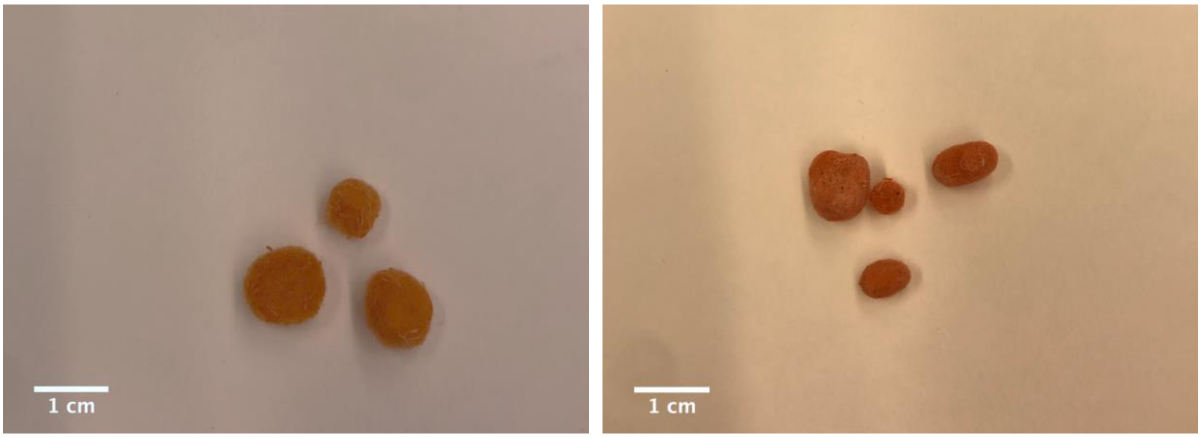

PAN (Orange) – SW medium (No Sand)

PAN (Orange) – SW medium with sand

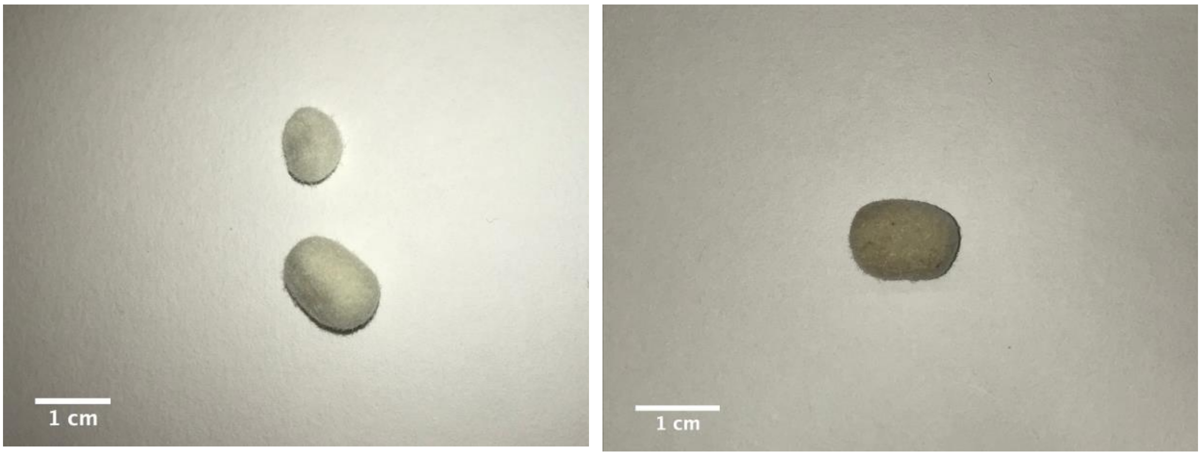

Wool – SW medium (No Sand)

Wool – SW medium with Sand

Figure D.2. MPFs and wool after mechanical abrasion studies at 5 degrees

Appendix E. LC-MS/MS study – Bisphenols and Benzophenones

Table E.1 Concentration of BP and BzP content (ng/g) in PET black, PET white, PA, PAN blue and PAN orange MPFs and wool fibre (N=3)

		BPA	BPAF	BPAP	BPB	BPF	BPM	BPP	BPS	BPZ	∑BPs	BzP1	BzP2	BzP3	4-OH-BzP	BzP8	∑BzPs
PET (Black)	Mean	131.58	<LOD	<LOD	<LOD	0.62	<LOD	<LOD	0.74	<LOD	132.95	3.51	<LOD	16.02	0.31	<LOD	19.86
	Median	86.64	<LOD	<LOD	<LOD	0.48	<LOD	<LOD	0.75	<LOD	87.88	0.48	<LOD	17.91	0.31	<LOD	18.68
	Min	66.91	<LOD	<LOD	<LOD	0.35	<LOD	<LOD	0.47	<LOD	67.74	<LOD	<LOD	11.13	0.28	<LOD	11.24
	Max	241.20	0.07	<LOD	<LOD	1.02	<LOD	<LOD	1.01	<LOD	243.35	10.07	<LOD	19.03	0.35	<LOD	29.65
	DR* (%)	100	33	0	0	100	0	0	100	0	100	100	0	100	100	100	100
PET (White)	Mean	24.63	<LOD	<LOD	<LOD	<LOD	<LOD	<LOD	0.58	<LOD	25.28	0.85	<LOD	20.22	0.17	<LOD	21.17
	Median	25.36	<LOD	<LOD	<LOD	<LOD	<LOD	<LOD	0.42	<LOD	25.82	0.10	<LOD	16.98	0.12	<LOD	17.12
	Min	17.38	<LOD	<LOD	<LOD	<LOD	<LOD	<LOD	0.38	<LOD	17.78	<LOD	<LOD	15.96	<LOD	<LOD	15.56
	Max	31.16	0.13	0.13	<LOD	<LOD	<LOD	<LOD	0.92	<LOD	32.40	2.77	<LOD	27.73	0.39	<LOD	30.85
	DR* (%)	100	33	33	0	0	33	0	100	0	100	100	100	100	100	0	100
PA (White)	Mean	89.35	<LOD	<LOD	<LOD	<LOD	<LOD	<LOD	0.51	0.07	89.96	<LOD	<LOD	15.37	<LOD	<LOD	14.93
	Median	73.11	<LOD	<LOD	<LOD	<LOD	<LOD	<LOD	0.52	<LOD	73.62	<LOD	<LOD	13.61	<LOD	<LOD	13.12
	Min	67.45	<LOD	<LOD	<LOD	<LOD	<LOD	<LOD	0.41	<LOD	67.86	<LOD	<LOD	8.59	<LOD	<LOD	7.99
	Max	127.47	<LOD	<LOD	<LOD	<LOD	<LOD	<LOD	0.59	0.26	128.42	<LOD	<LOD	23.90	<LOD	<LOD	23.69
	DR* (%)	100	0	0	0	0	0	0	100	100	100	100	100	100	100	0	100
PAN (Blue)	Mean	169.22	1.15	<LOD	<LOD	<LOD	<LOD	<LOD	0.67	<LOD	171.03	0.39	<LOD	4.78	0.16	<LOD	5.49

		BPA	BPAF	BPAP	BPB	BPF	BPM	BPP	BPS	BPZ	∑BPs	BzP1	BzP2	BzP3	4-OH-BzP	BzP8	∑BzPs
	Median	163.35	1.16	<LOD	<LOD	<LOD	<LOD	<LOD	0.69	<LOD	165.20	0.40	<LOD	4.33	0.11	<LOD	4.97
	Min	99.90	1.01	<LOD	<LOD	<LOD	<LOD	<LOD	0.59	<LOD	101.51	0.11	<LOD	3.29	0.09	<LOD	3.49
	Max	244.42	1.28	<LOD	<LOD	<LOD	<LOD	<LOD	0.72	<LOD	246.48	0.68	0.10	6.72	0.29	<LOD	8.00
	DR* (%)	100	100	0	0	0	0	0	100	0	100	100	33	100	100	0	93
PAN (Orange)	Mean	112.48	<LOD	<LOD	<LOD	<LOD	<LOD	<LOD	0.43	<LOD	112.97	0.26	<LOD	9.23	0.47	<LOD	9.95
	Median	104.98	<LOD	<LOD	<LOD	<LOD	<LOD	<LOD	0.29	<LOD	105.33	0.35	<LOD	7.77	0.38	<LOD	8.49
	Min	75.06	<LOD	<LOD	<LOD	<LOD	<LOD	<LOD	0.10	<LOD	75.20	<LOD	<LOD	7.29	0.34	<LOD	7.37
	Max	157.40	<LOD	<LOD	<LOD	<LOD	<LOD	<LOD	0.91	<LOD	158.40	0.61	<LOD	12.61	0.69	<LOD	13.98
	DR* (%)	100	0	33	0	0	33	0	100	67	100	100	0	100	100	0	100
Wool	Mean	809.59	<LOD	4.17	<LOD	46.99	<LOD	<LOD	1.95	<LOD	862.81	3.51	<LOD	20.57	2.90	<LOD	26.99
	Median	500.60	<LOD	3.76	<LOD	53.23	<LOD	<LOD	1.96	<LOD	559.67	3.27	<LOD	20.74	2.94	<LOD	26.93
	Min	343.94	<LOD	3.25	<LOD	24.91	<LOD	<LOD	1.24	<LOD	373.34	2.63	<LOD	18.05	2.23	<LOD	22.77
	Max	1584.22	<LOD	5.49	<LOD	62.82	<LOD	0.07	2.65	<LOD	1655.42	4.63	0.18	22.92	3.55	<LOD	31.29
	DR* (%)	100	0	100	100	100	100	33	100	0	100	100	100	100	100	0	100

*: Detection Rate (DR) refers to the number of samples with values above the LOD in percent

Calibration Curves – Bisphenols and benzophenones

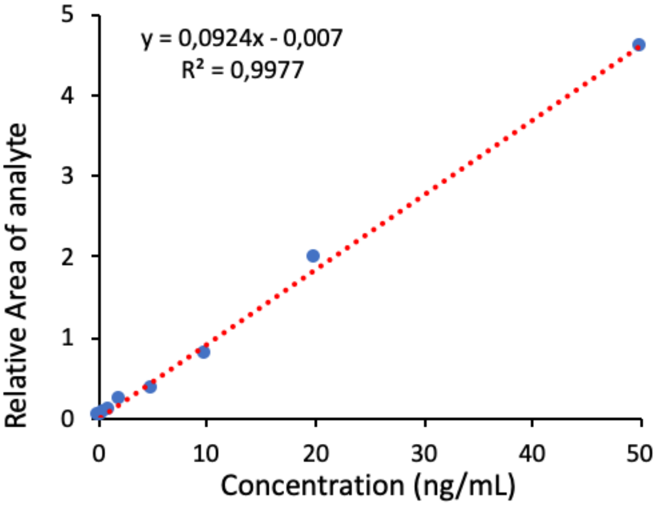

BPA

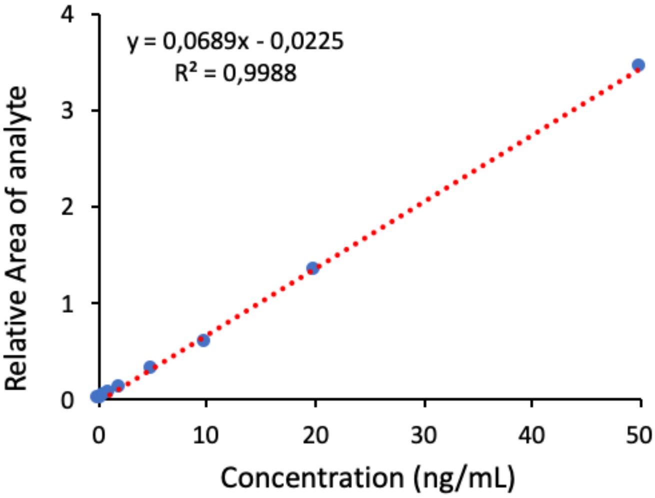

BPAF

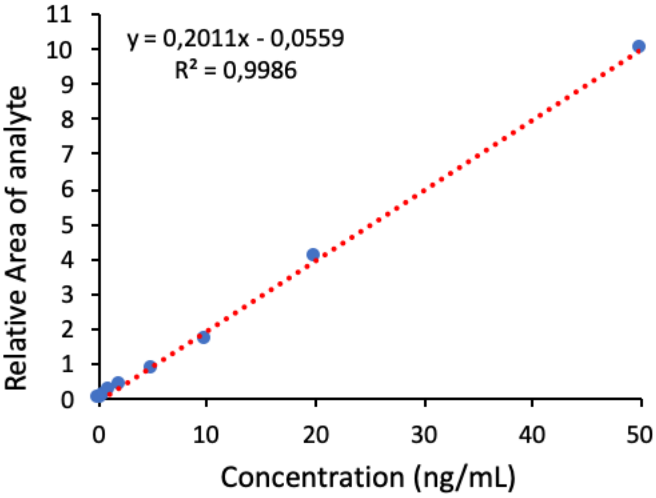

BPAP

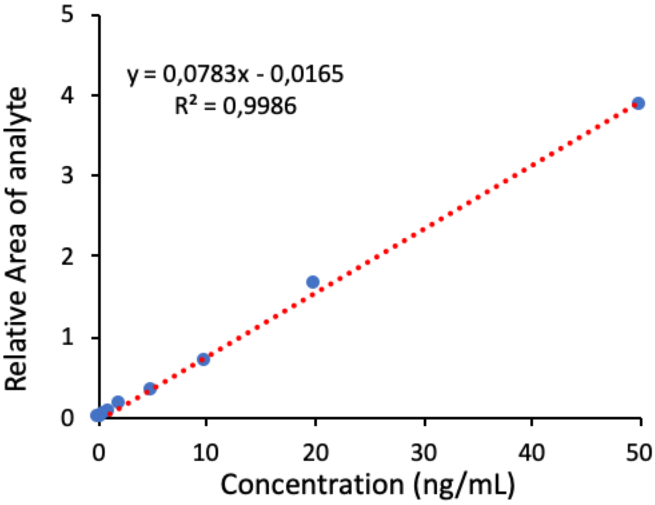

BPB

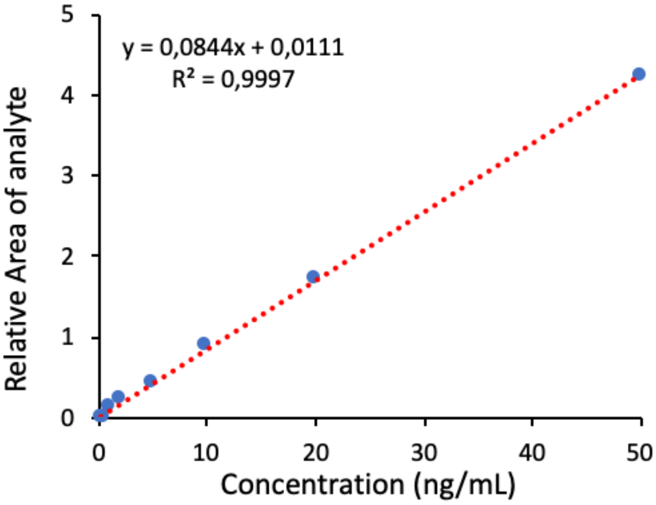

BPF

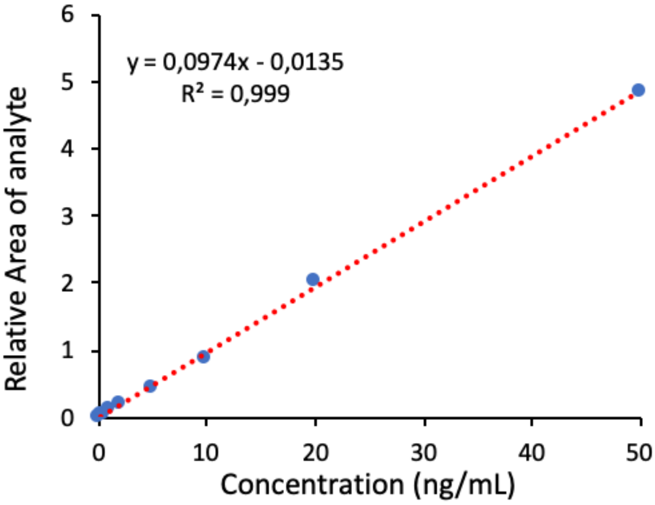

BPM

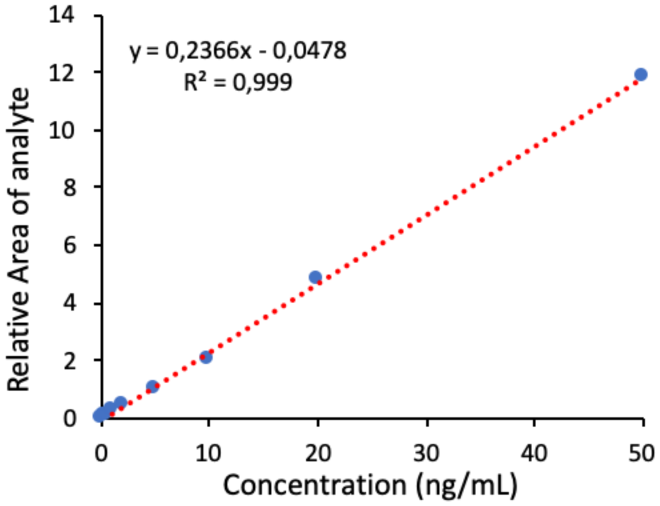

BPP

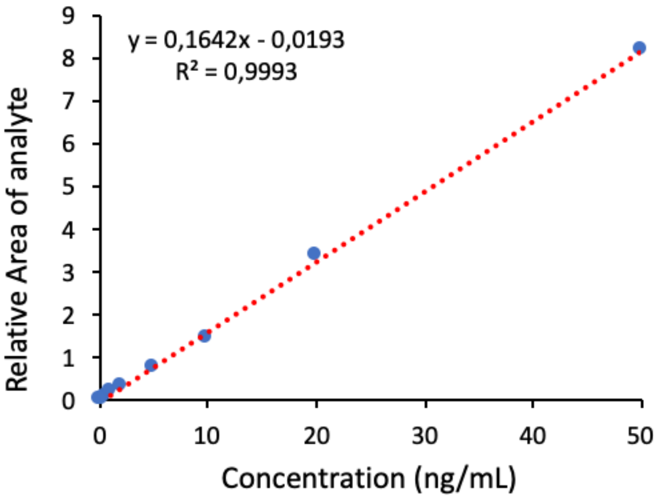

BPS

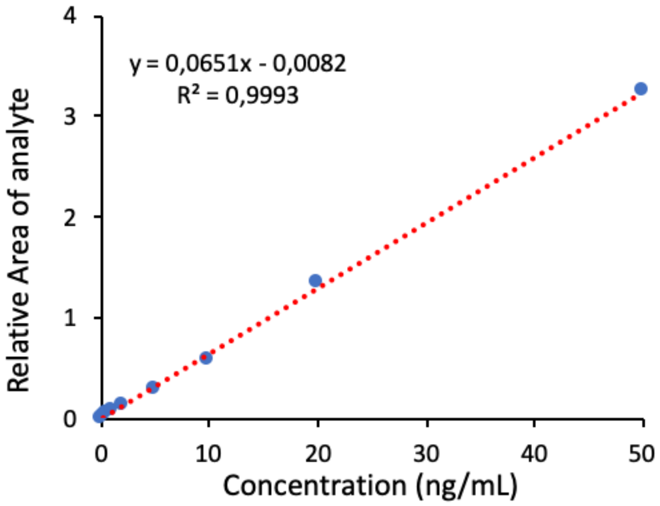

BPZ

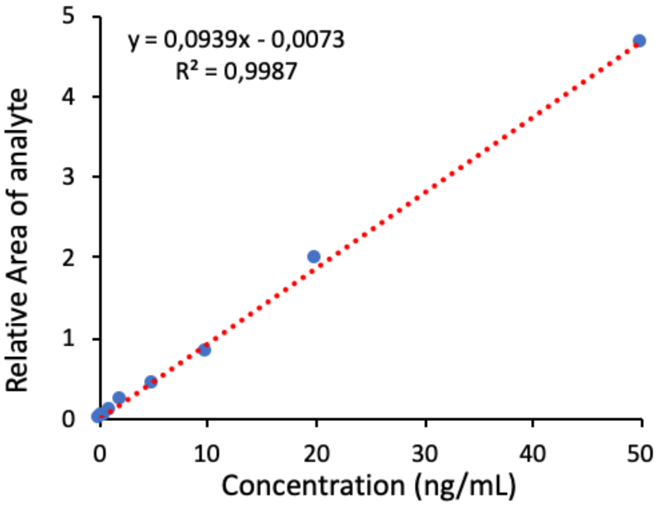

BzP-1

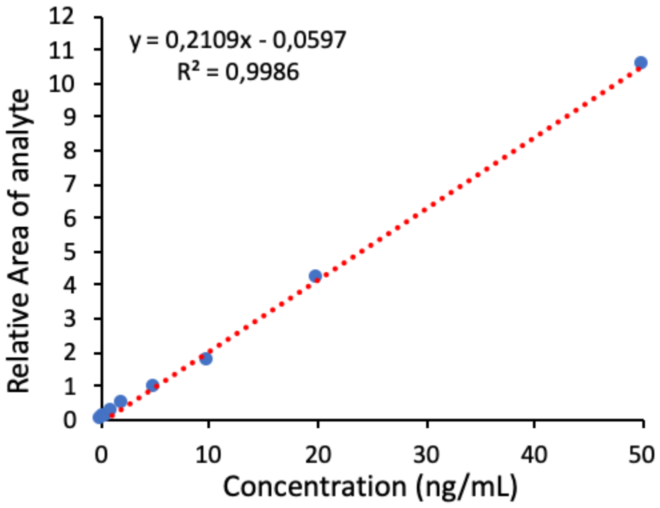

BzP-2

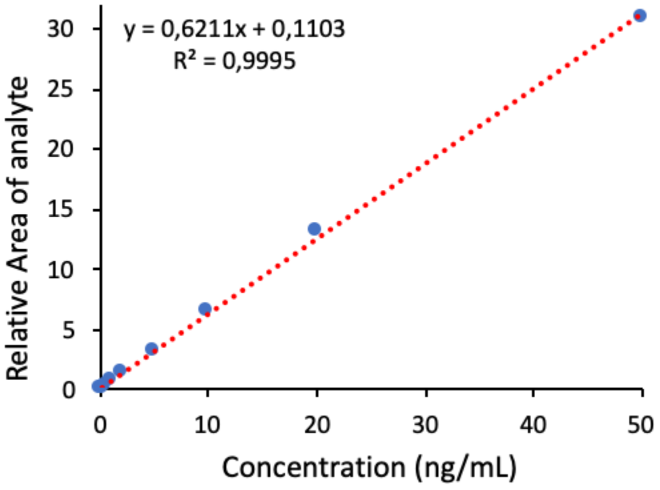

BzP-3

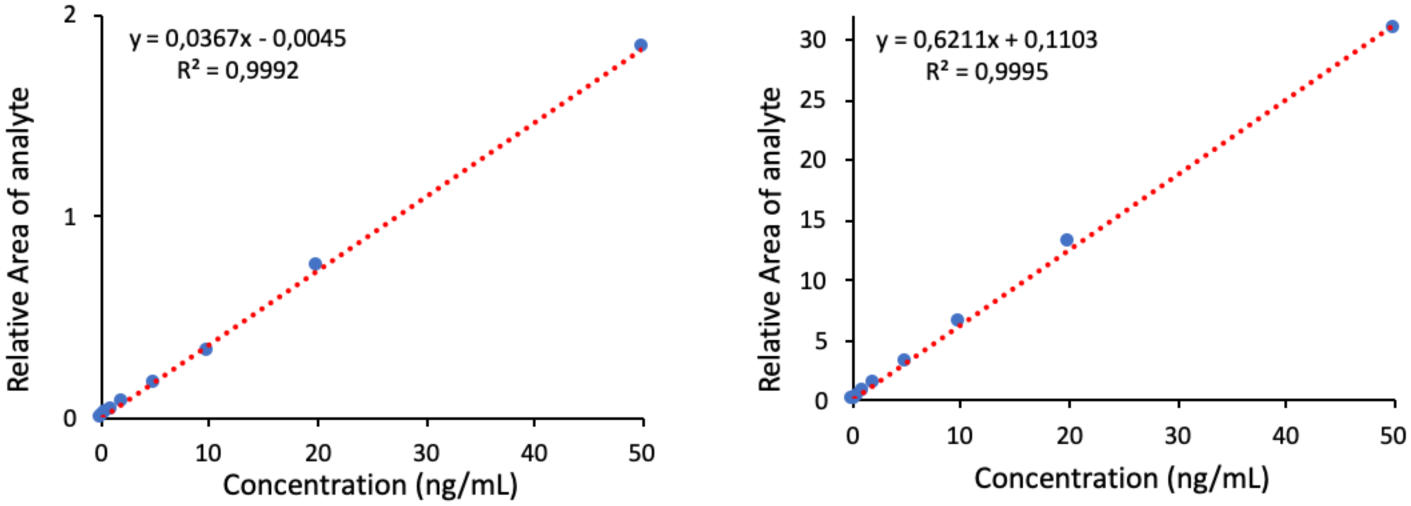

4-OH-BzP BzP-8

Figure E.1. Calibration curves for bisphenols (BPs) and benzophenones (BzPs)

Table E.2. Multiple reaction monitoring transitions for bisphenols and benzophenones and the compound specific parameters used in LC-MS/MS analysis.

Compound	Precursor ion (m/z)	Product ions (m/z)	Collision energy (V)	Cone voltage (V)
BPA	227	212	18	50
		133	24	
BPAF	335	265	24	40
		177	42	
BPAP	289	274	18	20
		195	28	
BPB	241	212	18	20
BPF	199	105	20	46
		93		
BPM	345	133	46	8
BPP	345	330	26	14
BPS	249	156	22	40
		108	26	
BPZ	267	173	24	40
		145	36	
BzP1	213	135	28	46
		91	18	
BzP2	245	135	14	40
		109	16	
BzP3	227	211	20	40
		183	34	
4-OH-BzP	197	120	22	60
		92	28	
BzP8	243	123	16	46
		93	18	
13C12 BPA	240	145	20	30
		224		
13C12 BPAF	348	277	24	20
13C12 BPF	212	82	28	22
		98	24	
		110	26	
13C12 BPB	254	224	20	16
		217	18	
13C12 BPS	262	98	36	20
		114	28	
		162	20	

Table E.3. Absolute and relative recovery (%) N=3

Compound	Absolute recovery (%)		Relative recovery (%)	
	Fibre	Leachate	Fibre	Leachate
BPA	76.54	86.43	99.80	101.99
BPAF	76.76	89.05	99.70	104.67
BPAP	73.10	79.75	106.63	93.43
BPB	70.20	84.31	102.19	97.52
BPF	72.87	89.77	98.73	99.93
BPM	73.53	82.77	107.40	96.82
BPP	73.48	82.31	107.23	96.46
BPS	72.17	87.92	103.10	103.33
BPZ	70.25	86.44	102.63	99.74
BzP1	65.62	83.14	92.56	98.97
BzP2	65.40	85.98	92.25	101.77
BzP3	57.11	64.56	87.07	75.34
4-OH-BzP	67.93	85.24	95.88	103.67
BzP8	64.53	68.04	88.46	76.98

Table E.4. Ion ratio (IR), RT and RRT (± RSD%) for target analytes

Compound	IR (%)	RT	RRT
BPA	43.09 ± 41.53	1.84 ± 0.22	1.00 ± 0.22
BPAF	8.05 ±1.34	1.72 ± 0.30	1.00 ± 0.32
BPAP	5.86 ± 6.46	2.29 ± 0.23	1.07 ± 0.23
BPB	N/A	2.14 ± 0.19	1.00 ± 0.19
BPF	99.13 ± 0.06	1.39 ± 0.37	1.00 ± 0.59
BPM	N/A	3.16 ± 0.13	1.48 ± 0.13
BPP	N/A	3.16 ± 0.17	1.47 ± 0.17
BPS	32.43 ± 1.41	0.32 ± 10.51	1.00 ± 0.00
BPZ	57.75 ± 4.72	2.48 ± 0.22	1.16 ± 0.22
BzP1	106.04 ± 18.07	0.39 ± 3.01	1.24 ± 9.94
BzP2	58.83 ± 6.09	0.32 ± 11.35	1.02 ± 1.57
BzP3	2.39 ± 8.42	2.51 ± 0.21	1.17 ± 0.21
4-OH-BzP	23.12 ± 7.97	0.39 ± 2.67	1.23 ± 11.08
BzP8	88.66 ± 6.24	1.51 ± 0.50	1.08 ± 0.72

Table E.5. Lower limit of quantification (LLOQ) and limit of detection (LOD) for target analytes (ng/ml)

Compound	LLOQ	LOD
BPA	0.10	0.03
BPAF	0.10	0.03
BPAP	0.10	0.03
BPB	0.50	0.17
BPF	0.20	0.07
BPM	0.10	0.03
BPP	0.10	0.03
BPS	0.10	0.03
BPZ	0.10	0.03
BzP1	0.10	0.03
BzP2	0.10	0.03
BzP3	0.20	0.07
4-OH-BzP	0.10	0.03
BzP8	0.50	0.17

Table E.6. Reproducibility (RSD%, N = 3; [20 ng/mL] of target analytes

Compound	Fibres
BPA	5.83
BPAF	6.00
BPAP	1.63
BPB	4.03
BPF	3.49
BPM	1.54
BPP	1.23
BPS	2.58
BPZ	1.35
BzP-1	1.13
BzP-2	4.30
BzP-3	2.61
BzP-8	5.54
4-OH-BzP	3.23

Table E.7. Matrix factors (MF) and effects (ME) of PET (white) fibre (N=3)

Compound	MF	ME (%)
BPA	0.98	-2.05
BPAF	1.19	19.35
BPAP	0.71	-28.76
BPB	0.76	-23.96
BPF	1.17	16.61
BPM	0.86	-13.62
BPP	0.88	-12.06
BPS	0.65	-34.57
BPZ	0.82	-17.71
BzP1	0.79	-21.12
BzP2	0.70	-30.43
BzP3	0.76	-24.08
4-OH-BzP	1.19	18.51
BzP8	1.07	7.33

Appendix F. ICP-MS – Investigation of inorganic content

Table F.1. High-pressure microwave digestion conditions

Step	Time (min)	Temp 1 (°C)	Temp 2 (°C)	Energy (Watt)
1	5	50	60	1000
2	10	50	60	1000
3	10	100	60	1000
4	8	110	60	1000
5	15	190	60	1000
6	5	210	60	1000
7	15	245	60	1000
8	10	245	60	1000

Table F.2. Determined quantification limits (QL) in MPFs

Element	Resolution	QL	Element	Resolution	QL	Element	Resolution	QL
Ag	Medium	0.03	Hf	Low	0.001	Rh	Low	0.0006
Al	Medium	0.26	Hg	Low	0.003	S	Medium	6.40
As	High	0.03	Ho	Low	0.0003	Sb	Medium	0.003
Au	Low	0.0003	I	Medium	1.28	Sc	Medium	0.005
B	Low	0.06	In	Low	0.0006	Se	Low	0.06
Ba	Medium	0.02	Ir	Low	0.0006	Si	Medium	12.8
Be	Low	0.003	K	Medium	1.28	Sm	Low	0.0006
Bi	Low	0.001	La	Low	0.0006	Sn	Low	0.001
Br	High	3.84	Li	Low	0.006	Sr	Medium	0.03
Ca	Medium	2.56	Lu	Low	0.0003	Ta	Low	0.0003
Cd	Low	0.003	Mg	Medium	0.13	Tb	Low	0.0003
Ce	Low	0.0003	Mn	Medium	0.008	Te	Medium	0.1
Cl	Medium	128.00	Mo	Medium	0.03	Th	Low	0.0006
Co	Medium	0.01	Na	Medium	12.80	Ti	Medium	0.03
Cr	Medium	0.03	Nb	Low	0.001	Tl	Low	0.0003
Cs	Low	0.001	Nd	Low	0.0003	Tm	Low	0.0006
Cu	Medium	0.04	Ni	Medium	0.02	U	Low	0.0003
Dy	Low	0.001	P	Medium	0.51	V	Medium	0.004
Er	Low	0.000	Pb	Low	0.003	W	Low	0.001
Eu	Low	0.001	Pd	High	0.06	Yb	Low	0.0005
Fe	Medium	0.03	Pr	Low	0.0004	Zn	Medium	0.03
Ga	Medium	0.009	Pt	Low	0.001	Zr	Low	0.0006
Gd	Medium	0.03	Rb	Medium	0.015			
Ge	High	0.03	Re	High	0.05			

Table F.3. Inorganic content (ng/mL) in PET (Black, White) and PA MPFs

	PET (Black)				PET (White)				PA (White)			
	Median	Mean	Min	Max	Median	Mean	Min	Max	Median	Mean	Min	Max
Ag	0.008	0.006	0.005	0.012	0.037	0.048	0.011	0.053	0.027	0.026	0.022	0.032
Al	3.620	3.514	3.299	4.045	4.869	5.117	4.012	5.477	2.801	2.686	2.181	3.536
Au	0.002	0.002	0.002	0.002	0.004	0.004	0.003	0.005	0.004	0.004	0.003	0.004
B	0.316	0.350	0.180	0.418	0.720	0.333	0.263	1.564	0.343	0.199	0.172	0.659
Ba	0.168	0.184	0.122	0.199	0.238	0.268	0.178	0.269	0.059	0.053	0.047	0.076
Bi	0.087	0.076	0.068	0.117	0.213	0.204	0.194	0.240	0.223	0.170	0.118	0.381
Ca	4.701	4.513	3.892	5.698	7.183	7.667	4.717	9.165	3.915	4.275	1.844	5.625
Cd	0.002	0.002	0.002	0.003	0.010	0.003	0.002	0.024	0.003	0.003	0.002	0.004
Ce	0.003	0.003	0.003	0.003	0.011	0.003	0.002	0.028	0.003	0.003	0.002	0.003
Co	0.036	0.036	0.034	0.038	0.028	0.028	0.027	0.029	0.023	0.002	0.002	0.066
Cr	0.196	0.197	0.190	0.202	0.248	0.244	0.232	0.269	2.275	0.160	0.128	6.536
Cs	0.000	0.000	0.000	0.000	0.000	0.000	0.000	0.000	0.000	0.000	0.000	0.000
Cu	0.253	0.239	0.238	0.281	0.300	0.308	0.244	0.346	0.391	0.300	0.218	0.655
Fe	2.598	2.558	2.232	3.003	3.440	3.444	2.920	3.957	10.709	2.526	2.462	27.139
Hf	0.003	0.003	0.002	0.003	0.003	0.003	0.002	0.003	0.002	0.002	0.002	0.002
Hg	0.002	0.002	0.000	0.005	0.003	0.003	0.002	0.003	0.005	0.005	0.003	0.006
K	13.442	12.822	10.942	16.563	17.255	18.010	11.407	22.347	21.773	14.910	8.878	41.530
L	0.003	0.003	0.003	0.003	0.007	0.003	0.003	0.016	0.001	0.001	0.001	0.002
Li	0.002	0.002	0.002	0.002	0.003	0.004	0.002	0.004	0.003	0.002	0.002	0.004
Mg	1.790	1.815	1.677	1.877	3.033	3.153	2.426	3.522	2.875	2.189	2.001	4.437
Mn	0.045	0.046	0.042	0.048	0.043	0.041	0.034	0.055	6.665	6.577	6.473	6.945

Mo	0.031	0.029	0.028	0.038	0.030	0.030	0.029	0.032	0.102	0.006	0.003	0.298
Na	8.298	7.888	7.854	9.153	10.945	12.510	7.554	12.773	16.901	11.982	6.887	31.833
Ni	0.045	0.045	0.045	0.046	0.066	0.066	0.063	0.069	1.533	0.056	0.053	4.490
P	4.129	3.927	3.897	4.562	4.824	4.684	4.593	5.196	9.555	9.750	8.491	10.424
Pb	0.135	0.123	0.123	0.159	0.120	0.124	0.096	0.139	0.050	0.046	0.042	0.063
Pr	0.000	0.000	0.000	0.000	0.000	0.000	0.000	0.001	0.000	0.000	0.000	0.000
Rb	0.009	0.009	0.006	0.012	0.014	0.013	0.010	0.018	0.013	0.009	0.006	0.023
S	90.195	91.749	85.612	93.223	13.840	14.324	12.493	14.705	10.788	10.542	7.434	14.389
Sc	0.000	0.000	0.000	0.000	0.000	0.000	0.000	0.000	0.000	0.000	0.000	0.000
Sb	138.476	138.020	136.723	140.687	146.032	147.356	142.640	148.099	0.621	0.602	0.597	0.665
Si	25.703	22.279	19.623	35.205	30.677	27.796	26.962	37.272	17.605	17.268	8.205	27.341
Sn	0.014	0.014	0.012	0.015	0.028	0.030	0.021	0.034	0.014	0.013	0.010	0.019
Sr	0.032	0.031	0.020	0.045	0.054	0.052	0.046	0.063	0.015	0.015	0.009	0.022
Th	0.000	0.000	0.000	0.000	0.000	0.000	0.000	0.000	0.000	0.000	0.000	0.000
Ti	37.405	34.275	29.297	48.644	47.269	45.513	42.453	53.841	87.361	87.832	77.843	96.409
U	0.000	0.000	0.000	0.000	0.000	0.000	0.000	0.000	0.000	0.000	0.000	0.000
V	0.031	0.029	0.029	0.034	0.032	0.031	0.031	0.033	0.029	0.023	0.023	0.040
Y	0.001	0.001	0.001	0.001	0.002	0.002	0.001	0.004	0.001	0.000	0.000	0.001
Zn	0.774	0.761	0.729	0.832	0.829	0.907	0.595	0.983	1.065	1.092	0.566	1.537
Zr	0.084	0.087	0.072	0.094	0.081	0.082	0.077	0.084	0.045	0.045	0.042	0.046

Table F.4. Inorganic content (ng/mL) in PAN (Blue, Orange) MPFs and wool (natural) fibre

	PAN (Blue)				PAN (Orange)				Wool			
	Median	Mean	Min	Max	Median	Mean	Min	Max	Median	Mean	Min	Max
Ag	0.012	0.012	0.006	0.018	0.023	0.023	0.018	0.029	0.021	0.019	0.015	0.029
Al	16.726	16.726	14.903	18.549	10.507	10.507	9.993	11.021	15.356	15.646	13.241	17.182
Au	0.005	0.005	0.004	0.005	0.010	0.010	0.008	0.013	0.016	0.017	0.010	0.021
B	0.001	0.001	0.001	0.001	0.000	0.000	0.000	0.001	0.001	0.001	0.001	0.001
Ba	1.039	1.039	0.878	1.199	1.838	1.838	1.776	1.900	0.718	0.677	0.634	0.844
Bi	0.221	0.221	0.186	0.255	0.186	0.186	0.182	0.189	0.220	0.219	0.214	0.227
Ca	193.659	193.659	185.537	201.781	172.329	172.329	163.443	181.215	188.701	131.707	128.046	306.350
Cd	0.008	0.008	0.006	0.009	0.006	0.006	0.006	0.007	0.015	0.014	0.012	0.018
Ce	0.021	0.021	0.010	0.032	0.006	0.006	0.006	0.006	0.025	0.024	0.021	0.030
Co	0.006	0.006	0.006	0.006	0.011	0.011	0.006	0.015	0.027	0.028	0.026	0.028
Cr	0.260	0.260	0.189	0.331	0.262	0.262	0.241	0.283	0.194	0.187	0.166	0.229
Cs	0.001	0.001	0.000	0.001	0.001	0.001	0.001	0.001	0.002	0.002	0.002	0.002
Cu	0.771	0.771	0.726	0.816	1.512	1.512	1.405	1.619	3.912	3.982	3.729	4.026
Fe	8.566	8.566	6.517	10.615	10.143	10.143	9.844	10.442	19.687	19.737	17.040	22.285
Hf	0.001	0.001	0.001	0.001	0.001	0.001	0.001	0.001	0.001	0.001	0.000	0.001
Hg	0.003	0.003	0.003	0.003	0.001	0.001	0.001	0.001	0.008	0.008	0.008	0.009
K	88.029	88.029	69.789	106.270	107.381	107.381	84.531	130.230	49.600	14.523	13.330	120.948
L	0.014	0.014	0.005	0.024	0.004	0.004	0.004	0.004	0.013	0.012	0.011	0.016
Li	0.012	0.012	0.012	0.012	0.009	0.009	0.009	0.010	0.013	0.011	0.011	0.017
Mg	21.981	21.981	21.633	22.328	16.782	16.782	15.629	17.934	27.679	17.606	15.714	49.718

	PAN (Blue)				PAN (Orange)				Wool			
	Median	Mean	Min	Max	Median	Mean	Min	Max	Median	Mean	Min	Max
Mn	0.136	0.136	0.108	0.163	0.134	0.134	0.120	0.147	1.304	1.076	0.983	1.854
Mo	0.024	0.024	0.023	0.026	0.007	0.007	0.006	0.007	0.026	0.026	0.026	0.027
Na	283.546	283.546	273.101	293.992	142.442	142.442	132.179	152.705	159.352	52.160	46.932	378.964
Ni	0.244	0.244	0.145	0.344	0.159	0.159	0.141	0.177	0.162	0.152	0.144	0.191
P	191.972	191.972	184.426	199.518	47.349	47.349	47.262	47.436	130.807	127.533	125.894	138.994
Pb	0.090	0.090	0.080	0.099	0.076	0.076	0.066	0.085	0.174	0.167	0.145	0.212
Pr	0.001	0.001	0.001	0.001	0.001	0.001	0.001	0.001	0.002	0.002	0.002	0.002
Rb	0.051	0.051	0.039	0.062	0.078	0.078	0.061	0.094	0.054	0.032	0.029	0.101
S	1480.541	1480.541	1464.889	1496.194	1372.988	1372.988	1351.683	1394.293	31282.880	31270.802	31032.101	31545.739
Sc	0.001	0.001	0.000	0.001	0.001	0.001	0.001	0.001	0.001	0.001	0.001	0.001
Sb	0.028	0.028	0.027	0.029	0.015	0.015	0.013	0.016	0.019	0.019	0.015	0.023
Si	285.340	285.340	240.258	330.423	28.436	28.436	26.649	30.223	84.461	83.755	78.206	91.422
Sn	0.161	0.161	0.101	0.222	0.041	0.041	0.041	0.042	0.043	0.039	0.036	0.053
Sr	1.232	1.232	1.223	1.240	0.596	0.596	0.556	0.635	0.686	0.398	0.366	1.295
Th	0.001	0.001	0.001	0.001	0.001	0.001	0.001	0.001	0.002	0.002	0.001	0.002
Ti	88.115	88.115	87.533	88.698	62.140	62.140	61.856	62.423	6.696	6.802	5.189	8.096
U	0.015	0.015	0.013	0.017	0.001	0.001	0.000	0.001	0.003	0.003	0.003	0.003
V	0.031	0.031	0.029	0.033	0.013	0.013	0.011	0.014	0.032	0.033	0.027	0.036
Y	0.004	0.004	0.003	0.004	0.004	0.004	0.004	0.004	0.008	0.007	0.006	0.010
Zn	24.421	24.421	24.293	24.549	8.757	8.757	8.236	9.279	101.793	102.353	100.655	102.373
Zr	0.028	0.028	0.028	0.029	0.029	0.029	0.027	0.032	0.020	0.018	0.016	0.026

Table F.5. Inorganic content of 14day aqueous leachates of PET (black) MPF in FW medium at 20 °C and SW at 5 and 20 degrees.

	PET (Black) – Freshwater – 20 °C				PET (Black) – Seawater – 20 °C				PET (Black) – Seawater – 5 °C			
	Mean	Median	Min	Max	Mean	Median	Min	Max	Mean	Median	Min	Max
Ag	0.09	0.05	0.04	0.21	0.24	0.25	<LOD	0.48	0.02	<LOD	<LOD	0.06
Al	46.15	32.30	29.65	90.35	39.51	39.43	29.87	49.30	29.50	29.65	28.98	29.86
B	2809	2756	2372	3354	7220	7289	6368	7936	6261	6268	6141	6372
Ba	2.17	2.18	1.31	3.02	13.26	13.18	10.86	15.83	12.13	12.46	10.96	12.96
Bi	2.11	2.05	0.06	4.29	0.02	0.03	0.01	0.04	0.02	0.03	<LOD	0.03
Ca	5004	5180	4301	5356	358462	360305	331041	382198	345813	349059	333864	354516
Cd	0.04	0.04	0.02	0.05	2.13	2.30	0.23	3.68	0.10	0.10	0.04	0.15
Cd	0.02	0.03	0.01	0.03	2.13	2.33	0.25	3.60	0.09	0.08	0.08	0.10
Ce	0.06	0.07	0.03	0.07	0.05	0.05	0.05	0.07	0.05	0.05	0.03	0.06
Co	0.30	0.32	0.22	0.37	0.04	0.04	0.01	0.06	0.03	0.04	0.00	0.04
Cr	0.56	0.37	0.26	1.23	1.13	1.04	0.51	1.93	0.25	0.29	0.05	0.40
Cs	0.02	0.01	0.01	0.05	0.21	0.21	0.20	0.22	0.23	0.24	0.22	0.25
Cu	154.47	116.34	114.59	270.59	69.03	72.85	26.85	103.58	44.17	36.56	22.07	73.88
Fe	10.68	9.70	5.75	17.59	2.91	2.81	2.15	3.90	1.03	<LOD	<LOD	4.08
Hf	0.02	0.02	0.01	0.02	0.01	0.01	0.01	0.03	0.01	0.01	0.01	0.01
Hg	<LOD	<LOD	<LOD	<LOD	<LOD	<LOD	<LOD	<LOD	<LOD	<LOD	<LOD	<LOD
K	512	525	436	563	350242	352852	322416	372848	330507	330782	329440	331300
La	0.04	0.02	0.01	0.10	0.04	0.04	0.03	0.06	0.06	0.04	0.02	0.11
Li	2.25	2.11	1.46	3.33	160.40	159.08	152.49	170.97	159.34	158.75	156.14	163.13
Mg	2213	2217	2132	2286	1096195	1097032	1034403	1156311	1078755	1079806	1046599	1109861

Mn	90.13	91.70	84.57	92.55	0.50	0.55	0.28	0.64	0.24	0.21	0.17	0.33
Mo	3.02	3.07	2.27	3.68	15.72	15.49	14.42	17.45	14.21	14.38	13.31	14.94
Na	19136	19480	17906	19679	8944944	9062090	8132886	9522712	8680625	8605448	8424404	9012024
Ni	0.80	0.79	0.66	0.98	0.31	0.34	0.00	0.54	0.59	0.61	0.50	0.65
P	472.53	340.25	332.81	876.82	78.07	79.64	69.03	83.97	104.75	40.84	14.62	258.78
Pb	2.16	1.25	1.05	5.10	12.70	11.43	11.30	16.65	1.30	0.86	0.79	2.24
Pr	0.01	0.01	0.00	0.03	0.01	0.01	0.01	0.02	0.01	0.01	0.01	0.01
Rb	0.18	0.18	0.08	0.27	109.34	109.21	102.61	116.31	109.97	108.93	108.10	112.87
S	1244	1217	960	1583	828511	824626	779584	885207	790884	795192	768706	808754
Sb	9.52	9.97	1.27	16.90	8.17	8.10	6.77	9.70	2.81	2.31	1.50	4.62
Sc	0.01	0.01	0.00	0.03	0.02	0.02	0.01	0.03	0.02	0.01	0.00	0.03
Si	5613	5521	4833	6579	5399	5640	3426	6891	1705	1515	1296	2304
Sn	0.08	0.08	0.06	0.09	0.11	0.11	0.08	0.12	0.02	0.01	0.00	0.06
Sr	4	4	2	4	8250	8246	7719	8790	8127	8024	7993	8365
Th	0.03	0.02	0.02	0.05	0.09	0.09	0.08	0.10	0.01	0.01	0.00	0.02
Ti	1.02	1.00	0.77	1.34	0.80	0.88	0.43	1.03	1.06	1.11	0.83	1.22
U	0.02	0.02	0.01	0.02	3.07	3.04	2.87	3.31	3.15	3.19	2.99	3.28
V	0.10	0.12	0.02	0.15	1.36	1.35	1.29	1.44	1.34	1.32	1.27	1.43
W	0.04	0.03	0.02	0.07	0.03	0.03	0.02	0.05	0.02	0.01	0.01	0.04
Y	0.06	0.03	0.01	0.16	0.13	0.14	0.12	0.14	0.14	0.12	0.11	0.19
Zn	28.85	29.58	17.92	38.33	29.87	30.87	23.74	34.03	18.12	15.97	14.96	23.42
Zr	0.63	0.62	0.46	0.81	0.23	0.23	0.14	0.31	0.32	0.33	0.19	0.43

Table F.6. Inorganic content of 14day aqueous leachates of PET (white) MPF in FW medium at 20 °C and SW at 5 and 20 degree

	PET (White) – Freshwater – 20 °C				PET (White) – Seawater – 20 °C				PET (White) – Seawater – 5 °C			
	Mean	Median	Min	Max	Mean	Median	Min	Max	Mean	Median	Min	Max
Ag	0.03	0.00	0.00	0.1	0.05	0.03	0.00	0.14	0.01	0.00	0.00	0.03
Al	29.84	29.23	25.57	34.73	37.38	34.88	33.43	43.82	28.95	27.97	27.27	31.61
B	3107	2953	2699	3670	7166	7281	6859	7358	6247	6261	6134	6347
Ba	1.63	1.56	1.17	2.16	10.9	10.83	8.55	13.32	11.24	10.32	10.14	13.27
Bi	0.01	0.01	0.01	0.02	0.04	0.04	0.02	0.04	0.01	0.01	0.01	0.02
Ca	4569	4449	4340	4919	35668	35101	345654	373384	344280	348777	334071	349992
Cd	0.03	0.01	<LOD	0.07	0.13	0.12	0.07	0.19	0.14	0.13	0.12	0.19
Cd	0.01	0.01	0.00	0.01	0.1	0.09	0.07	0.13	0.10	0.10	0.08	0.11
Ce	0.02	0.01	0.01	0.03	0.03	0.03	0.03	0.04	0.03	0.03	0.02	0.03
Co	0.39	0.43	0.27	0.47	0.07	0.05	0.04	0.11	0.03	0.04	-0.01	0.06
Cr	0.48	0.26	0.04	1.15	0.68	0.77	0.41	0.84	0.17	0.13	-0.1	0.47
Cs	0.000	0.000	0.000	0.000	0.22	0.22	0.2	0.24	0.23	0.23	0.21	0.24
Cu	56.79	40.96	13.81	115.61	148.09	169.86	31.14	243.26	32.83	29.95	28.58	39.97
Fe	48.94	2.26	1.41	143.14	6.12	2.04	0.99	15.33	<LOD	<LOD	<LOD	<LOD
Hf	0.01	0.01	0.01	0.02	0.01	0.01	0.01	0.01	0.01	0.01	0	0.01
Hg	<LOD	<LOD	<LOD	<LOD	<LOD	<LOD	<LOD	<LOD	<LOD	<LOD	<LOD	<LOD
K	439.84	437.15	432.09	450.29	343957	34019	336415	355262	328399	330494	318925	335779
La	0.02	0.02	0.01	0.03	0.05	0.06	0.03	0.07	0.03	0.03	0.03	0.03
Li	2.16	2.02	1.55	2.91	157.07	154.65	152.12	164.44	158.1	158.56	155.63	160.12
Mg	2190	2204	2136	2231	1095585	1068520	1067711	1150523	1053472	1068202	1023535	1068679

Mn	88.59	87.28	84.79	93.71	0.44	0.43	0.36	0.53	0.22	0.23	0.21	0.23
Mo	3.08	3.1	2.9	3.23	15.19	15.5	14.26	15.82	14.45	14.68	13.52	15.15
Na	19347	19399	18628	20014	8812954	8693254	8617839	9127769	8478422	8538324	8262743	8634199
Ni	0.29	0.28	0.05	0.53	1.22	1.19	1.12	1.35	0.56	0.72	0.04	0.92
P	270.85	182.98	169.92	459.65	215.96	223.92	133.6	290.37	16.47	19.98	6.12	23.3
Pb	2.32	2.22	1.81	2.94	5.01	4.78	4.08	6.17	3.39	3.64	2.84	3.69
Pr	<LOD	<LOD	<LOD	<LOD	<LOD	<LOD	<LOD	<LOD	<LOD	<LOD	<LOD	<LOD
Rb	0.11	0.09	0.06	0.17	109.21	108.64	105.19	113.78	106.57	107.96	101.99	109.77
S	1164	1167	1145	1180	821351	802397	791789	869868	787148	792503	764613	804329
Sb	12.22	10.81	9.85	16	14.69	14.83	12.74	16.51	12.04	10.72	6.71	18.68
Sc	0.02	0.02	0.02	0.03	0.01	0.01	0.00	0.04	0.00	0.00	0.00	0.01
Si	5543	4998	4761	6870	4992	4874	4542	5560	1207	1224	956	1443
Sn	0.1	0.09	0.08	0.12	0.35	0.05	0.05	0.95	0.07	0.07	0.05	0.08
Sr	1.85	1.35	1.22	2.99	8335.17	8167.27	8131.31	8706.93	8010.02	8112.88	7727.46	8189.73
Th	0.02	0.02	0.02	0.03	0.04	0.05	0.02	0.05	0.01	0.01	0.01	0.01
Ti	0.8	0.8	0.65	0.96	4.33	2.12	0.67	10.19	0.8	0.77	0.67	0.96
U	0.01	0.01	0.00	0.01	3.14	3.05	3.02	3.33	3.08	3.08	3.08	3.09
V	0.05	0.04	0.02	0.07	1.28	1.23	1.19	1.42	1.34	1.35	1.27	1.41
W	0.02	0.02	0.02	0.02	0.02	0.01	0.01	0.05	0.04	0.03	0.02	0.06
Y	0.02	0.01	0.01	0.03	0.14	0.14	0.1	0.19	0.11	0.11	0.1	0.11
Zn	23.78	22.59	21.77	26.97	36.09	40.95	26.08	41.23	20.93	19.6	18.48	24.71
Zr	0.22	0.19	0.15	0.31	0.36	0.36	0.25	0.46	0.25	0.21	0.21	0.34

Table F.7. Inorganic content of 14day aqueous leachates of PA (white) MPF in FW medium at 20 °C and SW at 5 and 20 degrees.

	PA (White) – Freshwater – 20 °C				PA(White) – Seawater – 20 °C				PA (White) – Seawater – 5 °C			
	Mean	Median	Min	Max	Mean	Median	Min	Max	Mean	Median	Min	Max
Ag	0.05	0.04	0.00	0.12	0.07	0.06	0.03	0.12	0.04	0.03	0.00	0.10
Al	32.09	33.66	23.46	37.59	30.75	30.23	29.51	33.04	32.86	32.45	31.95	34.17
B	1647	1634	1417	1903	6289	6305	6153	6393	6061	6084	5931	6168
Ba	1.85	1.90	1.19	2.40	10.09	10.26	7.92	11.94	10.87	10.80	10.19	11.61
Bi	0.02	0.02	0.01	0.02	0.02	0.01	0.01	0.04	0.01	0.02	0.00	0.02
Ca	4536	4544	4258	4799	346154	348466	326818	360864	347909	350774	340643	352311
Cd	0.16	0.15	0.07	0.26	0.11	0.13	0.06	0.14	0.24	0.21	0.19	0.32
Cd	0.12	0.09	0.07	0.21	0.10	0.10	0.09	0.11	0.24	0.20	0.13	0.38
Ce	0.02	0.02	0.01	0.03	0.04	0.04	0.02	0.05	0.03	0.04	0.03	0.04
Co	0.43	0.42	0.30	0.56	0.04	0.05	0.01	0.08	0.02	0.01	0.00	0.05
Cr	0.38	0.36	0.03	0.77	0.69	0.36	0.14	1.91	0.31	0.40	<LOD	0.63
Cs	0.01	0.01	0.00	0.01	0.21	0.20	0.20	0.21	0.26	0.25	0.24	0.28
Cu	46.43	51.32	11.70	71.36	69.68	70.40	36.45	101.47	25.70	23.00	12.16	41.95
Fe	2.39	1.61	1.28	5.06	1.21	0.55	<LOD	5.12	5.62	0.33	<LOD	16.99
Hf	0.01	0.01	0.00	0.02	0.01	0.01	0.00	0.02	0.01	0.01	0.01	0.01
Hg	<LOD	<LOD	<LOD	<LOD	<LOD	<LOD	<LOD	<LOD	<LOD	<LOD	<LOD	<LOD
K	609	586	555	709	337926	341218	318219	351047	336308	333703	330841	344381
La	0.02	0.02	0.02	0.03	0.05	0.04	0.03	0.10	0.04	0.04	0.03	0.04
Li	1.19	1.19	0.84	1.53	153.94	153.89	152.60	155.41	161.15	160.47	158.65	164.34

Mg	2250	2197	2071	2535	1049416	1057311	993556	1089487	1072002	1072351	1068944	1074710
Mn	103.51	103.95	100.00	106.13	36.85	36.57	32.25	42.00	12.40	11.87	10.81	14.54
Mo	3.07	3.17	2.43	3.48	14.48	14.64	12.70	15.94	14.66	14.72	14.42	14.83
Na	18216	17263	16690	21649	8712444	8793984	8112293	9149516	8826948	8818512	8759121	8903213
Ni	0.76	0.85	0.26	1.10	0.77	0.82	0.35	1.10	0.61	0.57	0.42	0.84
P	281.58	290.07	215.76	330.40	173.98	167.82	155.66	204.61	18.75	19.69	11.15	25.43
Pb	2.49	2.32	2.04	3.29	6.26	6.22	5.66	6.93	2.35	2.85	1.16	3.05
Pr	0.00	0.01	0.00	0.01	0.01	0.01	0.00	0.01	0.01	0.01	0.00	0.01
Rb	0.17	0.15	0.12	0.27	106.43	108.90	94.77	113.16	107.59	107.91	104.19	110.68
S	1206	1192	866	1574	797366	802072	751698	833620	793693	795743	786679	798656
Sb	0.52	0.43	0.28	0.94	0.32	0.37	0.07	0.46	0.32	0.35	0.23	0.38
Sc	0.01	0.01	0.00	0.02	0.02	0.01	0.00	0.03	0.02	0.01	0.01	0.03
Si	3154	3126	2913	3451	2801	2753	2324	3375	-30	2	-191	100
Sn	0.05	0.05	0.02	0.07	0.11	0.13	0.05	0.14	0.07	0.04	0.02	0.15
Sr	2.09	1.68	1.24	3.74	7772	7956	7021	8155	8028	7932	7838	8312
Th	0.01	0.01	0.00	0.02	0.01	0.01	0.01	0.02	0.01	0.01	0.00	0.01
Ti	0.76	0.76	0.50	1.04	0.96	0.98	0.39	1.50	0.77	0.88	0.53	0.92
U	0.01	0.01	0.00	0.01	3.07	3.07	3.04	3.11	3.47	3.49	3.37	3.56
V	0.04	0.04	0.00	0.08	1.21	1.25	1.06	1.28	1.29	1.35	1.05	1.47
W	0.01	0.01	0.01	0.02	0.02	0.02	0.01	0.04	0.04	0.04	0.03	0.06
Y	0.03	0.03	0.02	0.03	0.12	0.12	0.11	0.13	0.11	0.10	0.10	0.13
Zn	19.96	19.05	17.43	24.33	32.56	26.49	23.85	53.40	18.68	17.17	16.63	22.23
Zr	0.05	0.05	0.03	0.06	0.48	0.46	0.21	0.79	0.32	0.33	0.21	0.42

Table F.8. Inorganic content of 14 day aqueous leachates of PAN (Blue) MPF in FW medium at 20 °C and SW at 5 and 20 degrees.

	PAN (Blue) – Freshwater – 20 °C				PAN (Blue) – Seawater – 20 °C				PAN (Blue) – Seawater – 5 °C			
	Mean	Median	Min	Max	Mean	Median	Min	Max	Mean	Median	Min	Max
Ag	0.03	0.05	0.00	0.05	0.03	0.00	0.00	0.09	0.03	0.03	0.00	0.06
Al	27.92	26.30	25.67	31.79	33.94	35.19	28.52	38.09	33.38	34.07	31.79	34.29
B	1817	1778	1622	2051	6088	6121	5988	6156	6230	6194	6176	6319
Ba	2.09	2.52	1.12	2.62	11.10	11.35	10.47	11.47	11.53	11.84	10.02	12.74
Bi	0.01	0.01	0.00	0.01	0.02	0.02	0.00	0.04	0.01	0.01	0.01	0.01
Ca	4336	4278	4206	4525	334865	347691	308820	348085	348030	351530	339000	353559
Cd	0.03	0.03	0.02	0.04	0.10	0.09	0.08	0.12	0.15	0.15	0.07	0.24
Cd	0.04	0.02	0.02	0.07	0.10	0.09	0.09	0.12	0.15	0.15	0.10	0.21
Ce	0.01	0.02	0.01	0.02	0.03	0.03	0.01	0.04	0.03	0.04	0.01	0.04
Co	0.43	0.44	0.41	0.45	0.05	0.07	0.01	0.08	0.04	0.05	0.03	0.05
Cr	2.58	0.48	0.44	6.81	0.35	0.03	-0.21	1.23	0.41	0.42	0.30	0.50
Cs	0.01	0.01	0.01	0.02	0.24	0.24	0.22	0.24	0.24	0.23	0.22	0.28
Cu	90.99	114.48	27.35	131.15	119.71	121.91	73.43	163.79	103.37	93.17	28.03	188.91
Fe	17.45	1.73	0.70	49.91	1.94	1.85	0.01	3.95	0.90	0.89	0.69	1.12
Hf	0.02	0.02	0.02	0.02	0.02	0.02	0.01	0.03	0.02	0.02	0.01	0.03
Hg	<LOD	<LOD	<LOD	<LOD	<LOD	<LOD	<LOD	<LOD	<LOD	<LOD	<LOD	<LOD
K	403	394	388	428	332632	337621	318980	341293	328307	334245	313497	337178
La	0.01	0.01	0.01	0.02	0.03	0.03	0.02	0.04	0.07	0.07	0.01	0.12
Li	1.29	1.08	0.93	1.85	169.20	163.36	161.99	182.25	176.97	171.97	166.46	192.47
Mg	2131	2125	2088	2181	1032822	1062866	920362	1115239	1090730	1110025	1051949	1110215

Mn	84.66	86.97	79.51	87.51	0.37	0.35	0.35	0.41	0.31	0.25	0.18	0.49
Mo	2.55	2.44	2.35	2.85	13.77	14.69	11.92	14.70	14.45	14.38	13.22	15.75
Na	16868	16972	16284	17347	8555405	8702403	7994182	8969630	8740946	8876630	8467867	8878341
Ni	0.48	0.64	0.14	0.67	0.83	0.88	0.62	1.00	0.76	0.77	0.54	0.96
P	489.17	481.20	459.85	526.45	234.96	227.47	190.31	287.10	185.27	243.88	54.68	257.23
Pb	0.45	0.43	0.41	0.51	1.32	1.22	0.83	1.92	1.19	1.31	0.92	1.34
Pr	0.01	0.01	0.01	0.01	0.01	0.01	0.00	0.01	0.01	0.01	0.01	0.02
Rb	0.13	0.12	0.11	0.17	106.81	108.58	99.90	111.95	108.50	108.59	104.20	112.69
S	1319	1289	1081	1587	789435	804527	752844	810935	798860	800205	780803	815573
Sb	0.20	0.21	0.19	0.21	0.29	0.34	0.18	0.34	0.45	0.47	0.40	0.49
Sc	0.01	0.01	0.00	0.02	0.01	0.01	0.00	0.03	0.01	0.02	0.00	0.02
Si	3362.02	3550.55	2857.77	3677.75	425.72	188.08	<LOD	1125.41	286.49	207.23	<LOD	659.78
Sn	0.07	0.08	0.05	0.09	0.12	0.10	0.05	0.21	0.08	0.06	0.03	0.13
Sr	1.71	1.95	1.14	2.03	7714	7979	6871	8294	8135	8117	7943	8346
Th	0.00	0.00	0.00	0.01	0.01	0.01	0.00	0.02	0.01	0.01	0.01	0.01
Ti	0.62	0.64	0.55	0.67	1.25	1.31	0.99	1.44	0.78	0.82	0.67	0.84
U	0.01	0.01	0.01	0.01	3.35	3.26	3.25	3.53	3.52	3.48	3.28	3.78
V	0.08	0.09	0.05	0.10	1.41	1.39	1.27	1.58	1.25	1.29	1.16	1.32
W	0.02	0.02	0.00	0.04	0.02	0.02	0.00	0.03	0.04	0.05	0.04	0.05
Y	0.03	0.03	0.02	0.03	0.11	0.10	0.09	0.13	0.14	0.15	0.07	0.21
Zn	32.64	29.74	26.02	42.17	53.99	53.56	43.61	64.81	38.73	42.86	29.41	43.92
Zr	0.06	0.05	0.04	0.08	0.24	0.22	0.17	0.34	0.37	0.25	0.18	0.69

Table F.9. Inorganic content of 14 day aqueous leachates of PAN (orange) MPF in FW medium at 20 °C and SW at 5 and 20 degrees.

	PAN (orange) – Freshwater – 20 °C				PAN (orange) – Seawater – 20 °C				PAN (orange) – Seawater – 5 °C			
	Mean	Median	Min	Max	Mean	Median	Min	Max	Mean	Median	Min	Max
Ag	0.05	0.07	0.00	0.09	0.06	0.06	0.00	0.11	0.04	0.03	0.00	0.08
Al	31.31	29.93	27.09	36.90	33.14	32.68	31.62	35.10	31.44	30.59	30.41	33.33
B	1837	1775	1698	2038	6045	5987	5946	6201	6045	6049	5987	6098
Ba	5.99	6.32	5.15	6.51	12.75	12.63	12.25	13.37	14.47	13.22	11.62	18.57
Bi	0.01	0.01	0.00	0.02	0.02	0.03	0.00	0.04	0.02	0.01	0.00	0.03
Ca	4481	4462	4216	4765	341732	347284	325217	352696	357660	355513	352098	365369
Cd	0.16	0.19	0.04	0.25	0.10	0.11	0.05	0.13	0.38	0.14	0.14	0.86
Cd	0.11	0.11	0.03	0.20	0.08	0.07	0.06	0.11	0.32	0.10	0.09	0.79
Ce	0.02	0.02	0.01	0.03	0.03	0.03	0.02	0.04	0.03	0.03	0.02	0.04
Co	0.42	0.43	0.40	0.44	0.03	0.03	0.00	0.05	0.04	0.04	0.03	0.07
Cr	0.57	0.46	<LOD	1.27	0.64	0.66	0.05	1.20	0.01	0.14	-0.28	0.16
Cs	0.01	0.01	0.01	0.01	0.22	0.23	0.21	0.24	0.24	0.23	0.22	0.25
Cu	67.31	76.38	31.41	94.14	61.91	51.43	44.19	90.10	36.02	20.95	12.37	74.73
Fe	61.91	3.75	3.22	178.76	58.20	22.76	4.48	147.35	23.62	4.25	-0.38	67.00
Hf	0.02	0.01	0.01	0.02	0.01	0.01	0.00	0.01	0.01	0.01	0.00	0.01
Hg	<LOD	<LOD	<LOD	<LOD	<LOD	<LOD	<LOD	<LOD	<LOD	<LOD	<LOD	<LOD
K	424	419	407	446	333833	336988	321725	342786	337504	340925	330164	341423
La	0.02	0.02	0.02	0.03	0.03	0.03	0.02	0.03	0.05	0.04	0.03	0.08
Li	0.98	1.04	0.85	1.05	154.68	151.86	151.78	160.39	164.35	161.69	160.37	170.98
Mg	2205	2213	2138	2264	1049417	1055722	1003464	1089065	1122156	1127003	1110763	1128702

Mn	94.73	92.01	90.05	102.11	1.05	0.42	0.24	2.50	0.42	0.47	0.29	0.51
Mo	3.02	3.09	2.83	3.13	14.11	14.13	13.03	15.18	14.97	14.95	14.35	15.59
Na	17342	17918	16135	17974	8625712	8574699	8453128	8849309	9027535	9060399	8877363	9144843
Ni	0.63	0.42	0.04	1.43	1.09	1.15	0.92	1.19	0.36	0.38	0.19	0.51
P	326.87	334.88	293.26	352.48	182.97	172.97	158.66	217.29	65.69	52.40	49.49	95.19
Pb	1.06	1.15	0.87	1.16	1.08	1.07	0.92	1.24	0.77	0.76	0.69	0.86
Pr	0.00	0.00	0.00	0.00	0.00	0.01	0.00	0.01	0.01	0.01	0.00	0.02
Rb	0.10	0.11	0.06	0.13	109.12	106.94	106.47	113.95	111.67	112.48	109.57	112.95
S	1150	1114	1040	1297	804553	792992	781937	838730	822643	828235	810268	829425
Sb	0.07	0.07	0.03	0.10	0.30	0.33	0.18	0.40	0.26	0.25	0.25	0.27
Sc	0.01	0.00	0.00	0.02	0.01	0.00	0.00	0.01	0.02	0.02	0.00	0.04
Si	3528	3219	3013	4353	1290	911	787	2172	894	878	593	1209
Sn	0.09	0.12	0.03	0.12	0.08	0.07	0.05	0.12	0.03	0.01	0.01	0.07
Sr	1.66	1.71	1.54	1.75	8009	8215	7465	8348	8381	8418	8242	8483
Th	0.01	0.01	0.00	0.01	0.01	0.01	0.01	0.02	0.00	0.00	0.00	0.01
Ti	0.76	0.71	0.63	0.92	0.75	0.58	0.57	1.12	0.86	0.67	0.52	1.39
U	0.01	0.01	0.00	0.01	3.01	2.98	2.80	3.23	3.30	3.29	3.27	3.34
V	0.07	0.07	0.05	0.10	1.36	1.34	1.32	1.42	1.28	1.26	1.15	1.42
W	0.01	0.01	0.00	0.01	0.04	0.03	0.03	0.05	0.03	0.03	0.00	0.05
Y	0.03	0.02	0.02	0.04	0.11	0.11	0.10	0.11	0.12	0.10	0.10	0.15
Zn	25.07	25.00	17.30	32.90	31.71	30.93	28.94	35.26	21.85	22.66	19.62	23.26
Zr	0.10	0.12	0.03	0.14	0.35	0.37	0.23	0.43	0.33	0.32	0.27	0.41

Table F.10. Inorganic content of 14 day aqueous leachates of Wool natural fibre in FW medium at 20 °C and SW at 5 and 20 degrees.

	Wool – Freshwater – 20 °C				Wool – Seawater – 20 °C				Wool – Seawater – 5 °C			
	Mean	Median	Min	Max	Mean	Median	Min	Max	Mean	Median	Min	Max
Ag	0.01	0.00	0.00	0.03	0.00	0.00	0.00	0.00	0.03	0.03	0.00	0.06
Al	26.64	27.81	23.49	28.63	63.61	37.46	36.51	116.87	33.15	33.00	32.27	34.20
B	2146	2099	1964	2375	6185	6165	6133	6256	6293	6306	6202	6371
Ba	6.66	5.66	5.35	8.96	14.67	13.72	12.65	17.63	16.25	14.23	13.57	20.95
Bi	0.02	0.02	0.01	0.05	0.11	0.04	0.01	0.27	0.03	0.03	0.01	0.05
Ca	4462	4455	4447	4483	325222	327679	314462	333524	347565	350964	339362	352368
Cd	0.03	0.01	0.01	0.05	0.06	0.08	0.04	0.08	0.08	0.07	0.07	0.09
Cd	0.01	0.01	0.00	0.01	0.04	0.04	0.01	0.06	0.07	0.07	0.07	0.07
Ce	0.04	0.03	0.03	0.05	0.02	0.02	0.02	0.03	0.03	0.02	0.02	0.05
Co	0.11	0.09	0.09	0.14	0.02	0.02	0.00	0.04	0.03	0.04	0.02	0.04
Cr	0.14	0.05	-0.24	0.62	0.23	0.08	0.00	0.61	0.06	0.03	-0.08	0.24
Cs	0.01	0.01	0.00	0.02	0.23	0.24	0.23	0.24	0.23	0.22	0.20	0.27
Cu	56.84	36.20	23.30	111.01	104.29	86.64	72.95	153.29	62.48	35.31	9.73	142.40
Fe	20.52	8.43	7.31	45.83	4.75	4.53	2.25	7.48	3.99	3.94	3.13	4.91
Hf	0.02	0.02	0.02	0.03	0.01	0.01	0.00	0.02	0.01	0.00	0.00	0.03
Hg	<LOD	<LOD	<LOD	<LOD	<LOD	<LOD	<LOD	<LOD	<LOD	<LOD	<LOD	<LOD
K	308.50	313.57	297.98	313.94	325180	323124	321925	330492	333345	340445	316654	342936
La	0.03	0.04	0.03	0.04	0.03	0.04	0.02	0.04	0.04	0.03	0.01	0.07
Li	1.03	1.04	1.01	1.05	155.21	154.13	151.69	159.81	168.52	169.07	161.77	174.73
Mg	2207	2193	2173	2254	1011316	1022349	978856	1032744	1074467	1087458	1042797	1093145

Mn	87.07	87.29	85.17	88.77	12.49	10.60	10.48	16.40	11.24	7.07	5.37	21.28
Mo	1.21	0.98	0.93	1.73	14.44	14.00	13.98	15.33	14.90	14.23	14.19	16.29
Na	17156	17107	17069	17290	8394009	8411843	8184852	8585331	8841795	8980359	8457424	9087602
Ni	0.37	0.34	0.33	0.43	0.60	0.69	0.24	0.89	0.27	0.23	0.16	0.42
P	36.96	28.05	18.92	63.89	208.57	193.03	182.64	250.03	82.63	66.22	58.20	123.48
Pb	1.02	0.67	0.60	1.78	1.76	1.48	1.47	2.32	0.99	1.08	0.74	1.15
Pr	0.01	0.01	0.01	0.01	0.01	0.01	0.00	0.01	0.01	0.00	0.00	0.02
Rb	0.16	0.17	0.11	0.19	108.09	109.40	103.66	111.22	110.09	111.53	105.91	112.82
S	6182	6140	6010	6395	786479	783482	783324	792630	815233	822995	783846	838858
Sb	0.05	0.00	0.00	0.14	0.32	0.37	0.22	0.38	0.31	0.35	0.23	0.36
Sc	0.01	0.01	0.00	0.01	0.01	0.01	-0.01	0.02	0.01	0.00	0.00	0.01
Si	2360	2346	2302	2432	2025	1921	1460	2695	557	397	326	947
Sn	0.07	0.08	0.00	0.13	0.05	0.04	0.03	0.09	0.03	0.02	0.01	0.05
Sr	2.66	2.74	2.22	3.04	7536	7594	7218	7796	7977	8049	7631	8250
Th	0.00	0.00	0.00	0.01	0.02	0.02	0.01	0.02	0.01	0.00	0.00	0.01
Ti	0.62	0.57	0.48	0.81	0.96	0.98	0.88	1.01	0.60	0.50	0.48	0.83
U	0.00	0.00	0.00	0.01	0.49	0.39	0.35	0.74	1.25	1.00	0.93	1.81
V	0.01	0.01	0.00	0.01	0.44	0.47	0.37	0.48	0.36	0.35	0.26	0.46
W	0.02	0.01	0.01	0.03	0.03	0.02	0.02	0.04	0.03	0.02	0.00	0.06
Y	0.04	0.03	0.03	0.06	0.11	0.13	0.08	0.13	0.12	0.11	0.10	0.13
Zn	85.53	87.07	80.47	89.03	67.05	71.91	56.48	72.77	42.05	41.37	34.00	50.79
Zr	0.04	0.02	0.01	0.09	0.35	0.35	0.31	0.38	0.07	0.08	0.00	0.12

Appendix G. Short leachate studies

Table G.1. Detailed sample description of 14 day short leachate studies

Sample name	Fibre types (colour)	MPF amount (mg)			MPF size (mm)*	Medium	Medium amount (mL)	Exposure time	Exposure temp (°C)
PES-B_SW_20	Polyester (Black)	201.39	201.87	200.38	5	SW	20	14 days	20
PES-W_SW_20	Polyester (White)	201.33	201.27	199.79	5	SW	20	14 days	20
PA-W_SW_20	Polyamide (White)	351.29	350.03	350.21	5	SW	35	14 days	20
PAC-B_SW_20	Polyacrylonitrile (Blue)	349.31	350.70	350.18	5	SW	35	14 days	20
PAC-O_SW_20	Polyacrylonitrile (Orange)	350.97	350.30	350.97	5	SW	35	14 days	20
Wool_SW_20	Wool (white/beige)	350.72	350.40	351.35	5	SW	35	14 days	20
SW_20	N/A	N/A	N/A	N/A	5	SW	35	14 days	20
PES-B_SW_5	Polyester (Black)	199.01	201.30	201.11	5	SW	20	14 days	5
PES-W_SW_5	Polyester (White)	201.39	201.96	201.13	5	SW	20	14 days	5
PA-W_SW_5	Polyamide (White)	349.88	350.33	350.15	5	SW	35	14 days	5

PAC-B_SW_5	Polyacrylonitrile (Blue)	349.41	348.77	350.65	5	SW	35	14 days	5
PAC-O_SW_5	Polyacrylonitrile (Orange)	349.97	350.73	351.47	5	SW	35	14 days	5
Wool_SW_5	Wool (white/beige)	350.72	351.67	351.36	5	SW	35	14 days	5
SW_5	N/A	N/A	N/A	N/A	5	SW	35	14 days	5
PES-B_FW_20	Polyester (Black)	200.42	200.79	201.08	5	FW(TG201)	20	14 days	20
PES-W_FW_20	Polyester (White)	200.92	200.56	200.59	5	FW(TG201)	20	14 days	20
PA-W_FW_20	Polyamide (White)	351.25	350.33	349.87	5	FW(TG201)	35	14 days	20
PAC-B_FW_20	Polyacrylonitrile (Blue)	350.03	350.17	349.99	5	FW(TG201)	35	14 days	20
PAC-O__FW20	Polyacrylonitrile (Orange)	351.88	350.79	349.43	5	FW(TG201)	35	14 days	20
Wool__FW_20	Wool (white/beige)	350.87	351.27	352.84	5	FW(TG201)	35	14 days	20
FW_20	N/A	N/A	N/A	N/A	5	FW(TG201)	35	14 days	20

*MPF size refers to an average fibre length of 5 mm

Appendix H. Non-target – GC-MS

Table H.1. Tentatively identified hydrocarbons in PET

Compound Name	Formula	CAS ID	RT	Match	Polymer Extracts					Aqueous Leachates			Colour		Compound Type
					DCM	EtOAc	IPA	MeOH	Hex	14 days	UV (5 m)	UV (9 m)	B	W	
Undecane	$C_{11}H_{24}$	1120-21-4	13.06	90						×			×	×	Hydrocarbon
Dodecane	$C_{12}H_{26}$	112-40-3	15.57	91						×		×	×	×	Hydrocarbon
Nonane, 3,7-dimethyl-	$C_{11}H_{24}$	17302-32-8	15.57	83	×	×		×	×			×* (FW)	×	×	Hydrocarbon
Heptane, 2,5,5-trimethyl-	$C_{10}H_{22}$	1189-99-7	15.58	81	×	×						×* (SW)	×*	×	Hydrocarbon
Tridecane/Undecane, 4,7-dimethyl- (17301-32-5)	$C_{13}H_{28}$	629-50-5	17.93	93						×		×	×	×	Hydrocarbon
1-Undecene, 9-methyl-	$C_{12}H_{24}$	74630-41-4	19.98	87						x(FW)			×*	×	Hydrocarbon
Decane, 5-propyl-**	$C_{13}H_{28}$	17312-62-8	25.08	87	×*	×							×	×	Hydrocarbon
Octane, 2,3-dimethyl-**	$C_{10}H_{22}$	7146-60-3	25.13	81	×	×		×	×			×* (FW/SW)	×	×	Hydrocarbon
Heptadecane	$C_{17}H_{36}$	629-78-7	26.10	96	×	×							×	×	Hydrocarbon
Decane, 2-methyl-	$C_{11}H_{24}$	6975-98-0	26.21	82	×								×		Hydrocarbon

Compound Name	Formula	CAS ID	RT	Match	Polymer Extracts					Aqueous Leachates			Colour		Compound Type
					DCM	EtOAc	IPA	MeOH	Hex	14 days	UV (5 m)	UV (9 m)	B	W	
Hexane, 2,3,5-trimethyl-	C16H32	1069-53-0	27.03	95	×*	×*							×		Hydrocarbon
Undecane, 3-methyl-	C12H26	1002-43-3	27.97	82	×	×*			×	×* (SW_20)		× (SW.D)	×	×	Hydrocarbon
Undecane, x,x-dimethyl-**	C13H28	17301-26-7	28.61	86	×	×	×	×	×	×* SW20)		×* (SW)	×	×	Hydrocarbon
Decane, 2,4-dimethyl-**	C12H26	2801-84-5	28.63	84	×	×							×	×	Hydrocarbon
Octadecane, 3-methyl-	C19H40	6561-44-0	29.11	91	×*	×*								×	Hydrocarbon
Nonadecane, 4-methyl-	C20H42	25117-27-5	30.54	91	×	×								×	Hydrocarbon
Eicosane	C20H42	112-95-8	31.25	90	×	×								×	Hydrocarbon
Tridecane, 2-methyl-	C14H30	1560-96-9	31.37	81	×	×	×	×	×				×	×	Hydrocarbon
Hexadecane	C16H32	629-73-2	32.55	96	×	×	×	×	×				×	×	Hydrocarbon
Heneicosane	C21H44	629-94-7	32.79	92	×	×							×	×	Hydrocarbon
Tetracosane	C24H50	646-31-1	32.92	90	×	×							×	×	Hydrocarbon
Dodecane, 3-methyl-	C13H28	17312-57-1	34.27	85	×*	×								×	Hydrocarbon
Squalene	C30H50	111-02-4	42.44	91	×	×	×	×	×				×	×	Hydrocarbon

** indicates compound was identified by NIST at more than one RT across samples; * indicates compound was present in only 1 sample

Table H.2. Tentatively identified hydrocarbons in PA

Compound Name	Formula	CAS ID	RT	Match	Polymer Extracts					Aqueous Leachates			Compound Type
					DCM	EtOAc	IPA*	MeOH*	Hex*	14 days	UV (5 m)	UV (9 m)	
Octane, 4-methyl-**	C9H20	2216-34-4	13.06	86.30									Hydrocarbon
Hexane, 3,3-dimethyl-**	C8H18	563-16-6	13.12	91.06	×	×	×	×		×		× (FW)	Hydrocarbon
Cyclopentane, 1,1,3-trimethyl-	C8H16	4516-69-2	15.37	89.25						× (FW)	×	×	Hydrocarbon
Undecane, 2,4-dimethyl-*	C13H28	17312-80-0	17.92	80.25	×	×		×		×		×	Hydrocarbon
Octane, 2,7-dimethyl-**	C10H22	1072-16-8	23.53	80.85	×	×		×	×			×* (FW)	Hydrocarbon
Pentadecane, 3-methyl-	C16H34	2882-96-4	23.68	80.38	×	×			×				Hydrocarbon
Cycloheptane, methyl-	C8H16	4126-78-7	23.77	83.16	×								Hydrocarbon
Hexadecane	C16H34	544-76-3	24.22	96.53	×	×	×	×	×				Hydrocarbon

Compound Name	Formula	CAS ID	RT	Match	Polymer Extracts					Aqueous Leachates			Compound Type
					DCM	EtOAc	IPA*	MeOH*	Hex*	14 days	UV (5 m)	UV (9 m)	
Pentadecane, 2,6,10-trimethyl-	$C_{18}H_{38}$	3892-00-0	25.15	88.36	×	×	×		×				Hydrocarbon
3,5-Dimethyldodecane	$C_{14}H_{30}$	107770-99-0	25.15	88.63	×	×							Hydrocarbon
Hexadecane, 3-methyl-	$C_{17}H_{36}$	6418-43-5	25.56	88.94	×	×*							Hydrocarbon
Heptadecane	$C_{17}H_{36}$	629-78-7	26.10	98.82	×	×	×	×	×				Hydrocarbon
Pentadecane, 2,6,10,14-tetramethyl-	$C_{19}H_{40}$	1921-70-6	26.21	95.56	×	×	×		×				Hydrocarbon
Undecane, 4-ethyl-	$C_{13}H_{28}$	17312-59-3	26.89	89.51	×	×	×						Hydrocarbon
Tetradecane, 4-ethyl-	$C_{16}H_{34}$	55045-14-2	27.03	85.67	×	×							Hydrocarbon
Heptadecane, 4-methyl-	$C_{18}H_{38}$	26429-11-8	27.14	80.49	×	×			×				Hydrocarbon

Compound Name	Formula	CAS ID	RT	Match	Polymer Extracts					Aqueous Leachates			Compound Type
					DCM	EtOAc	IPA*	MeOH*	Hex*	14 days	UV (5 m)	UV (9 m)	
Hexadecane, 2,6,10,14-tetramethyl-**	$C_{20}H_{42}$	638-36-8	28.61	86.91	×	×			×				Hydrocarbon
Octadecane, 4-methyl-	$C_{19}H_{40}$	10544-95-3	28.88	84.26	×	×							Hydrocarbon
Octadecane, 3-methyl-	$C_{19}H_{40}$	6561-44-0	29.11	83.31	×	×							Hydrocarbon
Octane**	C_8H_{18}	111-65-9	29.26	81.93	×	×							Hydrocarbon
Nonadecane	$C_{19}H_{40}$	629-92-5	29.58	89.99	×								Hydrocarbon
Tridecane, 2-methyl-	$C_{14}H_{30}$	1560-96-9	29.65	84.57	×	×							Hydrocarbon
Heptane, 2,4-dimethyl-	C_9H_{20}	2213-23-2	30.42	81.64		×							Hydrocarbon
Nonadecane, 4-methyl-	$C_{20}H_{42}$	25117-27-5	30.53	81.14		×							Hydrocarbon
Heptacosane	$C_{27}H_{56}$	593-49-7	31.37	85.67	×	×							Hydrocarbon
Tridecane, 7-propyl-	$C_{16}H_{34}$	55045-09-5	31.82	87.43	×								Hydrocarbon

Compound Name	Formula	CAS ID	RT	Match	Polymer Extracts					Aqueous Leachates			Compound Type
					DCM	EtOAc	IPA*	MeOH*	Hex*	14 days	UV (5 m)	UV (9 m)	
Decane, 3,8-dimethyl-	C12H26	17312-55-9	31.83	89.93		×							Hydrocarbon
Nonadecane, 2,3-dimethyl-	C21H44	75163-99-4	32.11	80.61		×							Hydrocarbon
Drometrizole	C13H11 N3O	2440-22-4	32.47	88.59	×		×						Hydrocarbon
Hexacosane**	C26H54	630-01-3	32.90	86.50	×	×			×				Hydrocarbon
Pentacosane	C25H52	629-99-2	33.34	84.43	×	×			×				Hydrocarbon

** indicates compound was identified by NIST at more than one RT across samples; * indicates compound was present in only 1 sample

Table H.3. Tentatively identified hydrocarbons in PAN

Compound Name	Formula	CAS ID	RT	Match	Polymer Extracts					Aqueous Leachates			Colour		Compound Type
					DCM	EtOAc	IPA*	MeOH*	Hex*	14 days	UV (5 m)	UV (9 m)	Bl	O	
1-Decene, 2,4-dimethyl-	C12H24	55170-80-4	12.53	90.09						× (FW)			×		Hydrocarbon
Cyclopentane, 1,1,3-trimethyl-	C8H16	4516-69-2	15.37	89.59						× (FW20)	× (inc.D)	×	×	×	Hydrocarbon
Dodecane	C12H26	112-40-3	15.56	80.28	×	×				× (FW20/SW5)		×* (SW)	×	×	Hydrocarbon
Undecane, 4,7-dimethyl-	C13H28	17301-32-5	15.57	94.38						×* (FW20)		× (FW)	×*	×	Hydrocarbon
Decane, 6-ethyl-2-methyl-	C13H28	62108-21-8	15.58	89.47						× (FW_20		×*(FW)	×*	×	Hydrocarbon
Dodecane, 2,6,11-trimethyl-	C15H32	31295-56-4	17.49	93.63	×*				×	× (FW20)			×	×	Hydrocarbon
Tridecane	C13H28	629-50-5	17.93	94.58	×	×				×	×	×	×	×	Hydrocarbon
Decane, 2,9-dimethyl-	C12H26	1002-17-1	17.99	91.64	×*	×				×*(FW20)			x*	×	Hydrocarbon

Compound Name	Formula	CAS ID	RT	Match	Polymer Extracts					Aqueous Leachates			Colour		Compound Type
					DCM	EtOAc	IPA*	MeOH*	Hex*	14 days	UV (5 m)	UV (9 m)	Bl	O	
Hexadecane	C16H34	544-76-3	22.18	91.92	×	×	×		×	× (FW20)*			×	×	Hydrocarbon
Undecane, 3,8-dimethyl-	C13H28	17301-30-3	22.49	91.77	×			×		× (FW20)*			×	×	Hydrocarbon
Nonadecane	C19H40	629-92-5	23.47	91.39	×	×	×	×	×	× (FW20)*			×*	×	Hydrocarbon
Cetene	C16H32	629-73-2	29.27	93.31		×	×						×	×	Hydrocarbon
Heneicosane	C21H44	629-94-7	30.06	91.03	×	×	×	×	×	× (FW20)			×	×	Hydrocarbon
Hexadecane, 2,6,10,14-tetramethyl-	C20H42	638-36-8	30.70	90.91	×*	×				× (FW20)*			×	×	Hydrocarbon
Eicosane	C20H42	112-95-8	31.12	94.91	×		×	×	×	× (FW20)*			×	×	Hydrocarbon
Octane, 2,7-dimethyl-	C10H22	1072-16-8	34.23	82.07	×	×		×	×				x*	×	Hydrocarbon
Dodecane, 2,6,10-trimethyl-	C15H32	3891-98-3	35.66	85.95	×*	×		×						×	Hydrocarbon
Tetracosane	C24H50	646-31-1	37.02	96.66	×	×			×	× (FW20)*			×*	×	Hydrocarbon

Compound Name	Formula	CAS ID	RT	Match	Polymer Extracts					Aqueous Leachates			Colour		Compound Type
					DCM	EtOAc	IPA*	MeOH*	Hex*	14 days	UV (5 m)	UV (9 m)	Bl	O	
Pentacosane	$C_{25}H_{52}$	629-99-2	38.33	96.53	×	×	×		×	× (FW20)*			×*	×	Hydrocarbon
Hexacosane	$C_{26}H_{54}$	630-01-3	39.60	95.34	×	×			×	× (FW20)*			×	×	Hydrocarbon
Heptacosane	$C_{27}H_{56}$	593-49-7	39.60	95.31	×	×	×		×					×	Hydrocarbon
2-Propenoic acid	$C_3H_4O_2$	79-10-7	41.83	81.43							×		×*	×*	Hydrocarbon
Octacosane	$C_{28}H_{58}$	630-02-4	42.00	96.35	×	×	×	×	×	×* (FW20)			×	×	Hydrocarbon
Supraene	$C_{30}H_{50}$	7683-64-9	42.40	84.01	×	×	×	×	×			×*(FW)	×	×	Hydrocarbon
Squalene	$C_{30}H_{50}$	111-02-4	42.41	85.63	×	×			×				×	×	Hydrocarbon
Decane, 3,8-dimethyl-	$C_{12}H_{26}$	17312-55-9	43.83	91.9	×		×							×	Hydrocarbon
Hentriacontane	$C_{31}H_{64}$	630-04-6	44.24	95.06	×				×					×	Hydrocarbon
Heptadecane	$C_{17}H_{36}$	629-78-7	46.33	90.1	×									×	Hydrocarbon

** indicates compound was identified by NIST at more than one RT across samples; * indicates compound was present in only 1 sample

Table H.4. Tentatively identified hydrocarbons in wool

Compound Name	Formula	CAS ID	RT	Match	Polymer					14 day leachates	Compound origin
					DCM	EtOAc	IPA*	MeOH*	Hex*		
Hexane, 2,3,4-trimethyl- **	C9H20	921-47-1	13.12	95						× (20)	Hydrocarbon
Hexane, 2,3,5-trimethyl- **	C9H20	1069-53-0	13.27	84	×	×	×		×		Hydrocarbon
Isopropylcyclobutane	C7H14	872-56-0	15.37	91	×	×				× (FW)	Hydrocarbon
Dodecane	C12H26	112-40-3	15.57	97						× (FW)	Hydrocarbon
Tridecane	C13H28	629-50-5	17.93	97						×	Hydrocarbon
Cyclopentane, 1,1-dimethyl-	C7H14	1638-26-2	19.99	90	×					×* (FW)	Hydrocarbon
Octane, 2,7-dimethyl-	C10H22	1072-16-8	26.09	87	×	×			×		Hydrocarbon
Octane, 2,7-dimethyl-	C10H22	1072-16-8	26.09	90	×	×				×	Hydrocarbon
Undecane, 2-methyl-	C12H26	7045-71-8	31.20	91	×						Hydrocarbon
Undecane, 3,8-dimethyl-	C13H28	17301-30-3	31.20	88	×	×					Hydrocarbon
Dodecane, 2,6,10-trimethyl-	C15H32	3891-98-3	31.22	91	×	×					Hydrocarbon

Compound Name	Formula	CAS ID	RT	Match	Polymer					14 day leachates	Compound origin
					DCM	EtOAc	IPA*	MeOH*	Hex*		
Docosane	C22H46	629-97-0	34.23	97	×	×	×	×	×		Hydrocarbon
Butane, 2,2-dimethyl-	C6H14	75-83-2	35.13	87	×						Hydrocarbon
Heneicosane**	C21H44	629-94-7	35.66	97	×	×	×	×	×		Hydrocarbon
Tricosane	C23H48	638-67-5	35.66	96	×	×	×	×	×		Hydrocarbon
Tetracosane	C24H50	646-31-1	37.03	98	×	×	×	×	×		Hydrocarbon
2-Methylpentacosane	C26H54	629-87-8	39.14	89	×						Hydrocarbon
2-Methylpentacosane	C26H54	629-87-8	39.14	91	×	×	×	×	×		Hydrocarbon
Tetracosane, 3-ethyl-	C26H54	55282-17-2	39.27	90	×	×	×	×	×		Hydrocarbon
Cyclopentane, heneicosyl-**	C26H52	6703-82-8	39.41	82	×	×					Hydrocarbon
Heptane, 3,4,5-trimethyl-	C10H22	20278-89-1	40.22	90	×						Hydrocarbon
2-Methylhexacosane	C27H56	1561-02-0	40.37	93	×	×					Hydrocarbon
3-Methylhexacosane	C27H56	65820-56-6	40.50	87	×	×	×	×	×		Hydrocarbon
Cyclohexane, undecyl-**	C17H34	54105-66-7	41.21	82	×	×*					Hydrocarbon
Cyclohexane, octyl-	C14H28	1795-15-9	41.21	81	×	×*					Hydrocarbon
2-Methylheptacosane	C28H58	1561-00-8	41.57	90	×	×		×	×		Hydrocarbon

Compound Name	Formula	CAS ID	RT	Match	Polymer					14 day leachates	Compound origin
					DCM	EtOAc	IPA*	MeOH*	Hex*		
3-Methylheptacosane	$C_{28}H_{58}$	14167-66-9	41.70	90	×	×	×	×	×		Hydrocarbon
Octacosane, 2-methyl-	$C_{29}H_{60}$	1560-98-1	42.72	97	×	×	×	×	×		Hydrocarbon
3-Methyloctacosane	$C_{29}H_{60}$	65820-58-8	42.85	83	×	×*	×	×	×		Hydrocarbon
Cyclopentane, 1-ethyl-1-methyl-	C_8H_{16}	16747-50-5	43.55	80	×	×*					Hydrocarbon
Nonacosane, 2-methyl-	$C_{30}H_{62}$	1560-75-4	43.84	87	×*	×	×	×	×		Hydrocarbon
Nonacosane, 3-methyl-	$C_{30}H_{62}$	14167-67-0	43.96	82	×	×			×		Hydrocarbon
2,2,6,6-Tetramethylheptane	$C_{11}H_{24}$	40117-45-1	43.99	83		×					Hydrocarbon
Triacontane	$C_{30}H_{62}$	638-68-6	44.26	97	×	×	×	×	×		Hydrocarbon
Cyclohexane, octadecyl-	$C_{24}H_{48}$	929696	48.53	85	×						Hydrocarbon

** indicates compound was identified by NIST at more than one RT across samples; * indicates compound was present in only 1 sample

Appendix I. Antioxidants, UV and thermal stabilisers

Table I.1. Antioxidants, UV and thermal stabilising additive compound specific parameters used in GC-MS analysis

Compound (Industry name)	Cas No.	Retention time (min)	Quantifier ion (m/z)	Qualifier ions (m/z)
Irgafos 38	N/A	23.2	205.1	202.1
Irgacure 1800 (bis(2,6-dimethoxybenzoyl)-2,4,4-trimethyl-pentylphosphineoxide: Iragcure 184 1:4)	N/A	26.15	99.1	81.0
Irganox HP 2215 (Irganox 1010: Irgafos 168: HP-136 2:4:1)	N/A	37.93	307.2	350.2 335.1
Cyasorb UV-5411	003147-75-9	39.54	252.1	323.1
Tinuvin 328	25973-55-1	40.53	322.2	351.2 146.2 132.5
Tinuvin 234	70321-86-7	40.66	342.1	357.2 286.0 149.5
Irgafos 168	31570-04-4	48.75	441.3	308.2 147.1
Irganox B220 (Irgafos 168 and Irganox 1010)	N/A	48.8	441.3	207.0 147.1
Tinuvin 327	3864-99-1	50.85	432.2	447.2 356.2 342.1 119.1 91.1

Degradation and toxicity of microplastic fibres and their role as a source of emerging pollutants

Andy M. Booth[1], Lisbet Sørensen[1] , Dina Tevik Rogstad[2] , Shannen Sait[2] , Dag Altin[3] ,
Martin Wagner[2] , Alexandros Asimakopoulos[2] , Iurgi Salaberria[2]

[1]SINTEF Ocean, Trondheim, Norway
[2]Norwegian University of Science and Technology (NTNU), Trondheim, Norway
[3]BioTrix, Trondheim, Norway

E-mail contact: andy.booth@sintef.no

Microplastic fibres (MPFs) are increasingly being reported as one of the dominant forms of microplastic pollution in aquatic environments. Clothing and textiles produced from synthetic fibres such as polyester (PES), polyacrylic (PAC) and nylon (PA) are considered some of the main sources of MPFs. However, there has been little focus on the environmental fate and effects of MPFs compared to microplastic particles and fragments. In the current study, the environmental fate of MPFs was studied by long-term UV degradation studies using a suite of 5 MPFs with different physical and chemical characteristics (PES, PAC and PA) under freshwater and marine conditions. A detailed chemical characterisation of the pristine test materials was conducted, using GC-MS, LC-MS and ICP-MS to identify the type of additive chemicals present. Degradation studies were conducted in sterile synthetic freshwater (algal culture medium, TG201) and sterile-filtered seawater. Exposures were conducted in 35 mL quartz glass tubes using an Atlas Suntest CPS+ with Xenon lamp generating 65 W/m2 light intensity and fitted with a daylight filter (300-400 nm). The endpoints studied after 5 and 10 months were changes in MPF size (light microscopy and SEM), polymer chemistry and surface properties (ATR-FTIR), and the leaching and degradation of additives (colorants, UV stabilizers, softeners). The release of additive chemicals and their possible photodegradation to intermediate products was investigated as part of the UV degradation studies. In addition, we investigate the potential for the same suite of MPFs and their leachates to elicit toxicological responses in a marine microalga. Effects on algal production, photosynthetic activity and lipid content were assessed as a function of polymer type, fibre length, concentration, as well as the additive chemical profiles of the different MPF leachates.

Keywords: fragmentation, leachate, additive chemicals, textile

Funding source: This work was funded through the Research Council of Norway project 'MICROFIBRE' (Grant agreement number 268404).

Degradation of plastic microfibres, leaching of additive chemicals and interaction with persistent organic pollutants in polar environments

Lisbet Sørensen[1*], **Shannen Sait**[2], **Torbjørn Nguyen**[2], **Alexandros Asimakopoulos**[2], **Rudolf Shmid** [2], **Iurgi Salaberria** [2], **Andy M. Booth**[1*]

[1]SINTEF Ocean, Trondheim, Norway, [2]Norwegian University of Science and Technology (NTNU), Trondheim, Norway.

*Corresponding authors: Lisbet.Sorensen@sintef.no and Andy.Booth@sintef.no

Introduction

- Microplastic fibres (MPFs) from synthetic clothing and textiles are one of the dominant types of microplastic pollution in aquatic environments.
- Polyester, polyacrylic and polyamide (nylon) are among the most abundant polymers in microfibres in the environment.
- MPF physical and chemical properties (e.g. surface-to-volume ratio and chemical additives) may play an key role in the distribution of harmful contaminants through adsorption, desorption and leaching.

The current study aims to investigate the environmental impact of MPFs released from washing of synthetic textiles through studies of:

- Degradation of fibres after long-term UV- and mechanical abrasion of MPFs in synthetic freshwater and marine environments.
- Release of polymer additives to seawater and freshwater.
- Interaction between polymer MPFs and persistent organic pollutants.

Environmental degradation of MPFs

Preparation of Fibres

Polyester (black and white), polyamide and polyacrylate (blue and orange) yarns used in studies.

Environmentally relevant particles

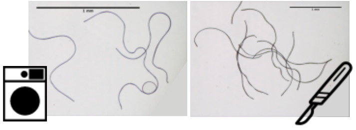

Fibres collected after washing of polyester fleece

Laboratory prepared fibres (scalpel cut)

UV Exposure Studies

- Nominally 2-3 mm fibres
- 9 month UV exposure in freshwater and seawater
- Irradiance = 65 W/m^2 (300-400 nm)
- Sampling at 5 and 9 months

Atlas Suntest CPS+ system fitted with a Xe lamp (1500 W) and daylight filter.

FTIR chromatogram of polyester (white) after 5 months UV exposure

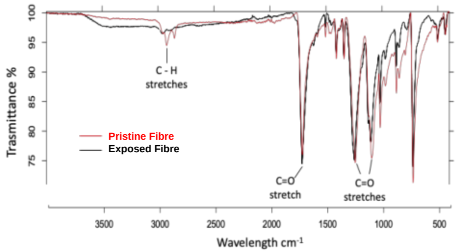

Before UV exposure

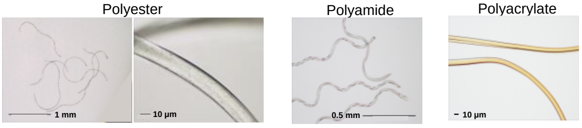

Polyester

Polyamide

Polyacrylate

After 5 month exposure

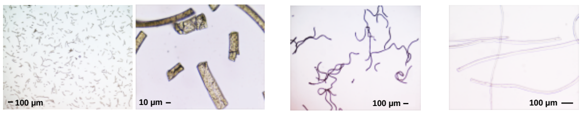

Change in MPF length after 5 month UV exposure

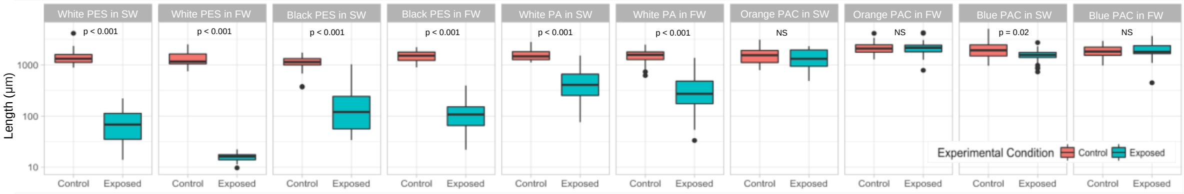

Additive leachates

GC-MS full scan chromatograms of polyester (white) leachates

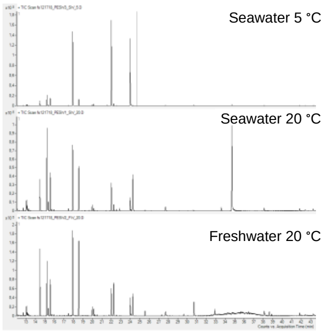

- Leachates were prepared by shaking pristine 5 mm MPFs (10 mg/mL) in sterile seawater (5 and 20 °C) and freshwater (20 °C) for 14 days.
- MPFs were removed and the leachates solvent extracted (DCM-hexane) and subjected to full scan GC-MS analysis (*mz* 50-500).
- Relative to the respective polymer solvent extracts, there were generally few compounds leaching into aqueous media under environmental conditions.
- Some tentatively identified compounds include UV-stabilisers (identification ongoing).
- Appears to be a difference in leachate profiles between freshwater and seawater.
- Leachate concentrations were also relatively higher at higher temperature.

Sorption of phenanthrene

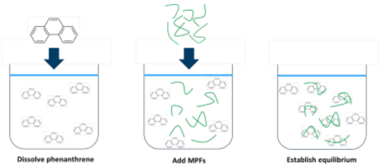

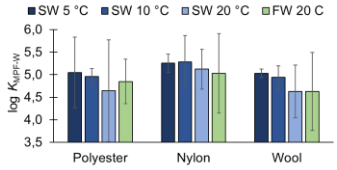

Sorption of phenanthrene at ~50 % solubility in seawater (SW) and freshwater (FW).

Acknowledgements

This research is funded by NRC Grant nr. 268404. We thank the laboratory staff at SINTEF Ocean for practical assistance.

Toxicity and degradation of microplastic fibres and their role as a source of emerging pollutants

Dina Tevik Rogstad[1], **Shannen Sait**[1], Lisbet Sørensen[2], Dionis J. Lyakurwa[1], Dag Altin[3], Alexandros Asimakopoulos[1], Martin Wagner[1], Andy M. Booth[2*], Iurgi Salaberria[1*]

[1]Norwegian University of Science and Technology (NTNU), Trondheim, Norway, [2]SINTEF Ocean, Trondheim, Norway, [3]BioTrix, Trondheim, Norway

*Corresponding authors: andy.booth@sintef.no and iurgi.salaverria@ntnu.no

Introduction

- Microplastic fibres (MPFs) from synthetic clothing and textiles are one of the dominant types of microplastic pollution in aquatic environments
- They mainly comprise of polyester (PES), polyacrylic (PAC) and nylon (PA) polymers
- Few studies have assessed the long-term environmental fate, biological impacts on aquatic primary producers, and role as emerging pollutants
- Physical and chemical properties (e.g. surface-to-volume ratio and presence of chemical additives) might have an important role in the distribution of harmful contaminants through adsorption, desorption and leaching into the environment

Aims & Objectives

To determine the environmental degradation of textile MPFs, and their toxicity towards the marine microalgae *Isochrysis galbana* via:

- Long-term UV- and mechanical degradation of MPFs in simulated freshwater (FW) and saltwater (SW) environments
- Assessing the effects of MPFs on cell production, chlorophyll *a* fluorescence and lipid storage in the marine microalgae *I. galbana*

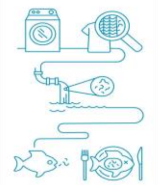

© 2018, Coraball

Approaches, Methods and Results

Preparation of Fibres

Environmentally relevant size!

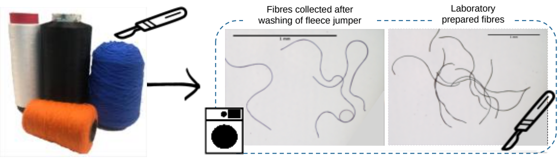

Additive Chemical Content

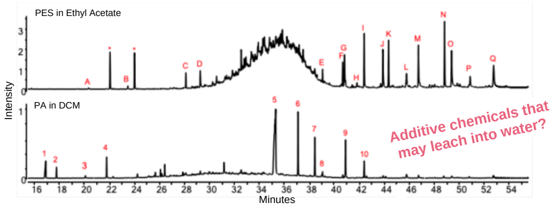

GC chromatograms of PES and PA extracted with ethyl acetate and DCM. Identification of compounds A-Q and 1-10 is ongoing

Toxicity Studies

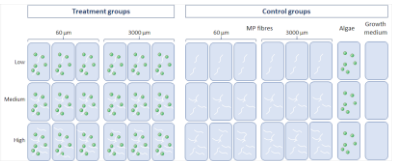

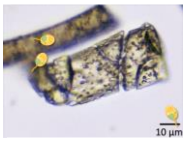

Approximate size comparison between PES and marine microalgae *I. galbana*

Exposed vs. Non-Exposed

Any quantitative changes in:

- Photosynthetic efficiency (Fv/Fm)?
- Neutral lipid accumulation?
- Chlorophyll *a* fluorescence?
- Daily cell production and mean size?

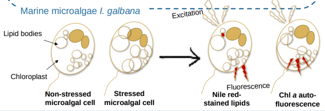

Growth rate of *I. galbana*

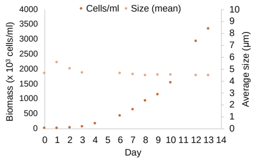

Does MPF size matter? Chemical composition? Concentration?

UV Exposure Studies

- 5 materials: PES in white and black; PA in white and PAC in blue and orange
- Exposed in SW and FW (TG201) medium
- 10 month exposure with sampling at 5 and 10 months
- Irradiance = 65 W/m^2 (300-400 nm)

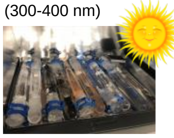

Samples at start of exposure in Atlas Suntest CPS+ system fitted with a xenon lamp (1500 W) and daylight filter

Before UV exposure

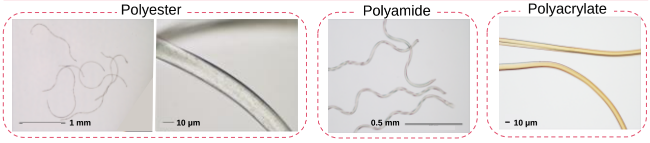

After 5 month exposure

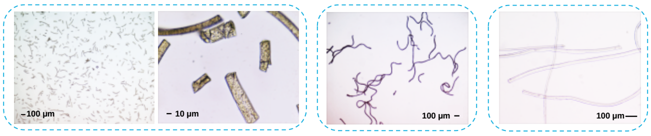

FTIR chromatogram of PES (white) in FW

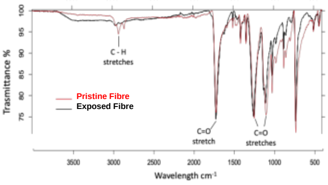

Based on preliminary results

- Significant fragmentation in PES and some fragmentation in PA, formation of nanoparticles to be investigated
- No evidence of fragmentation in PAC
- No evidence of chemical changes in UV exposed samples

Change in Fibre length after 5 month UV exposure

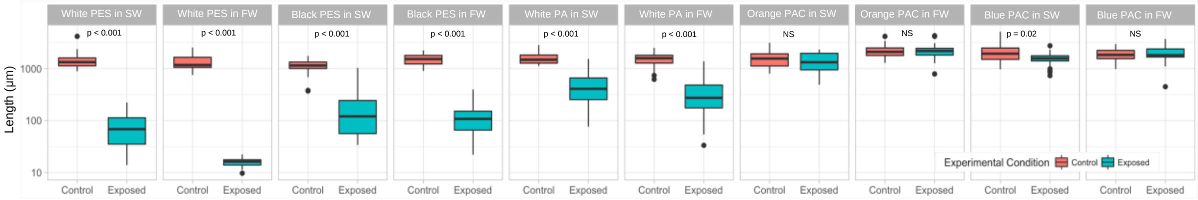

Ongoing and Future Work

- Identify additives across different fibre types via GC/MS and LC-MS/MS and determine if additive leaching is impacted by degradation
- Assess the effects of different physical and chemical properties of MPFs on *I. galbana*
- Assess extent of photodegradation after 10 month UV exposure
- Determine the extent of mechanical degradation after 5 and 10 month sand abrasion studies

Acknowledgements
This research is funded through the Research Council of Norway project MICROFIBRE (Grant agreement no. 268404).